

DOKUZ EYLÜL UNIVERSITY
GRADUATE SCHOOL OF NATURAL AND APPLIED
SCIENCES

IMPACT ON LAMINATED COMPOSITES

by
Berk ALGAN

December, 2009
İZMİR

IMPACT ON LAMINATED COMPOSITES

**A Thesis Submitted to the
Graduate School of Natural and Applied Sciences of Dokuz Eylül University
In Partial Fulfillment of the Requirements for the Degree of Master of Science
in Mechanical Engineering, Mechanics Program**

**by
Berk ALGAN**

December, 2009

İZMİR

M. Sc. THESIS EXAMINATION RESULT FORM

We have read the thesis entitled “**IMPACT ON LAMINATED COMPOSITES**” completed by **BERK ALGAN** under supervision of **PROF. DR. RAMAZAN KARAKUZU** and we certify that in our opinion it is fully adequate, in scope and in quality, as a thesis for the degree of Master of Science.

.....
Prof. Dr. Ramazan KARAKUZU

Supervisor

.....

(Jury Member)

.....

(Jury Member)

Prof. Dr. Cahit HELVACI

Director

Graduate School of Natural and Applied Sciences

ACKNOWLEDGEMENTS

First of all, I am deeply indebted to Prof. Dr. Ramazan KARAKUZU who has never been false in his advices through this thesis. He has patiently supervised my studies and has shared his experiences in a friendly atmosphere.

I also acknowledge research assistant Mehmet Emin Deniz for his guidance and assistance in framing my research.

I would like to dedicate this work to my family; the steps through this point would have been less meaningful without them. I would like to thank my family for their continuous support during my education.

I would like to express my thanks to the EGE TEKNİK POMPA MAKİNA LTD. CO. And it's owners Cengiz YEĞİTĞEL, Vahit AKÇAY and Hasan ATEŞ for their great help during my study.

Berk ALGAN

IMPACT ON LAMINATED COMPOSITES

ABSTRACT

An impact is a force which is applied over a short time period. Such a force can sometimes have greater effect than a lower force applied over a proportionally longer time period. Although many structures are some time subjected to these kinds of forces, many machines and machine parts are commonly subjected to such forces. That is why impact on materials has a big importance in mechanics. Impact on metallic materials will not result in greater effects because metallic materials have the ability to plastic strain and this will help them to absorb most of the energy which will occur as a result of the impact. On the other hand, the deformation which will occur as result of an impact on a composite can occur in an unexpected way and on an unexpected surface.

In this thesis it is discussed, the damage and the deformation of composites under different impact energies. Also it is discussed, in which conditions they can occur, by the help of experimental results and the experimental results are compared with finite element results.

The specimens that are used during the experiments are three kind of geometrical shapes; square with 76 mm per edge, square with 150 mm per edge and a circle with 76 mm of diameter. They are examined in Fractovis Plus impact tester machine.

Keywords: impact damage, laminated composite materials.

TABAKALI KOMPOZİTLER ÜZERİNE DARBE

ÖZ

Darbe kısa bir süre içerisinde tatbik edilen kuvvettir. Böyle bir kuvvet bazen daha düşük ölçüde fakat daha uzun süreli uygulanmış bir kuvvete göre daha fazla zarara yol açabilir. Birçok malzeme böyle kuvvetlere nadir maruz kalsa da, birçok makina ve parçaları böyle kuvvetler altında çalışmaktadır. Bu yüzden ki malzemeler üzerinde darbenin önemi büyüktür. Darbe hasarı genellikle metal malzemelerde çok büyük tehlike arz etmez çünkü metallerin plastik şekil değiştirme kabiliyeti, darbeden doğacak enerjinin büyük bir bölümünü absorbe etmelerini sağlar. Bu nedenle oluşacak kopmalar ani ve beklenmedik olmaz. Kompozit malzemelerde bir darbe sonucunda oluşan hasar, çarpmanın türüne göre beklenmeyen bir yüzeyde oluşabilir.

Bu çalışmada, kompozitlerin çeşitli darbe enerjileri altında hasar ve deformasyonları incelenmiştir. Ayrıca bu hasar ve deformasyonların hangi şartlar altında oluştukları deney sonuçları yardımıyla gözlenmiştir ve deney sonuçları sonlu elemanlar metodunun sonuçları ile karşılaştırılmıştır.

Deney süresince kullanılan numuneler üç farklı geometrik şekilden oluşmuştur; bir kenarının uzunluğu 76 mm olan kare, bir kenarının uzunluğu 150 mm olan kare ve çapı 76 mm olan bir daire. Bu numuneler Fractovis Plus darbe test makinası ile test edilmiştir.

Anahtar Sözcükler: darbe hasarı, tabakalı kompozit malzemeler.

CONTENTS

	Page
M. Sc. THESIS EXAMINATION RESULT FORM.....	ii
ACKNOWLEDGEMENTS	iii
ABSTRACT	iv
ÖZ	v
CHAPTER ONE – INTRODUCTION	1
CHAPTER TWO – COMPOSITE MATERIALS.....	7
2.1 Definition & Background.....	7
2.2 Classification and Characteristics of Composite Materials.....	10
2.2.1 Fibre Reinforced Composites	13
2.2.2 Particle Reinforced Composites	15
2.2.3 Laminated Composites	18
2.3 Design and Analysis with Composite Materials	20
2.4 Manufacturing Process of Composite Materials	23
2.4.1 Contact Moulding	24
2.4.2 Compression Moulding Methods	26
2.4.3 Filament Winding.....	31
2.5 Applications of Composite Materials.....	33
CHAPTER THREE – IMPACT MECHANICS OF LAMINATED COMPOSITES.....	37

3.1 Contact Laws	37
3.1.1 Hertzian Law of Contact.....	38
3.1.2 Indentation Law	39
3.1.3 Finite Element Formulation.....	40
3.2 Low Velocity Impact Damage	44
3.2.1 The Nature of Low Velocity Impact Damage	44
3.2.2 Prediction of Damage Threshold.....	47
3.2.3 Prediction of Damage Extent.....	50
3.3 Impact Tests	52
3.3.1 Importance of Impact Tests	52
3.3.2 Applicability of Impact Tests	54
CHAPTER FOUR–EXPERIMENTAL AND NUMERICAL RESULTS	57
4.1 Specimen Properties	57
4.2 Test Description	58
4.3 Experimental Results.....	61
4.3.1 Square with 76 mm per Edge.....	65
4.3.2 Circle with 76 mm of Diameter.....	69
4.3.3 Square with 150 mm per Edge.....	72
4.4 Damage Areas	76
4.4.1 Square with 76 mm per Edge.....	78
4.4.2 Circle with 76 mm of Diameter.....	87
4.4.2 Square with 150 mm per Edge.....	102
4.5 Numerical Results	118

CHAPTER FIVE–CONCLUSIONS 132

REFERENCES 134

CHAPTER ONE

INTRODUCTION

Composite materials have been increasingly used in aircraft and space structures. Different materials are suitable for different applications. When composites are selected over traditional materials such as metal alloys or woods, it is usually because of one or more of the advantages such as; cost, weight, strength and stiffness, dimension, surface properties, thermal properties, electrical properties.

Some specialists meeting are concerned with damage tolerance in helicopter structures. As the helicopter is an ideal fatigue machine and as most helicopter structures are still metallic (excluding rotor blades). It is natural that the emphasis should be on improving tolerance to cyclic loading and in using modern damage-tolerant methods to assess the time in which an inspectable crack will grow to an unstable situation which puts the structure at risk.

Laminated composite structures have their own brand of damage susceptibility and which is serious without the threat of cyclic loading (indeed carbon-epoxy composites have a rather good fatigue performance compared with metals) and that is the threat of impact damage. It will become increasingly important as more helicopter fuselages and empanages are built out of carbon-epoxy materials: the Bell 427 for example has 70% composite airframe structure.

The effect of impact damage, particularly on the compressive strength of aircraft structures, has been known for 15 years. The traditional way of coping with impact damage has been to limit design allowable strains in compression to 0.3% or thereabouts, where as the material can probably take 0.8% at least if dry at room temperature. Countless coupon tests have shown alarming reductions in the compression after-impact strength. Such tests on coupons are useful for comparing different materials, but are unsuitable for real structures where the nature of the structure can radically alter the amount of the damage, depending as it does on the history of the impact force and structural strains during the impact event. These will

depend on the dynamic response which will in turn depend on the structural mass, stiffness, geometry, substructure, internal stress field etc. A flexible structure may not be as badly damaged as a locally stiff one for example. How then does one assess the amount of impact damage in a real structure without conducting a large set of very expensive impact tests and in particular how to do this during the design phase when damage tolerance may be a key issue?

Many investigations about the impact on composite structures have been carried out. The problem of impact damage in laminated composite structures and the consequent reduction in residual strength, has been a topic of continual research for over two decades. The first attempts to characterize composite materials under dynamic loading were carried out by Rotem (1971) and Lifshitz (1976) and Sierakowski et al. Lifshitz (1976) has examined tensile strength of angle ply balanced laminated made of glass fibers and epoxy matrix under dynamic loading using an instrumented drop weight apparatus. A comparison of theoretical and experimental stress-strain curves reveals that good agreement exists for a certain range of fiber orientation. Different failure criteria have to be used for each range. Failure stresses in the dynamic case are found to be considerably higher than the corresponding static values for the complete range of fiber orientation. Failure strains and initial effective moduli are the same for static and for impact loadings.

Ramkumar and Chen (1983) employed the first order shear deformation theory developed by Whitney and Pagano (1970). They studied an analysis that predicts the response of anisotropic laminated plates to low velocity impact by a hard object. Transverse shear deformation in the plates is accounted for using Mindlin's theory and the governing equations are solved using Fourier integral transforms, assuming infinite dimensions for the plate. The contact area is assumed to vary with time, and the complex contact problem is replaced by the experimentally measured loading history. Computed plate response is used to predict initial failures, including back surface fiber/matrix failures, directly below the impact site and internal delaminations. Analytical predictions are shown to compare well with available experimental results and finite element solutions. Sankar (1992) presented semi-

empirical formula for predicting impact characteristics such as peak force, contact duration, and peak strain on back surface. By solving a one parameter differential equation, Olsson (1992) obtained an approximate analytical solution to the first phase of impact, or wave propagation dominated, response of composite plates. Various researchers have developed the three dimensional finite element models to investigate impact. Davies and Zhang (1993) eliminated some of the disadvantages of three dimensional analysis by describing a strategy for predicting the extent of internal damage in a brittle carbon fibre laminated composite structure, when subjected to low velocity impact by a single mass. The success of the predictions, which avoid expensive three dimensional analysis, is validated by test for a wide range of structures from small stiff plates through to large flexible stiffened compression panels whose residual strength is affected much more by internal delamination than tension structures.

Chang and Choi (1992) used the dynamic finite element method coupled with failure analysis to predict the threshold of impact damage. They studied the impact damage of graphite/epoxy laminated composites caused by a low velocity foreign object. The impact damage in terms of matrix cracking and delaminations resulting from a point-nose impactor was the primary concern. A model was developed for predicting the initiation of the damage and the extent of the final damage as a function of material properties, laminate configuration and the impactor's mass. The model consists of a stress analysis and a failure analysis. A transient dynamic finite element analysis was adopted for calculating the stresses and strains inside the composites during impact resulting from a point-nose impactor. Failure criteria were proposed for predicting the initial intraply matrix cracking and the size of the interface delaminations in the composites.

Jih and Sun (1993) studied prediction of delamination in composite laminates subjected to low velocity impact. They developed a method which is suitable for low velocity impact with heavy impactors. Static delamination fracture toughness was used to predict delamination crack growth under impact conditions. Curing stresses were also considered and found to play a significant role in evaluating the fracture

toughness of some laminates such as $[90_5/0_5/90_5]$. Experiments were performed to obtain the impact force history from which the peak force was used to determine the extent of delamination crack length. The prediction of delamination size using static fracture toughness was found to agree with experimental results. (Aslan, Karakuzu, Okutan, 2002)

Palazotto, Herup and Gummadi (2000) studied the response of composite sandwich plates to low velocity impact, the response was predicted by a displacement based, plate bending, finite element algorithm. Fifth order Hermitian interpolation allows three dimensional equilibrium integration for transverse stress calculations to be carried out symbolically on the interpolation functions so that transverse stresses within the elements could be expressed directly in terms of nodal quantities. Nomex honeycomb sandwich core was modeled using an elastic-plastic foundation and contact loading was simulated by Hertzian pressure distribution for which the contact radius was determined iteratively. Damage prediction by failure criteria and damage progression via stiffness reduction were employed. Comparison to experimental low-velocity impact and static indentation data has showed the ability to model some of the important features of static indentation of composite sandwich structures.

Several researchers have highlighted the importance of matrix cracking and delamination in laminated fiber reinforced fiber composites due to low velocity impact. An approach to predict the initiation and propagation of damage in laminated composite plates has been forwarded by Zhang, Zhu and Lai (2004). This approach was based on contact constraint introduced by penalty function method. The potential delamination and matrix cracking areas were considered as cohesive zone and the damage process as contact behavior between the interfaces. A scalar damage variable was introduced and the degradation of the interface stiffness was established. A damage surface which combines stress-based and fracture-mechanics-based failure criteria was set up to derive the damage evolution law. The damage model was implemented into a commercial finite element package, ABAQUS, via its user subroutine VUINTER. Numerical results on $(0_4, 90_4)_s$ carbon-epoxy laminate

plates due to transversely low velocity impact were in good agreement with experimental observations.

Review papers on the computational methods for predicting impact damage in composite structures have been written by Johnson, Pickett, Rozycki (2000). A continuum damage mechanics (CDM) model for fabric reinforced composites was developed as a framework within which both in-ply and delamination failure may be modelled during impact loading. Damage development equations were derived and appropriate materials parameters determined from experiments. The CDM model for in plane failure has been implemented in a commercial explicit finite element (FE) code, and new techniques were used to model the laminate as a stack of shell elements tied by contact interface conditions. This approach has allowed the interlaminar layers to be modelled and strength reduction due to delamination to be represented, it has also provided a computationally efficient method for the analysis of large-scale structural parts.

Zheng and Binienda (2008) have studied on analysis of impact response of composite laminates under prestress. An analytical solution for the impact response was obtained for the central impact of mass on a simply supported laminated composite plate under prestress based on the Fourier series expansion and Laplace transform technique. A linearized version of the elastoplastic contact law proposed was used in the analytical formulation to consider permanent indentation during the impact. Permanent indentation including damage effects was included in the elastoplastic contact law. The effects of initial stresses on the contact force, plate center displacement, as well as strain time histories are presented. It is shown that higher initial stresses increase the maximum value of the contact force but reduce the plate central displacement. Effects of impactor velocity, mass, interlaminar shear strength of the laminates, and plate thickness on the contact force and dynamic response of the plate under tensile prestresses are also discussed. Zheng and Binienda have also investigated semianalytical solution of wave-controlled impact on composite laminates. A modified Hertzian contact law was used to investigate the impact responses of composite laminates. The original non-linear governing equation

was transformed into two linear equations using asymptotic expansion. Closed –form solution can be derived for the first linear homogenous equation, which is the equation of motion for single degree of freedom system with viscous damping. The second linear nonhomogenous equation was solved numerically. The overall impact responses for wave-controlled impacts can be obtained semianalytically and agree well with the numerical solutions of nonlinear governing equations. The proposed is useful for providing guidance to numerical simulation of impact on complex composite structures with contact laws fitting from experimental data.

In this study, the influence of impact on laminated composites has been investigated experimentally. Composite specimens are tested both experimentally and numerically. Results of experiments and finite element solutions are compared. Finite element code which is used to compute the contact force is 3D IMPACT. Deflections, delaminations, damage zones, absorbed impact energies has been investigated to reach the exact results and also graphs has been drawn to make easier the comparison between the specimens under different energy values of impacts.

CHAPTER TWO COMPOSITE MATERIALS

2.1 Definition & Background

In most common way, we can define a composite material as a material which consists of at least two components with different physical and chemical properties from each other, macroscopic examination of a material wherein the components can be identified by the naked eye. Different materials can be combined on a macroscopic scale, such as in alloying of metals, but the resulting material is, for all practical purposes, macroscopically homogenous, the components can not be distinguished by the naked eye and essentially act together. The advantage of composite materials is that, if well designed, they usually exhibit the best qualities of their components or constituents and often some qualities that neither constituent possesses.

As we said we need two components, but to choose the right materials we must know that one will surround and support the other by saving its position in macroscopic level and the other will strengthen the composite by its mechanical and physical properties. These components are called “matrix” and “reinforcement” respectively.

Table 2.1 Roles of the matrix and reinforcements in a composite

Matrix	Reinforcements
<ul style="list-style-type: none">-Gives shape to the composite-Protects the reinforcements from the environment-Transfers loads to the reinforcements-Contributes to properties that depend upon both the matrix and the reinforcements, such as toughness	<ul style="list-style-type: none">-Give strength, stiffness, and other mechanical properties to the composite-Dominate other properties such as the coefficient of thermal expansion, conductivity, and thermal transport

Composite materials have a long history of usage, the beginning of this usage is not known exactly, but the most known and the older composite materials are straw and mud to form bricks. Straw was used by Israelites to strengthen mud bricks. A piece of dried mud is easy to break by bending but makes a good strong wall; on the other hand a piece of straw is hard to stretch but is too easy to crumple it up. But if you combine these materials they will form bricks which resist both squeezing and tearing. Here the mud is matrix and the straw is reinforcement. Another good example of known composites is plywood which was used by Egyptians when they realized that wood could be rearranged to achieve superior strength and resistance to thermal expansion as well as to swelling caused by the absorption of moisture.

One of the reasons which make composites so important is that matrix and reinforcement have complementary nature. However we can not say all of the properties of composites are advantageous. For each application advantages and disadvantages should be weighed carefully. Some of the advantages and disadvantages of composites are listed in Table 2.2.

Table 2.2 Advantages and disadvantages of composites

Advantages	Disadvantages
<ul style="list-style-type: none"> -Lightweight -High specific stiffness -High specific strength -Tailored properties (anisotropic) -Easily moldable to complex shapes -Part consolidation leading to lower overall system cost -Easily bondable -Good fatigue resistance -Good damping -Crash worthiness -Internal energy storage and release -Low thermal expansion 	<ul style="list-style-type: none"> -Cost of materials -Lack of well proven design rules -Metal and composite designs are seldom directly interchangeable -Long development time -Manufacturing difficulties -Fasteners -Low ductility (joints inefficient, stress risers more critical than in metals) -Solvent/moisture attack -Temperature limits -Damage susceptibility -Hidden damage

<ul style="list-style-type: none"> -Low electrical conductivity -Stealth (low radar visibility) -Thermal transport (carbon-fiber only) 	<ul style="list-style-type: none"> -EMI shielding required
---	---

Figure 2.1 represents a comparison between metals and composites regarding some important properties. We assume all kind of composites as one group and all kind of metals into another group in this figure.

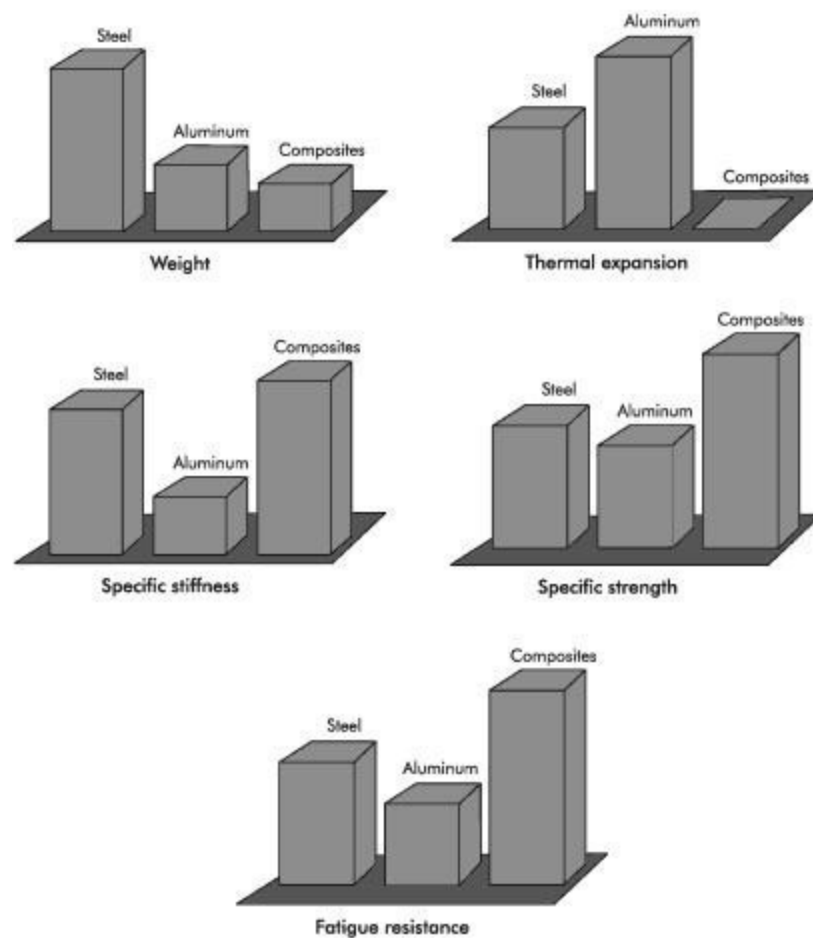


Figure 2.1 Comparison of metals and composites

Most common produced composites use a polymer matrix material often called a resin solution, there are many different polymers such as; polyester, vinly ester, epoxy, polyimide, polyamide, etc. Key point to choose the matrix material is the degree of protection desired for reinforcements. For instance, although polymeric matrices protect the reinforcements good against moderately hostile conditions, they

are not enough against high temperatures or some of the solvents. These extreme conditions may require a ceramic or metal matrix composite. The reinforcement materials are often fibers and ground minerals.

2.2 Classification and Characteristics of Composite Materials

It is already stated that a composite is a mixture of two or more distinct phases or constituents. However this definition is not sufficient and three other criteria have to be satisfied before a material can be said to be a composite. First, both constituents have to be present in reasonable proportions, say greater than 5%. Secondly, it is only when the constituent phases have different properties, and hence the composite properties are noticeably different from the properties of the constituents, that we have come to recognize these materials as composites. For example plastics, although they generally contain small quantities of lubricants, ultra-violet absorbers, and other constituents for commercial reasons such as economy and ease of processing, do not satisfy either of these criteria and consequently are not classified as composites. Lastly a man-made composite is usually produced by intimately mixing and combining the constituents by various means. Thus, an alloy which has two phase microstructure that is produced during solidification from a homogenous melt, or by a subsequent heat treatment whilst a solid, is not normally classified as a composite (Figure 2.2.). However if ceramic particles are somehow mixed with a metal to produce a material consisting of the metal containing a dispersion of the ceramic particles, then this is a true composite material (Figure 2.3.)

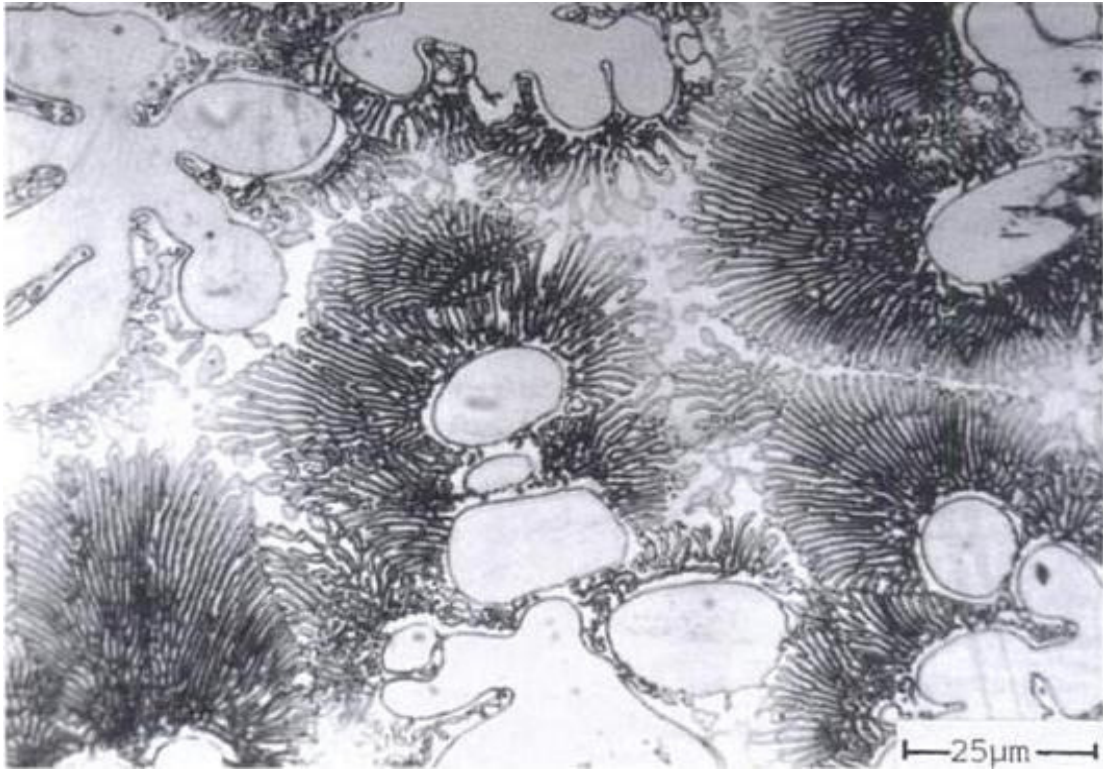


Figure 2.2 Micrograph of a cast Co-Cr-Si-Mo alloy with a multiphase microstructure (Halstead and Rawlings, 1986)

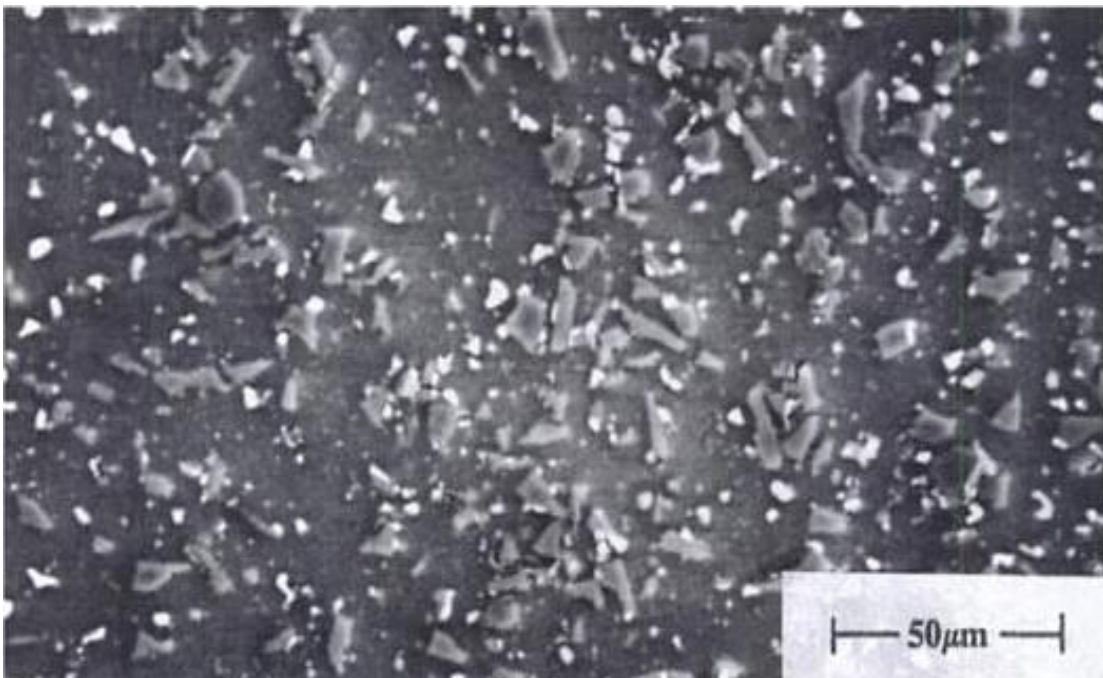


Figure 2.3 Scanning electron micrograph of an aluminium alloy reinforced with angular particles of silicon carbide. The white particles are a second phase in the aluminium alloy matrix (Courtesy D.J.B. Greenwood)

As a result we can say that properties of a composite material depends on,

- The properties of the constituents,
- The geometry of the reinforcements, their distribution, orientation, and concentration usually measured by the volume fraction or fiber volume ratio,
- The nature and quality of the matrix-reinforcement interface.

Composite materials can be classified by the form of the components or by their nature. There are two commonly accepted types of composite materials; fibrous composites, and particulate composites. But there is other kind of composites called “laminated composites” which are made of layers of different materials, including composites of the first two types. So we will also investigate laminated composites under a new topic (Figure 2.4.).

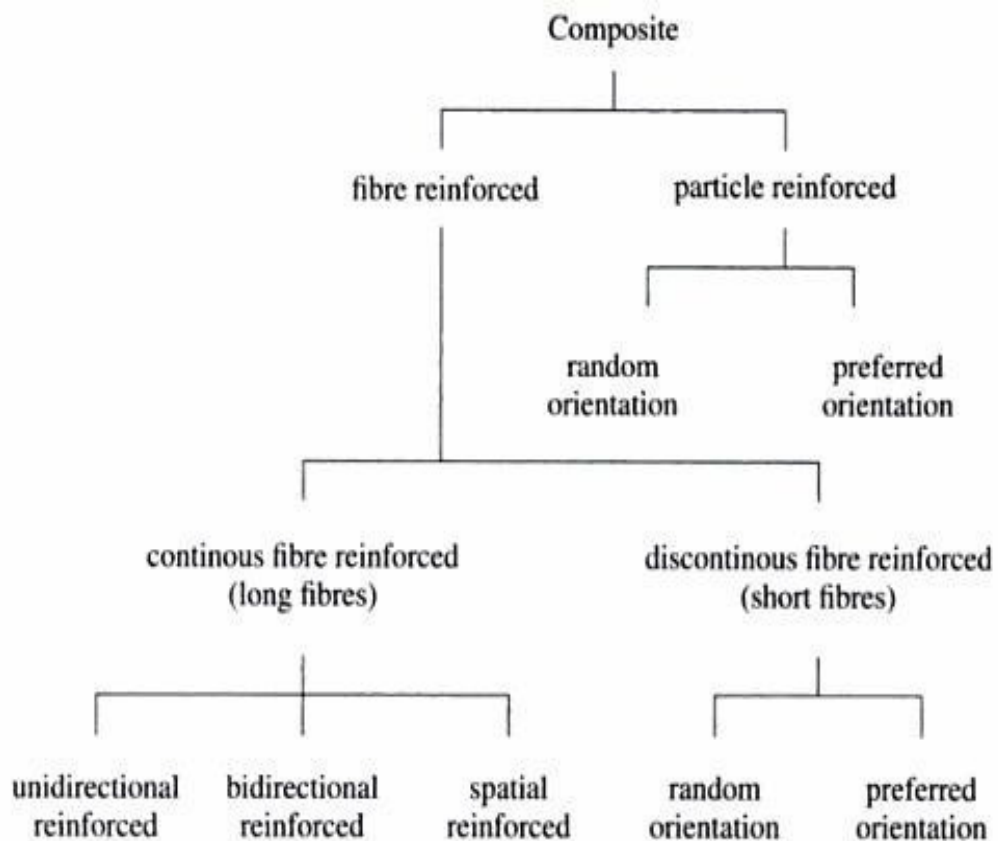


Figure 2.4 Classification of composite materials

2.2.1 Fibre Reinforced Composites

A composite material is a fibre composite if the reinforcement is in the form of fibres. The fibres used are either continuous or discontinuous in form. The short fibres (discontinuous) may be distributed at random orientations, or they may be aligned in some manner forming oriented short-fiber composites. A typical example of a random short-fiber composite is fiberglass.

Continuous fibre-reinforced composites are made up of bundles of small diameter circular fibers. Typically, the radii of these fibers are in the order 0.005 mm, such as the radius of carbon fibers. The largest diameter fibers, such as boron fibers, are in the order of 0.05 mm. Continuous fibre reinforced composite materials are commercially available in the form of unidirectional type.

Normally, fibres are much stiffer and stronger than the same materials in bulk form because fibres have fewer internal defects. Table 2.3 shows the mechanical properties of some commonly used materials made in the form of fibres

Table 2.3 Specific characteristics of materials, made in the form of fibres (Berthelot, 1999)

Fibres of	Modulus E (Gpa)	Ultimate Strength σ (Mpa)	Density ρ (kg/m ³)
E-Glass	72.4	3500	2540
S-Glass	85.5	4600	2480
Carbon with			
(a) High modulus	290 240	2100 3500	1900 1850
(b) High strength			
Kevlar (Aramid)	130	2800	1500
Boron	385	2800	2630

It is obvious that the arrangement of fibres and their orientations is crucial to the evaluation of strength and stiffness of a composite and also allows us to tailor the mechanical properties of the composite according to the performances required. One of the most important types of fibre composite material is the unidirectional composite. A unidirectional composite is made of parallel fibres arranged in a matrix. This type of material forms the basic configuration of fibre composite materials.

Matrix materials are of considerably lower density, stiffness and strength than fibres. However the combination of fibres and a matrix can have high strength and stiffness and still have low density.

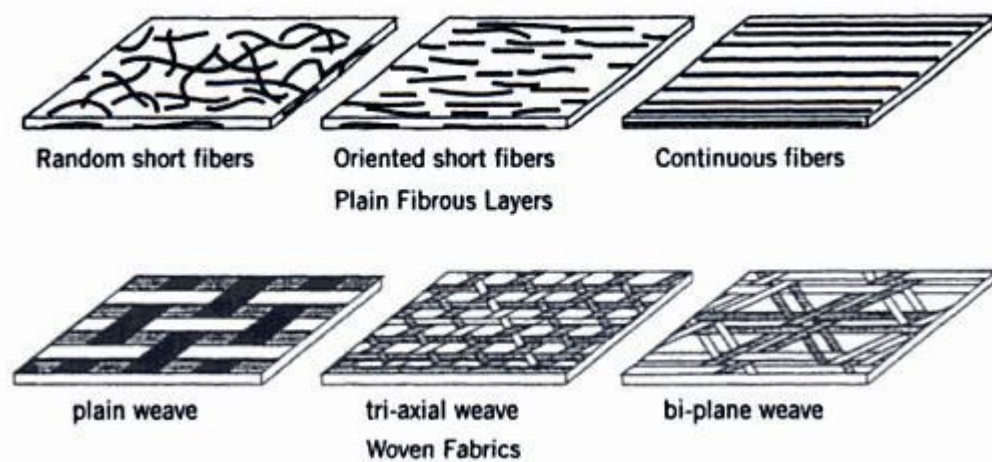


Figure 2.5 Fiber arrangement patterns in the layer of a fibre reinforced composite

Another classification of fibre reinforced composites has been done according to the matrix used, into four broad categories. They are polymer matrix composites, metal matrix composites, ceramic matrix composites and carbon/carbon composites Table 2.4. Polymer matrix composites are made of thermoplastic or thermoset resins reinforced with fibres such as glass, carbon or boron. Metal matrix composites consist of a matrix of metals or alloys reinforced with metal fibres such as boron or carbon. Ceramic matrix composites consist of ceramic matrices reinforced with ceramic fibres such as silicon carbide, alumina or silicon nitride. They are mainly effective for high temperature applications. Carbon /carbon composites consist of

graphite carbon matrix reinforced with graphite fibres. In addition to the above, there are other types of composites as well. The flake composites consist of a matrix reinforced with flakes which may be of different types such as glass flakes, mica flakes and metal flakes. The distribution of the flakes throughout the matrix provides a considerable barrier to moisture, gas and chemical transport. It can suitably be used for obtaining high thermal and electrical resistance or conductivity.

Table 2.4 Classification of fibre reinforced composites according to the matrix used

Matrix Type	Fibre	Matrix
Polymer	E-Glass S-Glass Carbon (graphite) Aramid (kevlar) Boron	Epoxy Polyimide Polyester Thermoplastics Polysulfone
Metal	Boron Borsil Carbon (graphite) Silicon Carbide Alumina	Aluminium Magnesium Titanium Copper
Ceramic	Silicon Carbide Alumina Silicon Nitride	Silicon Carbide Alumina Glass Ceramic Silicon Nitride
Carbon	Carbon	Carbon

2.2.2 Particle Reinforced Composites

A composite material is called a particle composite if the reinforcement is made of particles. The particles can be either metallic or non-metallic. A particle, in contrast to fibres, does not have a preferred orientation. Particles are generally used to improve certain properties of materials, such as stiffness, behaviour with

temperature, resistance to abrasion, decrease of shrinkage, etc. The load carrying capacity of particle composites however depends on the properties of matrix materials. The four possible combinations constituents will be summarized in the following paragraphs.

The most common example of a nonmetallic particle system in a nonmetallic matrix, indeed the most common composite material, is concrete. Concrete is particles of sand and gravel (rock particles) that are bonded together with a mixture of cement and water that has chemically reacted and hardened. The strength of the concrete is normally that of the gravel because the cement matrix is stronger than gravel. The accumulation of strength up to that of the gravel is varied by changing the type of cement in order to slow or speed the chemical reaction. Flakes of nonmetallic materials such as mica or glass can form an effective composite material when suspended in a glass or plastic, respectively. Flakes have a primarily two dimensional geometry with strength and stiffness in the two directions, as opposed to only one for fibres. Ordinarily, flakes are packed parallel to one another with a resulting higher density than fiber packing concepts. Accordingly, less matrix material is required to bond flakes than fibers. Flakes overlap so much that a flake composite material is much more impervious to liquids than an ordinary composite material of the same constituent materials. Mica in glass composite materials are extensively used in electrical applications because of good insulating and machining qualities. Glass flakes in plastic resin matrices have a potential similar to, if not higher than, that of glass fiber composite materials. Even higher stiffnesses and strengths should be attainable with glass flake composite materials than with glass fibre composite materials because of the higher packing density. However, surface flaws reduce the strength of glass flake composite materials from that currently obtained with more perfect glass fiber composite materials.

Solid-rocket propellants consist of inorganic particles such as aluminium powder and perchlorate oxidizers in a flexible organic binder such as polyurethane or polysulfide rubber. The particles comprise as much as 75% of the propellant leaving only 25% for the binder. The objective is a steadily burning reaction to provide

controlled thrust. Thus, the composite material must be uniform in character and must not crack; otherwise, burning would take place in unsteady bursts that could actually develop into explosions that would, at the very least, adversely affect the trajectory of the rocket. Metal flakes in a suspension are common. For example, aluminum paint is actually aluminum flakes suspended in paint. Upon application, the flakes orient themselves parallel to the surface and give very good coverage. Similarly, silver flakes can be applied to give good electrical conductivity. Cold solder is metal powder suspended in a thermosetting resin. The composite material is strong and hard and conducts heat and electricity. Inclusion of copper in an epoxy resin increases conductivity immensely. Many metallic additives to plastic increase the thermal conductivity, lower the coefficient of thermal expansion, and decrease wear.

Unlike an alloy, a metallic particle in a metallic matrix does not dissolve. Lead particles are commonly used in copper alloys and steel to improve the machinability (so that metal comes off in shaving form rather than in chip form). In addition, lead is a natural lubricant in bearings made from copper alloys. Many metals are naturally brittle at room temperature, so must be machined when hot. However, particles of these metals, such as tungsten, chromium, molybdenum, etc. can be suspended in a ductile matrix. The resulting composite material is ductile, yet has the elevated temperature properties of the brittle constituents. The actual process used to suspend the brittle particles is called liquid sintering and involves infiltration of the matrix material around the brittle particles. Fortunately, in the liquid sintering process, the brittle particles become rounded and therefore naturally more ductile.

Nonmetallic particles such as ceramics can be suspended in a metal matrix. The resulting composite material is called cermet. Two common classes of cermets are oxide based and carbide based composite materials. Oxide based cermets can be either oxide particles in a metal matrix or metal particles in an oxide matrix. Such cermets are used in tool making and high temperature applications where erosion resistance is needed. Carbide based cermets have particles of carbides of tungsten, chromium and titanium. Tungsten carbide in a cobalt matrix is used in machine parts

requiring very high hardness such as wire drawing dies, valves, etc. Chromium carbide in a cobalt matrix has high corrosion and abrasion resistance; it also has a coefficient of thermal expansion close to that of the steel, so is well suited for use in valves. Titanium carbide in either a nickel or a cobalt matrix is often used in high temperature applications such as turbine parts. Cermets are also used as nuclear reactor fuel elements and control rods. Fuel elements can be uranium oxide particles in stainless steel ceramic, whereas boron carbide in stainless steel is used for control rods.

2.2.3 Laminated Composites

A lamina or ply is a typical sheet of composite material. A laminate is a collection of laminae stacked to achieve the desired stiffness and thickness. A composite is called a laminated composite when it consists of layers of at least two different materials that are bonded together. Lamination is used to combine the best aspects of the constituent layers in order to achieve a more useful material. The ability to structure and orient material layers in a prescribed sequence leads to several particularly significant advantages of composite materials compared with conventional monolithic materials. The most important among these is the ability to tailor or match the lamina properties and orientations to the prescribed structural loads. The properties that can be emphasised by lamination are strength, stiffness, low weight, corrosion resistance, wear resistance, beauty or attractiveness, thermal insulation, acoustical insulation, etc.

To achieve the desired stiffnesses and thickness, unidirectional fiber reinforced laminae can be stacked so that the fibers in each lamina are oriented in the same or different directions (Figure 2.6). The sequence of various orientations of a fiber reinforced composite layer in a laminate is termed the lamination scheme or stacking sequence. The layers are usually bonded together with the same matrix material as that in a lamina. If a laminate has layers with fibers oriented at 30° or 45° , it can take shear loads. The lamination scheme and material properties of individual lamina

provide an added flexibility to designers to tailor the stiffness and strength of the laminate to match the structural stiffness and strength requirements as we said.

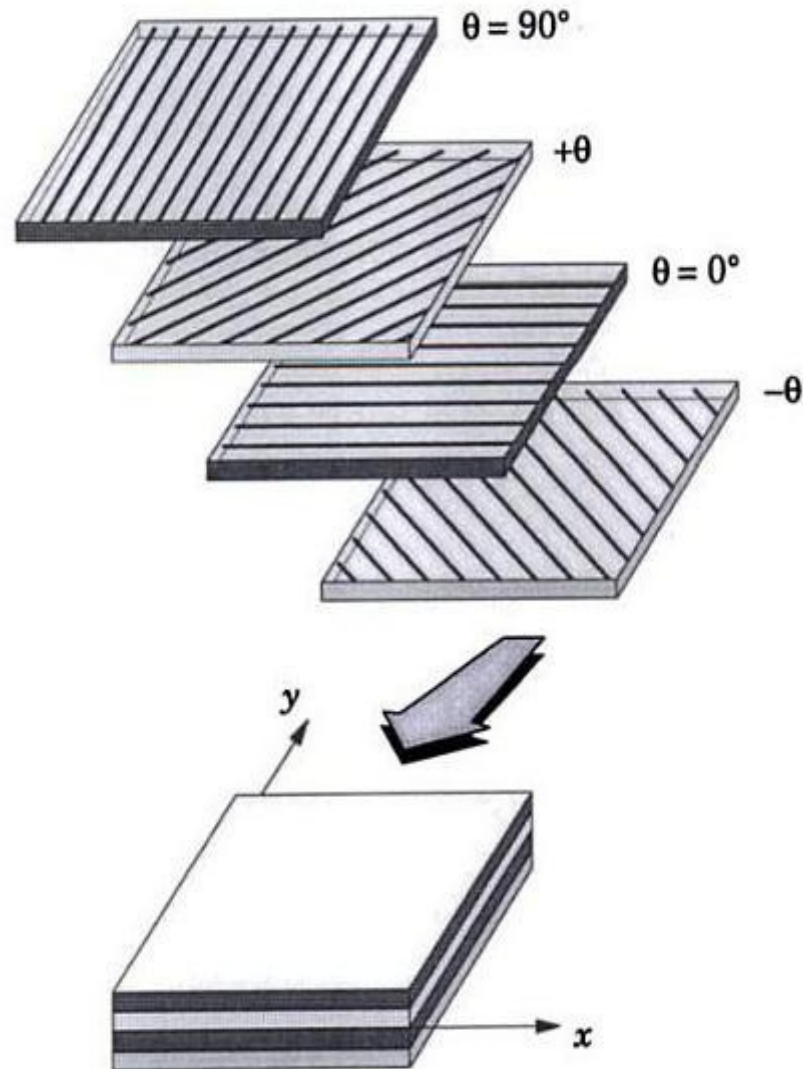


Figure 2.6 A laminate made up of laminae with different fiber orientations.

Laminates made of fiber reinforced composite materials also have disadvantages. Because of the mismatch of material properties between layers, the shear stresses produced between the layers, especially at the edges of a laminate, may cause delamination. Similarly, because of the mismatch of material properties between matrix and fiber, fiber debonding may take place. Also, during manufacturing of laminates, material defects such as interlaminar voids, delamination, incorrect orientation, damaged fibers, and variation in thickness may be introduced. It is

impossible to eliminate manufacturing defects altogether; therefore, analysis and design methodologies must account for various mechanisms of failure.

2.3 Design and Analysis with Composite Materials

In the theory of elasticity there are three sets of equations that are used;

- Equilibrium
- Stres-Strain (Constitutive Equations)
- Strain-Displacement Relations (Compatibility Equations)

To illustrate these equations consider a prismatic bar as shown in Figure 2.7 below subjected to a load P ,

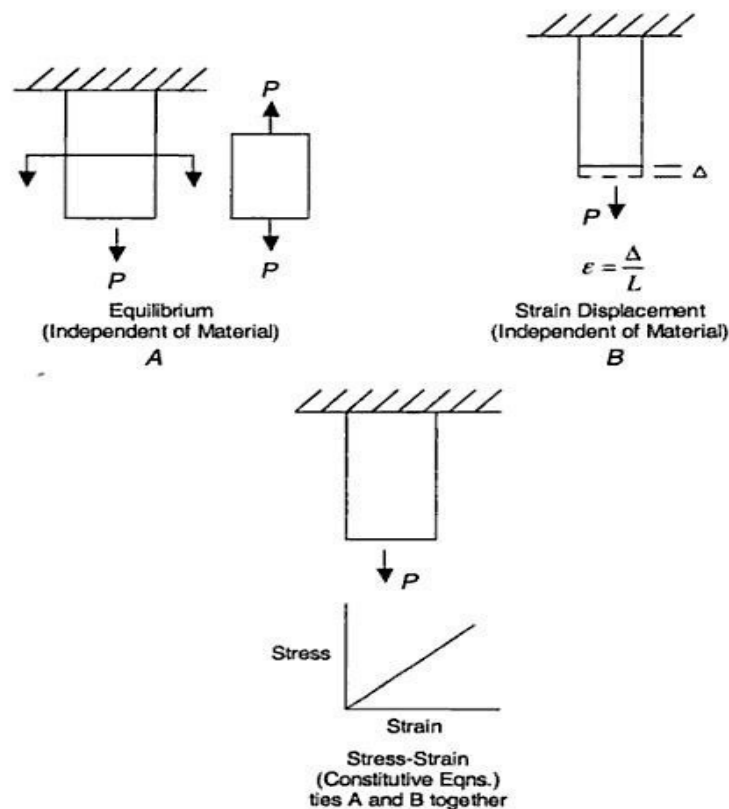


Figure 2.7 Simple tensile tests

In the above all but the stress-strain relations are independent of the material used in the structure. Therefore, the equilibrium equations, the strain-displacement relations and the compatibility equations are the same for an isotropic structure as for

an anisotropic composite material structure. The compatibility equations insure that all deflections are single valued and continuous.

The composite configuration is a key element in the selection of appropriate constitutive equations for determining the stresses and deformations in a specific structural member. Whether a composite material is unidirectional, cross-ply, angle-ply, woven, braided or any other configuration as well as the properties of the fibers and matrix used, all determine the details of the constitutive equations.

Using these sets of equations, the design and analysis of composite structures can be carried out. In design and analysis, there are four primary things to determine for any structure.

The location and magnitude of the maximum stresses: only by determining these maximum values can a comparison be made with the strength of the composite material at that location in each principal direction to determine if the structure is over-stressed or under stressed. A factor of safety (F.S.) is a number that is used and/or mandated to account for unknown considerations such as unanticipated loads, material aberrations, unanticipated uses, etc. A factor of safety can be as low as, for example 1.5 for fighter aircraft, and as high as 10 for elevator cables. The factor of safety is used to relate the strength of the material to an allowable stress (σ_{all}) to which a structure is designed and analyzed.

$$\sigma_{all} = \frac{\text{strength of the material}}{F.S.} \quad \text{OR} \quad \sigma_{all} = \frac{\text{buckling stress}}{F.S.}$$

The location and magnitude of maximum deflections: this calculation indicates whether the structure is adequately stiff. Many structures are stiffness critical; among these are aircraft wings, gyroscopes and the chassis of automobiles. If the structure is too flexible or compliant, it can not perform its intended tasks.

Determination of natural frequencies: almost every structure is subjected to dynamic loads. When a structure is subjected to dynamic loads, whether cyclical or one time impact, every natural frequency of the structure is excited. Therefore, it is

important to determine the important natural frequencies. If a cyclic loading occurs at one or more given frequencies it is important that no natural frequency of the structure be close to these imposed frequencies. Otherwise the resonances that will occur will cause structural failure by the time, or if failure does not occur, fatigue problems will most likely occur.

Determination of buckling loads: when a structure is subjected to compressive or and/or shear loading, an elastic instability can occur, termed buckling. Usually buckling is synonymous with collapse and termination of the usefulness of the structure. Depending upon the slenderness or frailty of the structure, the buckling stresses associated with the buckling load can be a fraction of the strength of the material.

Therefore, in analyzing a structural design, an analyst must check out each of the above four criteria to insure that the structure is sound. In designing a structure, one must therefore insure that the materials, stacking sequences, thickness and configuration details are such that the structure is adequate for the four important design considerations outlined above. To complicate matters one must also consider temperature considerations in order to use the mechanical properties at temperature extremes, consider any potential corrosion effects, weathering, damage, moisture and other environmental effects, and if the material is exposed to dynamic loads, consider high strain rate effects. For composites, design and manufacturing are inextricably entwined. The selection of a manufacturing process may be automatic, however, in many instances this selection is based on available equipment and/or prior experience. This affects the type of composite material used in the design. The geometry of the component, the number of parts to be made, surface finish and dimensional stability can have a pronounced effect on material selection and the resulting composite configuration.

2.4 Manufacturing Process of Composite Materials

Unlike most conventional metals, there is a very close relation between the manufacture of a composite material and its end use. The manufacture of the material is often actually part of the fabrication process for the structural element or even the complete structure. Thus, a complete description of the manufacturing process is not possible nor is it even desirable. In the other hand, we can define processing as a science of transforming materials from one shape to the other because composite materials involve two or more different materials. The processing techniques used with composites are quite different than those for metals processing. There are various types of composites processing techniques available to process the various types of reinforcements and resin systems. It is the job of a manufacturing engineer to select the correct processing technique and processing conditions to meet the performance, production rate, and cost requirements of an application. The engineer must make informed judgements regarding the selection of a process that can accomplish the most for the least resources. The discussion of manufacturing of laminated fiber reinforced composite materials is restricted in this section to how the fibers and matrix materials are assembled to make a lamina and how; subsequently laminae are assembled and cured to make a laminate.

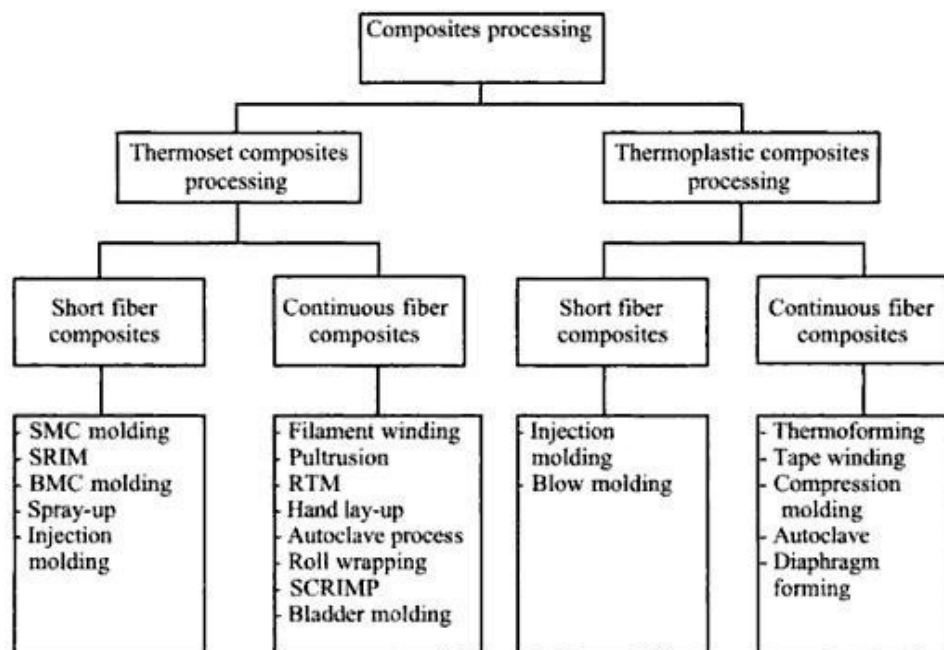


Figure 2.8 Classification of composites processing techniques

2.4.1 Contact Moulding

Mould preparation: By far the most common method of fabrication for large structures such as ship hulls is contact moulding in an open female mould using cold curing polyester resin and E-glass reinforcement. The first step in the fabrication process is the mould preparation. For small to medium size structures, moulds are usually fabricated in GRP (Glass reinforced plastics), in which case a male plug, commonly of wooden construction finished in GRP, is first assembled whose external shape defines the structure to be built. Very large moulds for ship construction may be of steel or aluminium construction lined with an epoxy paste or similar filler to allow fairing out of welded distortions. Mould preparation is usually completed by wax polishing and application of polyvinyl alcohol (PVA) or an equivalent release agent. Lamination is usually started by application of a pigmented gel coat of good quality resin, deposited in the mould by brush or spray, the main purpose of which is to provide a smooth external surface. Lamination is then continued, before the gel coat has fully cured, using one of the following two methods.

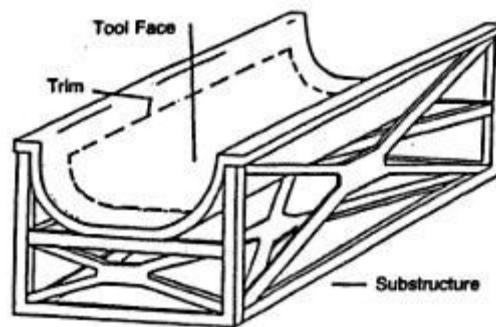


Figure 2.9 Mould preparation

Spray-up: Spray-up of chopped fiber on perforated models has been used for many years. One of the difficulties with this method has been creating a uniform and reproducible thickness of the preform. This problem is addressed with the new processes, where industrial robots are programmed to hold and move a specially designed spray gun and cutter that sprays the chopped fibers together with a thermoplastic powder on a perforated preform tool. After complete spray-up, hot air is forced through the preform for about 1 min. so that the thermoplastic powder

melts. After melting, the air stream is switched to cold and the preforming powder solidifies. Advantages with this method are that inexpensive raw material (glass-fiber roving) can be used and it can be automated to a high degree.

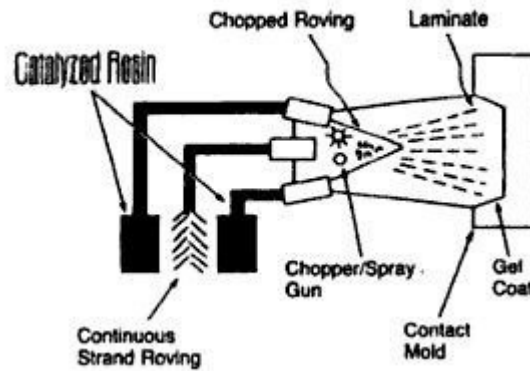


Figure 2.10 Spray-up

Hand lay-up: Resin mixed with a catalyst is deposited liberally on the gel coat or on a previous ply of impregnated reinforcement by a roller-dispenser, brush or spray gun. Each ply of reinforcement, in the form of CSM (chopped strand mat) with a real weight of 300-600 g/m² or woven rovings (WR) with a real weight of 400-800 g/m², is dispensed from a roll, typically 1-1.5 m wide, and is wetted out and consolidated by rolling or brushing into the wet resin. In WR adjacent strips of reinforcement within a ply may be lapped or butted; in either case the strips of reinforcement forming the subsequent plies must be staggered to avoid a continuous line of weakness in the material. This requires little capital equipment but is labour intensive. It is particularly suited for a limited number of a particular structure. The main disadvantages of the method are the low reinforcement content and difficulty in removing all the trapped air; hence the mechanical properties are not as good as in other processes.

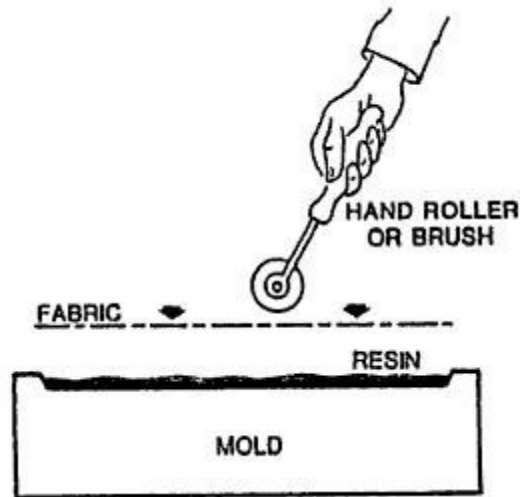


Figure 2.11 Hand lay-up

2.4.2 Compression Moulding Methods

Matched Die Moulding: Three types of matched die molding will be discussed: preform molding, SMC molding (sheet molding compounds), BMC (bulk molding compounds). These three methods all utilize the same type of high pressure molding equipment, but differ in the form of the material that is placed in the molds to form the part. The materials most commonly molded by this technique are fiberglass and either polyester or epoxy. The short fiber lengths generally preclude the use of this technique for high performance parts. The equipment is a press (usually hydraulically driven) that is fitted with both male and female dies (hence the term matched die molding). The dies are generally made of hard metal (such as tool steel) and can be highly polished and chrome plated in order to get a fine finish. The pressures developed by the press can range up to several hundred thousand kg. which is useful for obtaining good part uniformity and compression of the voids that may develop. Compression molding can be used for both addition type cross linking and condensation cross linking. When condensation polymers (such as phenolics) are molded, the condensate (usually water) must be allowed to escape to prevent gas pockets. Therefore, after the mold is closed, it is opened slightly for a few seconds to allow the gases formed by the heated condensate to escape. This process is called degassing or breathing the mold.

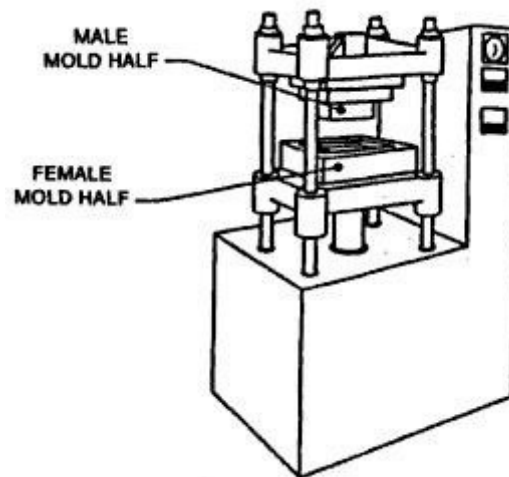


Figure 2.12 Matched die (compression) molding

Forming Methods Employing Gas Pressure: These forming methods sometimes known as bag molding processes and can be categorized under three broad headings. The first of these is vacuum bag molding in which, unlike the case of matched die molding, only one mould is required. This process may be regarded as an extension of the contact molding process. It involves placing over the mould a flexible membrane, separated from the uncured laminate by a film of PVA, polythene or equivalent material, sealing the edges and evacuating the air under the membrane so that the laminate is subjected to a pressure of up to 1 bar. Curing may be accelerated by placing the component in an oven or employing a heated mould.

Autoclave molding is a modification of vacuum forming that uses pressure in excess of atmospheric pressure to produce high density, reproducible products for critical applications such as those needed in the aerospace industry. The mould is situated in an autoclave which has facilities for heating and pressurizing by a gas, usually nitrogen.

The pressure bag works on a similar principle in that a pressure in excess of atmospheric pressure is used for shaping but it is cheaper as it does not require an autoclave. A flexible bag is placed over the lay-up on the mould. Inflation of the bag by compressed air, forces the lay-up into the mould.

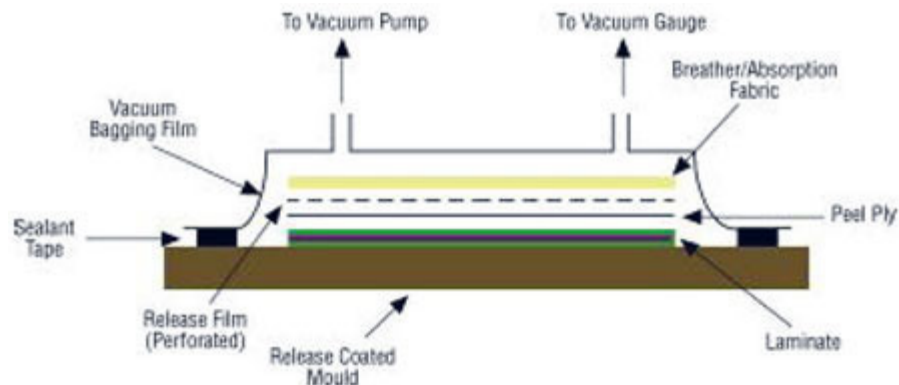


Figure 2.13 Vacuum forming

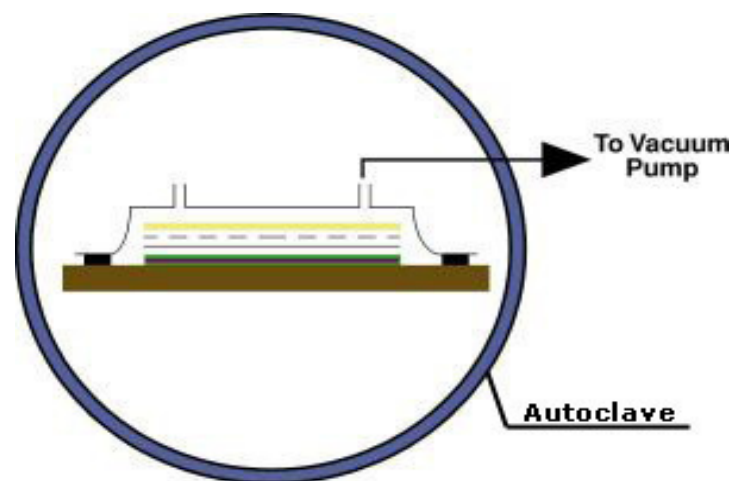
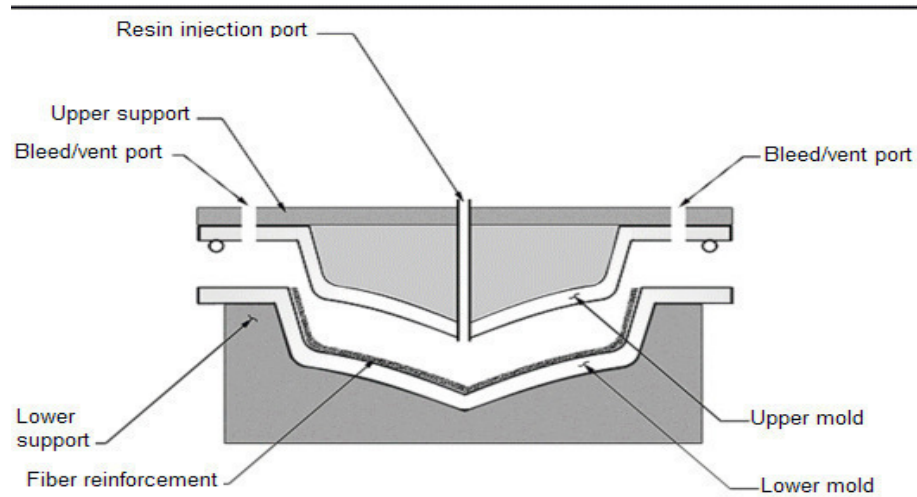


Figure 2.14 Autoclave molding

Low Pressure, Closed Mould System: The methods considered in this section consist of placing the reinforcement in a closed mould and then inserting the resin material into the mould to infiltrate the reinforcement.

In resin transfer molding (RTM): The low viscosity resin is injected into the closed mould using low pressure and is subsequently cured. A consequence of the use of low pressures is that inexpensive moulds, made for example from GRP, have sufficient strength. Such moulds facilitate the manufacture of complex shapes and large components without the need for high cost tooling. However as the mould material does not have good high temperature properties, curing have to be carried out slowly, to restrict any temperature rise which could damage the mould. In fact the production cycle is long. For large components it may even take days, as the infiltration stage is also slow owing to the low pressures involved.

The low pressures required for RTM may be obtained by extracting the air from the mould and allowing atmospheric pressure, or even lower pressure, to force the resin into the mould. This variant of RTM is called vacuum-assisted resin injection moulding (VARIM).



Small part removed from mold.



Top and bottom mold RTM boat hull.

Figure 2.15 Resin transfer molding (RTM)

Instead of using pre-catalysed resin with a slow cure, it is possible to mix two fast reacting components to make the resin just prior to injection into the mould containing the pre-form. The components are mixed at high pressures in an impingement mixing chamber and then injected into a mould where the pressure is usually less than 1 MPa. This is followed by a rapid curing so that the cycle time for this process, which is known as reinforced reaction injection moulding (RRIM), is far less than that for VARIM and is typically 1-2 min.

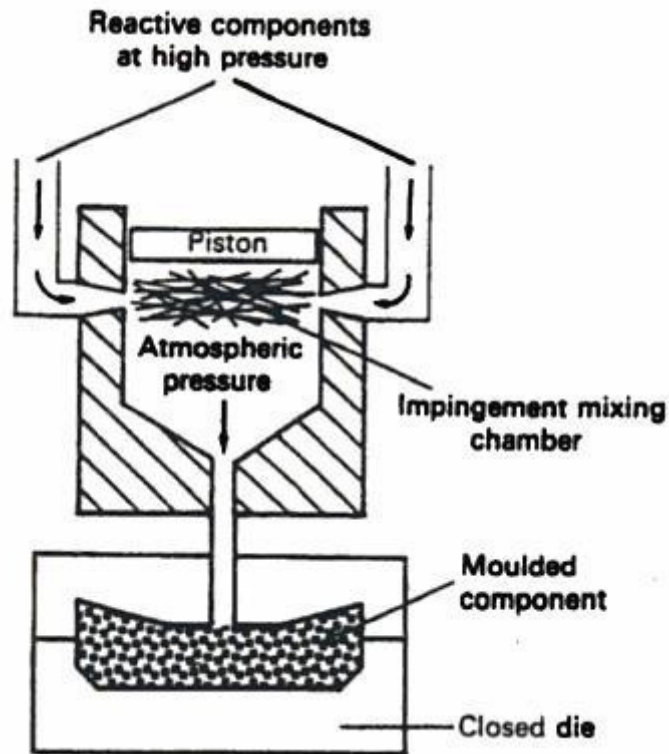


Figure 2.16 Diagram of reinforced reaction injection molding

Pultrusion: In the pultrusion process, continuous reinforcement fibers are impregnated with resin and shaped by drawing through a die and are then cured. This process is analogous to the extrusion of aluminium or thermoplastics (with the obvious exception that pultrusion incorporates fibers and involves thermoset resins in most cases). Pultrusion is a continuous processing method and therefore has great potential for high throughput. The major limitation of pultrusion, as with the extrusion processes, is that the cross section of the part normally must be constant, although both solid and hollow parts as well as many profiles can be made. Compliant dies that permit a change in thickness have been designed for special applications and permit some variation in cross section. Two types of pultrusion dies are commonly used fixed (with no movement) and floating (where one die segment floats and has pressure applied). The pressure can be applied by hydraulics, fire hoses, springs or other methods. The use of fixed dies can generate tremendous hydraulic forces in the resin to impregnate and wet out fibers. Floating dies rarely generate more pressure in the resin than the pressure being applied to the die. A properly designed pultrusion die will maintain accurate resin content because of the fixed cross section. As long as the fiber volume passing through the die is held

constant, as it is in normal production, excess resin will be squeezed out and will run back into the resin bath.

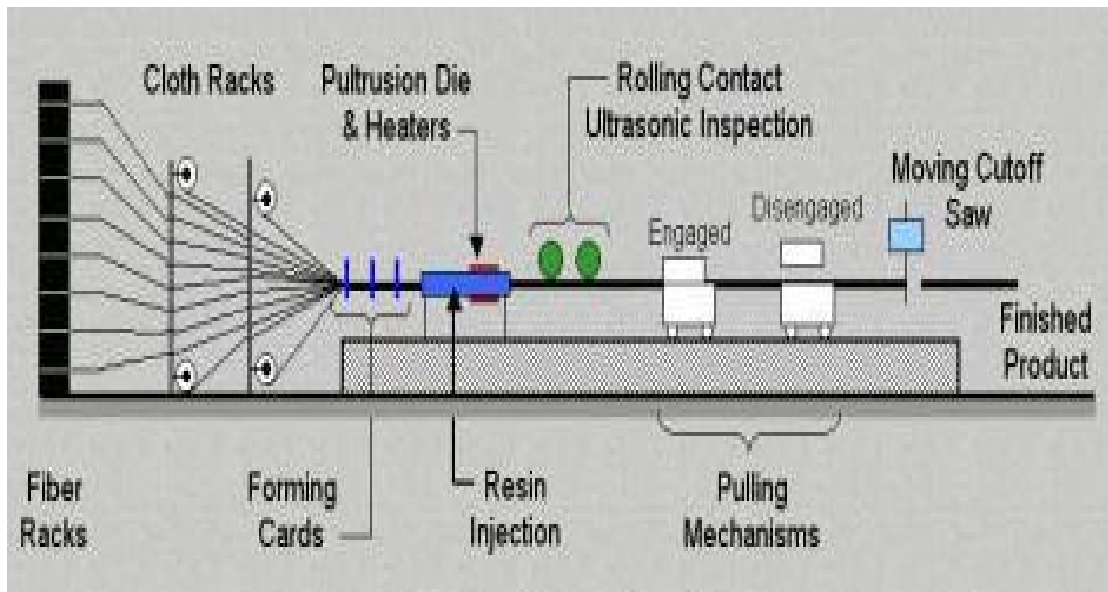


Figure 2.17 Schematic diagram of the pultrusion process

2.4.3 Filament Winding

Structures in the form of bodies of revolution, including cylindrical and spherical shells and cylinders with hemispherical or torispherical end closures may be fabricated economically and to high performance standards by filament winding. In this process resin impregnated fibers are wound over a rotating mandrel at the desired angle. A typical filament winding process is shown in Figures 2.18 and 2.19, in which a carriage unit moves back and forth and the mandrel rotates at a specified speed. By controlling the motion of the carriage unit and the mandrel, the desired fiber angle is generated. The process is very suitable for making tubular parts. The process can be automated for making high volume parts in a cost effective manner. Filament winding is the only manufacturing technique suitable for making certain specialized structures, such as pressure vessels.

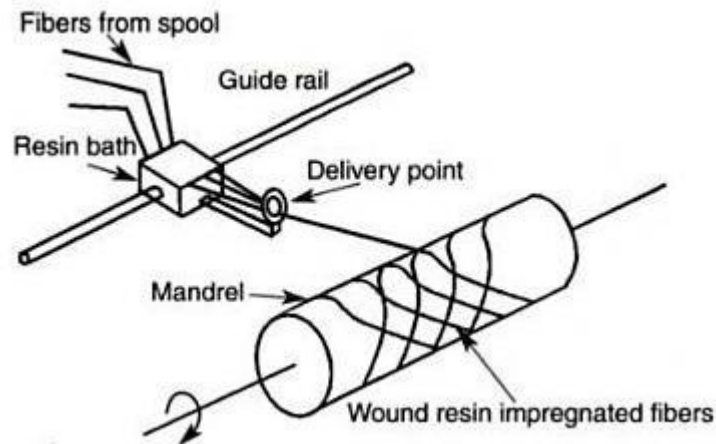


Figure 2.18 Schematic diagram of the filament winding process

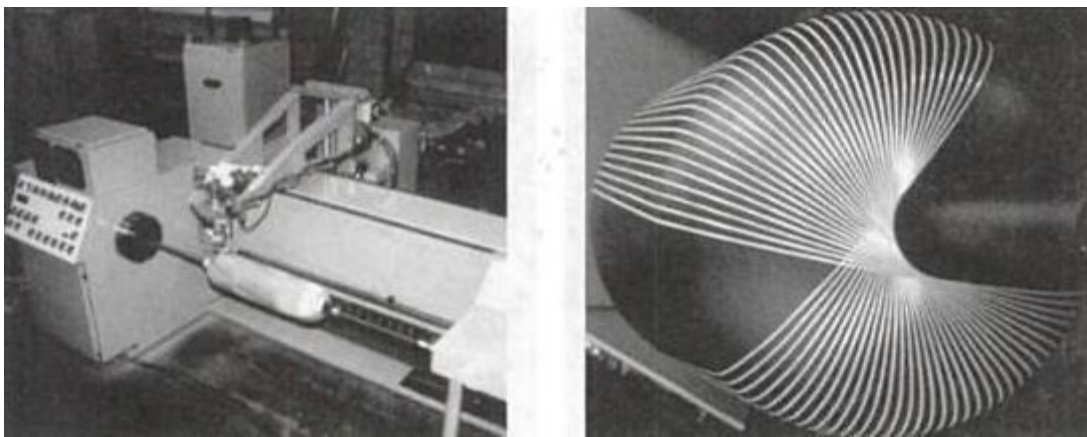


Figure 2.19 Demonstration of the filament winding operation. (Courtesy of Entec Composite Machines, Inc.)

It is important to appreciate the relative merits of the different processing methods and to know under what circumstances a particular method is likely to be selected for manufacture. It is therefore appropriate to recap some of the main features of the methods discussed so far. Hand lay-up can be used to produce complex and/or large structures and components in small quantities. The properties obtained are variables depending on the ratio of constituents used. Capital costs here are low, but it is labour intensive and slow. The equipment for matched die moulding methods is expensive, but components can be produced rapidly. These, and related methods, are especially suited for the production of large number of components, the complexity, of which is limited by the need to use steel dies. RTM processes lie between the two extremes, they are employed for relatively small runs on simple components and for

longer runs on more complex components. Figure 2.20 shows comparison of composite manufacturing processes where H represents “high”, M represents “medium”, and L represents “low”.

Manufacturing Process	Equipment Costs	Rate of Production	Part Strength	Operator Skill Required	Part complexity	Reproducibility	Possible Fibre Forms (R-Random/C-Continuous)
Hand Lay-up	L	L	L	H	H	L	R,C
Spray-up	M	M	L	H	H	L	R
Tape Lay-up (Manual)	L	L	---	H	N	L	C
Tape Lay-up (Automated)	H	H	---	L	M	H	C
Vacuum Bag Moulding (Wet Lay-up)	L	M	M	H	H	L	R,C
Autoclave Moulding (Tape Lay-up)	H	M	H	M	M	H	C
Filament Winding	M	M	H	L	L	H	C
Pultrusion	H	H	H	L	L	H	C
Compression Moulding	H	H	*	M	H	H	R,C
Resin Transfer Moulding	M	M	*	M	H	H	R,C
Reaction Injection Moulding	M	H	*	M	H	H	R,C
Injecting Moulding	H	H	L	H	H	H	R
Stitched/Thermoform Preforms	M	H	M	M	M	H	R,C
Random Fibre Preforms	M	L	L	H	H	L	R
3-D Woven/Braided Preforms	H	M	H	L	H	H	C

Figure 2.20 Comparison of composite manufacturing processes (Wittman and Shook, 1982)

2.5 Applications of Composite Materials

Composite materials are used in a very wide range of industrial applications. Commercial and industrial applications of composites are diverse and varied. Some of these applications are ships and submarines, aircrafts and spacecrafts, trucks and rail vehicles, automobiles, robots, civil engineering structures and prosthetic devices. The main uses of composite materials may be classified as follows;

Marine Field: Like in all other areas, uses of composites in the marine field are growing rapidly for years. Fiberglass boat manufacturers use a variety of materials including glass roving, woven fabrics, mats, vinylester and polyester resins, epoxy, balsa, foam and honeycomb cores, E-glass, S-glass, carbon and Kevlar fibers, with E-glass being the fiber of choice. The manufacturing techniques used for boats include hand lay-up, spray-up, RTM, and SMC processes. Currently the majority of fiberglass boats are produced using an open mold process. Boat builders use composite materials for the boat hulls, as well as decks, showers, bulkheads, cockpit covers, hatches, etc. The demand for high performance fibers is increasing in order to reduce weight, gain speed and save fuel. There is growing interest in carbon and Kevlar fibers for high performance applications such as power and racing boats. Other marine applications of FRP include submarine casings and appendages, superstructure of ships, warship radomes, sonar domes, ship's piping and ventilation systems, oil and water storage tanks, floats and buoys for fishing and mine sweeping purpose.

Aircraft and Space: The most important thing for an aircraft is weight reduction to attain greater speed and increased payload that is why composite materials are found to be ideal in aircrafts and space vehicles. Carbon fibers either alone or in the hybridized condition is used for a large number of aircraft components. Carbon and Kevlar have become the major material used in many wing, fuselage and empennage components. FRP with epoxy as the resin is used for the manufacture of helicopter blades. One of the main reasons why FRP is used for rotor blades is the ability of the material to tailor the dynamic frequency of the blade to its operating parameters.

Composite materials are used extensively in the F-18, an attack fighter made by McDonnell Douglas (now Boeing) and Northrop (now NorthropGrumman). The various speckled areas in Figure 2.21 are graphite-epoxy in primary structure: the vertical fin, the wings and the horizontal tail surfaces. Also, graphite-epoxy is used in various small doors and other regions around the entire plane, which are secondary structures.

Not only F-18 but also Boeing 777 has composite materials on its various parts. The Boeing 777 large twin engine wide-body aircraft in Figure 2.22 entered service in 1995 with more use of composite materials than any previous Boeing commercial aircraft. Approximately 8,400 kg of composite materials are used in each plane for both primary structure and secondary structure for a total of 10% of the structural weight.

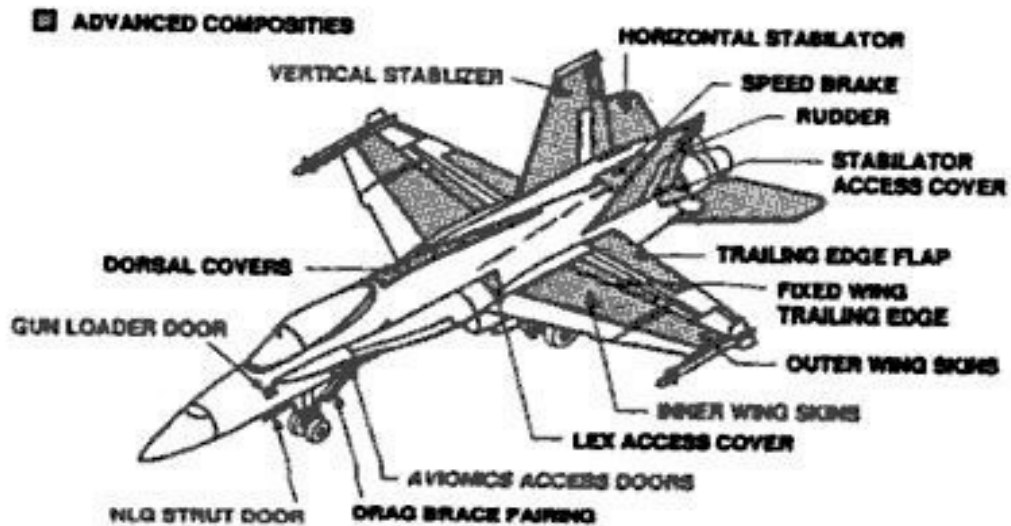


Figure 2.21 F-18C/D Composite materials usage (Courtesy of Boeing)

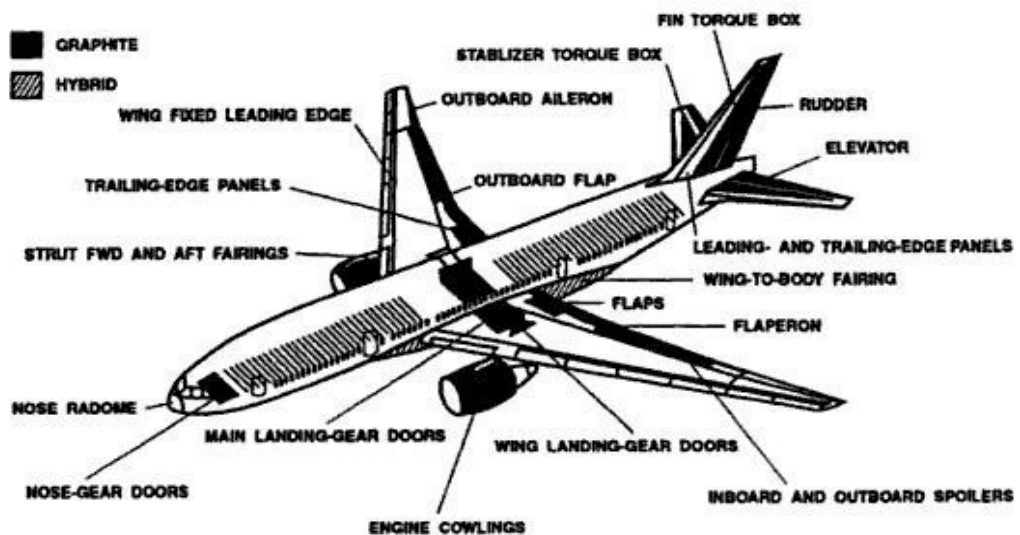


Figure 2.22 Boeing 777 Composite materials usage (Courtesy of Boeing)

Automotive Field: The reason that automotive field prefer composite materials is that, the exterior part of the car such as hood or door panels requires sufficient stiffness. The other requirement is that it should offer maximum resistance to dent

formation (damage tolerance). Resins like polyurethanes enable the damage tolerance to be limited to acceptable values. Further, a good surface finish is highly desirable. Crashworthiness and crash management strategies have been applied in the design of automobiles, particularly racing cars. Maximum energy absorption on impact at high speeds is the goal of the design of the front end of the vehicle for maximum energy absorption to protect or safeguard occupants from forces that cause serious injury or death. Although steel is effective in providing energy absorption 25 kJ/kg uses of orientated Carbon-Fiber/epoxy composite results in higher energy absorption of 120kJ/kg and due to energy absorbed by composite microfracture processes occurring during fragmentation on impact.

Sporting Goods: Many sporting goods are made of FRPs nowadays. One of the major advantages of using FRP is the reduction of weight. Tennis rackets or snow skis are made as a sandwich structure. FRP with carbon or boron fiber as the skin and the core formed by soft and light urethane foam which enables the structure to have a weight reduction without any decrease in stiffness. FRPs enable damping of vibrations. Therefore, shock resulting from the impact of the ball on the tennis racket which is transmitted to the arm of the player will dampen out at a quicker rate. Other application areas of composite materials in sports are fishing rods, bicycle frames, archery bows, sail boats, oars, paddles, canoe hulls, racket balls, rackets, javelins, helmets, golf club staff, hockey sticks, athletic shoe soles and heels, surfboards and many other items.



Figure 2.23 Schematic section through a hybrid carbon fiber/Boron monofilament construction for a golf club staff

CHAPTER THREE

IMPACT MECHANICS OF LAMINATED COMPOSITES

3.1 Contact Laws

The resistance to impact of laminated composites is important in applications such as a bullet hitting a military aircraft structure or even the contact of a composite leaf spring in a car to runaway stones on a gravel road. The resistance to impact depends on several factors of the laminate, such as the material system, interlaminar strengths, stacking sequence, and nature of the impact such as, velocity, mass, and size of the impacting object. Impact reduces strengths of the laminate and also initiates delamination in composites. Delamination becomes more problematic because, many times, visual inspection cannot find it.

In general, hard and soft objects result in different failure modes. If the object is relatively rigid and small, then the contact time is short and extensive damage occurs in the neighborhood of the contact region. The extent of the damage obviously depends on the contact force between the object and the target composite. An accurate account of the contact force and indentation is necessary to quantify the impact damage.

Direct measurement of the dynamic contact force is not an easy task due to the wide range of impact velocities and other parameters, and limitations of experimental techniques. The most famous elastic contact law, $F = k \alpha^{3/2}$, was derived by Hertz for the contact of two spheres of elastic isotropic materials based upon theory of elasticity. The contact between a sphere and a half-space is a limiting case, since this contact law is derived based upon the contact of elastic spheres. One faces several uncertainties when applying it to laminated composites: First of all, most laminated composites in use cannot be adequately represented by a half space. Second, the anisotropic and nonhomogenous property of laminated composites may alter the form of the law and finally, the strain rate which is not accounted for by the Hertzian law may have significant effects on the $F - \alpha$ relation.

Except for the strain rate effect, the first two uncertainties may be cleared by analyzing the exact contact problem of a sphere pressed into a laminated composite by using a three-dimensional elasticity.

3.1.1 Hertzian Law of Contact

When two solid bodies are in contact, deformation takes place in the contact zone and the contact force results. Once the contact force is obtained, conventional methods for stress analysis can be used to find the stress distribution in the bodies. Determination of the contact force-indentation relationship often becomes the most important step in analyzing the contact problem.

A special case of the Hertz contact problem is the contact of an elastic sphere and an elastic half space. The contact occurs in a circular zone with a radius of a in which the normal pressure p is;

$$p = p_0 \left[1 - \left(\frac{r}{a} \right)^2 \right]^{\frac{1}{2}} \quad (3.1)$$

where p_0 is the maximum contact pressure at the center of the contact zone, r is the radial position of an arbitrary point in the contact zone. Figure 3.1 represents two bodies of revolution for Hertzian analysis of contact.

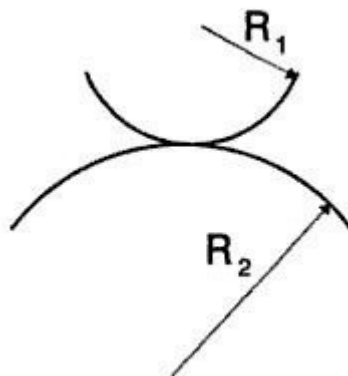


Figure 3.1 Two bodies of revolution for Hertzian analysis of contact

$$\frac{1}{R} = \frac{1}{R_1} + \frac{1}{R_2} \quad (3.2)$$

$$\frac{1}{E} = \frac{1-\nu_1^2}{E_1} + \frac{1-\nu_2^2}{E_2} \quad (3.3)$$

where R_1 and R_2 are the radii of two bodies. E is the Young modulus, and ν is the Poisson's ratio. The notation 1 represents the indenter, 2 represents the specimen properties.

$$a = \sqrt[3]{3 \frac{PR}{4E}} \quad (3.4)$$

$$\alpha = \frac{a^3}{R} = \sqrt[3]{\frac{9P^2}{16RE^2}} \quad (3.5)$$

$$p_0 = \frac{3P}{2\pi a^2} = \sqrt[3]{\frac{6PE^2}{\pi^3 R^2}} \quad (3.6)$$

$$P = k\alpha^{3/2} \quad (3.7)$$

where P is the contact force, k is the contact stiffness and α is the indentation. Equation (3.7) is referred as Hertz Contact Law and it can be applied to the laminated composites, although laminated composites are not homogenous and isotropic.

$$k = \frac{4}{3} E \sqrt{R} \quad (3.8)$$

3.1.2 Indentation Law

In the case of impact of a hard projectile, damage is expected to occur in the impact zone where direct contact of the projectile and the composite takes place. Thus, it is very important to estimate accurately the contact force and its history. A general dynamic contact law for a projectile of arbitrary shape striking the flat

surface of a laminated composite is not available. The classical Hertzian Contact Law for an elastic sphere pressed into an elastic isotropic half space has been given before as;

$$F = k\alpha^{2/3} \quad (3.9)$$

where F is the contact force (or it can be written as P), α is the indentation depth, and

$$k = \frac{4}{3} \frac{R_s^{1/2}}{\left(\frac{1-\nu_s^2}{E_s} + \frac{1-\nu_h^2}{E_h} \right)} \quad (3.10)$$

is the rigidity associated with the deformation. In Equation (3.10), R_s is the radius of the sphere; ν_s, E_s and ν_h, E_h are the Poisson's ratios and the Young's moduli of the sphere and the half space, respectively. The Hertzian law which was based on linear elasticity has been used widely for studying impact of elastic bodies. Equation (3.9) was found to be valid by Willis for a rigid sphere pressed on a transversely isotropic half space. In this work, the general expression of Equation (3.9) is adopted with

$$k = \frac{4}{3} \frac{R_s^{1/2}}{\left(\frac{1-\nu_s^2}{E_s} + \frac{1}{E_T} \right)} \quad (3.11)$$

where E_T is the transverse Young's modulus of fiber composites.

3.1.3 Finite Element Formulation

When subjected to impact of a mass, the beam receives an impulsive force which is the contact force between the mass and the beam. Calculation of the contact force depends on knowledge of the local deformation at the contact region. The local deformation represented by α is, in turn, affected by deflections of the beam. The interaction can be expressed by;

$$\alpha = w - v(x_0) \quad (3.12)$$

where w is the displacement of the projectile measured from the position of initial contact, and $v(x_0)$ is the displacement of the beam at the point of contact $x = x_0$. Once α is obtained, the contact force is obtained according to the Hertzian contact law. Thus, the first step toward solving the impact problem is to determine the histories of motion of both the projectile and the beam. The finite element method is used to accomplish this end.

The laminated composite is modeled by higher order beam finite elements derived based on the Bernoulli-Euler beam theory. Assuming that lamination is symmetric with respect to the midplane, the bending-extension coupling effect is eliminated. Thus, a transverse impact induces only flexural deformations. The displacement function for the transverse deflection of the beam element is taken as;

$$v = a_0 + a_1x + a_2x^2 + a_3x^3 + a_4x^4 + a_5x^5 \quad (3.13)$$

with this displacement function, there are three degrees of freedom at each node, namely, the transverse displacement v_i , the rotation θ_i , and the curvature K_i . The displacement function can also be expressed in terms of the six generalized nodal displacements. The element stiffness matrix and mass matrix are derived in the usual manner. The element equations of motion are expressed in the form;

$$\begin{Bmatrix} Q_1 \\ m_1 \\ \mu_1 \\ Q_2 \\ m_2 \\ \mu_2 \end{Bmatrix} = \frac{D}{70L^3} \begin{bmatrix} 1200 & 600L^2 & 30L^2 & -1200 & 600L & -30L^2 \\ - & 384L^2 & 22L^3 & -600L & 216L^2 & -8L^3 \\ - & - & 6L^4 & -30L^2 & 8L^3 & L^4 \\ - & - & - & 1200 & -600L & 30L^2 \\ - & - & - & - & 384L^2 & -22L^3 \\ - & sym & - & - & - & 6L^4 \end{bmatrix} \begin{Bmatrix} v_1 \\ \theta_1 \\ K_1 \\ v_2 \\ \theta_2 \\ K_2 \end{Bmatrix}$$

$$+ \frac{\rho AL}{55440} \begin{bmatrix} 21720 & 3732L & 281L^2 & 6000 & -1812L & 181L^2 \\ - & 832L^2 & 69L^3 & 1812L & -532L^2 & 52L^3 \\ - & - & 6L^4 & 181L^2 & -52L^3 & 5L^4 \\ - & - & - & 21720 & -3732L & 281L^2 \\ - & - & - & - & 832L^2 & -69L^3 \\ - & sym & - & - & - & 6L^4 \end{bmatrix} \begin{Bmatrix} \ddot{v}_1 \\ \ddot{\theta}_1 \\ \ddot{K}_1 \\ \ddot{v}_2 \\ \ddot{\theta}_2 \\ \ddot{K}_2 \end{Bmatrix}$$

where;

D = beam bending rigidity,

L = length of element,

ρ = mass density,

A = cross-sectional area,

a dot = time derivative, and Q_1 , m_1 , and μ_1 are the element generalized forces corresponding to the degrees of freedom v_1 , θ_1 , and K_1 respectively. The assembled equations of motion for the whole system can be symbolically written as;

$$\{P\} = [K]\{\Delta\} + [M]\{\ddot{\Delta}\} \quad (3.14)$$

where;

$\{P\}$ = external loads

$\{\Delta\}$ = nodal displacements, and

$[K]$ and $[M]$ = assembled stiffness matrix and mass matrix, respectively.

Integration of the equations of motion is performed numerically by employing a finite difference form proposed by Wilson and Clough. The nodal displacements, velocities, and accelerations at time $t + \Delta t$ are expressed as;

$$\{\Delta\}_{t+\Delta t} = \{\Delta\}_t + \Delta t\{\dot{\Delta}\}_t + \frac{\Delta t^2}{3}\{\ddot{\Delta}\}_t + \frac{\Delta t^2}{6}\{\ddot{\Delta}\}_{t+\Delta t} \quad (3.15)$$

$$\{\dot{\Delta}\}_{t+\Delta t} = \{\dot{\Delta}\}_t + \frac{\Delta t}{2}\{\ddot{\Delta}\}_t + \frac{\Delta t}{2}\{\ddot{\Delta}\}_{t+\Delta t} \quad (3.16)$$

$$[H]\{\ddot{\Delta}\}_{t+\Delta t} = \{P\}_{t+\Delta t} - [K]\{b\}_t \quad (3.17)$$

where;

$$[H] = [M] + \frac{\Delta t^2}{6}[K] \quad (3.18)$$

$$\{b\}_t = \{\Delta\}_t + \Delta t\{\dot{\Delta}\}_t + \frac{\Delta t^2}{3}\{\ddot{\Delta}\}_t \quad (3.19)$$

It should be noted that, in the present application, the external loads $\{P\}$ consists of only the contact force that exists at the point of impact $x = x_0$. The contact force depends on the motion of the projectile governed by the equation of motion.

$$m_s \ddot{w} = -k[w - v(x_0)]^{1/2} \quad (3.20)$$

where m_s is the mass of the sphere. From Equation (3.20) it is clear that motions of the beam and the projectile are coupled nonlinearly. To incorporate Equation (3.20) in the finite difference equations, Equations (3.15), (3.16), and (3.17), we assume that at time $t + \Delta t$

$$w_{t+\Delta t} = w_t + \Delta t \dot{w}_t + \frac{1}{2} \Delta t^2 \ddot{w}_t \quad (3.21)$$

$$v_{t+\Delta t}(x_0) = v_t(x_0) + \Delta t \dot{v}_t(x_0) + \frac{1}{2} \Delta t^2 \ddot{v}_t(x_0) \quad (3.22)$$

from Equation (3.20), we obtain

$$m_s \ddot{w}_{t+\Delta t} = -k[w_{t+\Delta t} - v_{t+\Delta t}(x_0)]^{1/2} \quad (3.23)$$

and the contact force at $t + \Delta t$ is given by

$$F_{t+\Delta t} = -m_s \ddot{w}_{t+\Delta t} \quad (3.24)$$

By using the above expression for the contact force in the finite element program, response of the beam can be computed step by step. This procedure has been used with success to study impact responses of beams of homogenous and isotropic materials.

3.2 Low Velocity Impact Damage

The response of materials and structures to impulsive loading is complex. Practical impact problems often involve impactors and targets whose behavior is influenced by their finite boundaries. As the intensity of impact energy increases, the material is driven from the elastic into the plastic stage. This process involves large deformations, exothermal processing, and fractures, resulting in target failure through a variety of mechanisms. The impact response composites depend on various combinations of materials, lay-ups, and fabrication processes, including the properties of the impactor.

It is essential to understand the effect of impact by foreign objects on structural strength when using composites for heavily loaded primary structural components, such as wings and fuselage. Aircraft structures damaged by large impact energy can also experience significant changes in stiffness at the component level. Within a wing, for example, severe skin damage, such as panel detachment or rupture, can reduce the torsional stiffness below the flutter requirements of the operating envelope. In this section we will identify the nature of the low velocity impact damage and describe possible courses in controlling damage growth in composites.

3.2.1 The Nature of Low Velocity Impact Damage

We will concentrate on low velocity impact which may cause significant damage by delamination in the middle region of a thin plate or it may cause tensile matrix and fiber failure on the back face, both of which are invisible to the outside observer. Barely visible impact damage (BVID) is a hidden menace.

Firstly it is necessary to define “low velocity”. If the incident velocity is high enough (ballistic or rotor blade damage) then high energy stress waves are set up through the thickness of the structure, sufficient energy may mean complete penetration, and the structural response will be very local and uninfluenced by the nature of the surrounding structure. Crudely it can be shown that these stress waves

give rise to a strain of order V/C , where V is the impactor velocity and C is the speed of sound through the plate thickness – governed primarily by the density and modulus of the resin matrix. Local failure will occur if these strains are of order (say) 1%. Now for epoxy resins C is of order 2000 m/sec which gives the threshold for V as 20m/sec. This is not commonly thought of as low, but experiments have shown a transition from low velocity behavior, when the thin plate has time to respond away from the impact site, when the velocity increases from roughly 20 to 60 m/sec. Accidents like tools dropped from heights up to 4m correspond to impact velocities up to 9 m/sec. It is these that form the scope of discussion.

Figure 3.2 shows three zones of damage developing as the plate deforms under impact. The bending strains cause (1) tensile failure on the back face in which matrix cracks occur first (and then precipitate local delamination where the cracks meet an interface) and (2) delamination in the interior where the shear strains are maximum and finally (3) compressive strains on the impacted surface. There may also be point (Hertzian) damage which is very local and does not debilitate the structure much, although up to 10% of the energy may be absorbed in this mode if the impact force is high. As far as the compression after impact strength is concerned, the internal delamination is the main threat, since the separated laminae may buckle locally and this local blister can then propagate.

. The distribution of these shear-driven delamination can be complex, consisting of a series of overlapping oblongs or “peanuts” aligned in the direction of the fibers on the lower surface. Figure 3.3 shows an X-ray which reveals these multi-level delamination. However, for this particular laminate with a quasi-isotropic stacking sequence $(+45, -45, 0, 90)_{4s}$, the envelope of the delamination is circular as revealed in the C-scan shown.

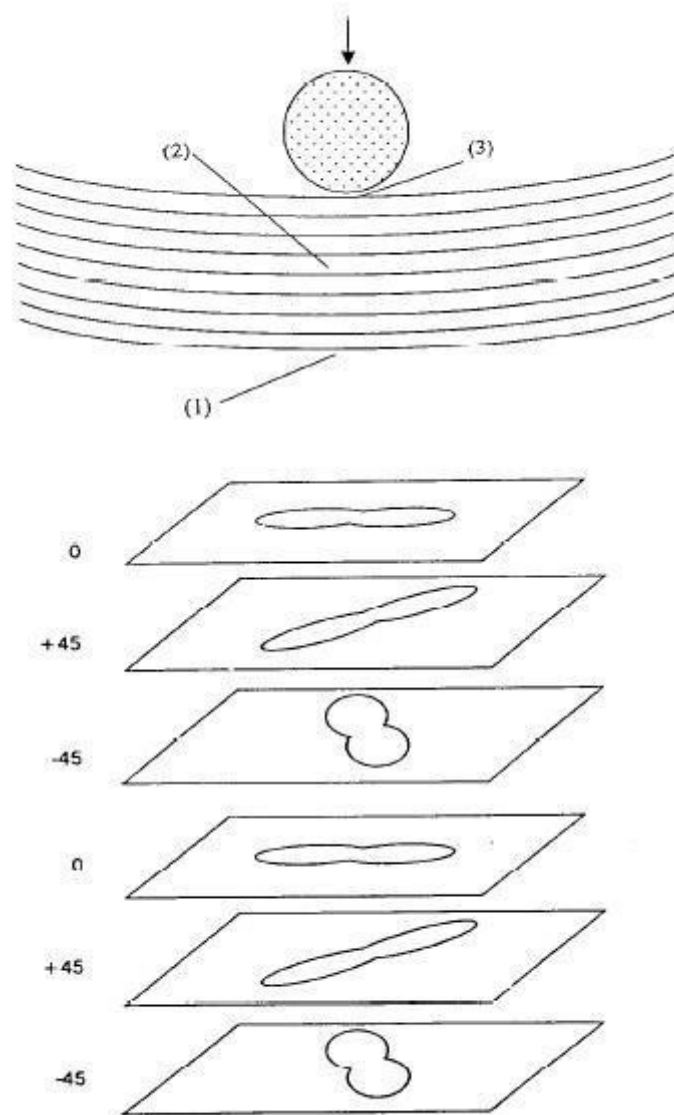


Figure 3.2 Low velocity impact damage zones

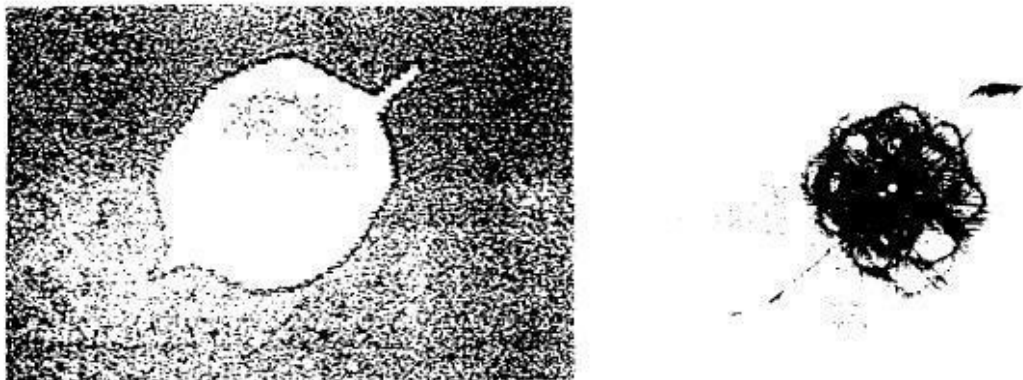


Figure 3.3 Internal delamination in the form of overlapping peanut shapes

Also can be seen the elongated delamination in the +45° direction, caused by tensile matrix cracking on the back face lamina. If we use the area enclosed by the envelope as a measure of the damage, we can construct a map of impact damage with incident energy.

3.2.2 Prediction of Damage Threshold

Having shown that the damage depends primarily on the maximum impact force it is now tempting to try and predict what clearly a threshold force is, below which no damage occurs at all. One route is to model the laminated plate using a very fine finite element mesh and then solve the equations of motion to reconstruct the damage evolution during the impact event. If no approximations are to be made this means using finite elements as one brick element per lamina, so that if we say the plate is 6 mm thick (48 ply) and the damage zone is 20 mm x 20 mm (which is not large) we then need $48 \times (20 : 1/8)^2 = 1.3\text{M}$ elements. Although not difficult to set up this model, this is a very expensive simulation, and more importantly it will be extremely difficult to understand the answers and the underlying physics, possibly more difficult than interpreting experimental results.

Suppose we attempt to use the interlaminar shear strength as a failure criteria, then the mean shear stress is a simple function of force and radius (stress = $P/2\pi r t$) and hence the area πr^2 , varies continuously with P. We therefore resorted to fracture mechanics which are capable of explaining sudden unstable propagation, and we are able to show that there is indeed a critical threshold force P_{crit} at which delamination will occur, and that this is independent of radius of the delamination circle.

$$P_{crit}^2 = \frac{8\pi^2 E t^3 G_{IIc}}{9(1-\nu^2)} \quad (3.25)$$

Notice that this force is a function of the plate stiffness (Et^3) and the mode II fracture toughness G_{IIc} , explaining why thermoplastics are less susceptible to

damage since the fracture toughness may be two or three times that of a thermoset. Equation is based on the highly simplifying assumption that the damage and the structural strains are axisymmetrical which is approximately true for a quasi-isotropic lay-up. Thus if we wish to avoid delamination completely it is only necessary to find the maximum impact force and then use equation. If we need only the force, and not a detailed history of the interior strain field, it is tempting to model the system as one degree of freedom - an impactor mass and a structural spring. This should be a reasonable model if the mass is heavier than the responding structure (which is likely) so that the structures inertia forces can be ignored. The structure should then respond in a fundamental mode and simple harmonic motion ensures that the maximum force is readily evaluated. The computing effort would be negligible since a simple static solution would give the required equivalent spring stiffness. This approach has naturally been tried by many investigators. Unfortunately there are two reason why this may not work. Firstly the response of a real structure with discontinuities in stiffness may not be a single fundamental mode, and a mixture of harmonics may respond with no guarantee that the force history is sinusoidal with a clear maximum. The other error source lies in ignoring the coupling between the bending strains and the shear driven force response. If the plate is flexible enough, and if the incident energy is sufficiently high, then the bending strains may exceed the fiber allowable strengths and failure will then decrease the flexural rigidity locally and hence attenuate the force.

To model this we presently need to use a finite element code, but there is no need to deploy an expensive model. Simple composite shell elements are used to assume the strain distribution through the shell thicknesses, as usual, linear, but each lamina at every level is monitored during the impact event, and if a conventional strain criteria is exceeded this element layer is deleted. The result is a quite gradual decrease in stiffness which has been shown to give force histories agreeing very well with many tests, sizes, and materials. Figure 3.4 shows the results of two such drop tests on the Boeing test specimens with (a) modest and (b) large incident energies. The C scans show a conventional shear-driven circular enveloped for (a) but for (b) there is much delamination in the 45° direction under the laminate near the tensile

back surface, which is a consequence of the massive matrix cracking in this region. The deflection in both cases exceeded the plate thickness of 1 mm and hence the code needed non-linear stiffness updates, but it also had the laminate strength failure routine here referred to as “degraded” capability. The need for this is clear in Figure (3.4) where the elastic undamaged prediction of 2400N is twice that of the true value of 1200N. It does look therefore that some FE modeling is unavoidable even if we wish only to find the force history and the threshold for delamination.

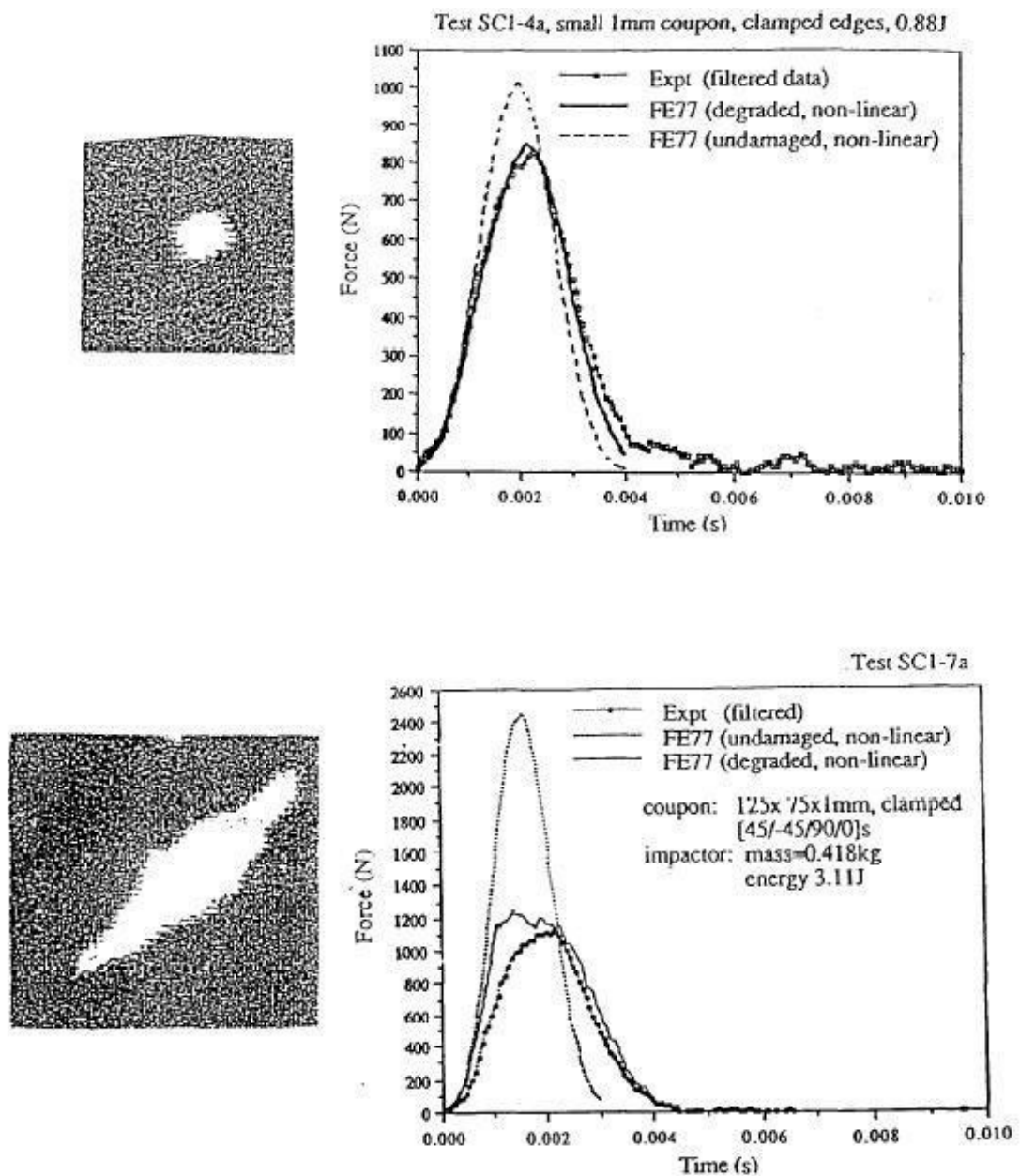


Figure 3.4 FE force predictions with and without extensive flexural damage

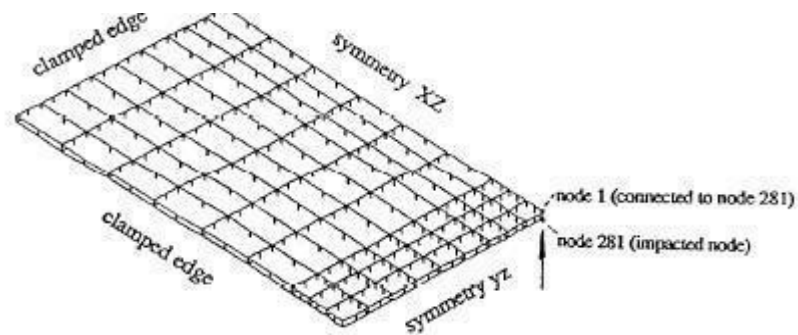
3.2.3 Prediction of Damage Extent

A thin-walled composite structure will still have residual compressive strength even when damaged, and there is an incentive to predict the extent of this delamination. At the moment there does seem to be no alternative to using a non-linear dynamic finite element code to predict delamination, and also flexural degradation. This is nowadays accepted in crashworthiness studies on metal aircraft and automobiles, and DYNA 3-D (to name one) has become common usage in car and aero-engine impact studies.

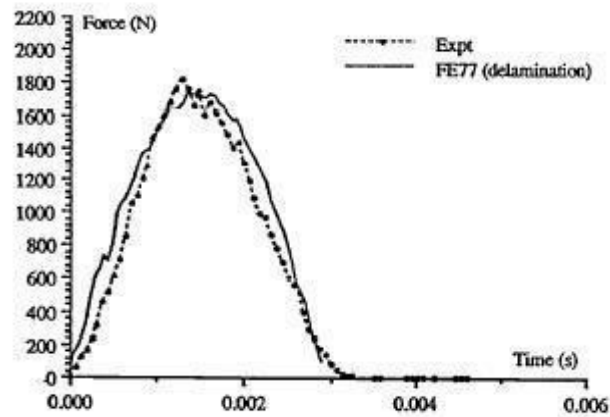
The problem in laminated composites has been noted as the complex nature of the impact-induced delamination. It will undoubtedly become routine as computing power becomes remorsefully cheaper and more accessible, and the commercial codes become more user-friendly in displaying damage and using it as an input to a residual CAI strength predictor.

In the meantime we have assessed the accuracy of using a simpler description of damage. Thus a delamination level was assumed and just two layers of shell elements arranged each side of it, with fictitious links joining the element node points, and which could be broken as the equivalent forces reach a value derived from the interlaminar shear strength or the peeling strength. This should predict the initiation of delamination but we need fracture (energy release rate) criteria to propagate. The results were encouraging as Figure 3.5 indicates. A more ambitious study was the damage threshold for impact over a stiffener in a top-hat stiffened compression panel. This is much more complex and not amenable to the simple analysis used for plate impact. Here the structure is locally very much stiffer than a single plate thickness and hence a much higher impact force is generated for a given energy. However a structure is better able to resist such a force since it will locally behave like a stiff beam many times stiffer than the thin plate, hence we may expect higher threshold energy, in this case. However, the shear stress rises to a peak and is then constant along the stiffener all the way to the nearest support, there being virtually no diffusion to the surrounding panel. This is potentially very dangerous as

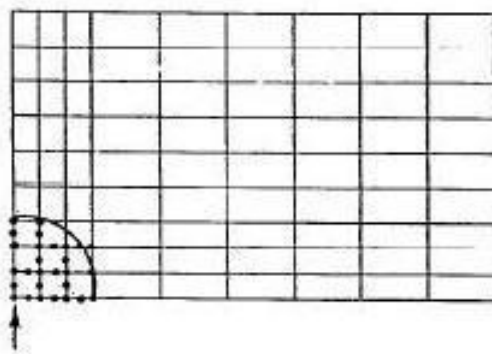
complete separation of a stiffener can reduce the buckling load of the stiffened panel by 75%.



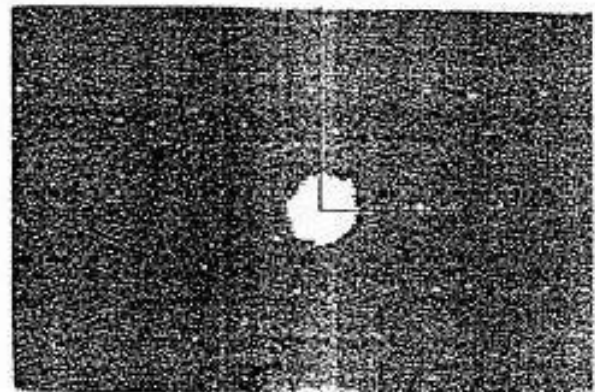
FE model of one quarter plate for delamination simulation.



Comparison of predicted and measured force histories.



predicted delamination area = 160 mm².



C-scan detected damage area = 140 mm².

Figure 3.5 Predictions of delamination size using just one array of breakable links

3.3 Impact Tests

Low velocity impact events are expected to occur during the manufacturing and service life of composite parts and structures. Foreign body impact can occur during manufacturing, routine maintenance or use of a laminated composite part. This has led to an abundance of research on low velocity impact damage to laminated composite plates. Typically, laminated plates are impacted by a “drop weight” method. This method usually consists of an instrumented striker that is secured to a carriage that falls along guideposts and collides with the plate. After an impact event has been performed, ultrasonic C-scans, X-radiography, and cross sectional photo microscopy are some of the common techniques used to document the damage area.

3.3.1 Importance of Impact Tests

Impact resistance is one of the most important properties for a part designer to consider, and without question, the most difficult to quantify. The impact resistance of a part is, in many applications, a critical measure of service life. More importantly these days, it involves the perplexing problem of product safety and liability.

One must determine;

- The impact energies the part can be expected to see in its lifetime.
- The type of impact that will deliver that energy, and then
- Choose the right components for material that will resist such assaults over the projected life span.

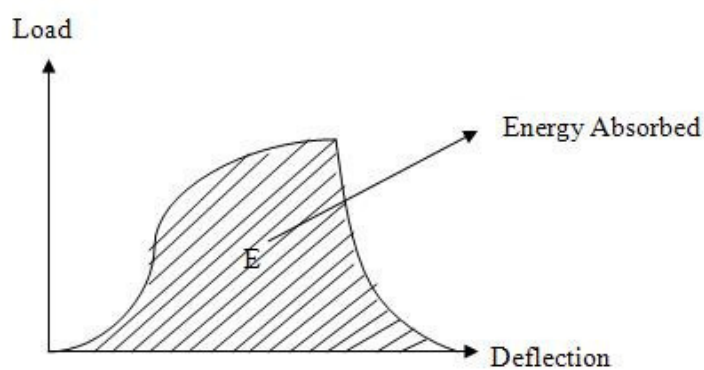


Figure 3.6 Relationship between impact energy and absorbed energy

Impact energy;

Impact energy = Potential energy + Kinetic energy

Absorbed energy;

A measure of material strength and ductility and also graphically the area beneath the load displacement curve.

Molded in-stresses, polymer orientation, weak spots and part geometry will affect impact performance. Most real world impacts are biaxial rather than unidirectional. Further complication is offered by the choice of failure modes: ductile or brittle. Brittle materials take little energy to start a crack, little more to propagate it to a shattering climax. Other materials possess ductility to varying degrees. Highly ductile materials fail by puncture in drop weight testing and require a high energy load to initiate and propagate the crack. Many materials are capable of either ductile or brittle failure, depending upon the type of test and rate and temperature conditions. They possess a ductile brittle transition that actually shifts according to these variables.

Instrumented drop weight impact testing has been used to study the impact performance of fiber reinforced polymer composites in many studies. Deformation processes and fracture mechanisms of thin-plate composite laminates are results of material parameters, plate thickness, stacking sequence, and impact loading rate. And it is clear that for the laminates containing tough fibers, such as high-strength polyethylene, plastic deformation is an important energy absorbing mechanism. High flexibility of these fibers allows the incident energy to be dispersed in a wider area and the impact load to be shared by a greater volume of material. A clean penetration crack can be observed in the samples that contain primarily brittle fibers, such as graphite.

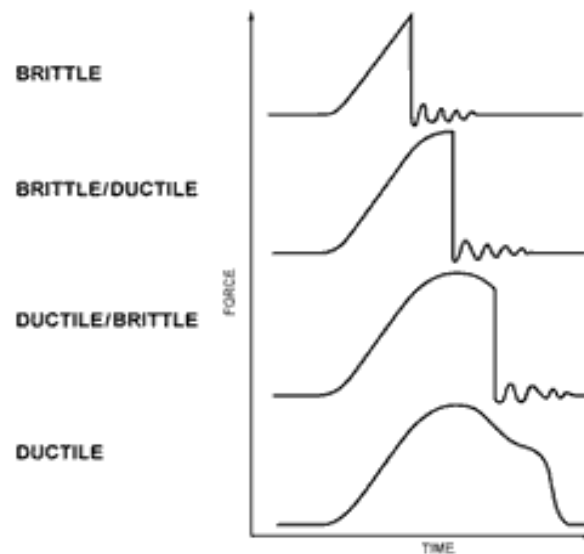


Figure 3.7 Material behaviors regarding to failure modes: ductile or brittle.

3.3.2 Applicability of Impact Tests

The ideal impact test would be one in which all the energy of a blow is transmitted to the test specimen. Actually this ideal is never realized; some energy is always lost through friction, through deformation of the supports and of the striking mass, and through vibration of various parts of the testing machine. In some test, it is impossible to obtain a truly accurate measure of the energy measured by a specimen. Further, the particular values obtained from an impact test depend very much upon the form of specimen used. These facts require close attention to standardization of details in any given type of test if concordant results are to be obtained, and usually preclude direct comparisons of results from various different types of impact tests. Each type of impact test has its own specialized field of use, and its applicability depends largely upon satisfactory correlation with performance under service conditions. In this connection, it may be also observed that the applicability of a test may not necessarily be confined to materials for use in parts that are to be subject to impact. In making an impact test, the load may be applied in flexure, tension compression, or torsion. Flexural loading is the most common; tensile loading is less common; compressive and torsional loadings are used only in special instances.

Table 3.1 Classification and summary of impact tests

Means Of Applying Blow	Type Of Loading	Single Blow Tests		
		Machine	Maximum Capacity(joule)	Maximum Striking Velocity (m/s)
Dropping Weight	Flexure	Hatt-Turner	4340	6.4
		Fremont	600	8.8
	Tension	Olsen Guillotine Calif. I. Tech.	4746	6.4 ...
	Compression	Olsen Calif. I. Tech.	4746	6.4 ...
Swinging Pendulum	Flexure	Charpy	3-325	3.35-5.5
		Izod	3-350	3.35-5.5
		Russell	680	3.35
Oxford		
	Tension	Modified Charpy or Izod	340	3.35-5.5
	Shear	Mc Adam	540	5
Rotating Flywheel	Flexure	Guillery	583	8.8
	Tension	Mann-Haskell Calif. I. Tech.	305
		Torsion	Carpenter	>187

The impact blow may be delivered through the use of a dropping weight, a swinging pendulum, or a rotating flywheel. Some tests are made so as to rupture the piece by a single blow; others employ repeated blows. In some tests of the latter type, the repeated blow is of constant magnitude; in others, the “increment-drop” tests, the height of drop of the weight is increased gradually until rupture is induced. In Table 3.1 several of the various impact tests are grouped in accordance with these classifications.

Nowadays, another type of test is being used by most investigators, although many details of the actual test apparatus may differ. Experimental studies attempt to

replicate actual situations under controlled conditions. For example, during aircraft take off and landing, debris flying from the runway can cause damage; this situation, with small high-velocity projectiles, is best simulated using a gas gun. On the other hand impact of a composite structure by a larger projectile with low velocity is representing the tools which are accidentally dropped on a structure. This situation is best simulated using a drop weight tester.

CHAPTER FOUR

EXPERIMENTAL AND NUMERICAL RESULTS

4.1 Specimen Properties

Composite laminates which has been impacted in this experiment were manufactured by Izoreel Firm in Izmir. Our laminated composites consists of glass fiber and epoxy resin. Unidirectional glass fiber weights 250 g/m^2 . Mass ratios of Epoxy CY225 and hardener HY225 is 10/8. Number of plies and the fiber orientations is chosen to be $[0/0/90/90/0/0/90/90]_s$. In other words, 16 plies laminate is designed symmetrically as defined orientation.

Except dimensions (width, length), there are no differences between the specimens. All the properties like; orientations, number of plies or thickness are same. All tests were performed at 20 C° and at 1 bar air pressure. The mechanical properties of the specimens can be listed as follows;

Table 4.1 Mechanical properties of the specimen

Mechanical Property	Value		
Longitudinal Young's Modulus	38	GPa	Exx
Transverse Young's Modulus	16	GPa	Eyy
Poisson's Ratio (x-y direction)	0.25		Vxy
Poisson's Ratio (y-z direction)	0.25		Vyz
Shear Modulus (x-y direction)	5.5	GPa	Gxy
Ply Thickness	0.23	mm	H
Density	1736	kg/m^3	RHO
Critical Indentation	1.02×10^{-4}		ACR
Longitudinal Tensile Strength	900	MPa	LT
Longitudinal Compressive Strength	275	MPa	LC
Transverse Tensile Strength	80	MPa	TT
Transverse Compressive Strength	153	MPa	TC
Interlaminar Shear Strength	75	MPa	IS

4.2 Test Description

The conditions for this drop test were defined as an impact onto laminated composites. Basic properties of laminated composites were defined as above. In this test laminated composites will be fixed to impact test machine by three different types of plate holders. Dimensional properties of the laminates and plate holders can be summarized as in Table 4.2.

Table 4.2 Dimensional properties of laminates and plate holders

Laminated Composites	Dimensions (Impacted Area)	Plate Holders
L.C. 1	Square with 76 mm per edge	Figure 4.2
L.C. 2	Square with 150 mm per edge	Figure 4.3
L.C. 3	Circle with 76 mm of diameter	Figure 4.4

All the experimental tests will be done with falling weight technique. Fractovis Plus is the impact testing machine for all experiments. Description of the impact testing machine is written below in Table 4.3.

In the falling weight drop test, the test specimens are usually supported with plate holders. Figure 4.1 (D) and an impactor Figure 4.1 (B) or strike (of known mass) is allowed to fall from a known height to strike the specimen. The energy absorbed may be deduced from the initial potential energy of the striker, taking into account any rebound of the striker or, may be deduced from the kinetic energy of the striker just prior to impact. Displacement gauges are often used to measure the velocity of the striker just prior to impact. Again, the striker is often instrumented to allow the force-time record of the impact event to be captured. This is the most popular impact test for composites and has the advantage that realistic specimen geometries can be tested. Also, the design of the striker can accurately simulate the geometry of any anticipated in service impact. A disadvantage of the test however, is that when penetration occurs, considerable energy is consumed by friction. Increasingly, hydraulic and pneumatic test machines are being used to perform impact tests. Also, that is why we are using Fractovis Plus in our tests. Figure 4.1



Figure 4.1 Fractovis Plus low velocity impact test machine

The steel impactor rod has a diameter of 12.7 mm and has a mass of 4.926 g. A piezoelectric head striker which is used in experiments is characterized by higher robustness so it is more suitable for testing hard materials like advanced composites.

Table 4.3 Fractovis Plus impact test machine and its equipments

Fractovis Plus Impact Test Machine	Equipments
A	Body of the impact tester
B1	Impactor nose
B2	Piezoelectric impactor nose
C	Data acquisition system (DAS)
D	Specimen holder mechanism
E	Springs

Knowing the weight of impactor, we can find the needed velocity to apply the previously determined energy and impactor can be set at a needed dropping height according to the law of conservation of energy. By the help of this information Table 4.4 is prepared. It shows the impactor velocity to apply the previously determined energy under constant impactor mass.

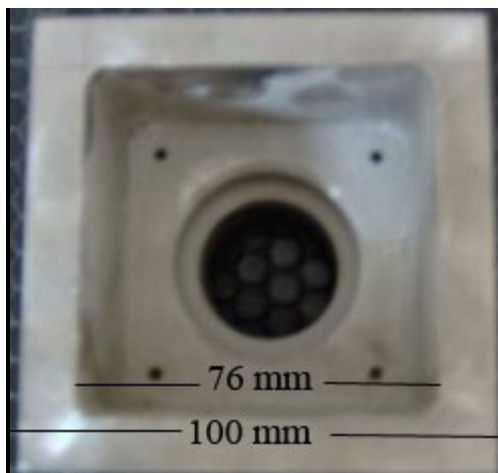


Figure 4.2 Plate holder for square with 76 mm per edge

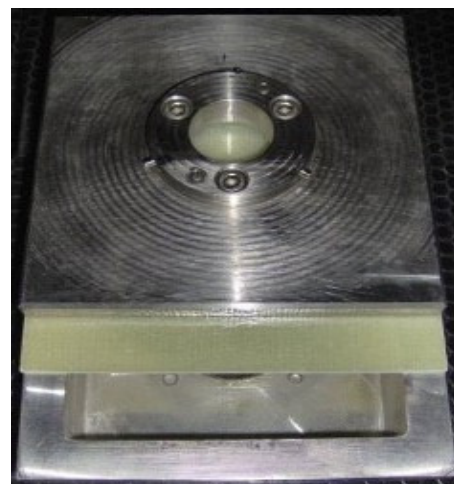
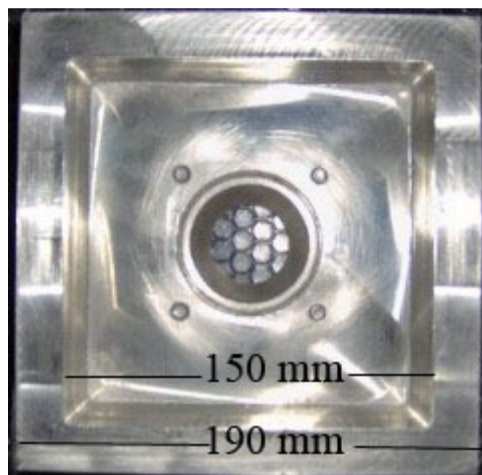


Figure 4.3 Plate holder for square with 150 mm per edge

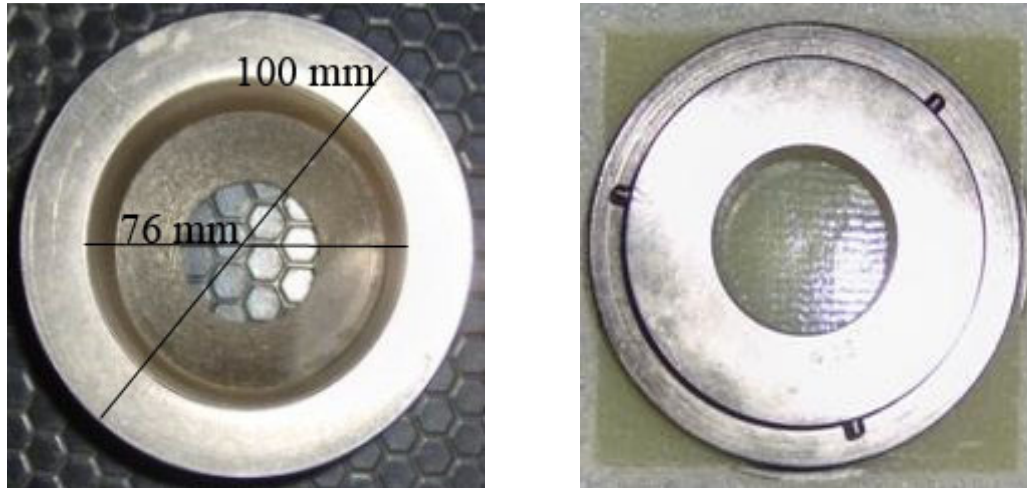


Figure 4.4 Plate holder for circle with a diameter 76 mm

As written before, we will use a 4.926 g of constant mass of impactor so; the bolded region will be evaluated during tests.

Table 4.4 Change of energy with impactor mass and velocity

	Mass of the impactor 4.926 kg													
Energy	10	20	30	40	50	60	65	70	75	78	80	85	90	100
Velocity	2,015	2,850	3,490	4,030	4,506	4,936	5,137	5,331	5,518	5,627	5,66	5,875	6,045	6,372

Data collected during the test will include maximum contact force, maximum deflection, contact duration, and energy absorbed. History of test data will be collected in DAS which is data acquisition system for Fractovis Plus. These data are collected to evaluate force-impact energy, absorbed energy-impact energy, and peak deformation-impact energy relations and to summarize them graphically.

4.3 Experimental Results

During the impact, the resistive force exerted by the sample on the striker is measured as a function of time and stored for subsequent display and analysis. That is the force transducer detected the contact forces at many consecutive instants and transient data were recorded for each sample tested, which include time, energy, velocity and deflection. The maximum contact force was termed peak force. The

system calculates the corresponding velocity history of the impactor by integrating the force history (after being divided by the mass of the impactor) and with the use of initial impact velocity. Similarly, the corresponding displacement history of the impactor was calculated from integrating the velocity history. Based on the force and displacement histories of the impactor, the energy history, which represented the history of energy transferred from the impactor to the composite, was calculated.

Before giving the graphs, we must understand more about the characteristics of the material being used. Physical modes of damage of the impacted composite include indentation, fiber breakage, surface cracking, delamination and perforation. Among these, perforation is the most apparent and severe. This implies that perforation is the most important mode of damage and the impact characteristics (such as peak force and absorbed energy) as a result, mechanical property degradation of composite laminates reach critical values when perforation takes place.

Penetration indicates the onset of perforation. During penetration, the impactor got stuck in the composite. Since rebound is negligible the impact energy was almost completely absorbed by the composite plate in different forms of damage. As the penetration preceded (the impactor moved deeper into the composite), it required more energy for the impactor to break through the composite and to overcome the friction between the impactor and the composite. Eventually, perforation of the composite would be achieved. Perforation causes the ultimate damage in composites subjected to impact loading. Once a composite is perforated, any excess impact energy would be retained as kinetic energy in the impactor except that an insignificant amount might be converted into additional damage. Hence, perforation threshold is an important parameter in characterizing the impact behavior of a composite structure. The perforation threshold indicates the completion of the perforation process.

The difference between the penetration and perforation thresholds, or the equal energy interval was believed to be dependent to the material type and the laminate

thickness. Although perforation is a significant damage stage, delamination plays an important role in the impact energy absorption and mechanical property degradation.

To explain the damage types, contact force, deflection, impact velocity and impact energy versus time graphs are given in Figure 4.5

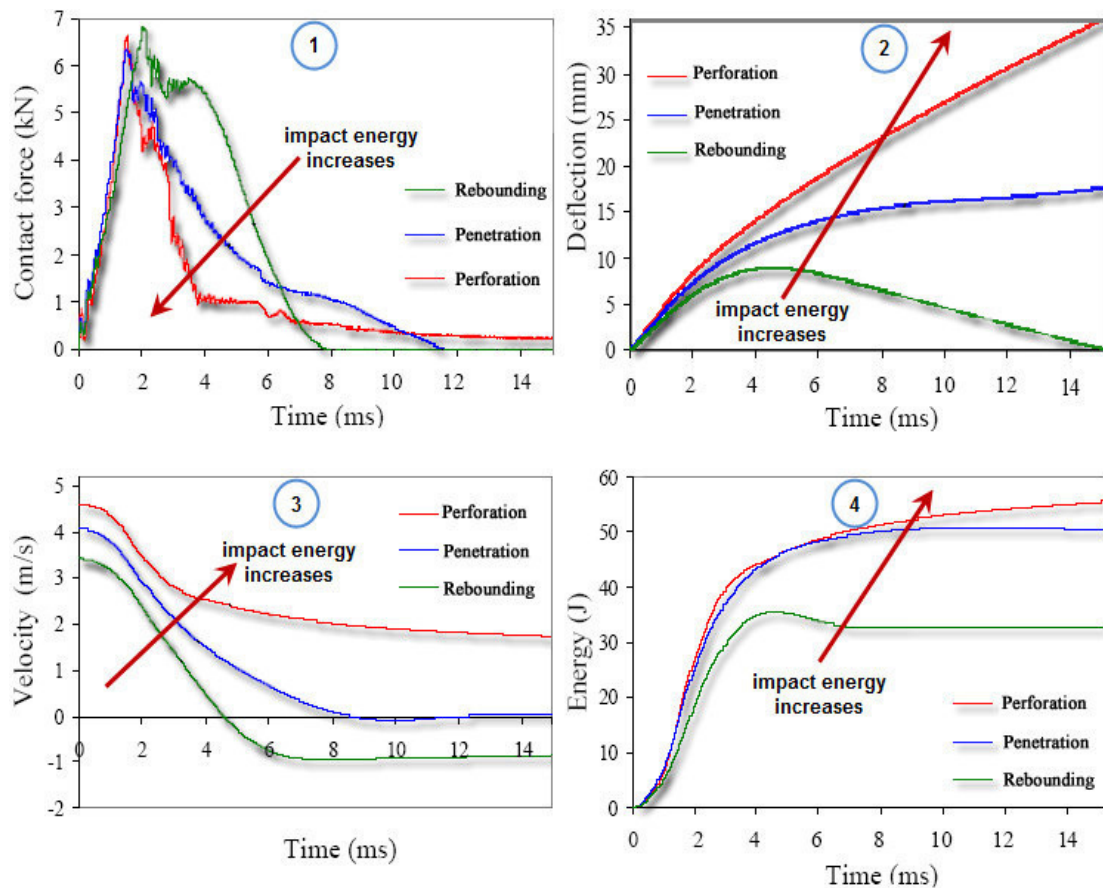


Figure 4.5 Main impact damage types (Aktaş,2007)

As we said, penetration indicates the onset of perforation. In Figure 4.5-1, we can see that lines for penetration and perforation may be similar with the increase of energy, because as the penetration precedes (the impactor moves deeper into the composite), it requires more energy for the impactor to break through the composite and to overcome the friction between the impactor and the composite. And as it moves deeper into the composite, the deflection will reach its maximum value like in Figure 4.5-2 It can be seen in Figure 4.5-3 that in rebounding condition velocity takes a negative value as the nature of rebounding and penetration results with a

velocity of zero because of friction. It's clear from the Figure 4.5-4 that rebounding occurs when the impact energy is greater than absorbed energy.

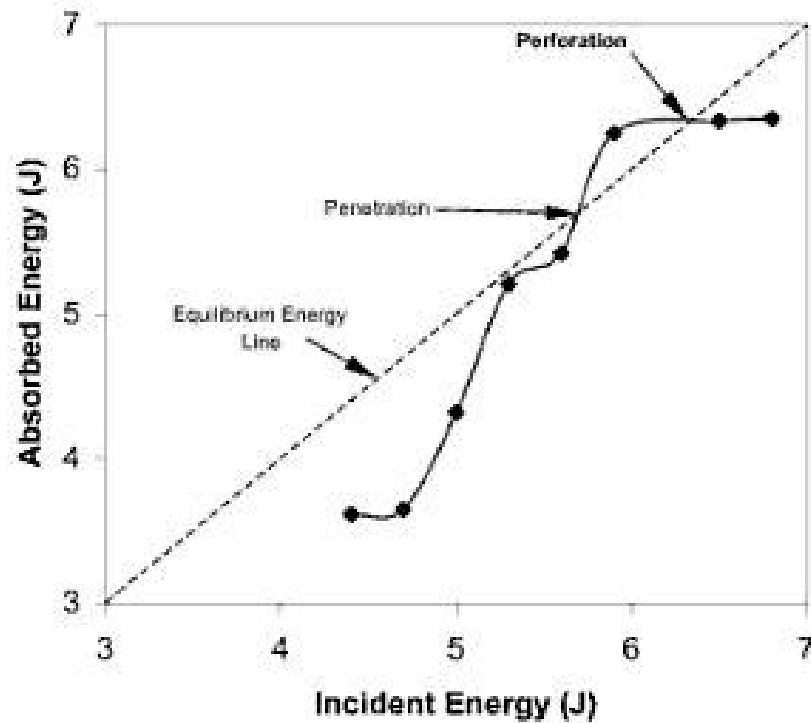


Figure 4.6 Complete energy profiles for a random specimen

To serve as a basis for us, this graph shows the situations in which penetration and perforation takes place. It also reveals that the absorbed energy increases with increase in the impact energy. It is suspected that the point above the equilibrium energy line indicating a greater value of energy absorbed compared to the impact energy, might be due to energy from some other source, such as vibration.

Experimental results will be given under three main titles. Titles will be named according to the specimens damaged impact zones; square with 76 mm per edge, circle with 76 mm diameter and square with 150 mm per edge. Before giving the titles, it is better to see absorbed energy-impact energy relations of these three titles in one graph so that we can compare them better and can comment on them easily.

It is clear from the Figure 4.7 that specimens with damage zones 76 mm circle and 76 mm square have similar response to the impact. Also we can say that for low energies both of the specimens act similar. It can be seen that for all specimens, the absorbed energy curves are congruent till 30J. Square specimens with 150 mm per edge as an impact zone, differs from the other two specimens in higher impact energy levels. Having a larger area, it resists better to impact and need more energy for penetration, but it absorbs lesser energy than other specimens.

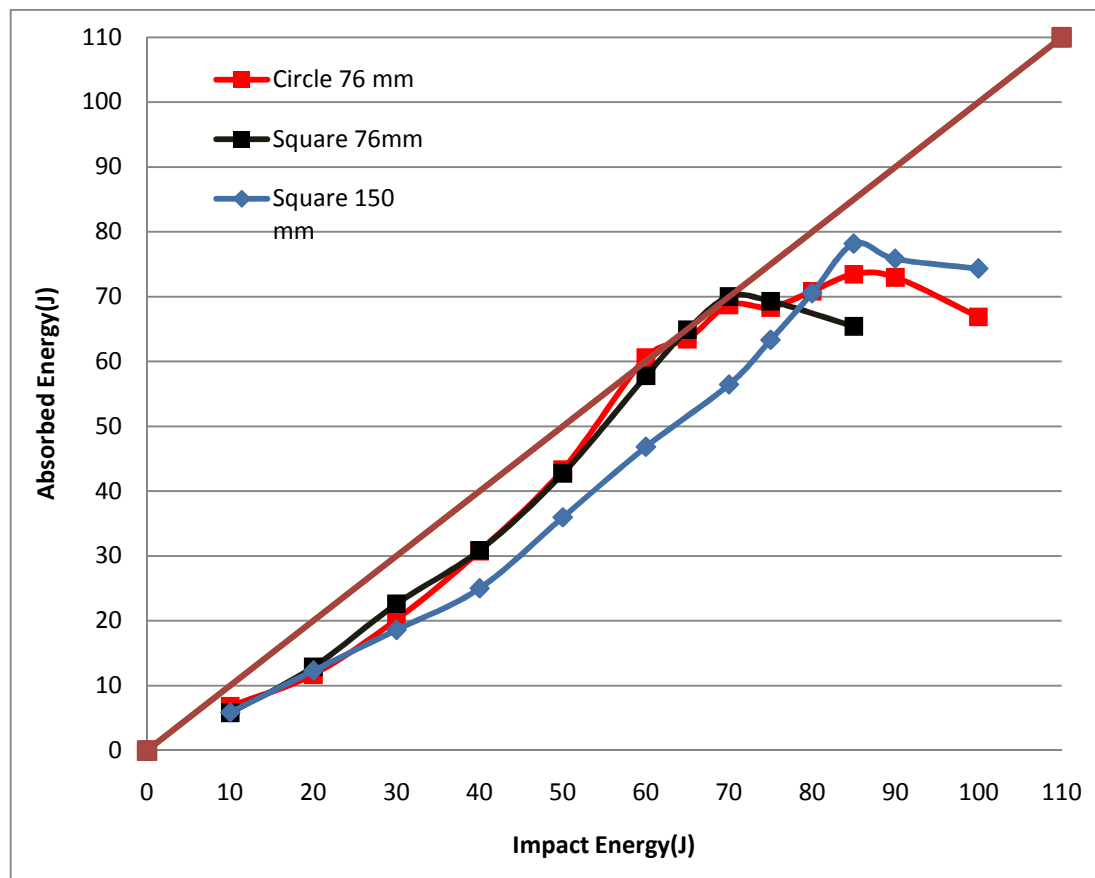


Figure 4.7 Absorbed energy-Impact energy histories for all three specimens

4.3.1 Square with 76 mm per Edge

In order to investigate impact resistance of the composite plates, 10 impact energy levels are determined from 10 J to 85 J. Energy levels are determined according to the response that we have investigated from the previous composite which we have impacted. Thus, some of the energy levels are repeated 3 times or more regarding to

the response that we examined. The values given in Table 4.5 are average values for the repeated tests.

Table 4.5 Test results for square with 76 mm per edge

Impactor Mass(Kg)	Impact Energy(J)	Max. Peak Force(N)	Max. Deflection(mm)	Contact Duration(ms)	Absorbed Energy(J)
4.926	10	3964	4.07	6.50	5.82
4.926	20	6045	6.07	6.57	12.91
4.926	30	6557	7.47	7.07	22.65
4.926	40	7679	8.65	7.01	30.89
4.926	50	7798	10.15	7.51	42.75
4.926	60	9447	11.26	8.59	57.79
4.926	65	7375	14.90	10.44	64.91
4.926	70	8787	15.58	9.66	70.02
4.926	75	8605	21.49	9.17	69.30
4.926	85	7824	22.41	5.00	65.42

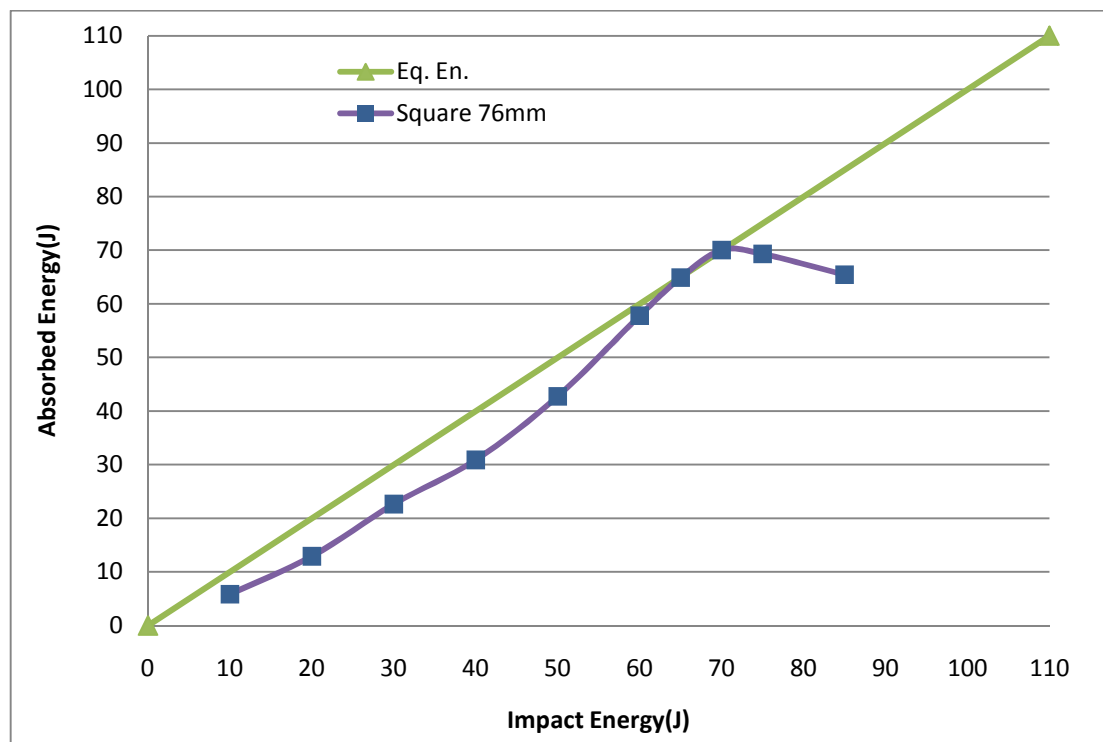


Figure 4.8 Absorbed energy-Impact energy history for square with 76 mm per edge

Ideally, when composites are used for resisting impact damage, the impact energy should be completely absorbed by the composite when perforation occurs. Thus, the perforation and penetration threshold of laminated composites can be identified on the equality between absorbed energy and impact energies.

It's seen that in Figure 4.8 first point of equality between absorbed energy and impact energy is at 65 J, here we can say 65J-70J is penetration threshold region for this specimen. Also penetration is onset of perforation, increasing the impact energy penetration will turn into perforation as we see in Figure 4.8 at point 70J and further energies.

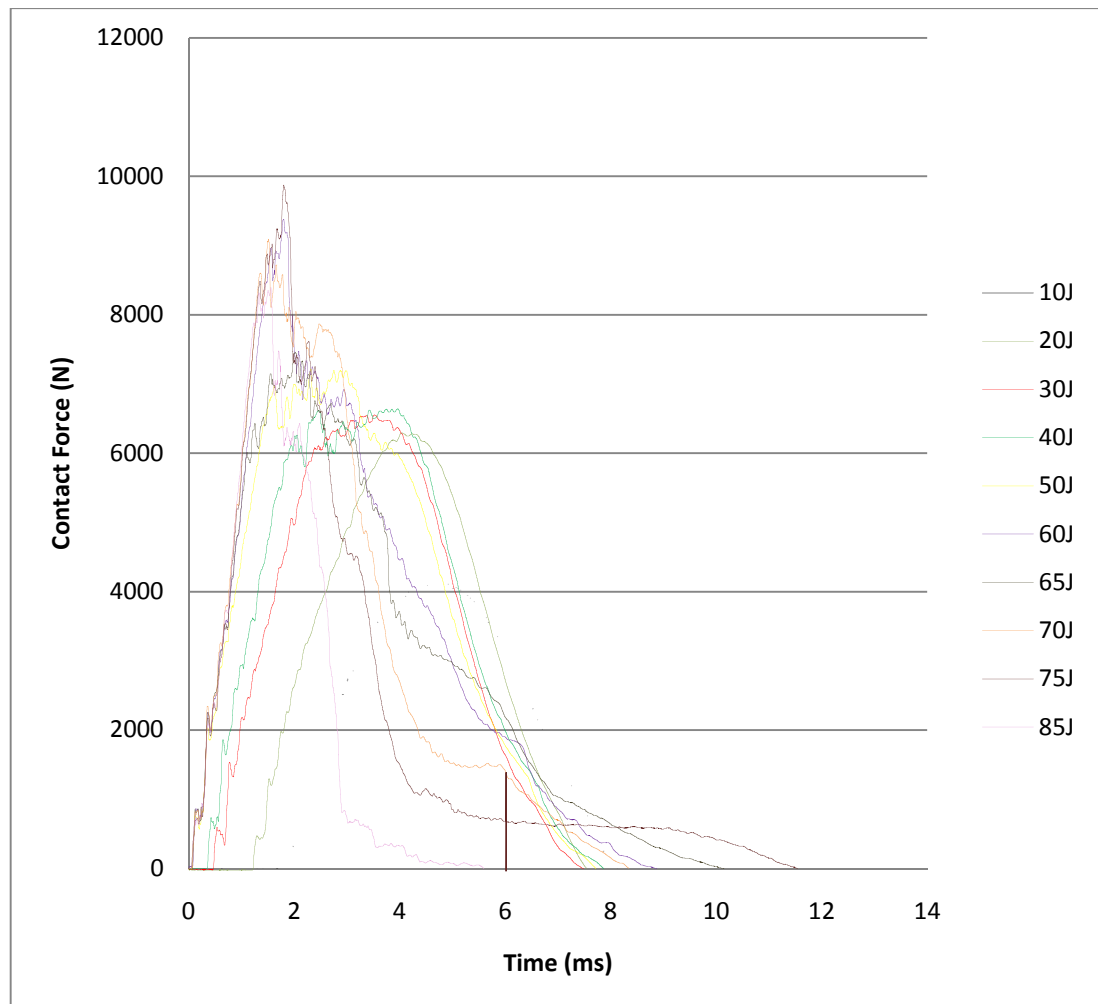


Figure 4.9 Contact force-Time history of square with 76 mm per edge

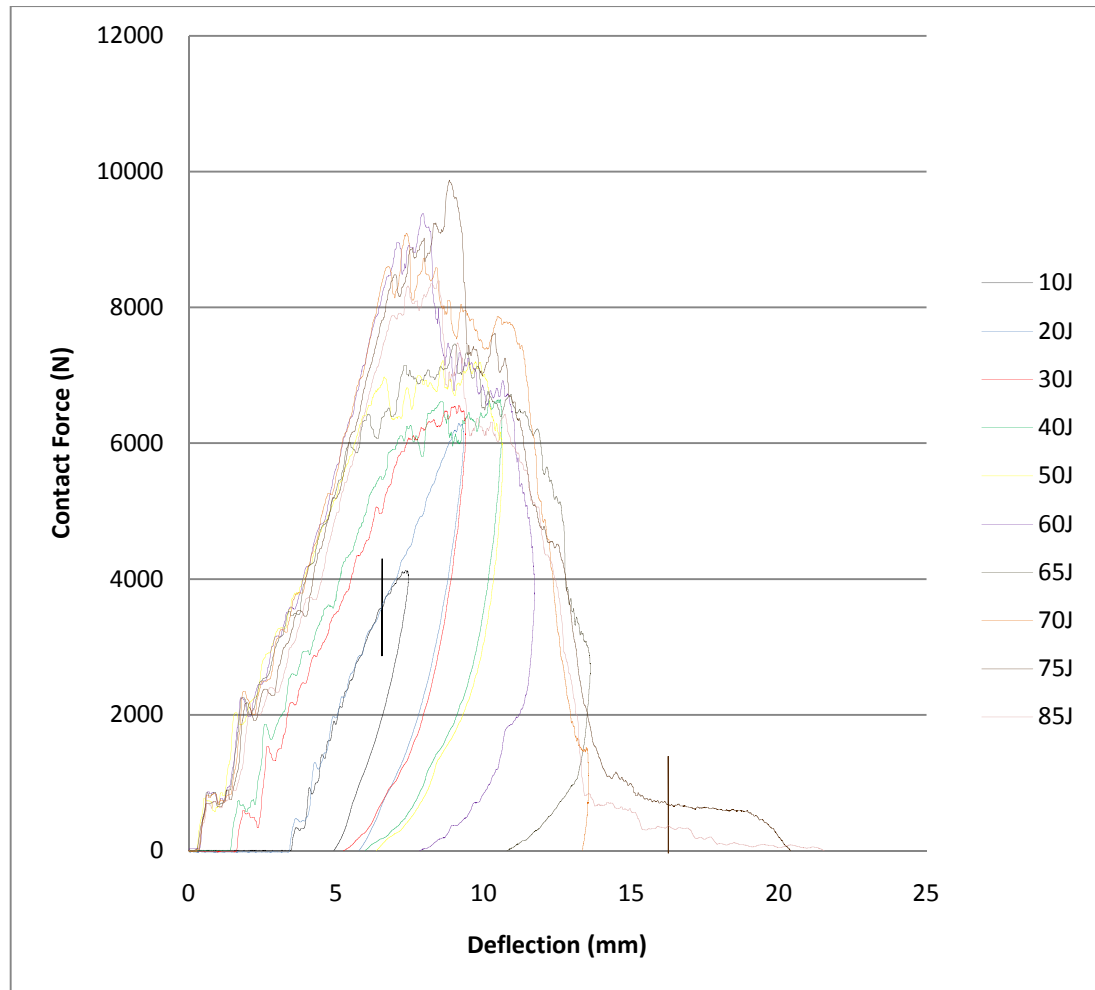


Figure 4.10 Contact force-Deflection history of square with 76 mm per edge

Generally it can be accepted that contact force increases by increasing impact energy, impact time decreases by increasing the impact energy and deflection of the specimens increases by increasing energy level.

As we will see from the photographs of the specimens, the damage zones till 50J energy level are no more than matrix cracks or basic failure modes. Thus, with the increasing contact force, other damage mechanisms may occur. Here 70J energy level can be said to be rebounding-penetration transition energy level. In Figure 4.10 it is clear that all energy lines act similar till they reach max. contact force and then their path differ from each other. This is because of the damage modes occurring in the specimen. Energy line for 70J is a good example of penetration; also we can observe perforation at 75J and 85J. Other energies are examples of rebounding conditions. (10J, 20J, 30J, 40J, 50J, 60J, 65J)

4.3.2 Circle with 76 mm of Diameter

Same with the previous test, to investigate impact resistance of the composite plates, this time 13 impact energy levels are chosen from 10 J to 100 J. and total number of 42 test have been done for these specimens. Average test results for the repeated test are given below in Table 4.6

Table 4.6 Test results for circle with 76 mm of diameter

Impactor Mass(Kg)	Impact Energy(J)	Max. Peak Force(N)	Max. Deflection(mm)	Contact Duration(ms)	Absorbed Energy(J)
4.926	10	4061	4.40	6.62	6.81
4.926	20	6733	5.88	6.27	11.70
4.926	30	7523	7.13	6.66	20.19
4.926	40	7552	8.65	7.16	30.75
4.926	50	8120	9.95	7.94	43.30
4.926	60	8707	12.72	9.30	60.61
4.926	65	8920	12.42	7.88	63.42
4.926	70	8420	13.70	9.03	68.70
4.926	75	8255	21.64	9.11	68.33
4.926	80	9110	24.18	9.47	70.81
4.926	85	8289	23.83	6.57	73.46
4.926	90	9259	26.18	7.54	72.98
4.926	100	7284	20.23	4.23	66.86

Energy profile of these specimens is given in Figure 4.11 Having an energy profile of a tested specimen, we can comment on penetration and perforation thresholds of this specimen as highlighted before.

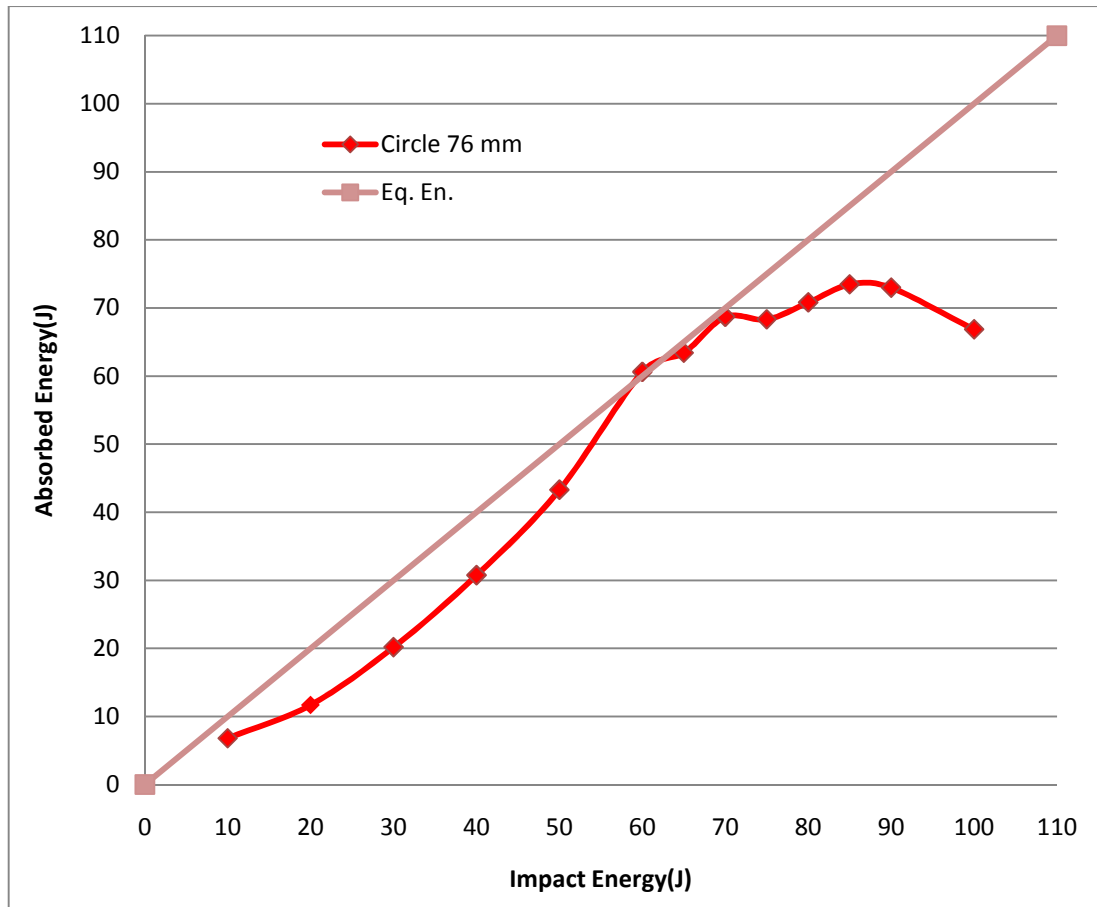


Figure 4.11 Absorbed energy-Impact energy history for circle with 76 of diameter

It's seen that in Figure 4.11 first point of equality between absorbed energy and impact energy is at 60 J, here we can say 60J-70J is penetration threshold region for this specimen. Also penetration is onset of perforation, increasing the impact energy penetration will turn into perforation as we see in Figure 4.11 at point 85J and further energies. Energy levels till 60 J represents a region in which specimens remain non-penetrated thus, we can call this region rebounding region.

We have seen two energy profiles thus far; first one was for the specimens which have an unclamped area of 76x76 mm square and the second one was for the specimens which have an unclamped area of circle with 76 mm diameter. Comparing these energy profiles gives us superficial data from which we can say that these two specimens act practically same against impact damage but some differences stand out like; although rebounding regions of both profiles reaches approximately same

energies, first energy profile reaches perforation threshold at 70 J on the other hand second profile reaches perforation at 85J.

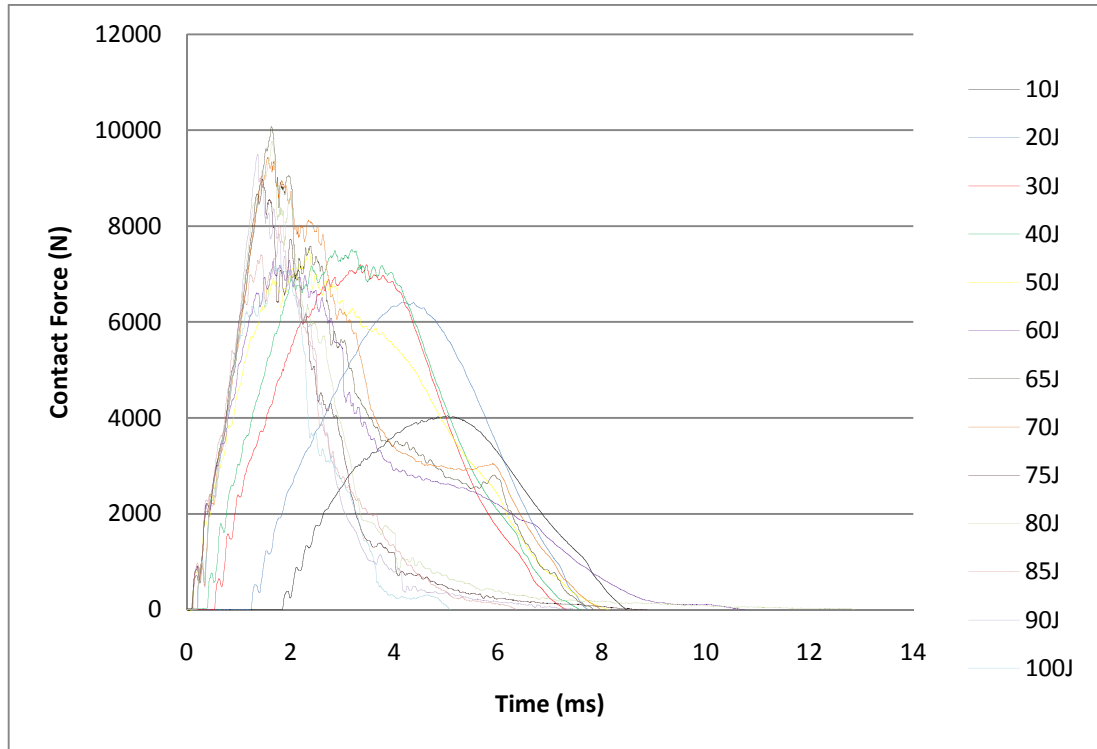


Figure 4.12 Contact force-Time history of circle with 76 mm of diameter

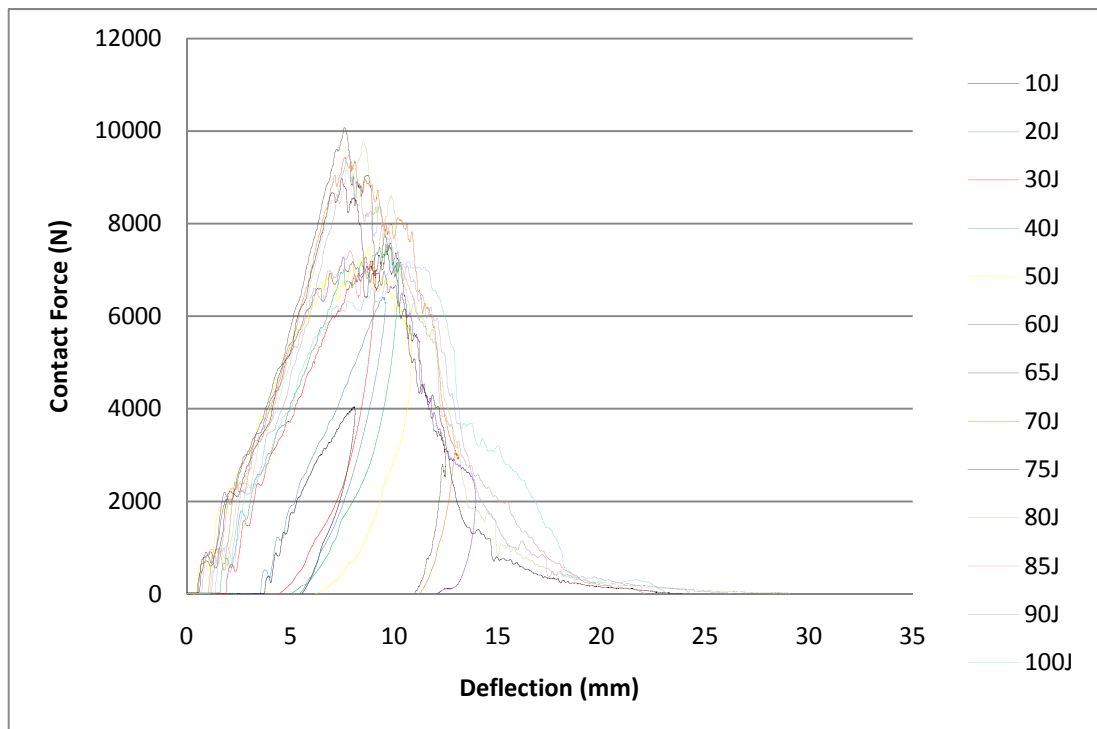


Figure 4.13 Contact force-Deflection history of circle with 76 mm of diameter

4.3.3 Square with 150 mm per Edge

Same with the previous tests, to investigate impact resistance of the composite plates, this time 13 impact energy levels are chosen from 10 J to 100 J. and total number of 45 test have been done for these specimens. Average test results for the repeated test are given below in Table 4.7

Table 4.7 Test results for circle with 150 mm per edge

Impactor Mass(Kg)	Impact Energy(J)	Max. Peak Force(N)	Max. Deflection(mm)	Contact Duration(ms)	Absorbed Energy(J)
4.926	10	3160	6.67	9.54	5.91
4.926	20	4780	8.84	9.42	12.34
4.926	30	6190	10.64	9.49	18.62
4.926	40	7644	11.74	9.17	25.02
4.926	50	8131	11.46	8.73	35.97
4.926	60	8374	13.43	9.26	46.84
4.926	70	8343	15.35	9.79	56.46
4.926	75	8369	16.31	9.98	63.33
4.926	78	9180	16.31	10.21	64.05
4.926	80	8555	17.23	8.13	70.55
4.926	85	8696	18.19	4.84	78.16
4.926	90	8459	18.75	4.38	75.84
4.926	100	8376	18.38	3.65	74.34

Energy profile of these specimens is given in Figure 4.14 We can better comment on the results with energy profile and can compare it with previous tests energy profiles.

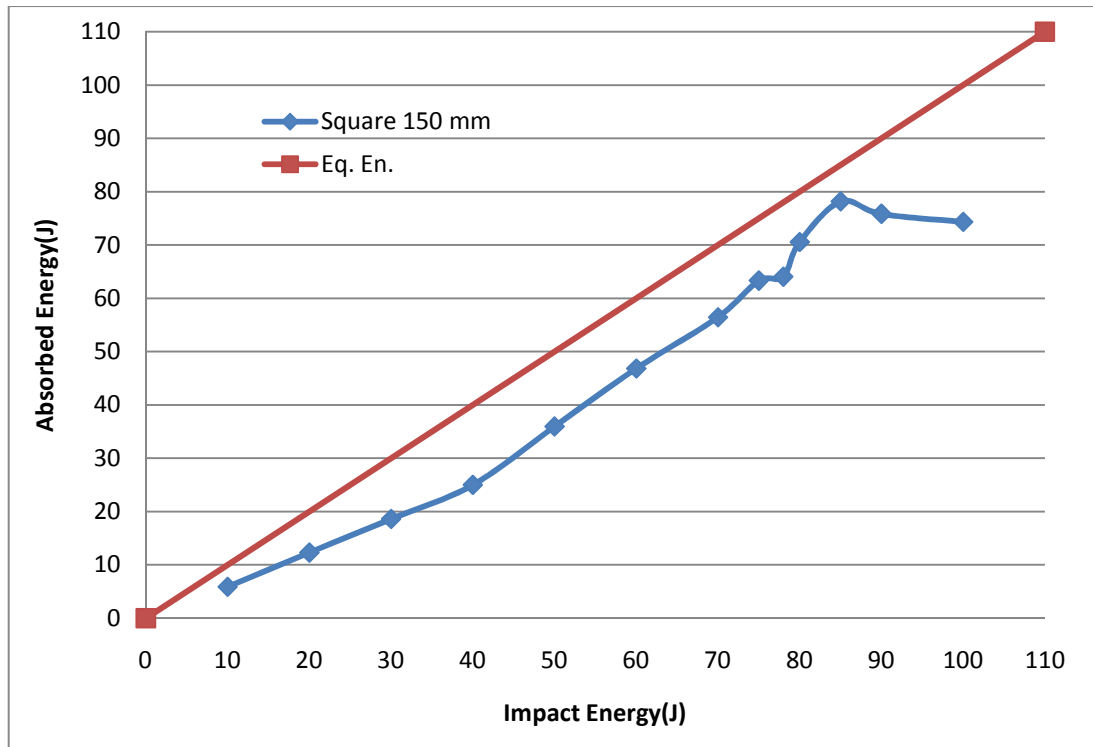


Figure 4.14 Absorbed energy-Impact energy history for square with 150 mm per edge

We have seen all the energy profiles now; first one was for the specimens which have an unclamped area of $76 \times 76 \text{ mm}^2$ square and the second one was for the specimens which have an unclamped area of circle with 76 mm diameter and the last one was for the specimens which have an unclamped area of $150 \times 150 \text{ mm}^2$ square. If we compare the last results with the first two profiles, we can see that at same impact energies square with 150 mm per edge absorbs lesser energies but as a result of this it can resist higher impact energies thus, penetration and perforation thresholds can be said to be higher than the others.

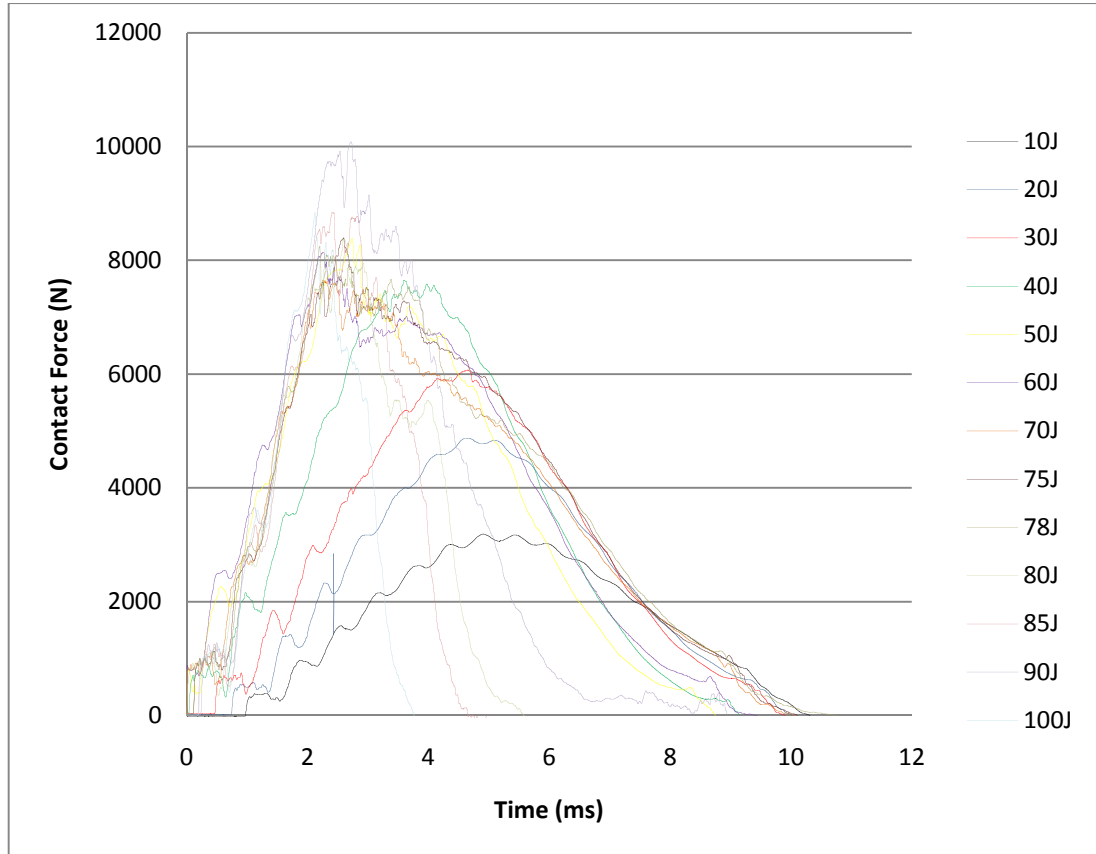


Figure 4.15 Contact force-Time history of square with 150 mm per edge

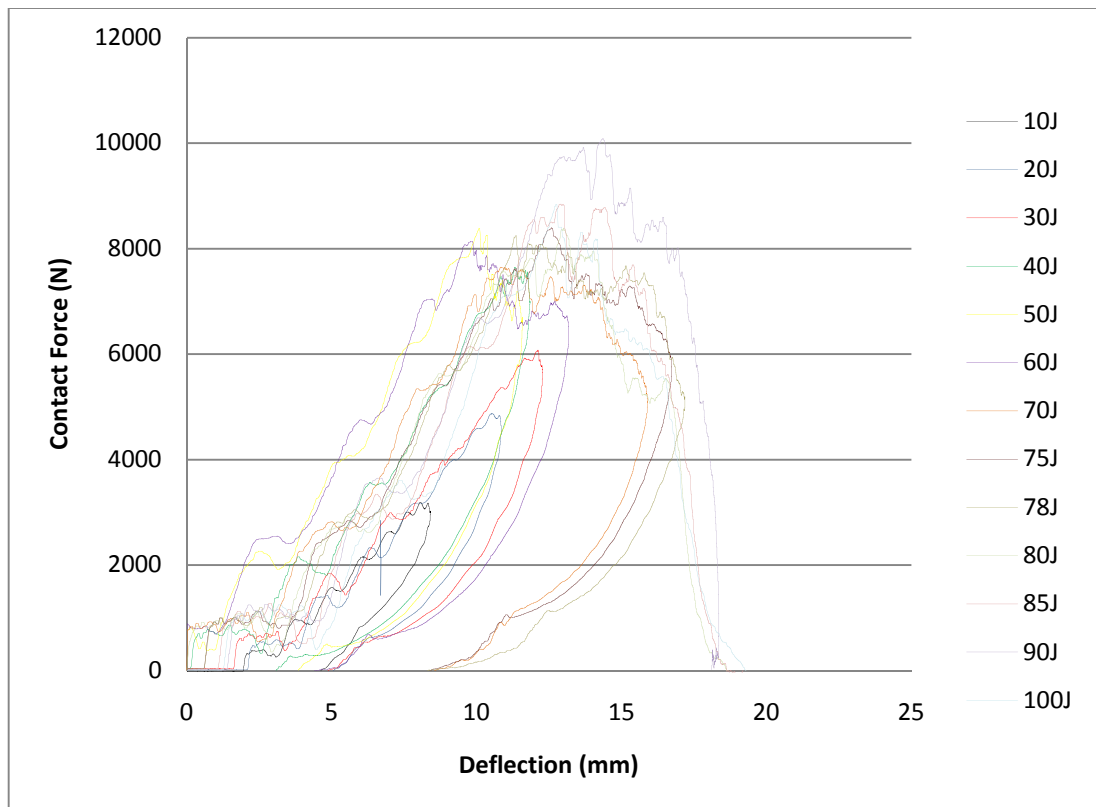


Figure 4.16 Contact force-Deflection history of square with 150 mm per edge

In Figure 4.16 it can be observed that 70J energy level is rebounding-penetration transition energy. 70-75-78J energy levels represent the region for penetration and 80-85-90-100J energy levels represent the region for perforation. Other energy levels i.e. 10-20-30-40-50J are in rebounding case, that is why loading curve and unloading curve of these energy levels returns parallel to each other.

As additional information for graphs through now, we can say that the starts of material failures are abrupt, because there is no plastic deformation. Instead there is a region of fiber breakage and pullout ending with an abrupt break. The fiber breakage region is characterized by oscillations in loading curve. In this region, load may remain essentially flat, drift up or drift down.

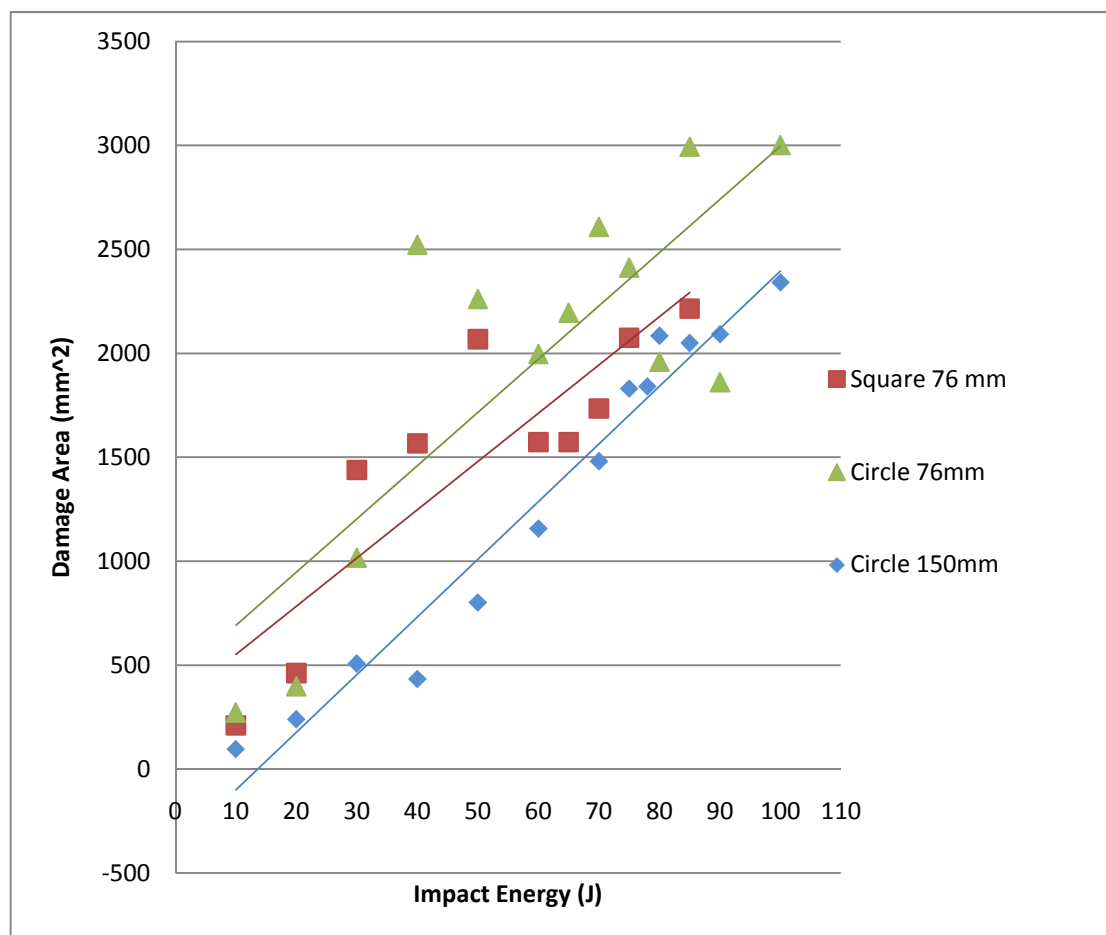


Figure 4.17 Damage area-Impact energy history for the specimens

4.4 Damage Areas

In impact loading of composite plates by cylindrical impactors several different failure mechanisms can operate. The dominant mechanism often changes during failure of a given plate and also depends upon the particular type of composite plate. In our tests among the mechanisms that have been observed are: fiber breakages, matrix cracks and delamination. One or more mechanisms can occur together.

We will observe these damage mechanisms from the photographs of impacted composites. It is particularly easy to observe in the epoxy matrix plates because the epoxy transmits light so photographs of both the normal and with a strong light behind the plate were taken to better observe damage areas.

During our tests the dominant and bare failure mechanism stands out as delamination so it is better to analyze delamination mechanism. For moderate impact velocities, the first stage of the delamination process is a through the thickness shear failure of the first lamina along two planes A-A and B-B parallel to fibers, separated by a distance $2R$, where R is the impactor radius. Thus, the impactor pushes forward a strip of the first lamina, of width $2R$, whose length increases with time as the two cracks propagate away from the vicinity of the impactor, until the propagation is stopped when the impactor has cut of all the fibers of the strip. In Figure 4.18 the two cracks are shown after they have stopped at length d_1 .

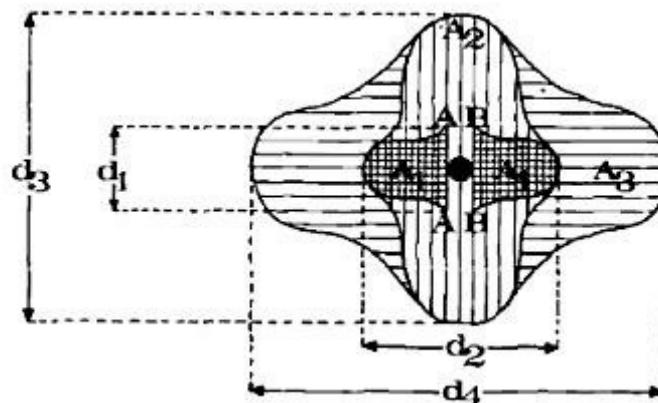


Figure 4.18 Delamination pattern

Until the fibers of the strip are cut through, this strip of width $2R$ from the first lamina loads transversely the second lamina along the entire length of the strip and thus initiates an interlaminar separation between lamina 1 and lamina 2 (the delamination area A_1). Because of its action in generating the delamination process this strip of the first lamina, of width $2R$ and length increasing to d_1 , will be called the first generator strip.

During the process just described very little energy is dissipated by matrix deformation or by the through-the-thickness crack formation, because of the low strength of the matrix material. The tensile forces in the fibers of the generator strip and in those fibers of the next lamina that are transversely loaded by the generator strip become quite high, however and as the generator strip is pushed forward, these tensile forces develop a component acting to decelerate the impactor. The tensile forces in the strip also tend to produce a lengthwise motion of the strip. The shearing forces in the fibers of the generator strip as they are cut off by the impactor also act to decrease the kinetic energy of the impactor.

After all the fibers of the first generator strip have been cut through or broken, the process is repeated with the second lamina. A second generator strip is formed by two through-the-thickness shear cracks in the second lamina, which propagate until all the fibers of the second generator strip have been cut off or broken. This second generator strip loads transversely the fibers of the third lamina and initiates delamination between lamina 2 and lamina 3, the delamination area is marked A_2 . This process just described may involve several laminas and it takes longer to penetrate the second generator strip than it took to cut through the first.

Same with in experimental results, damage areas also will be given under three main titles. Titles will be named again according to the specimens unclamped areas.

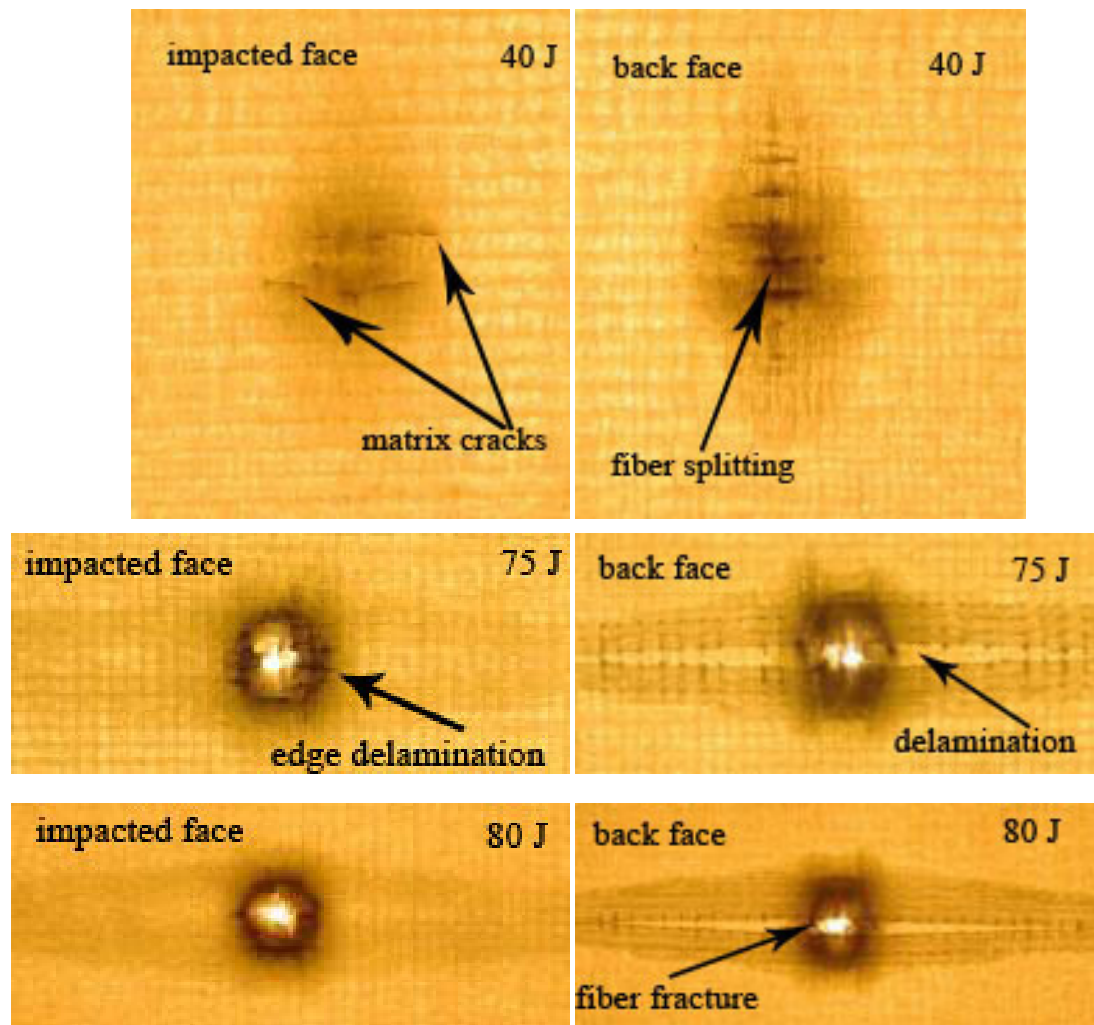
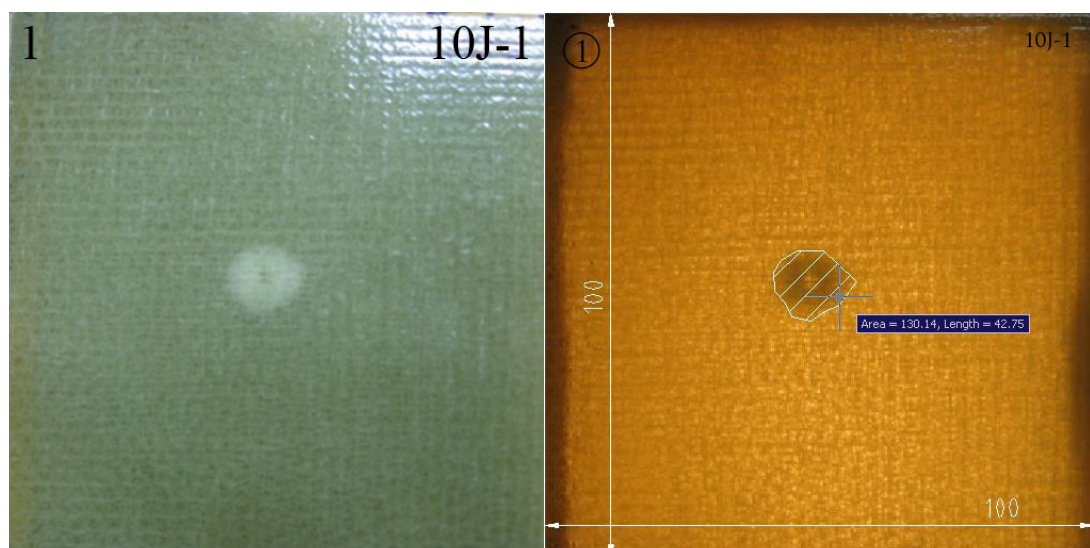
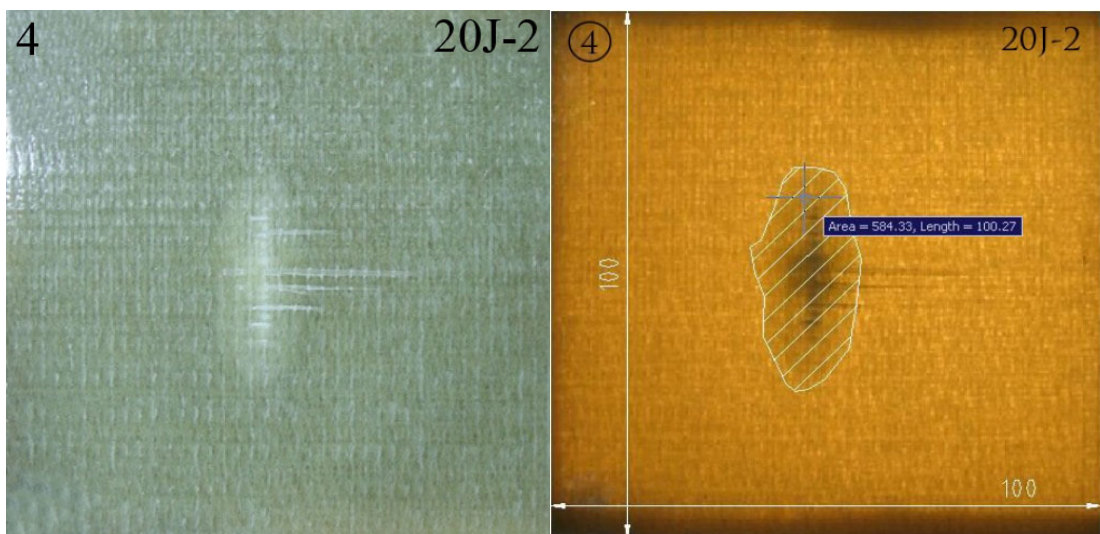
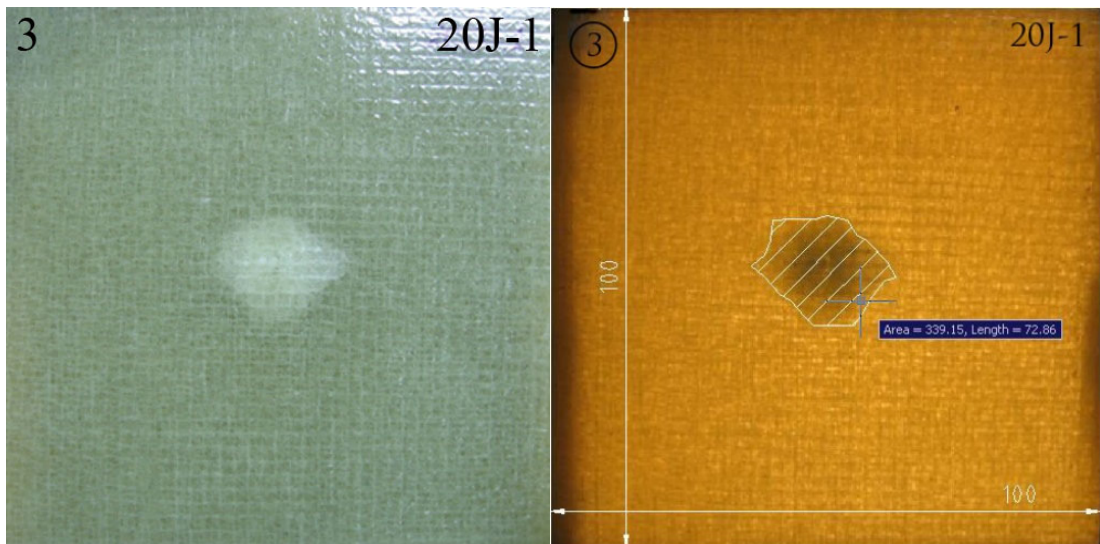
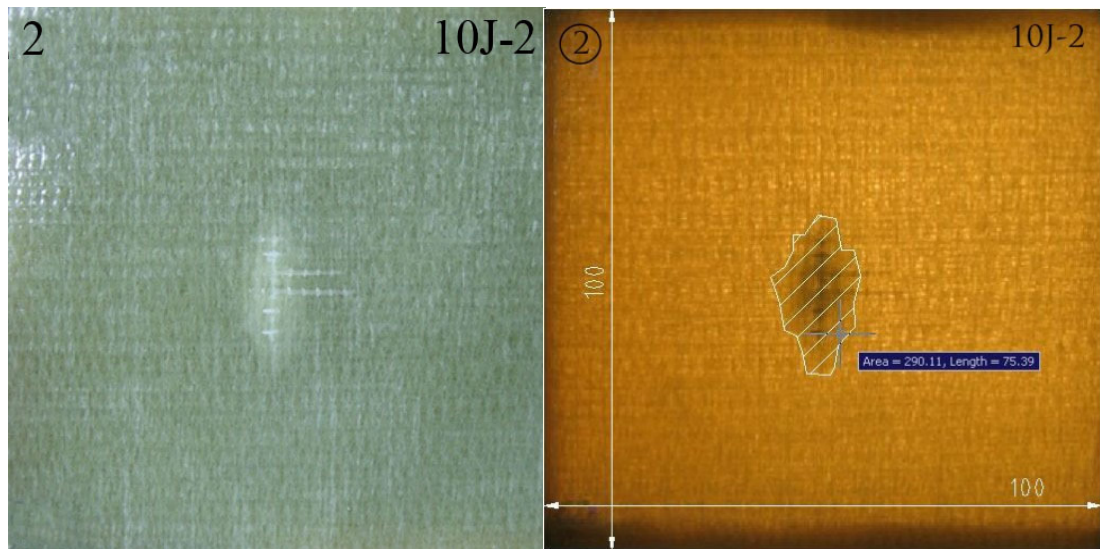
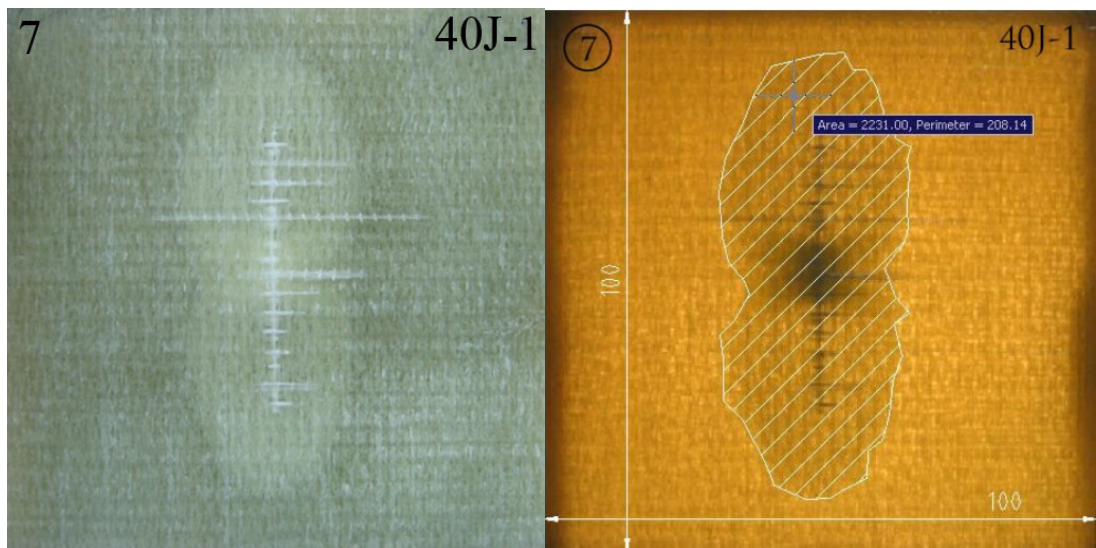
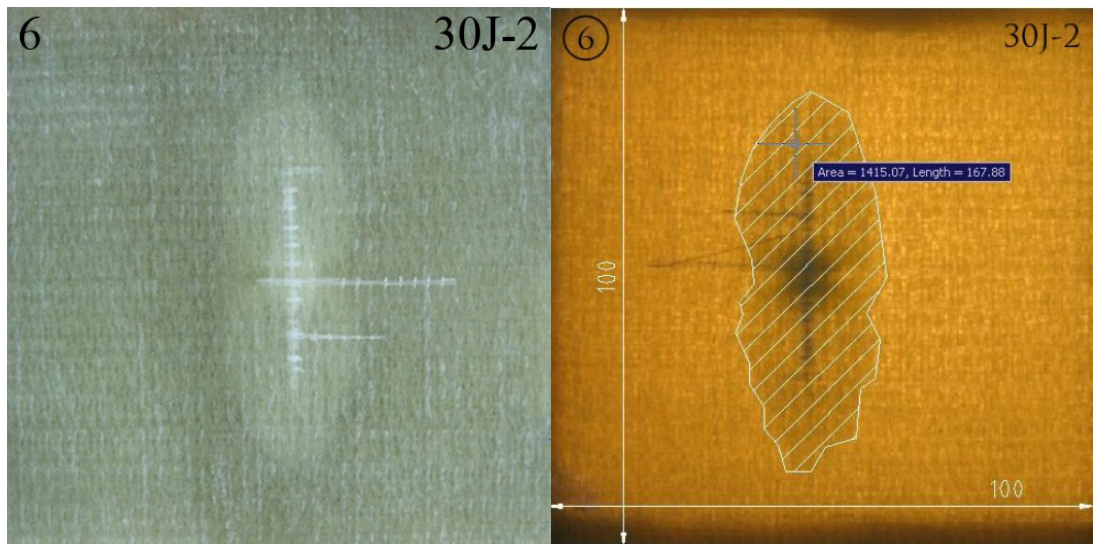
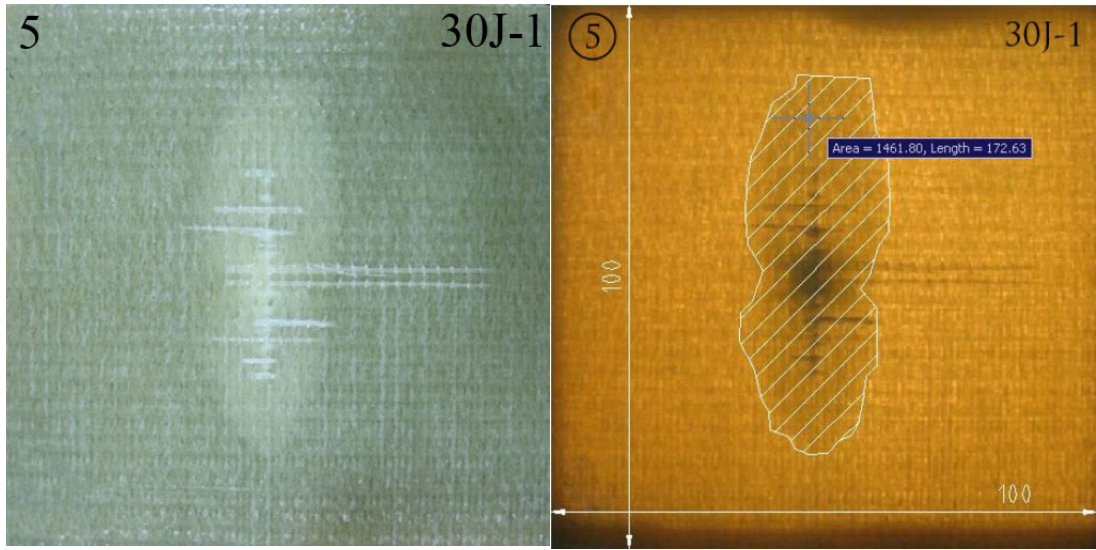


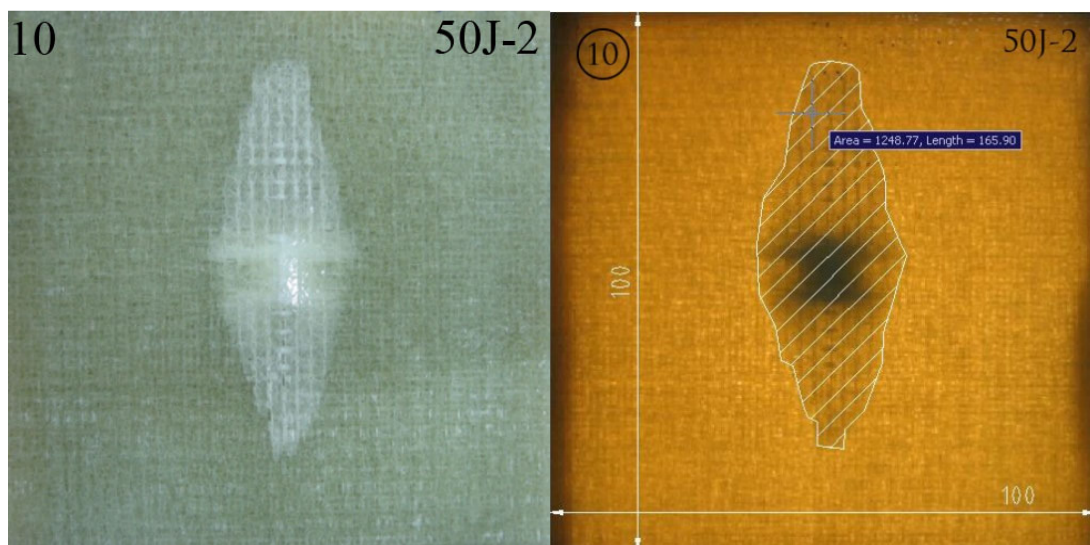
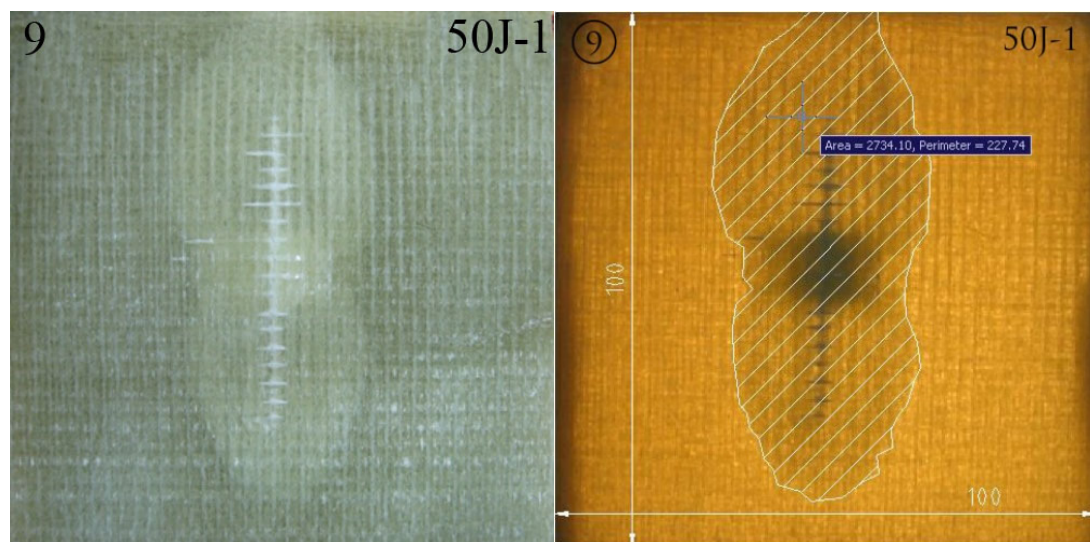
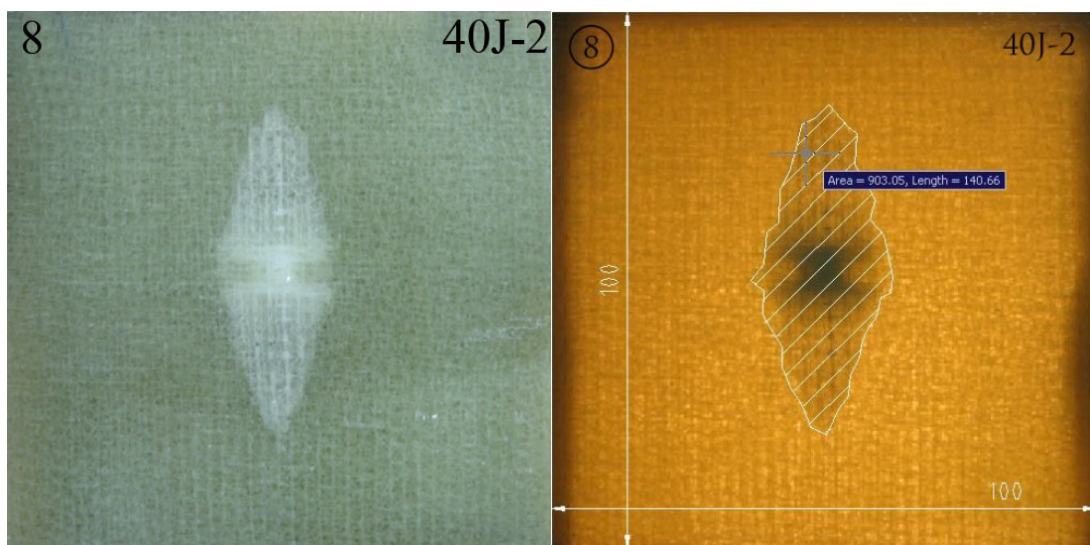
Figure 4.19 Some representative photographs of damaged samples taken with high intensity backlighting

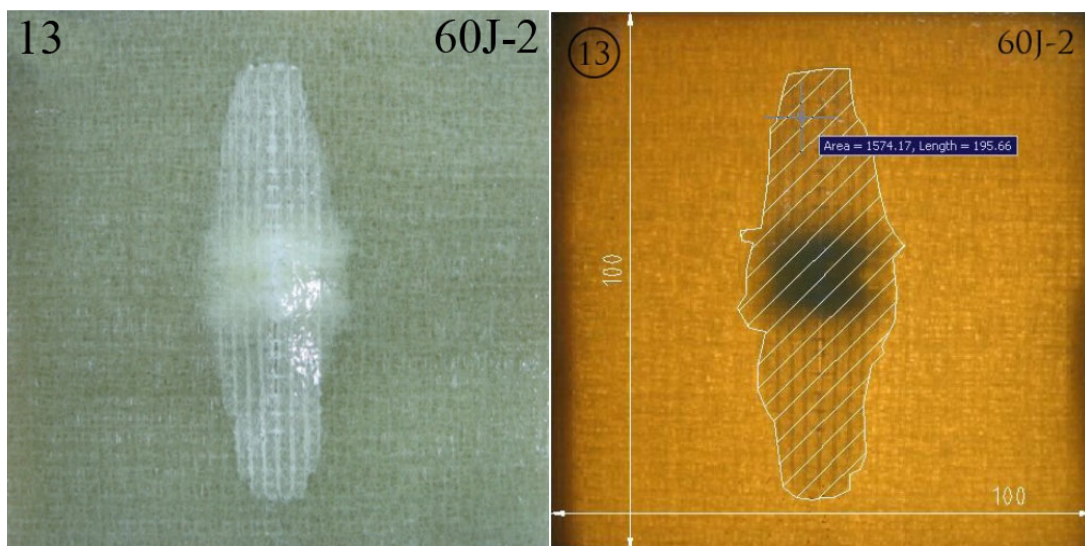
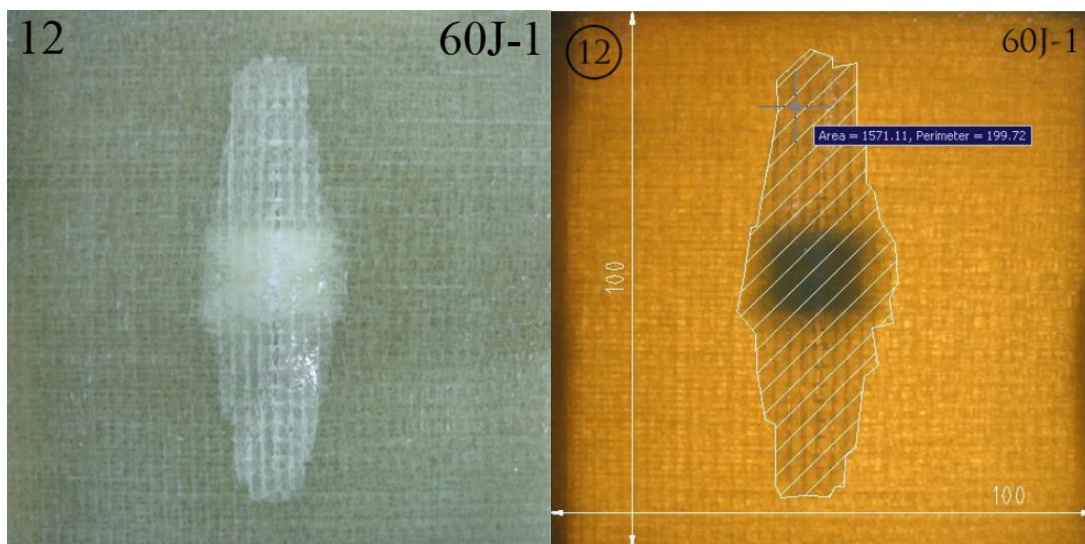
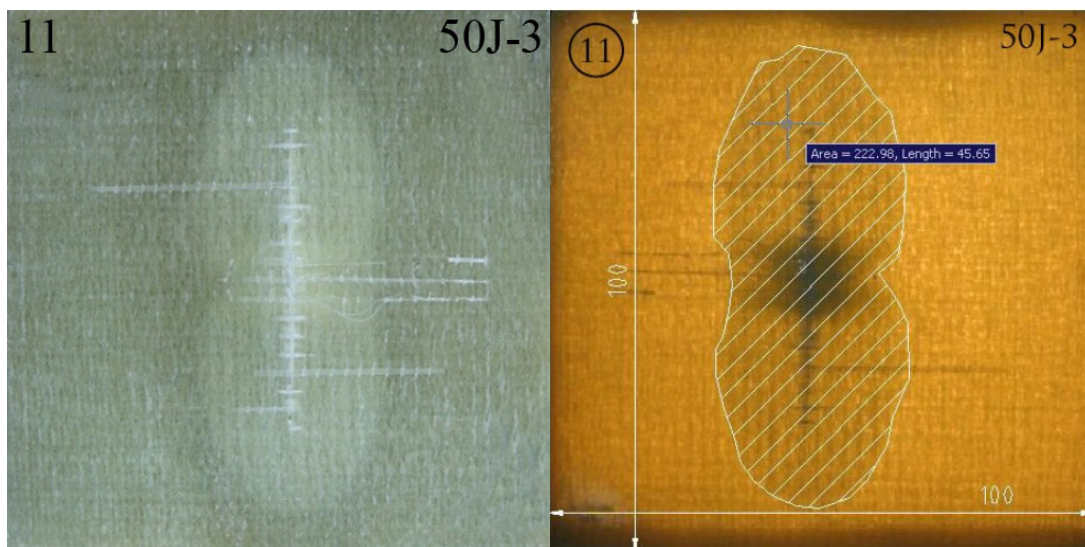
4.4.1 Square with 76 mm per Edge

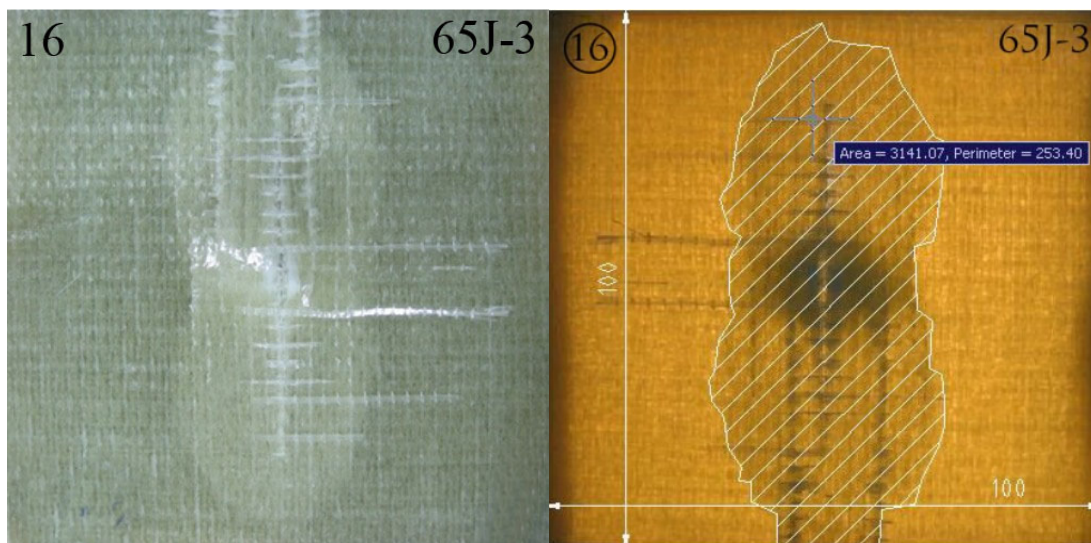
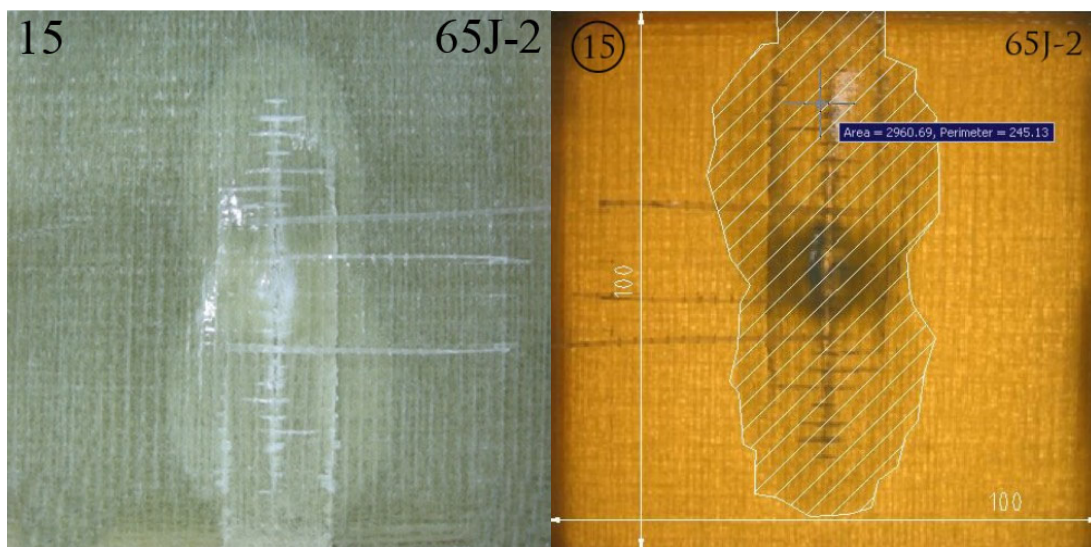
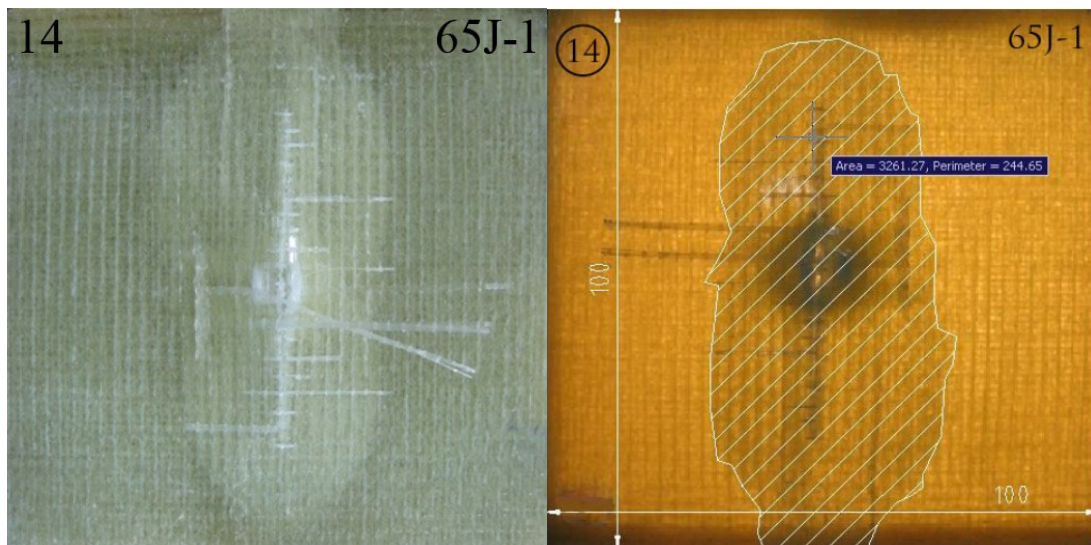


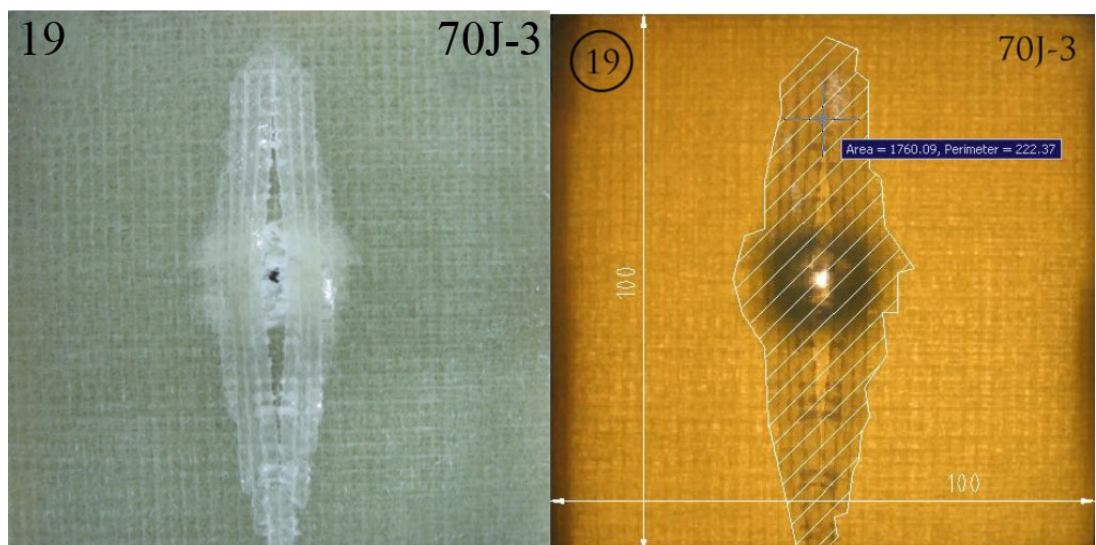
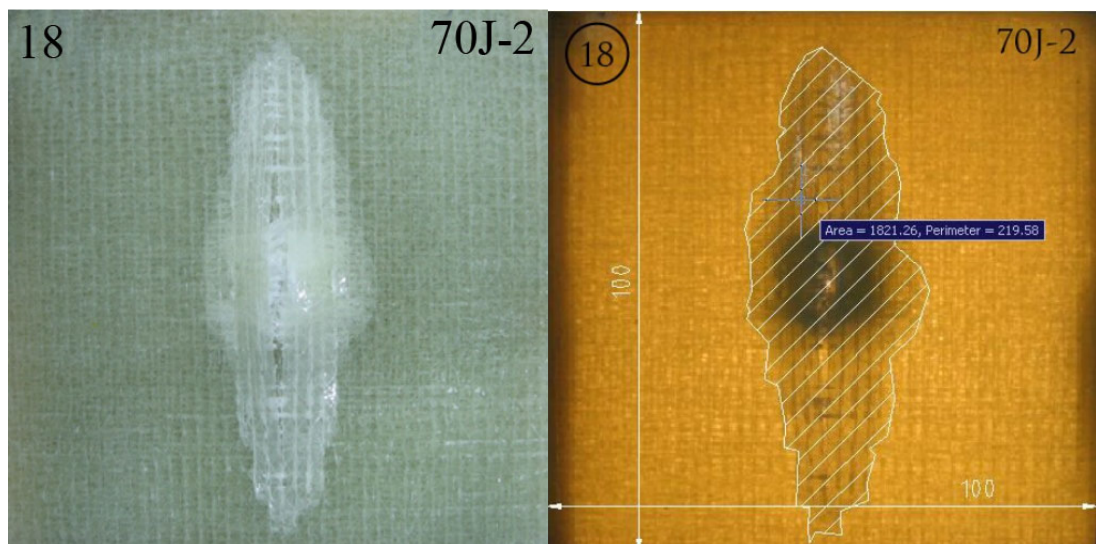
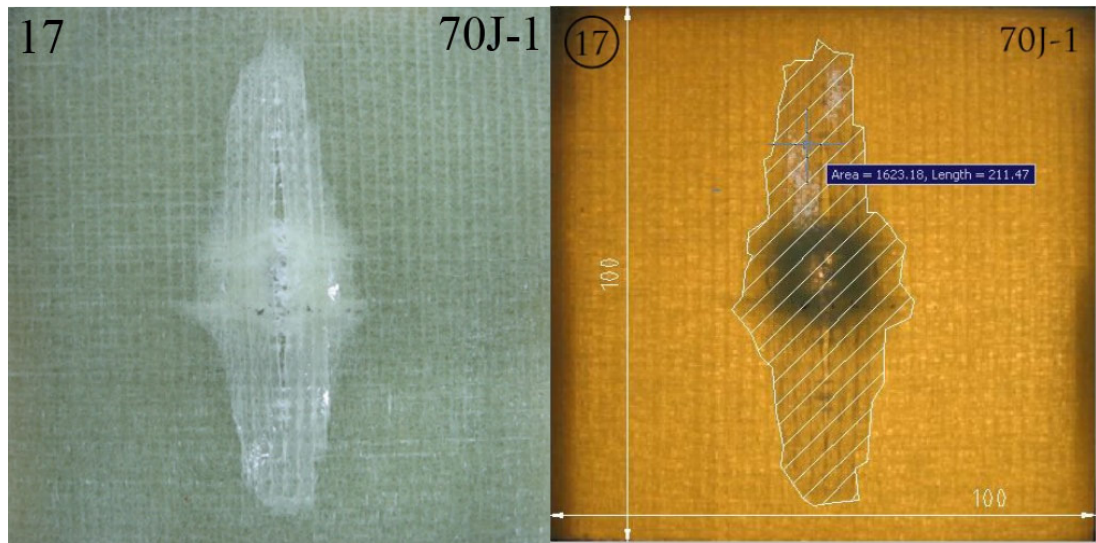


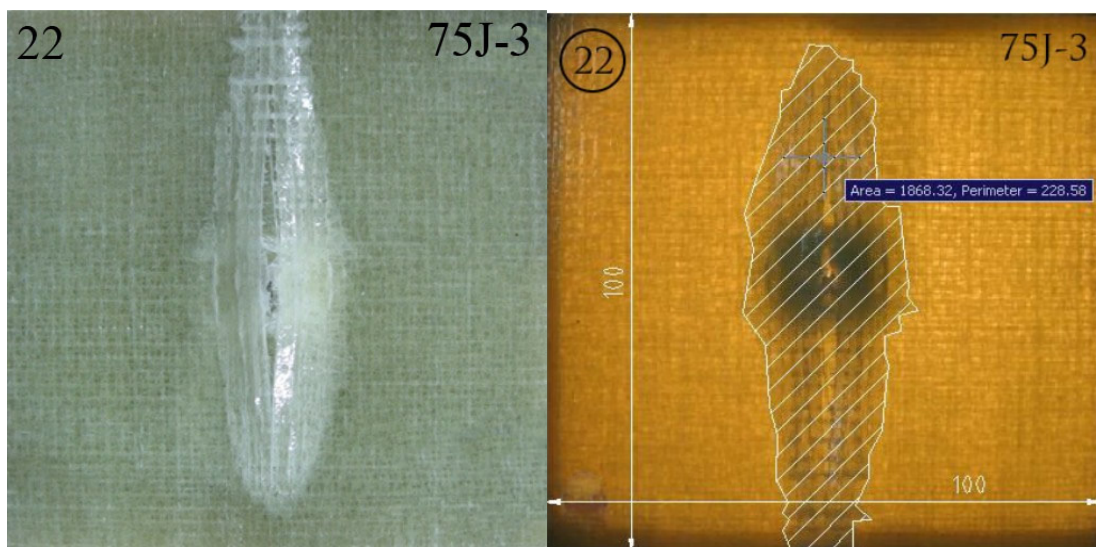
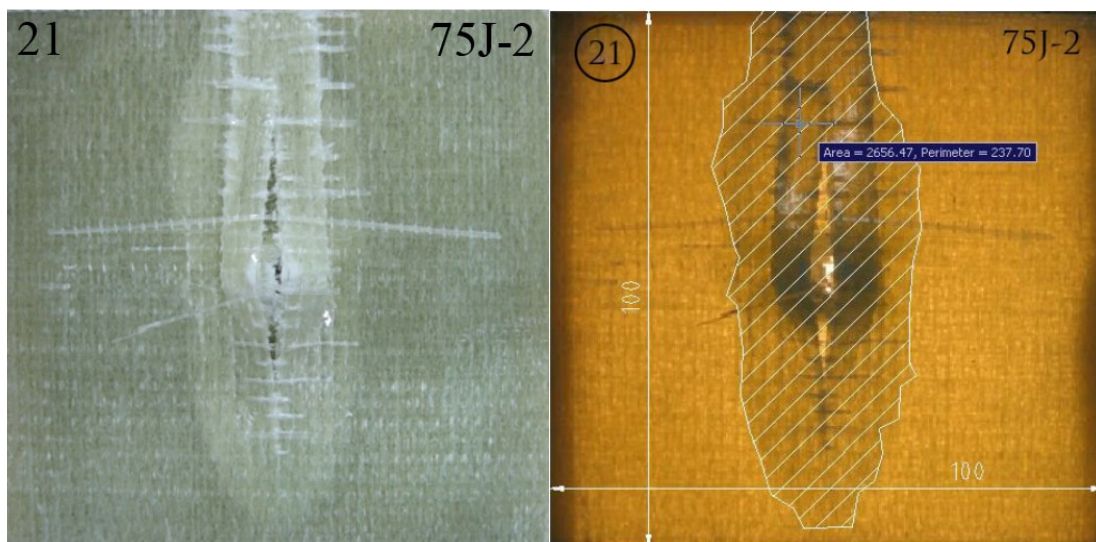
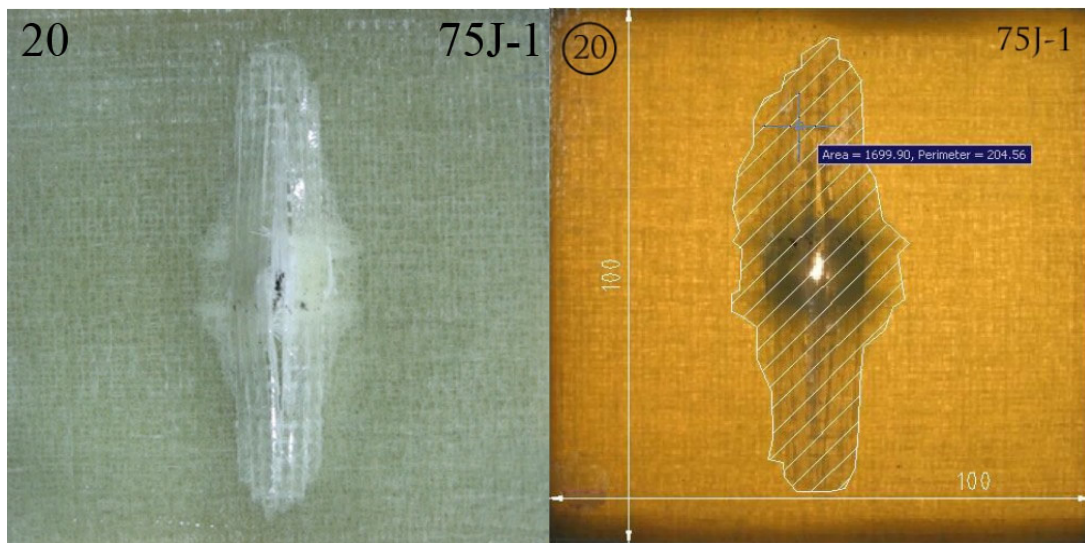












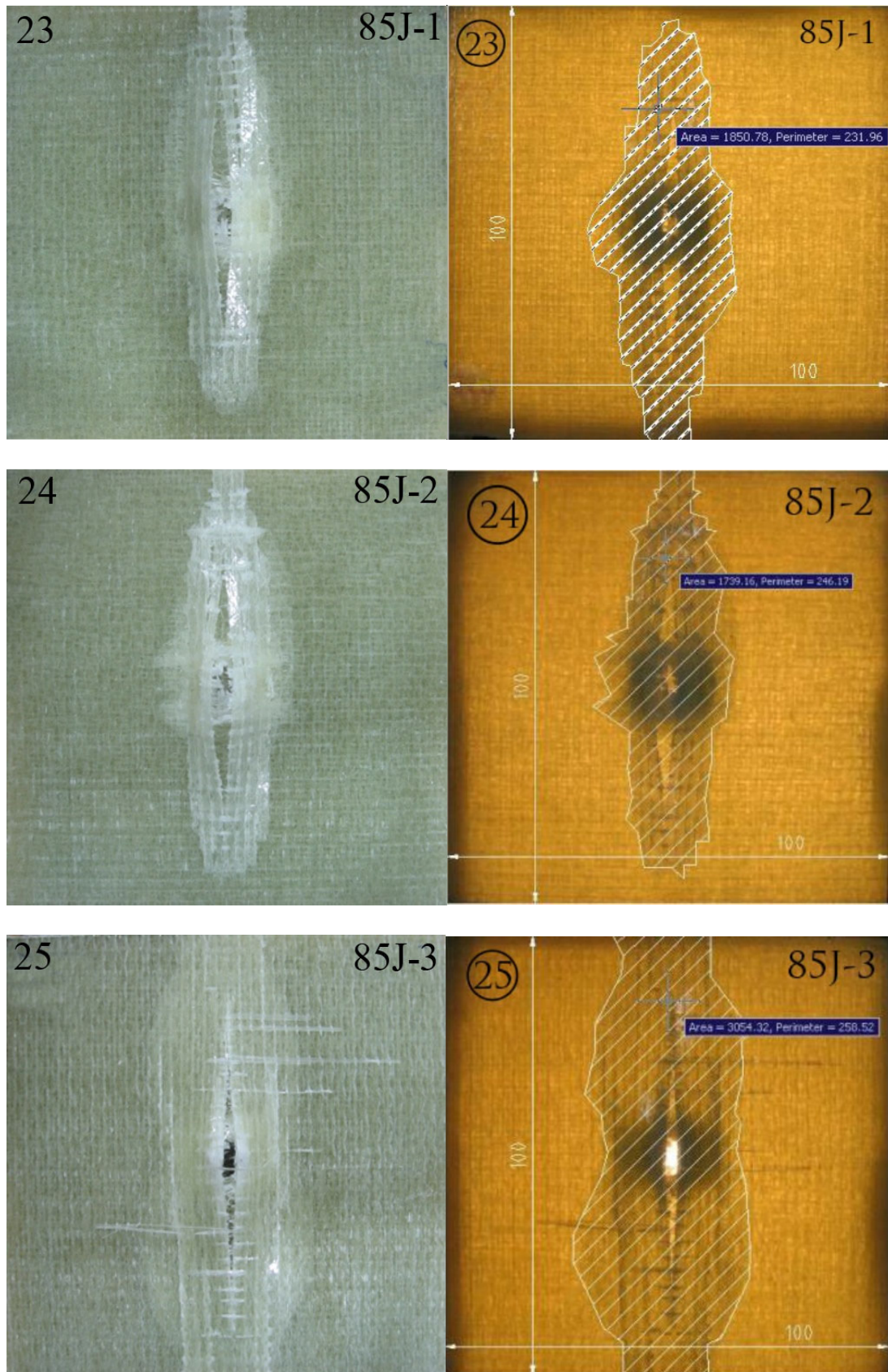


Figure 4.20 Photographs of the specimens (normal left, with a strong light behind right)

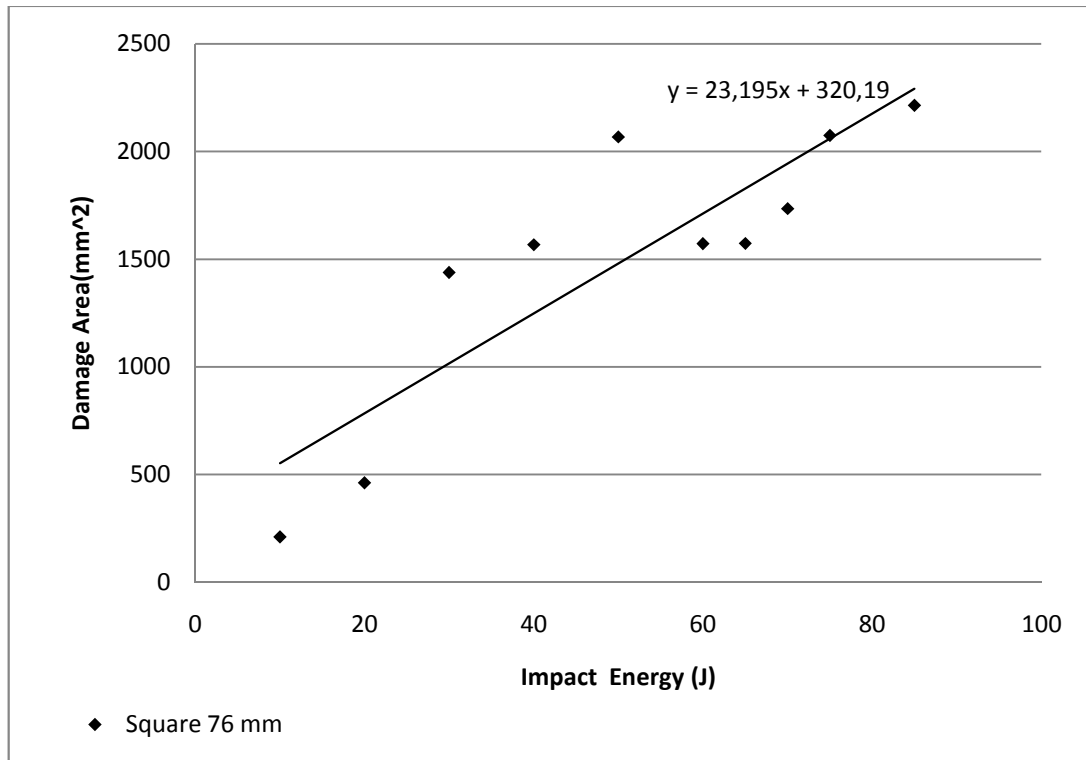
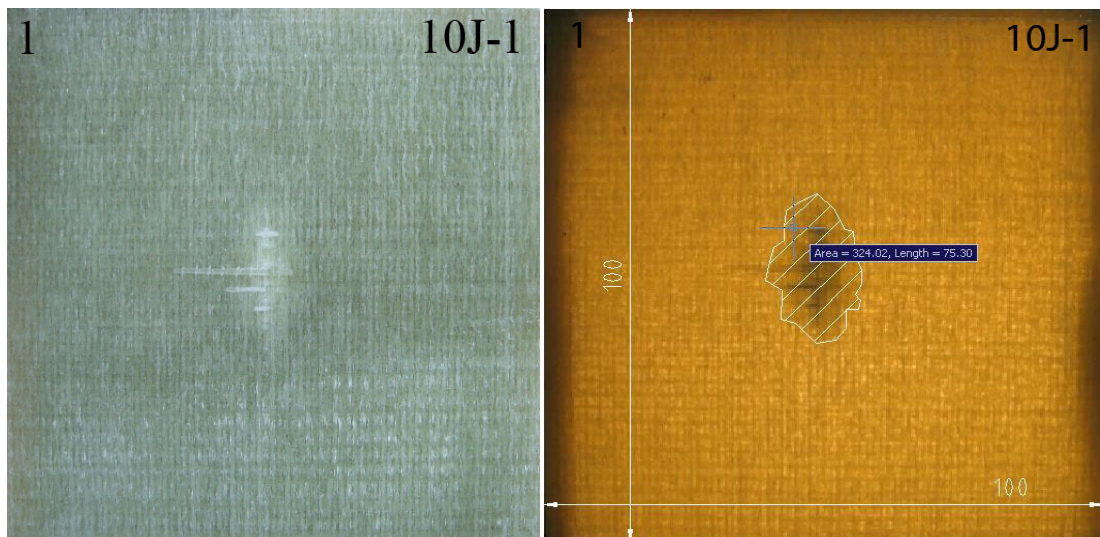
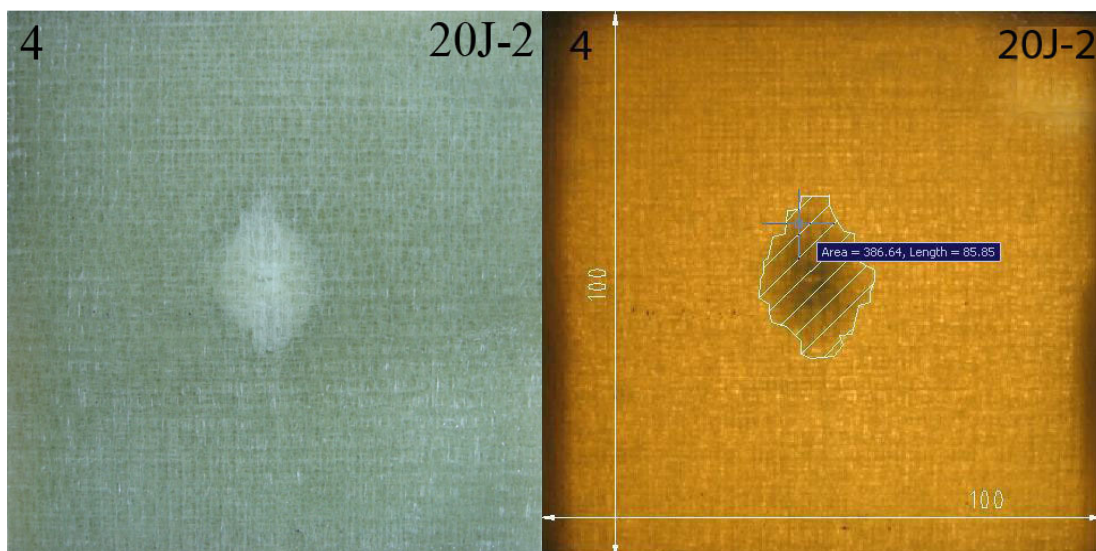
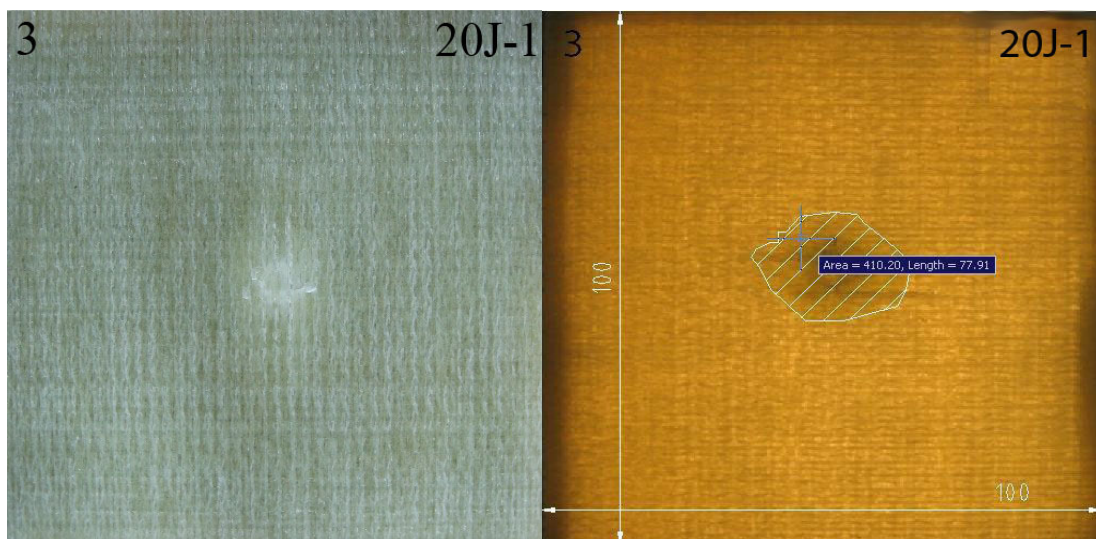
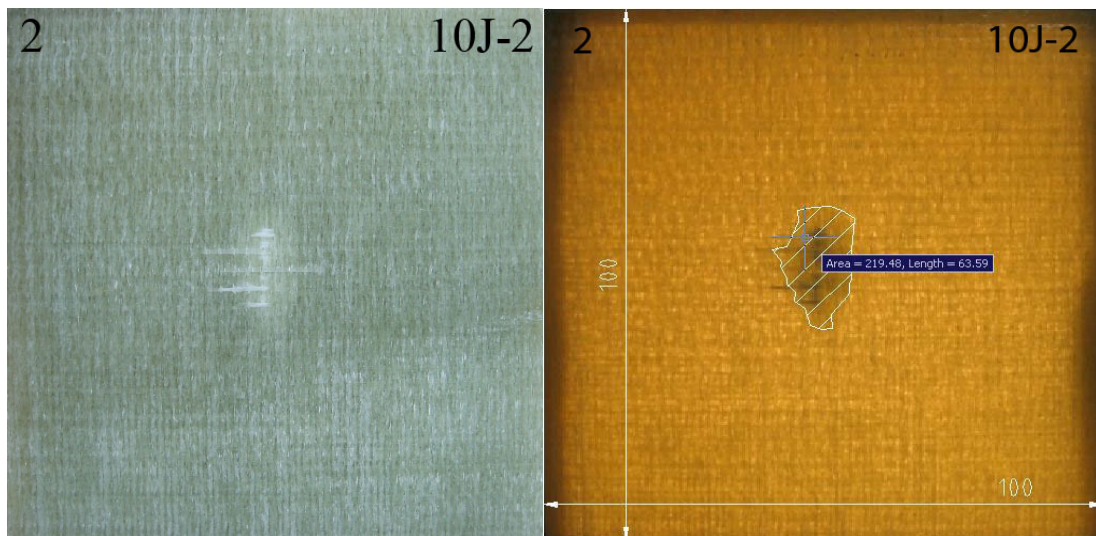
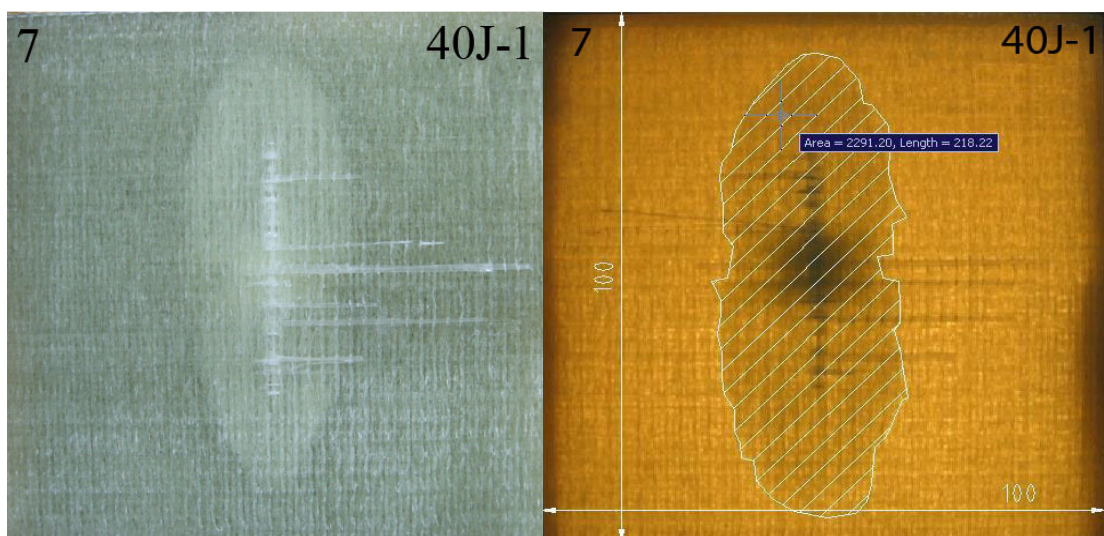
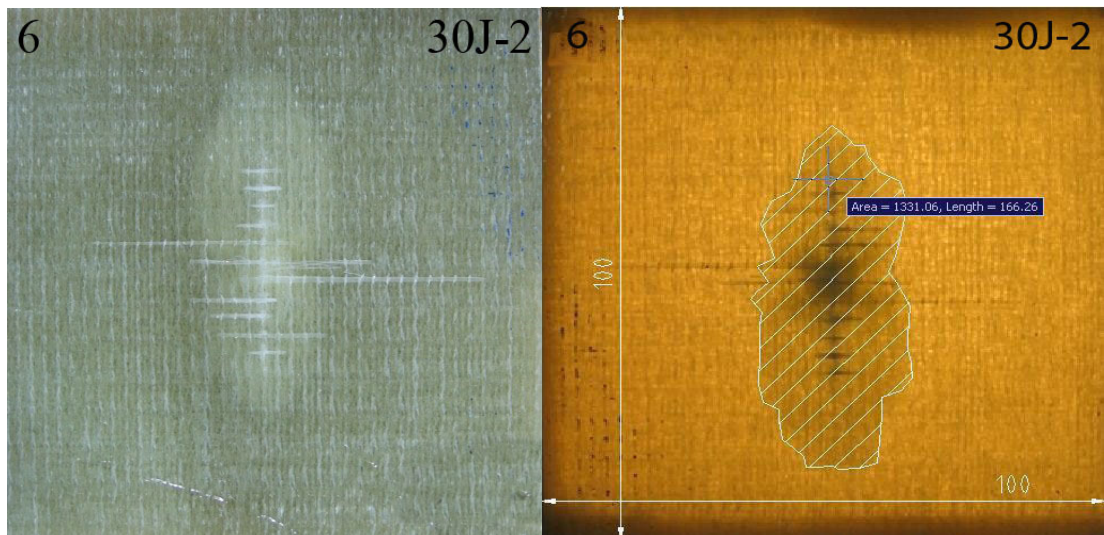
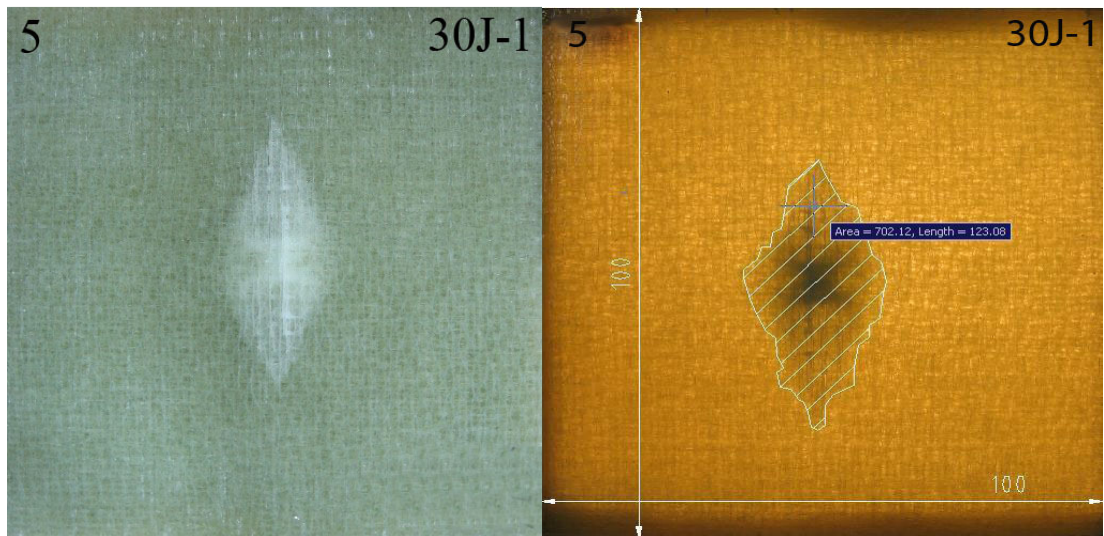


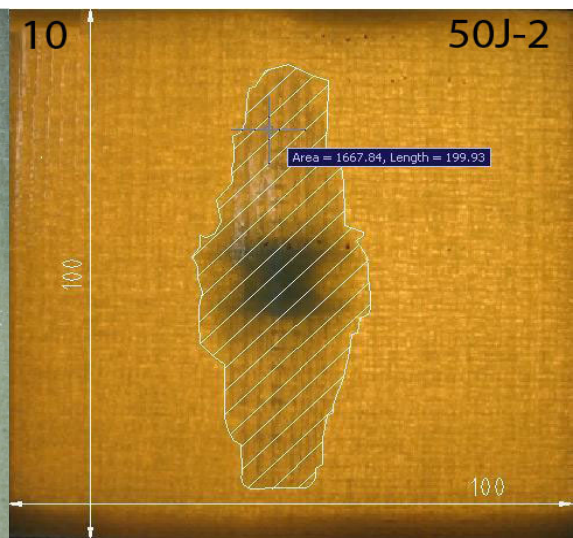
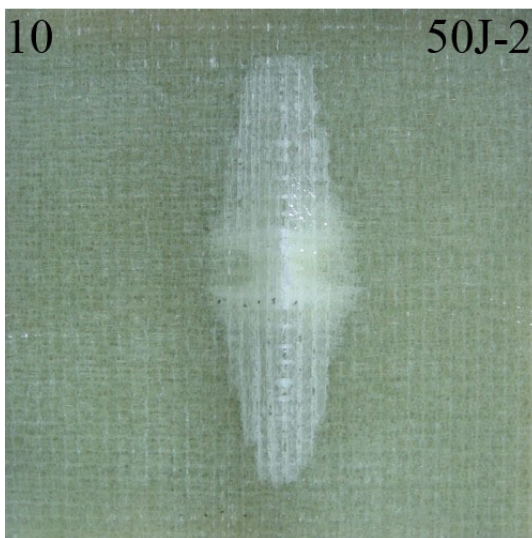
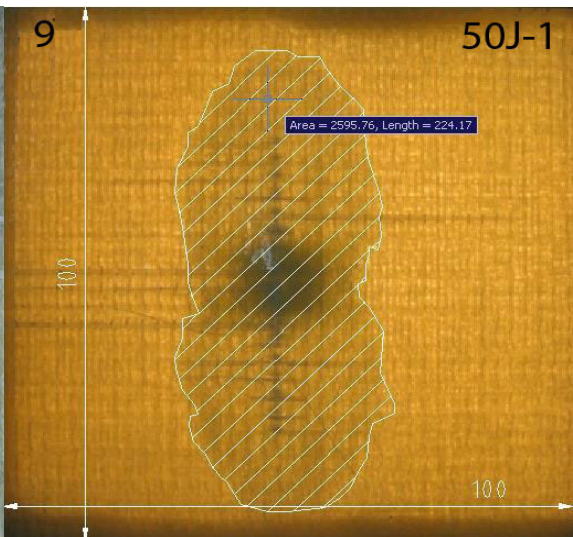
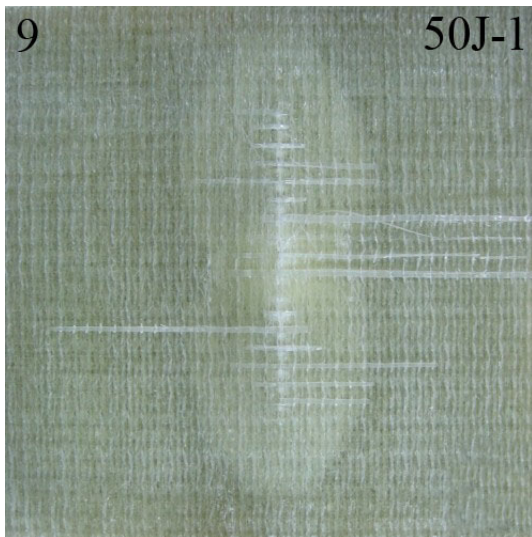
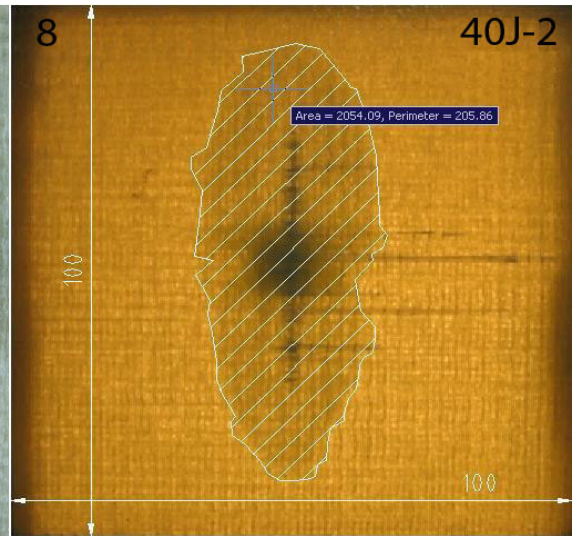
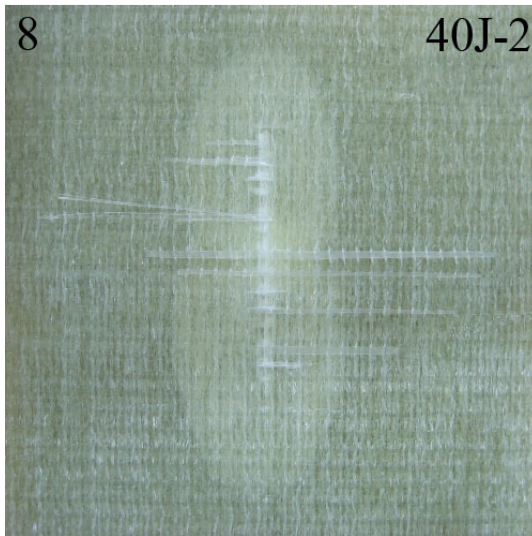
Figure 4.21 Damage area-Impact energy history of square with 76 mm per edge

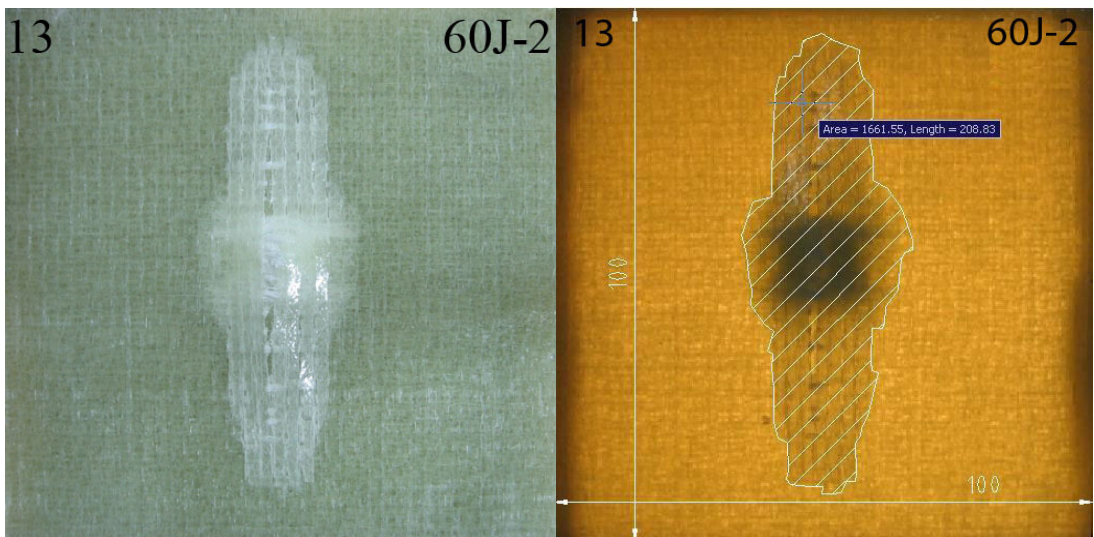
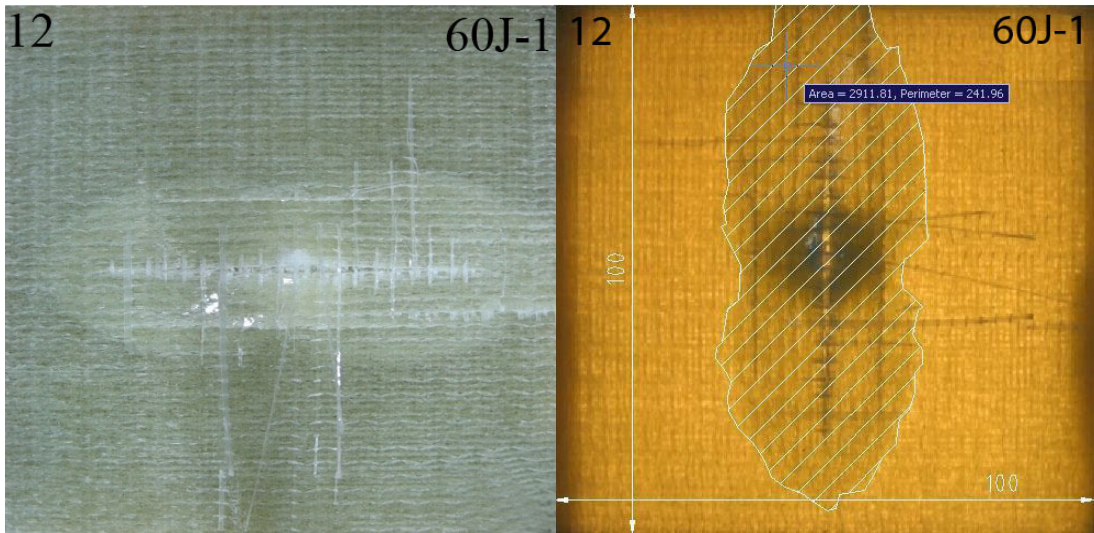
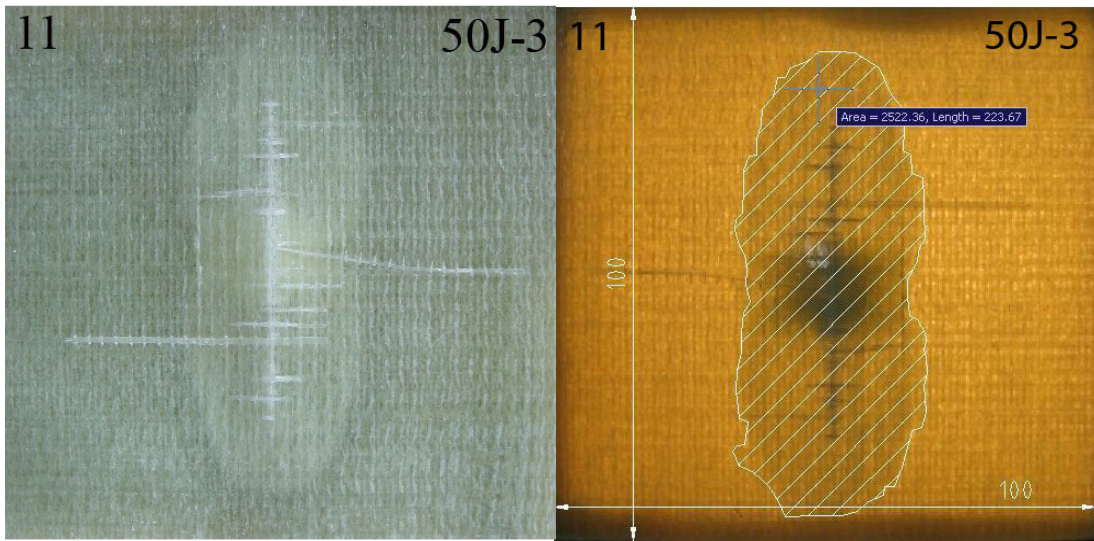
4.4.2 Circle with 76 mm of Diameter

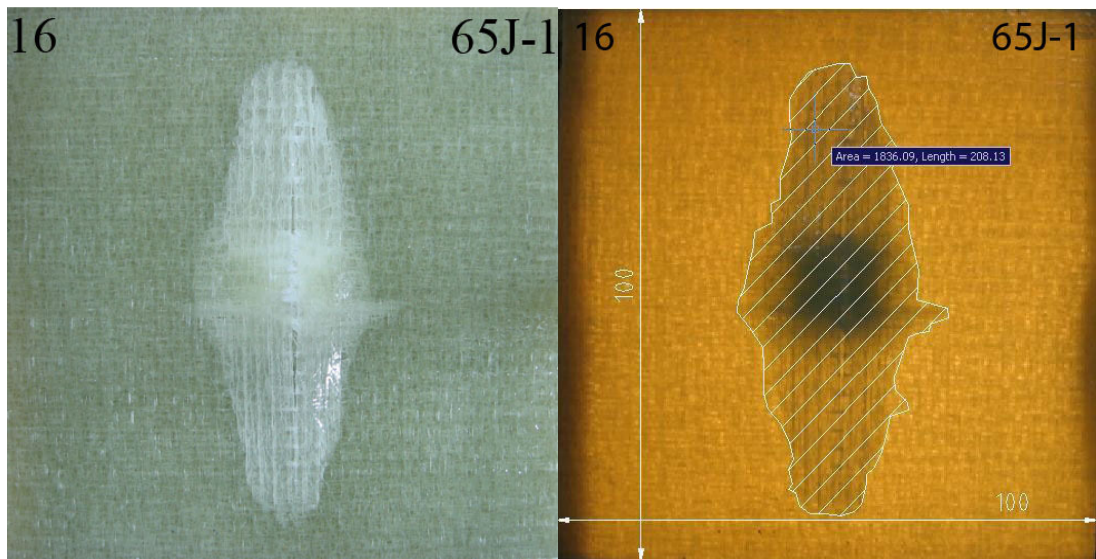
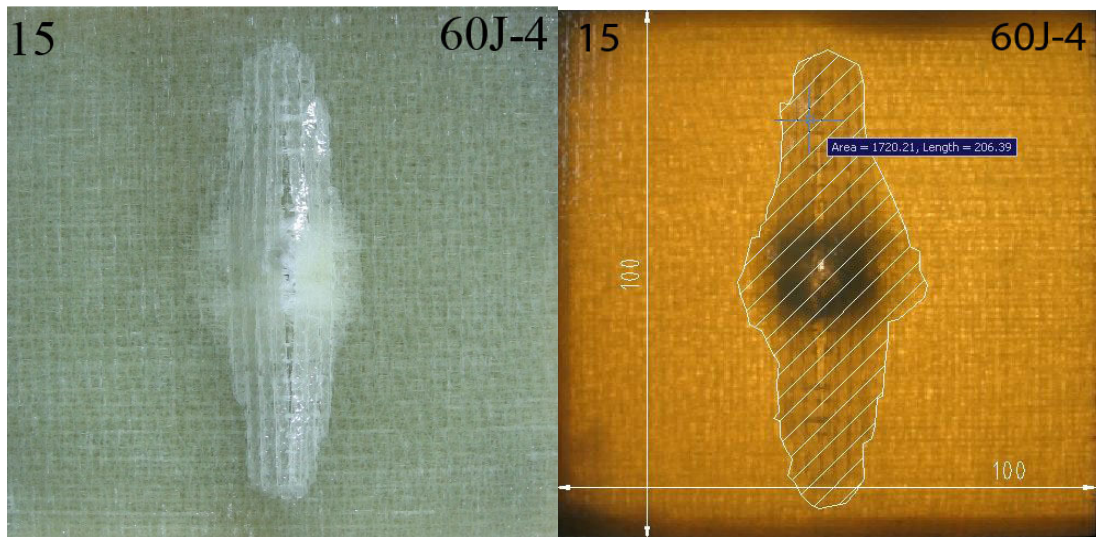
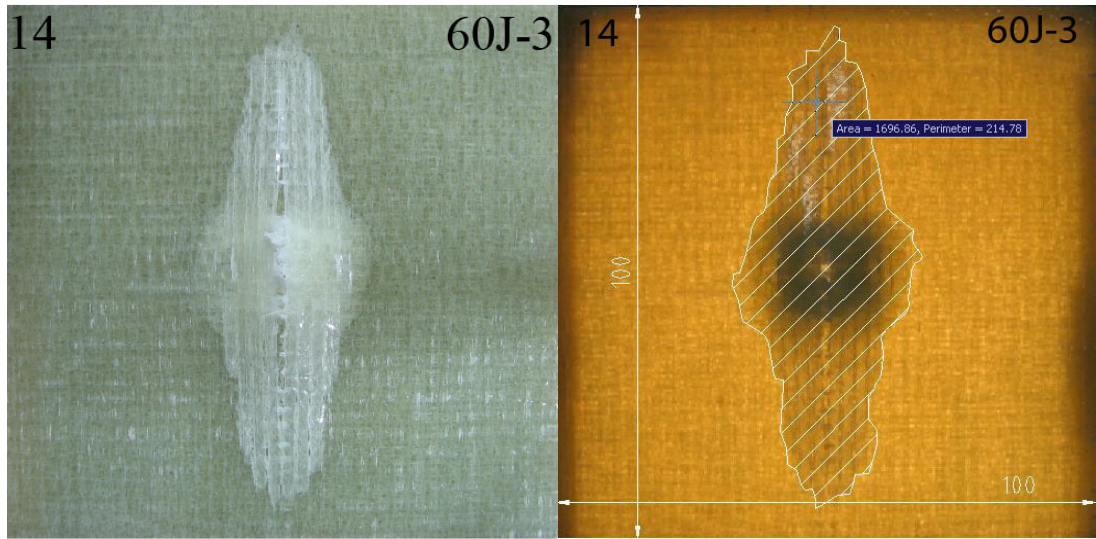


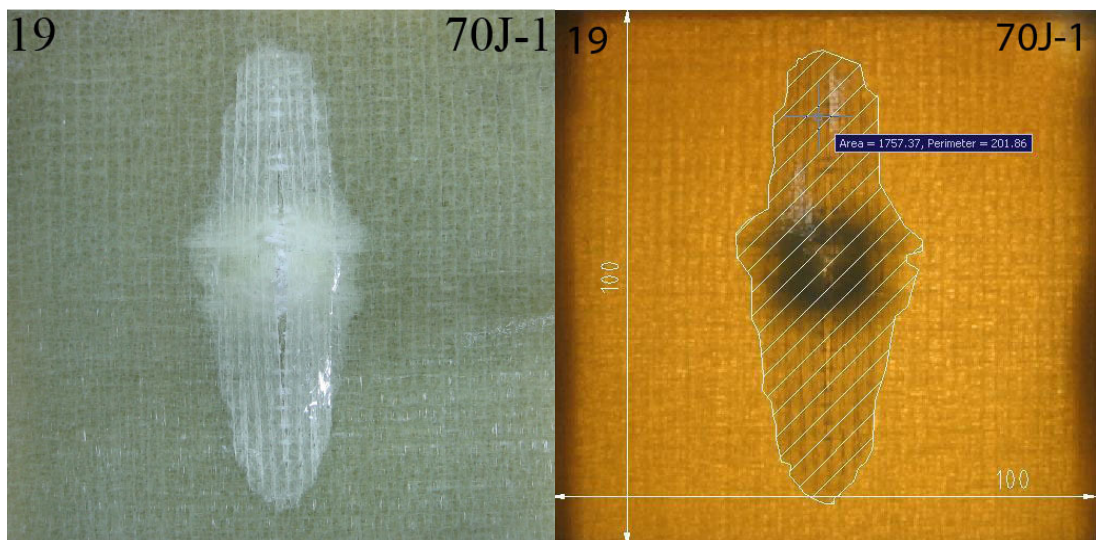
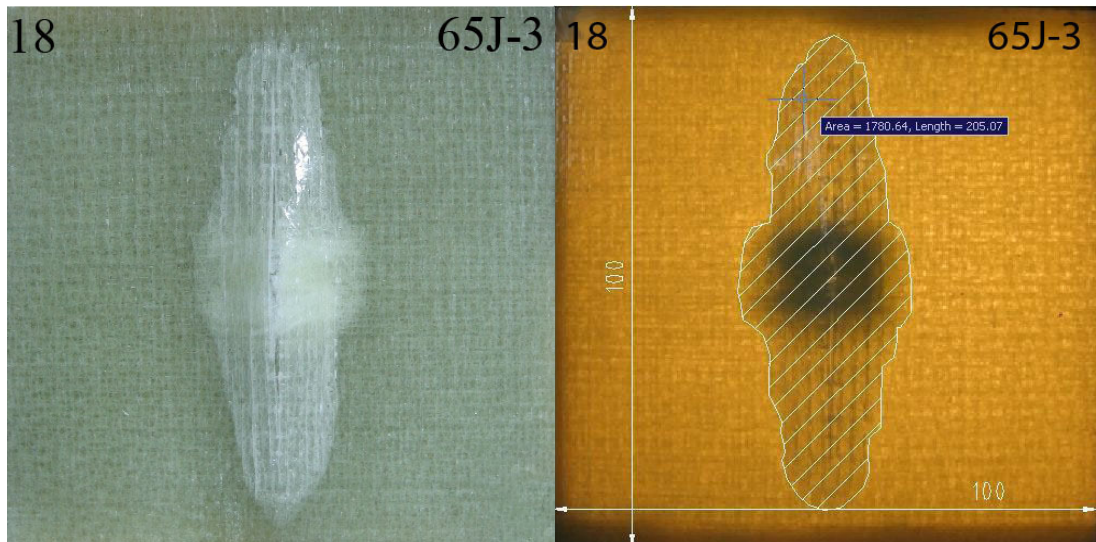
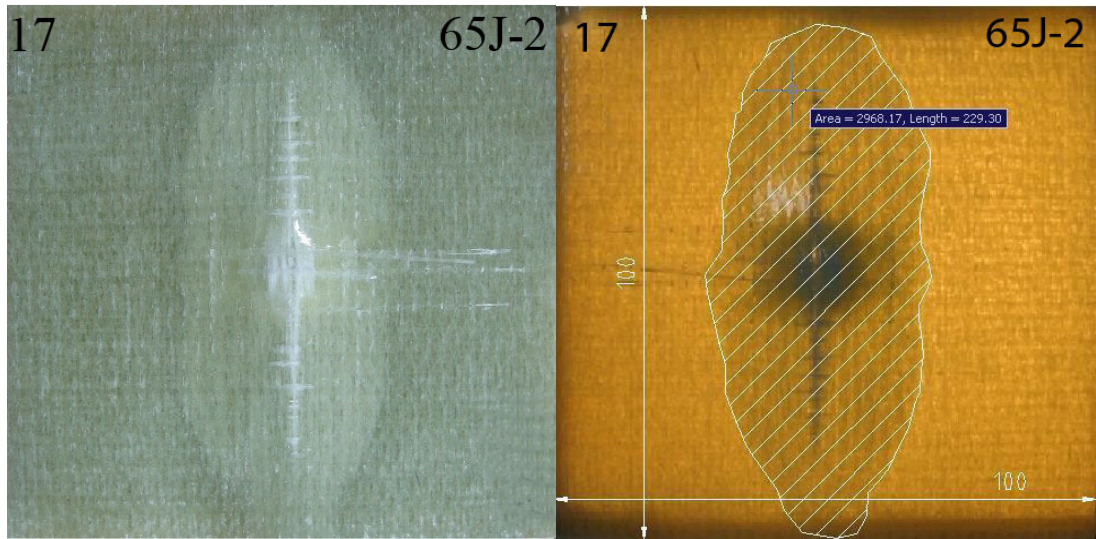


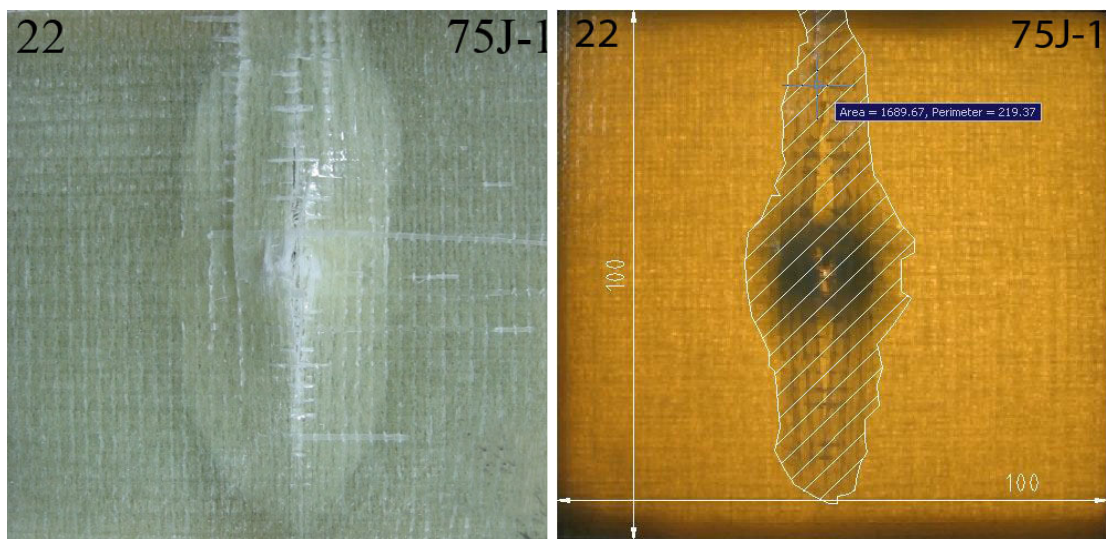
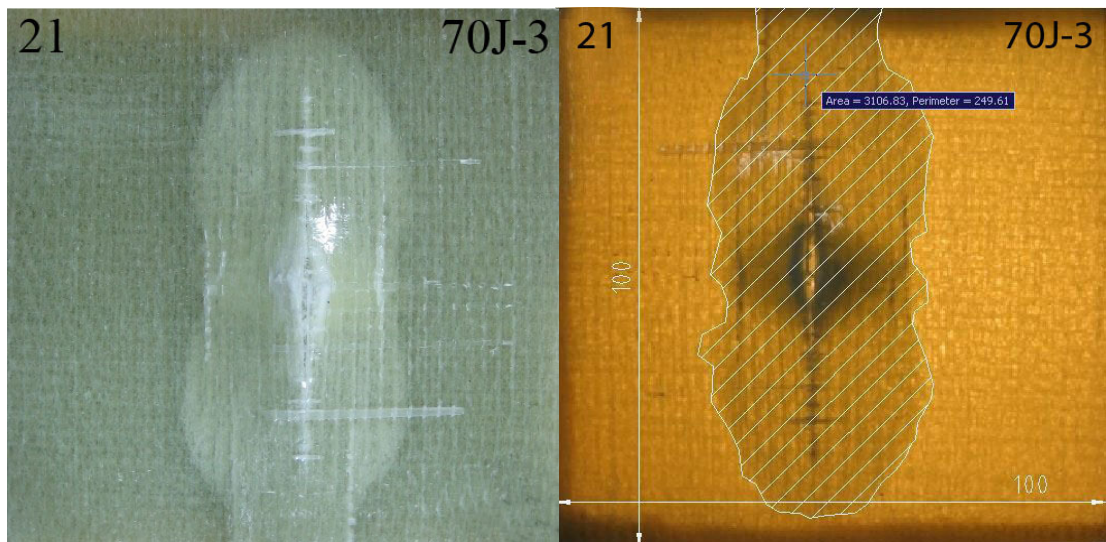
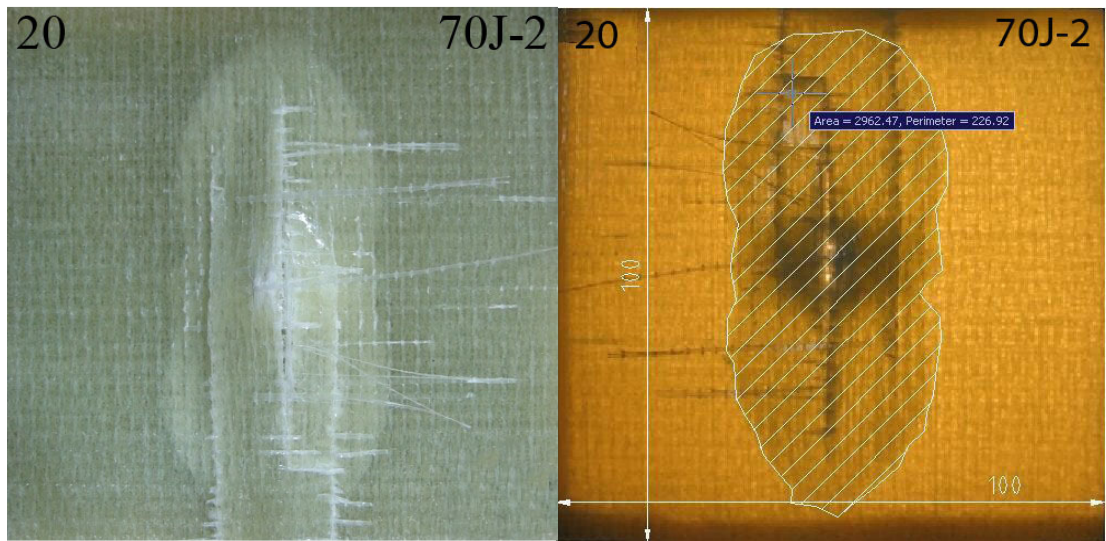


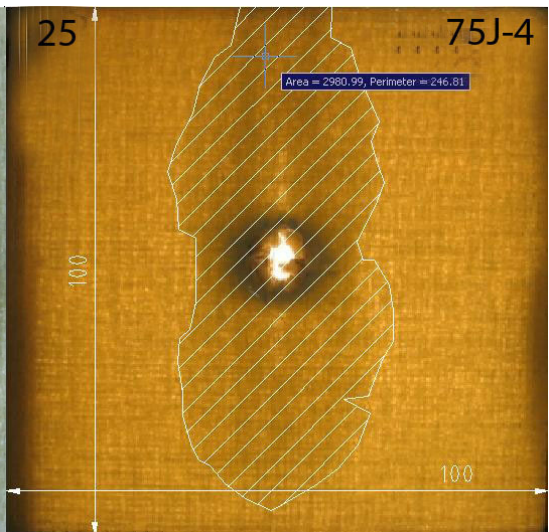
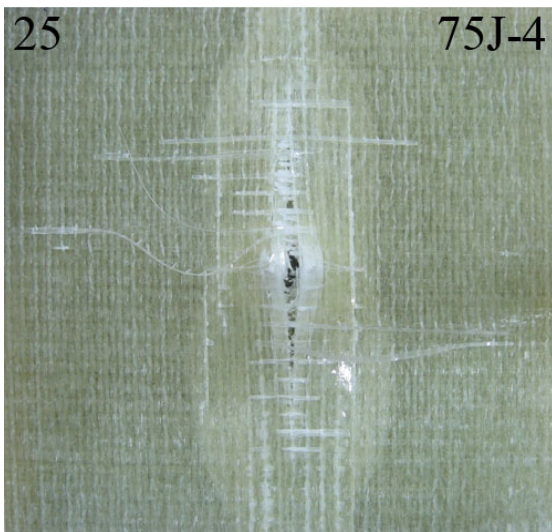
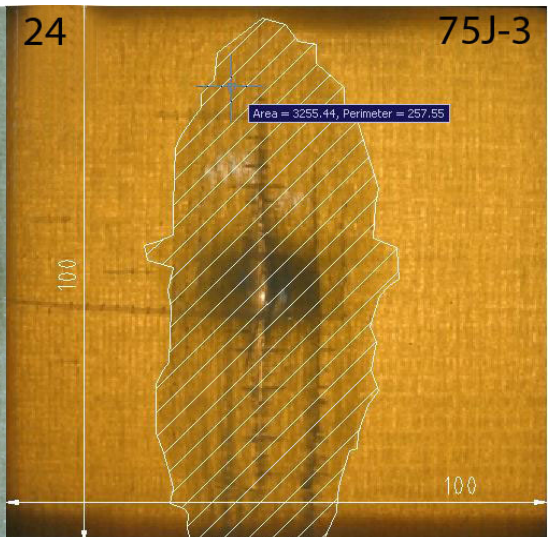
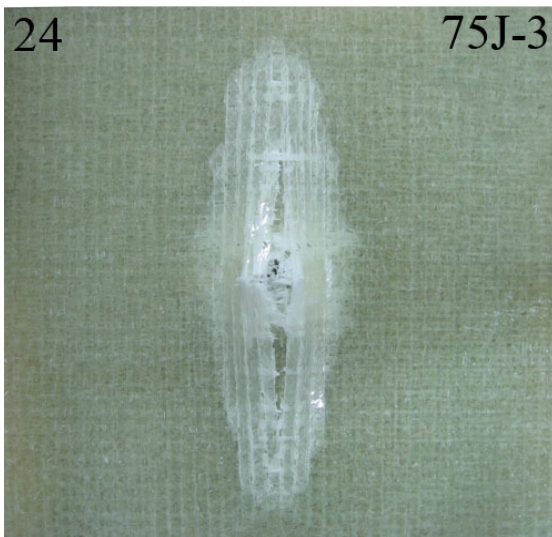
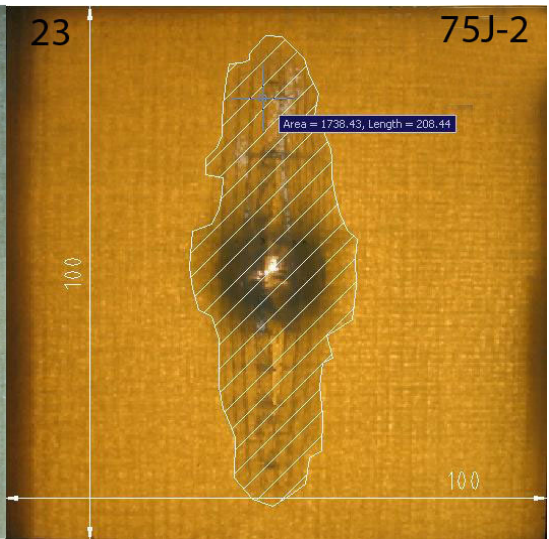
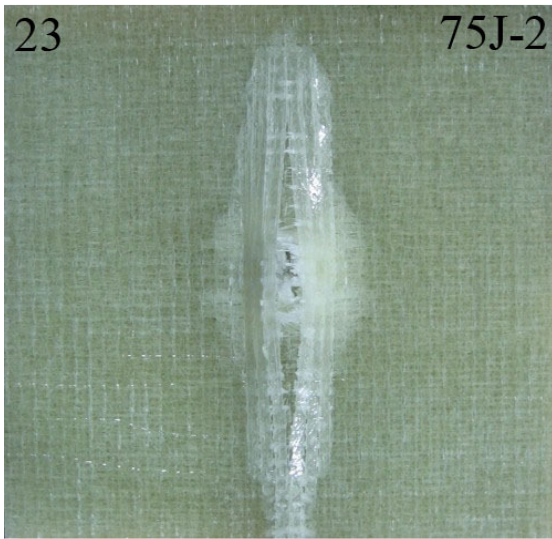


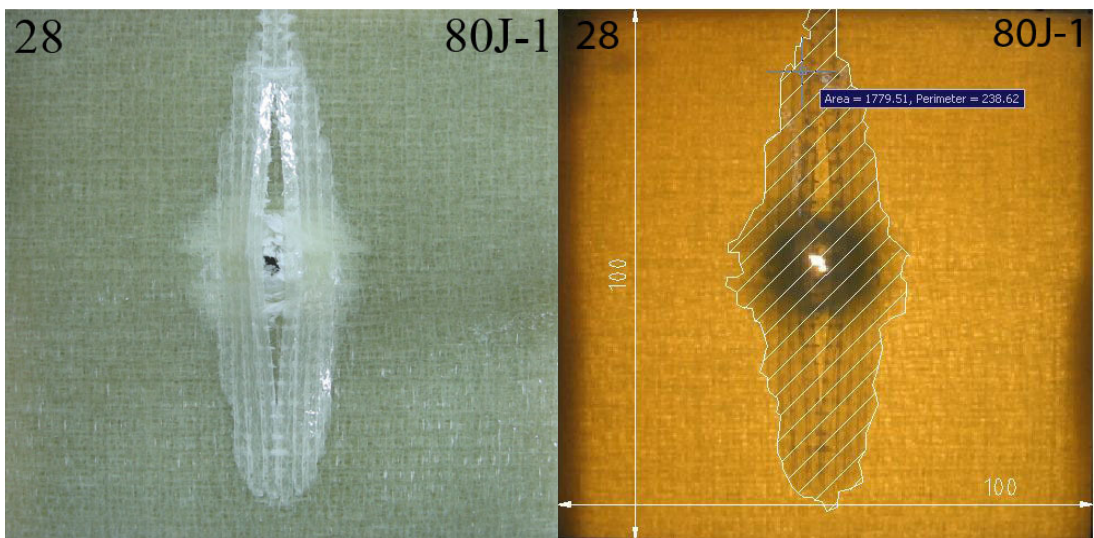
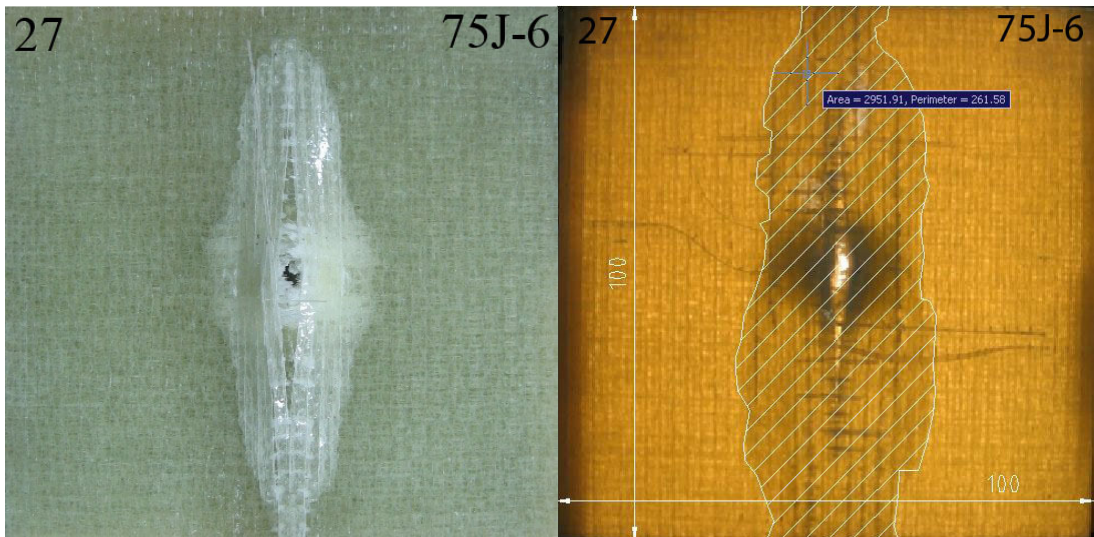
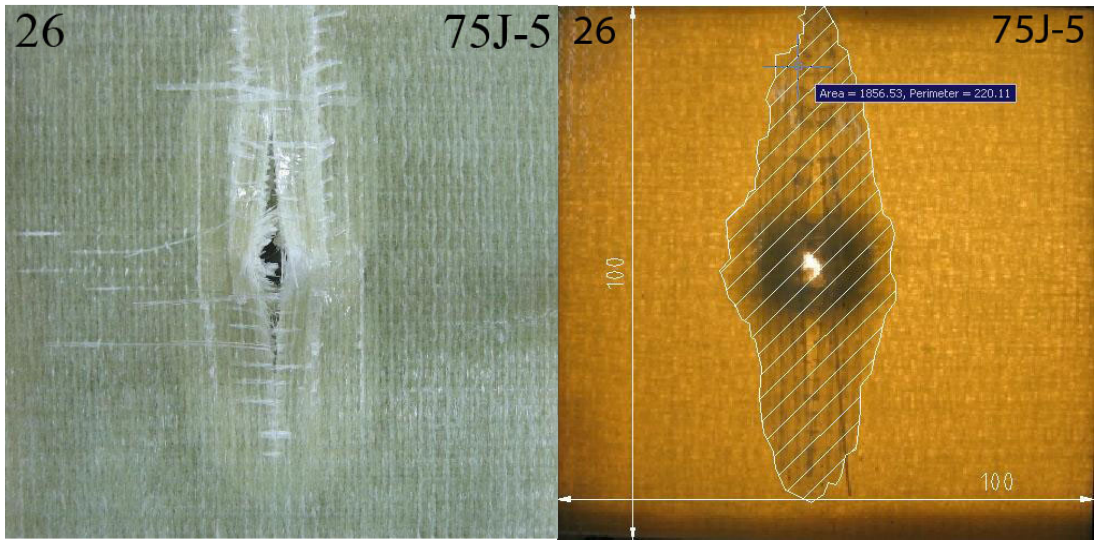


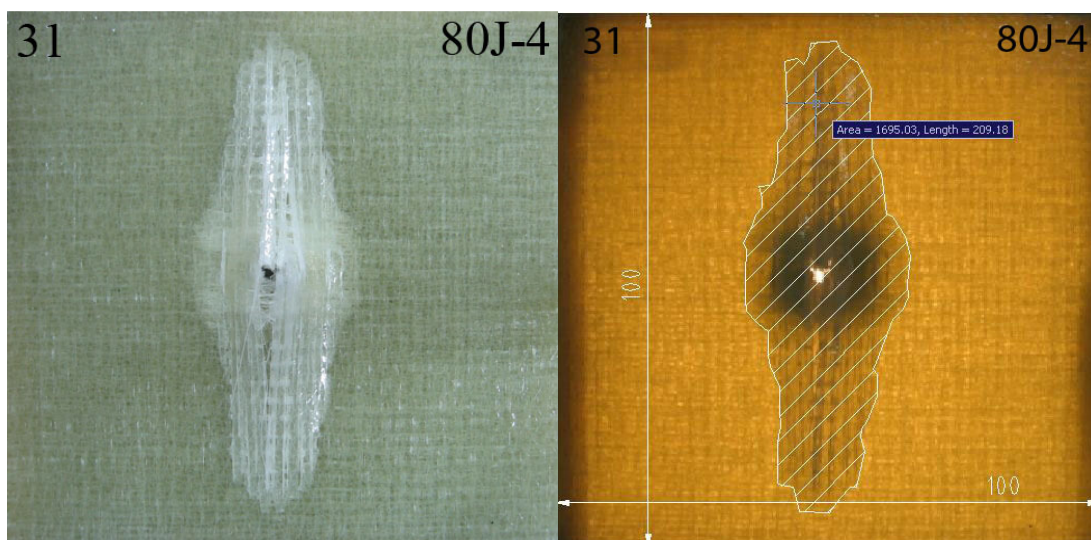
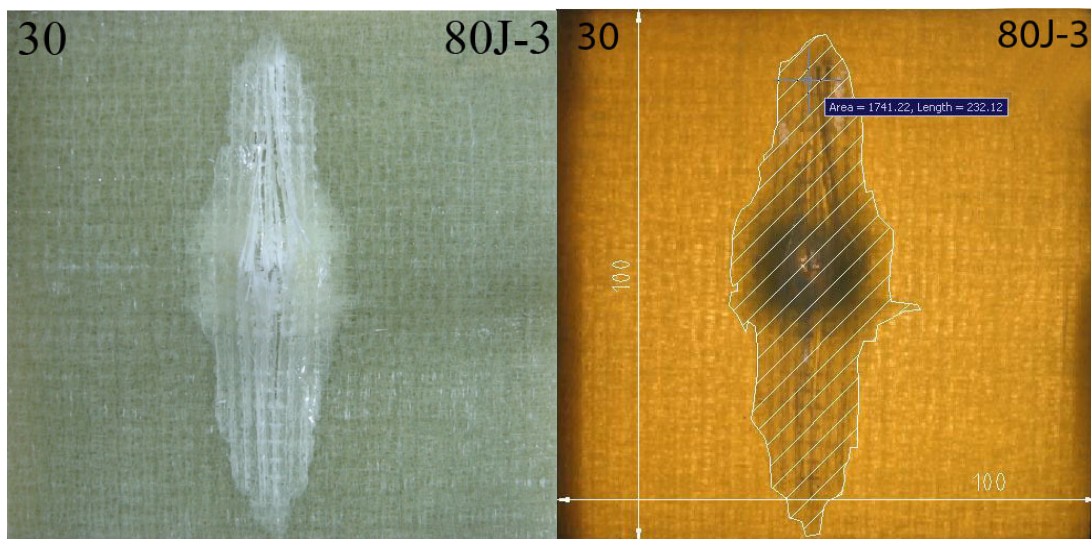
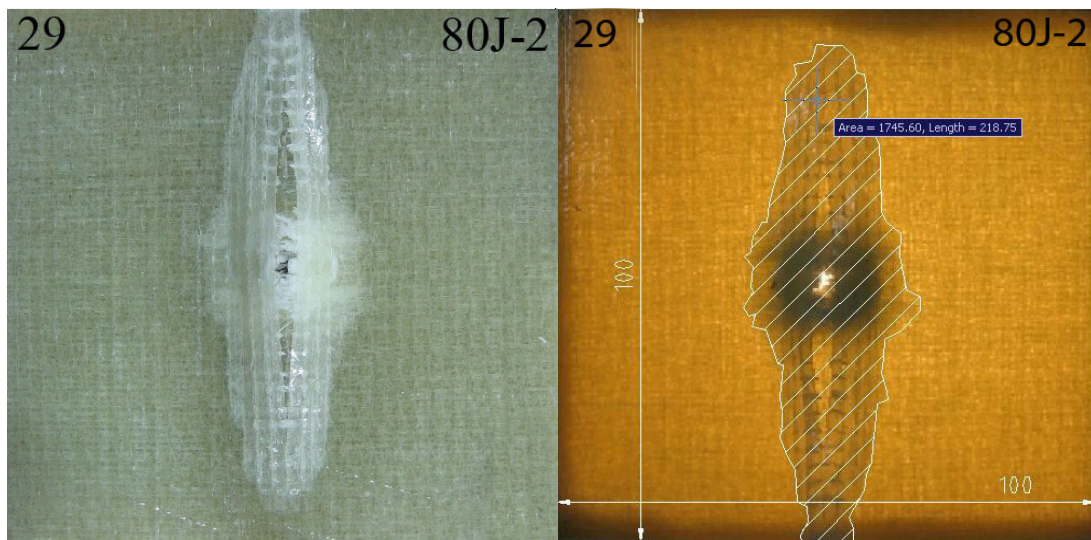


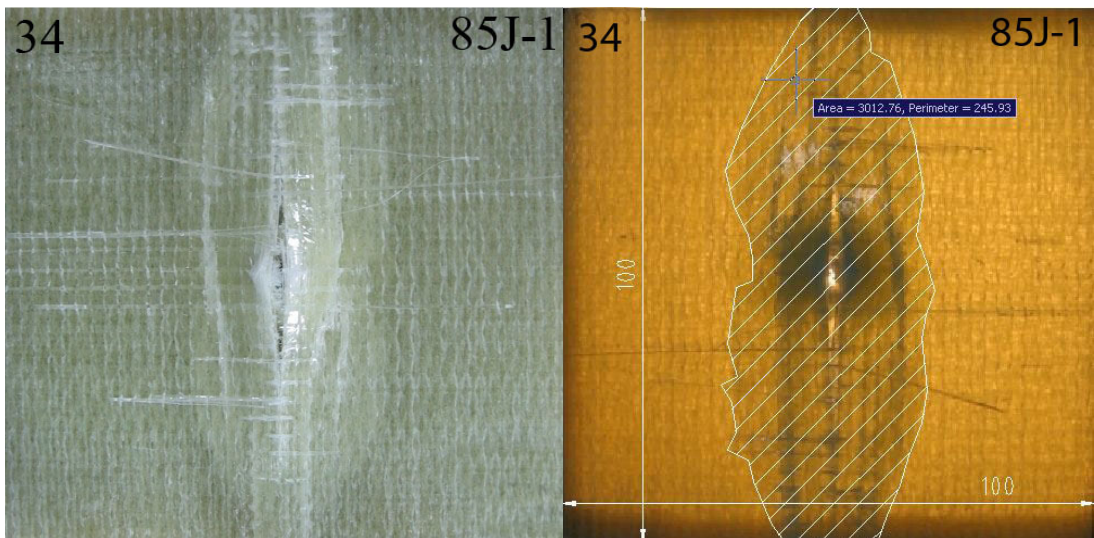
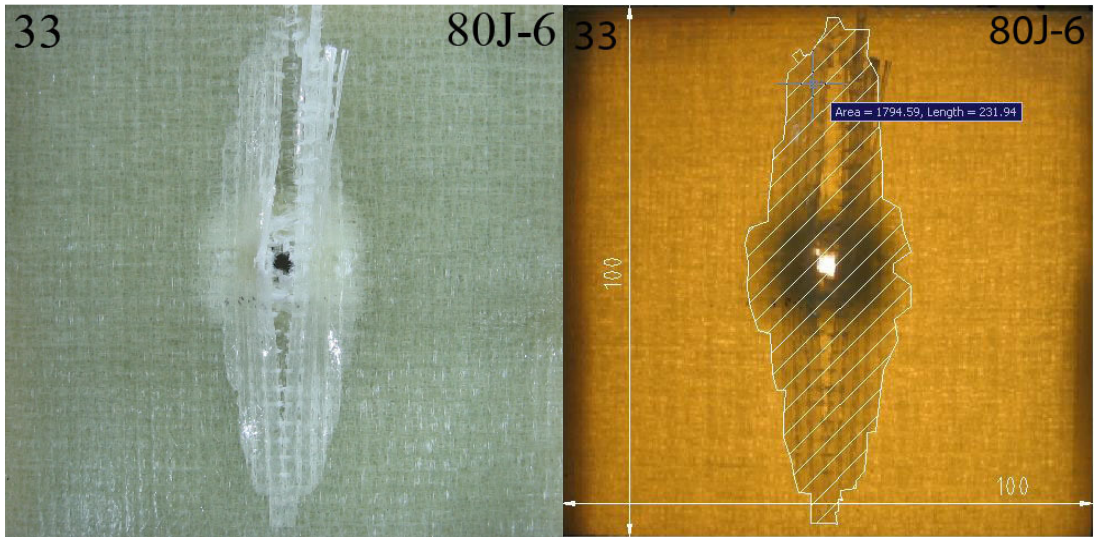
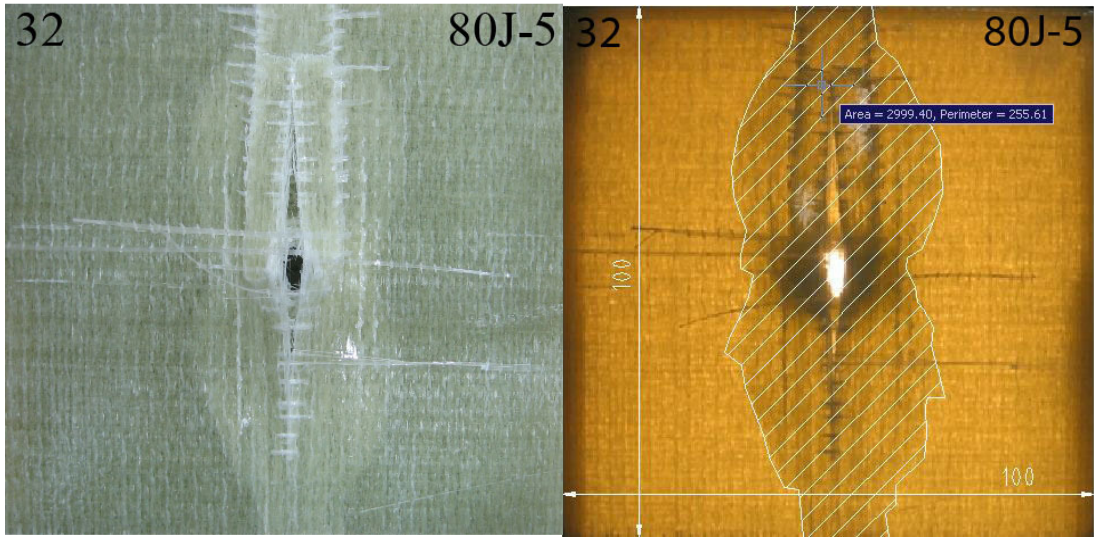


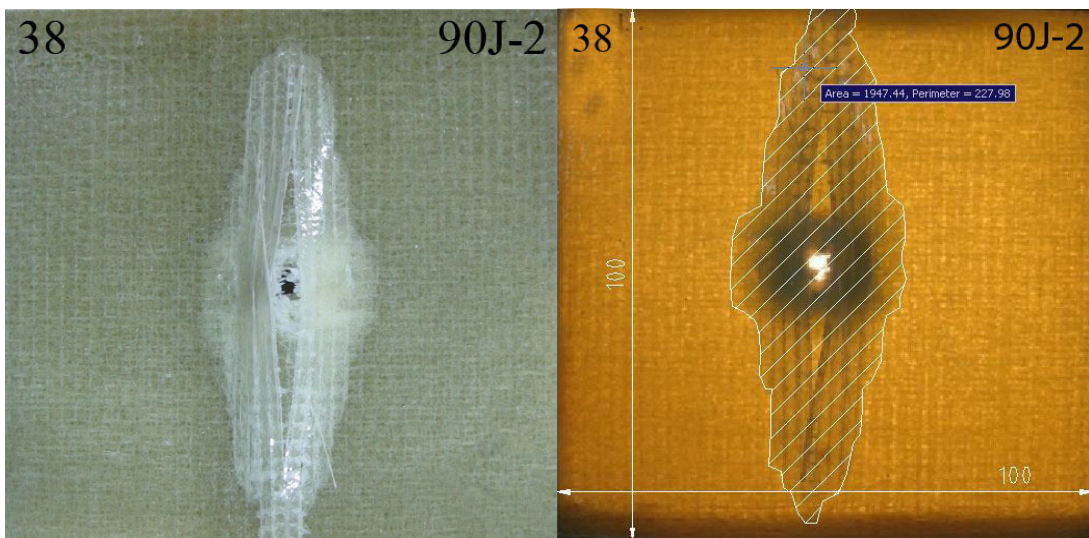
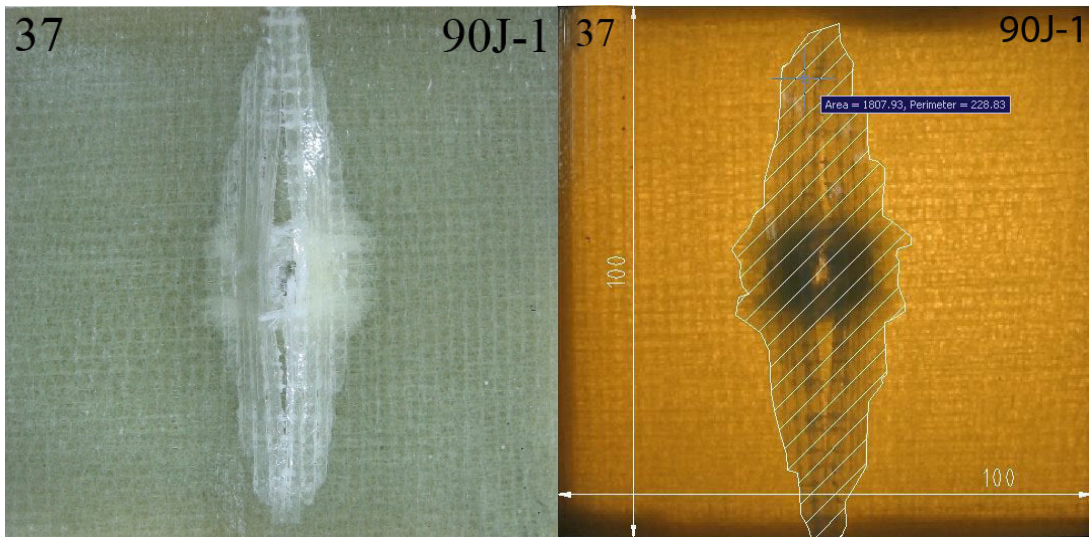
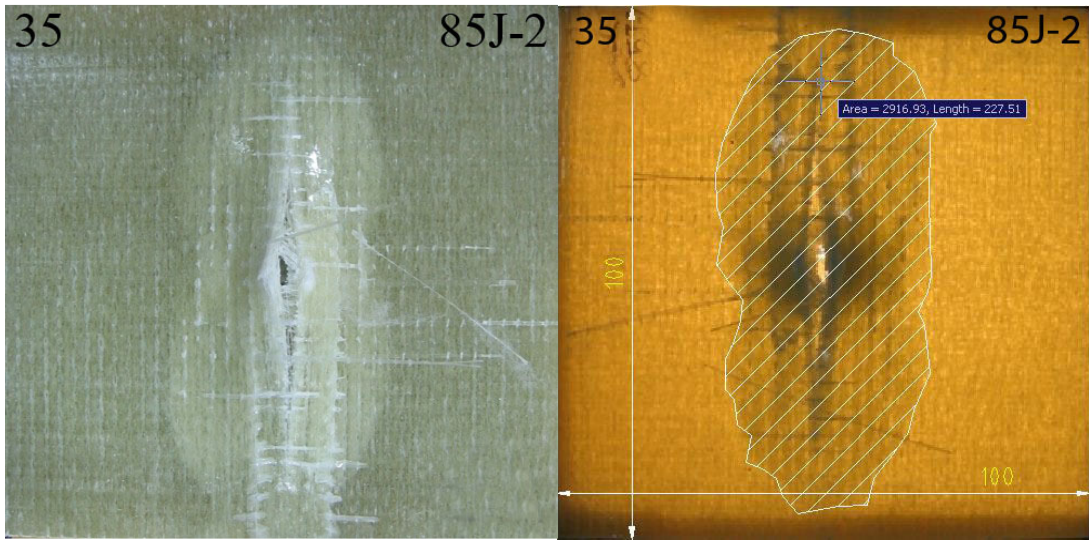


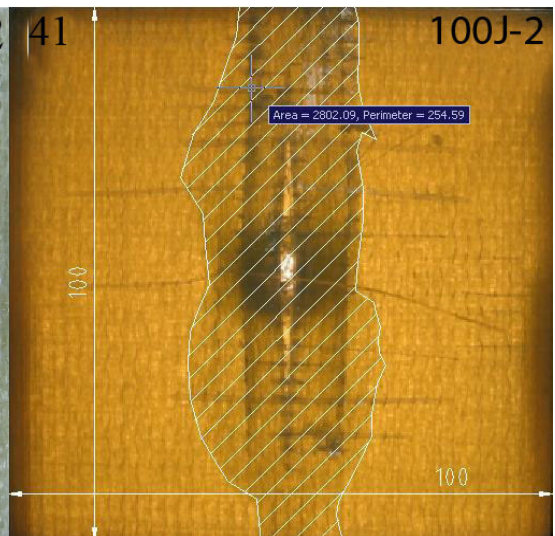
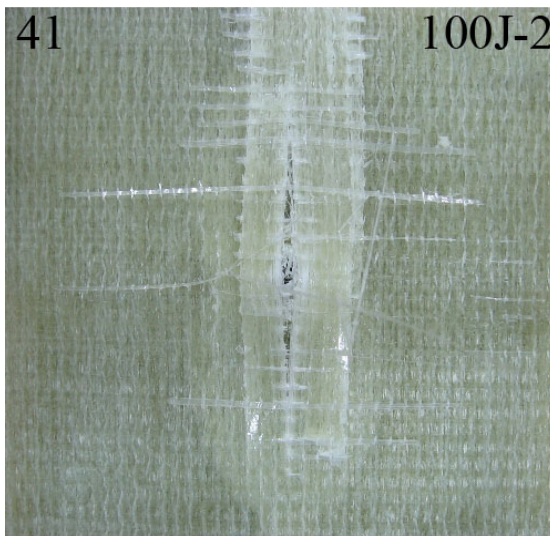
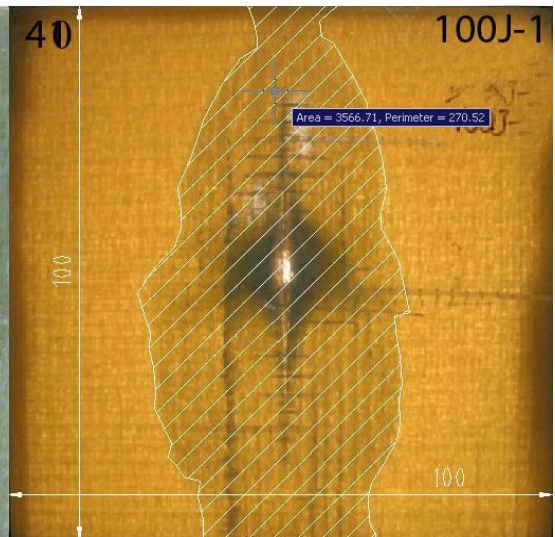
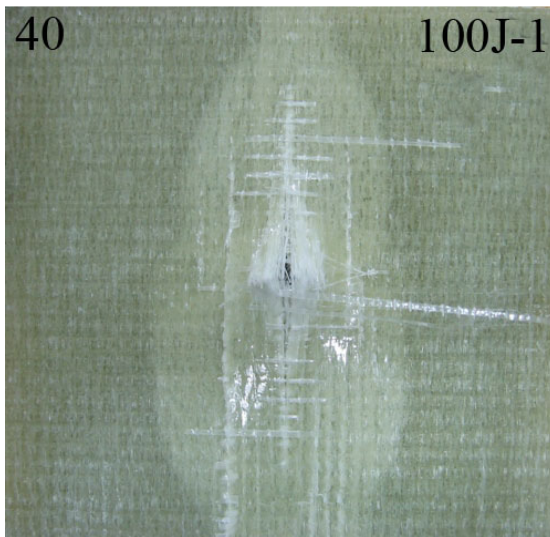
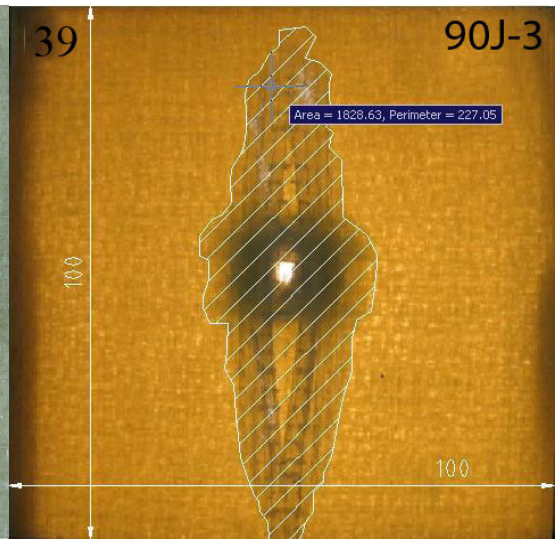
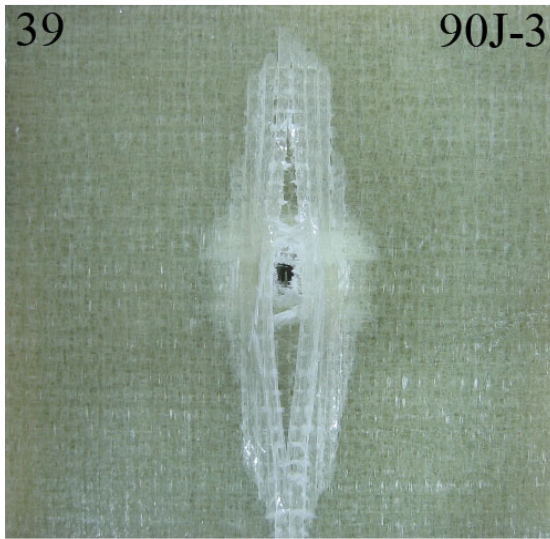












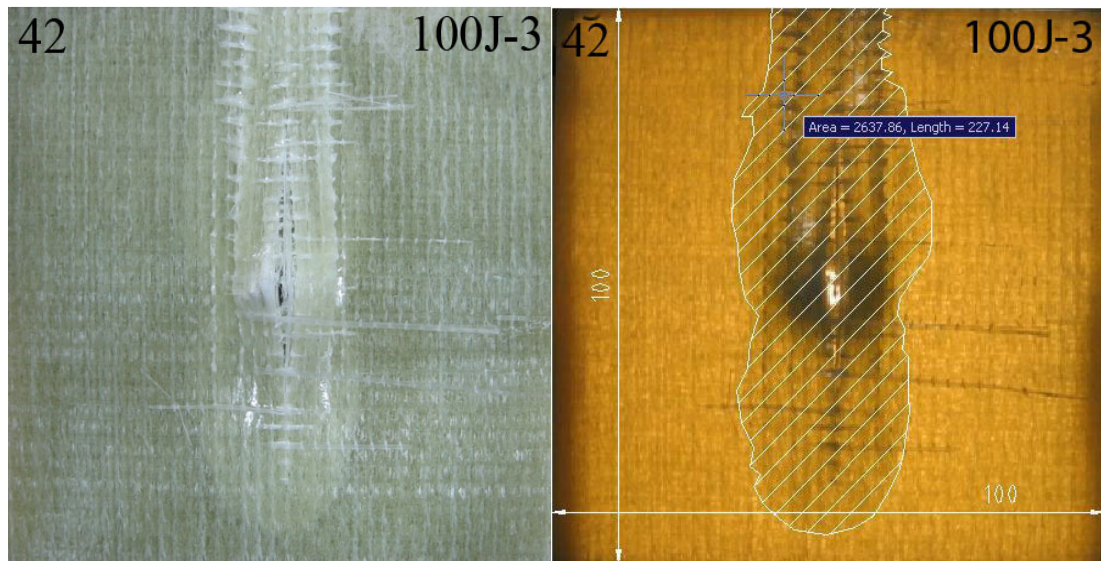


Figure 4.22 Photographs of the specimens (normal left, with a strong light behind right)

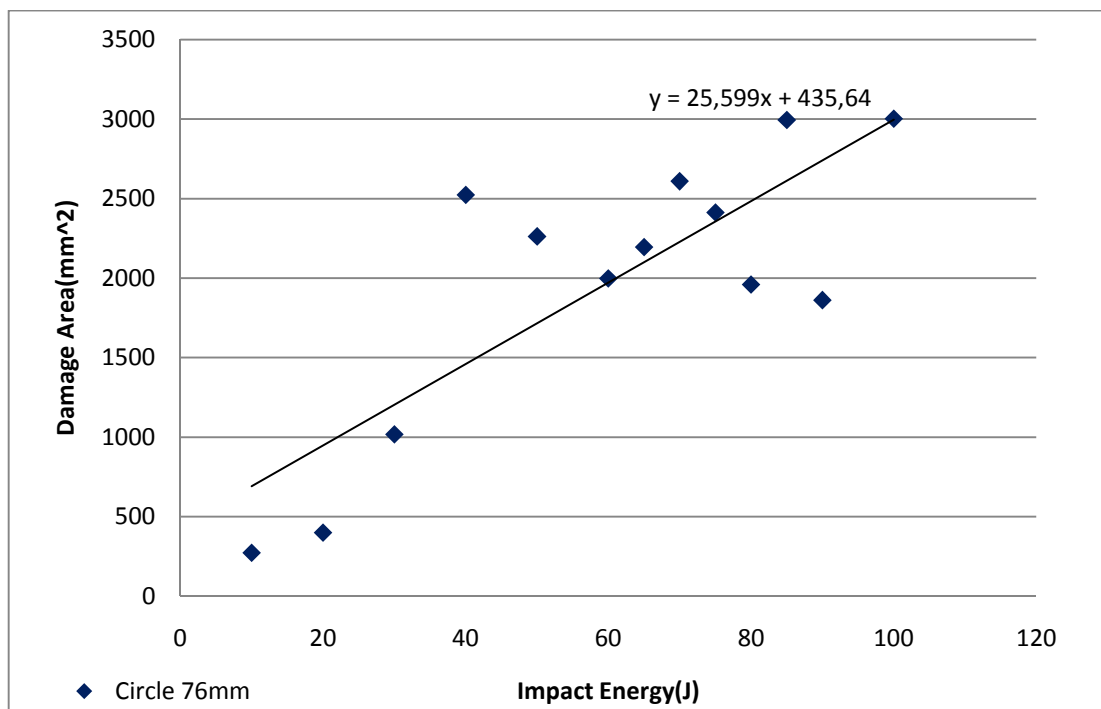
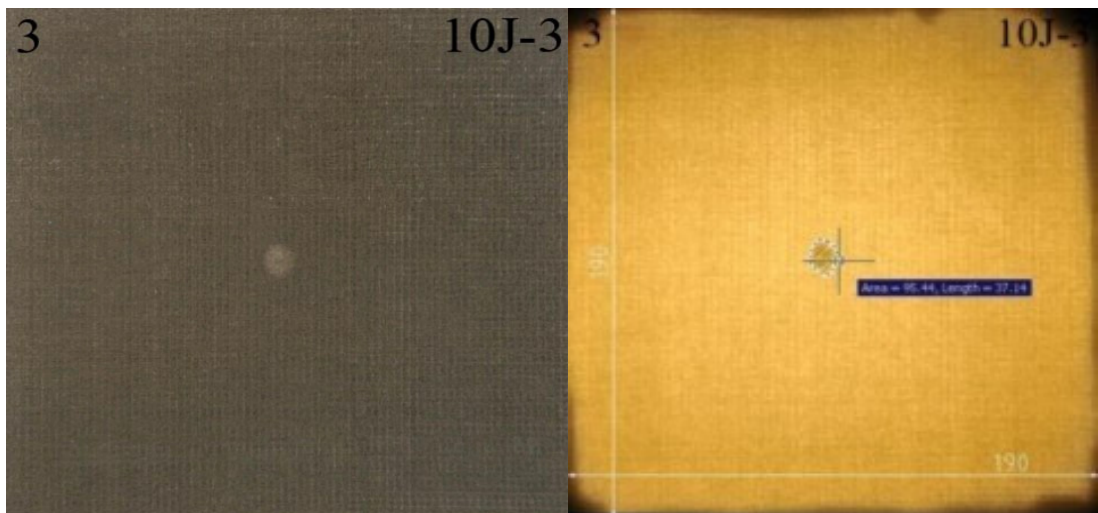
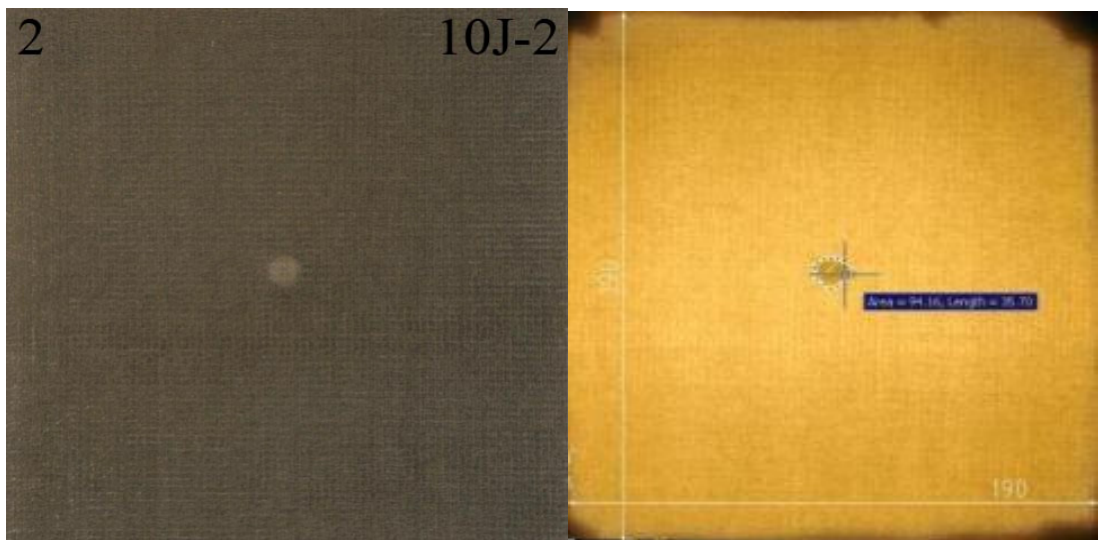
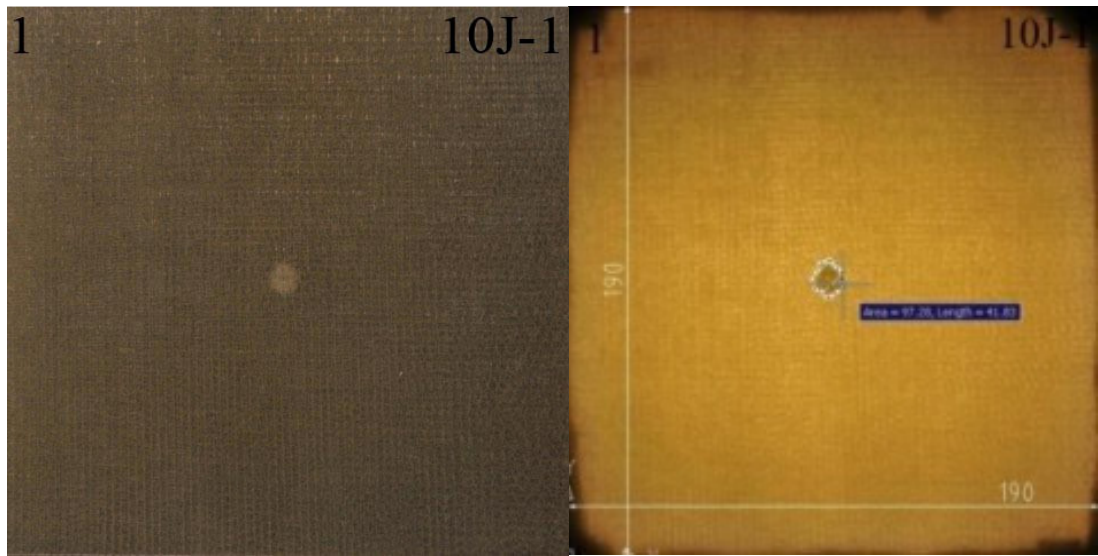
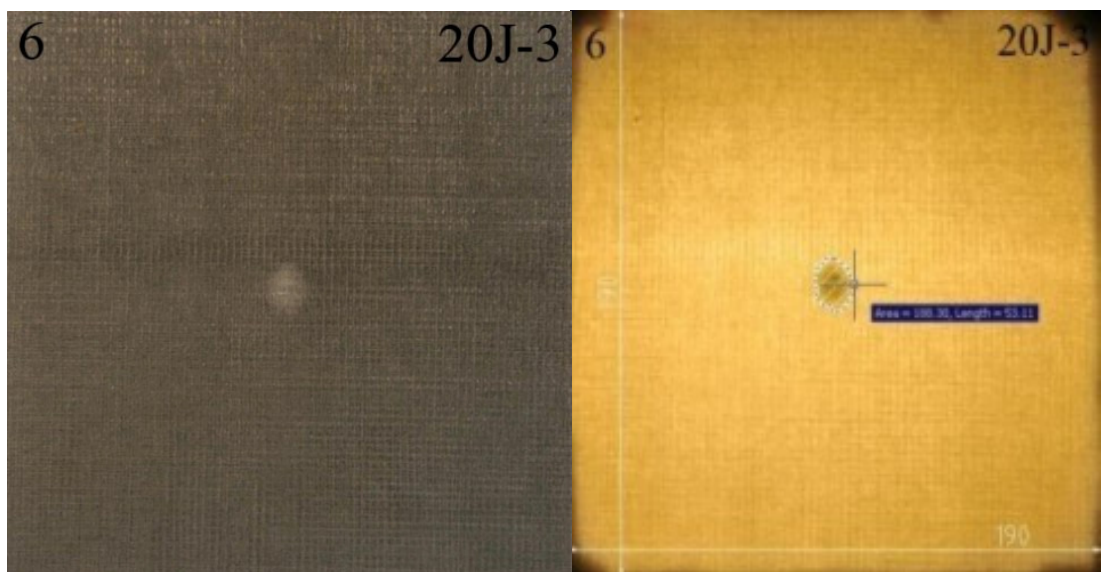
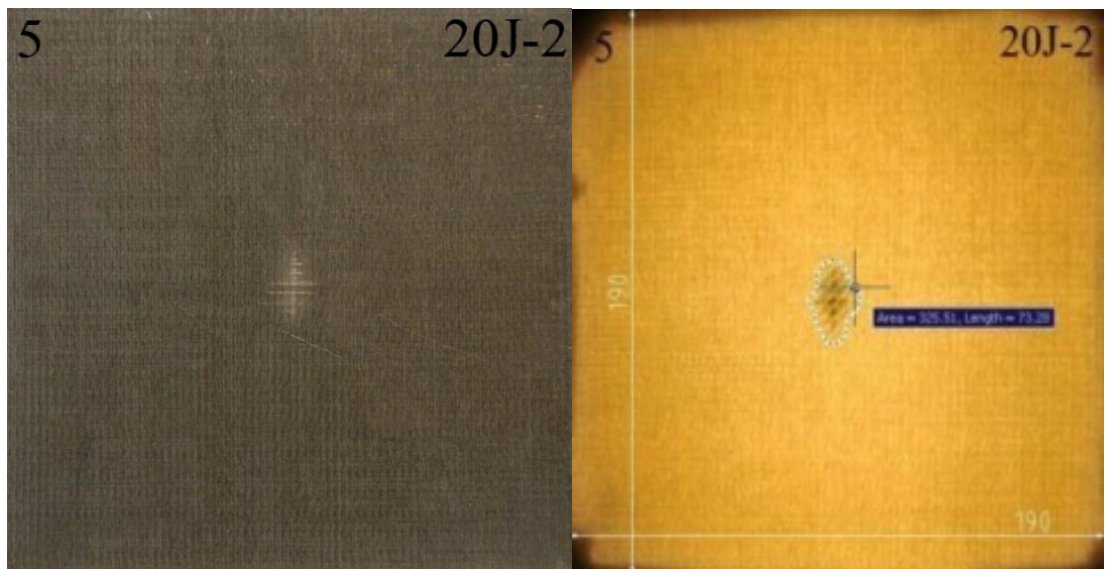
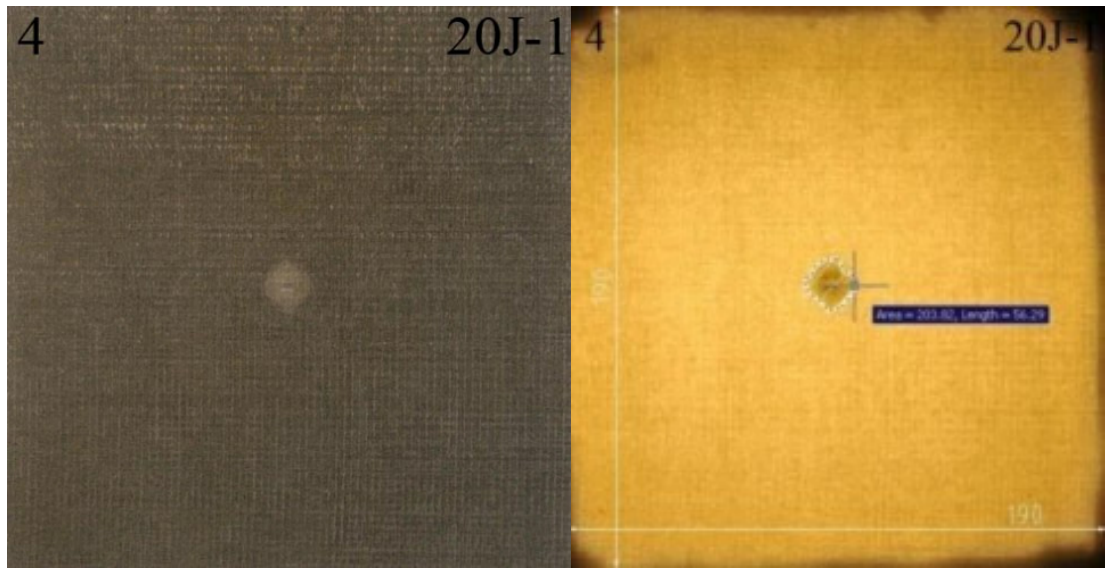
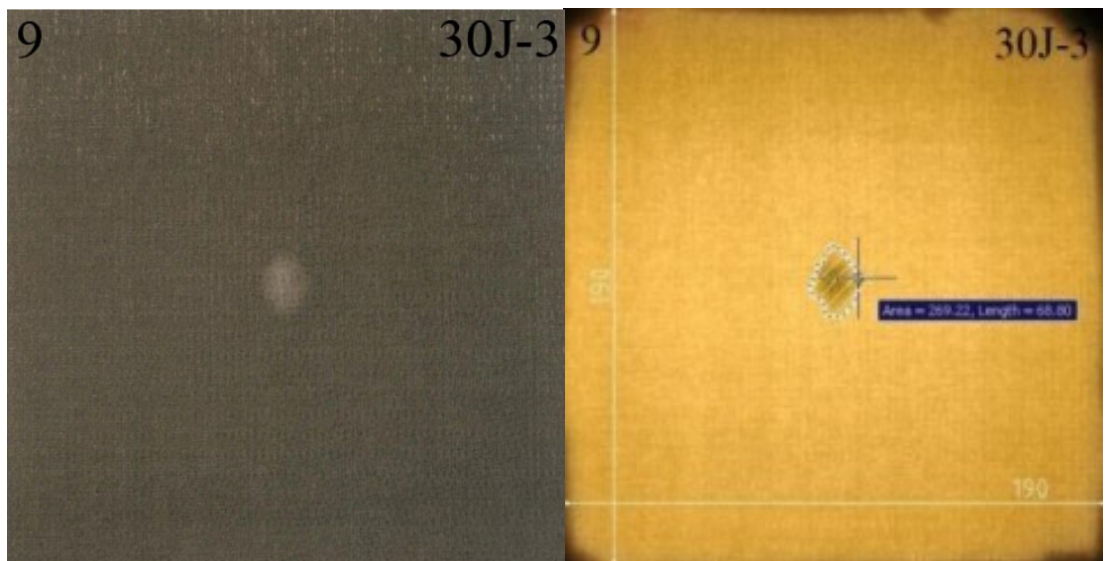
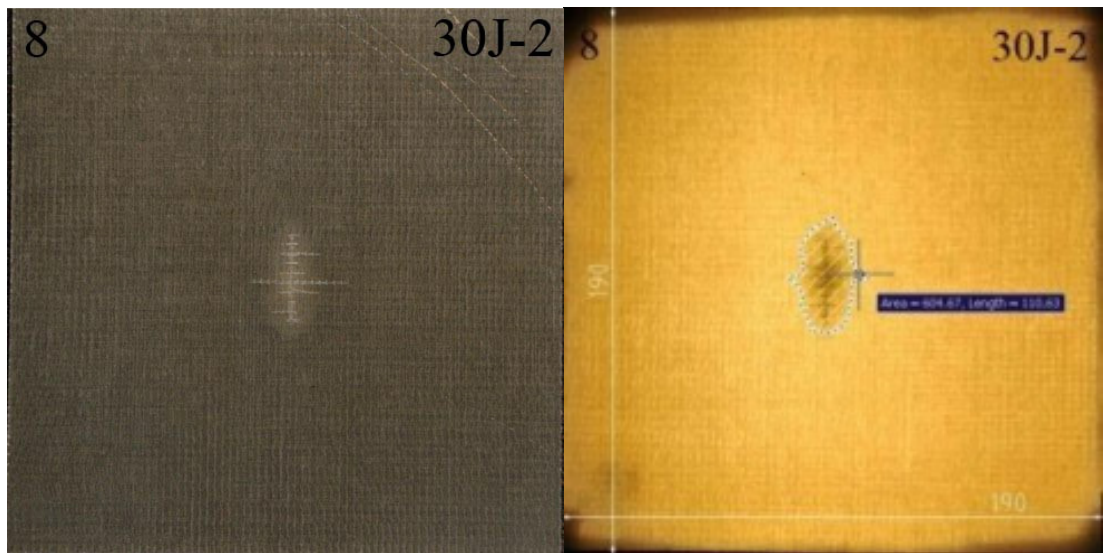
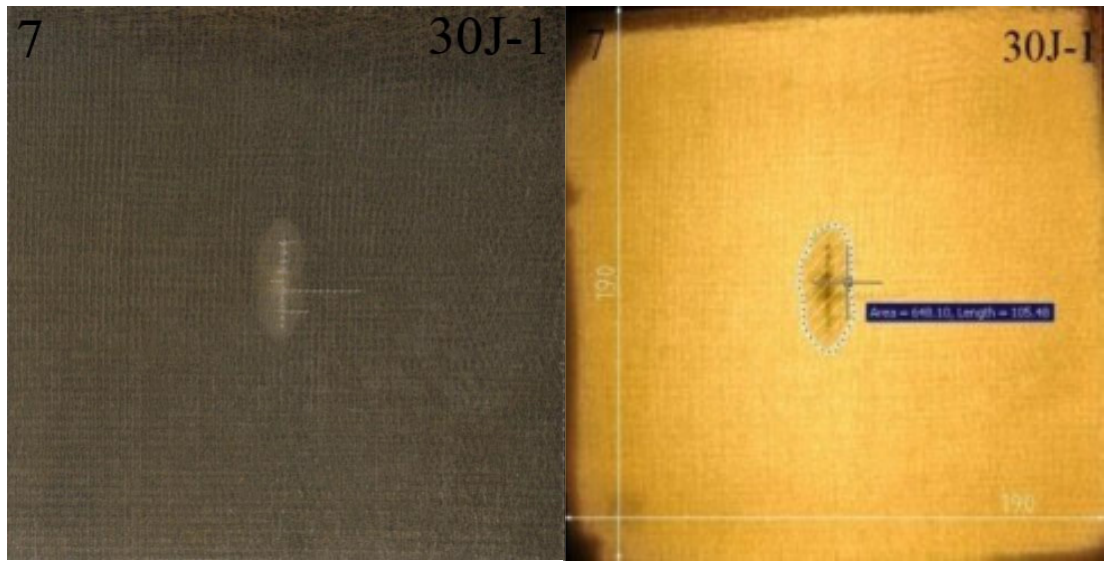


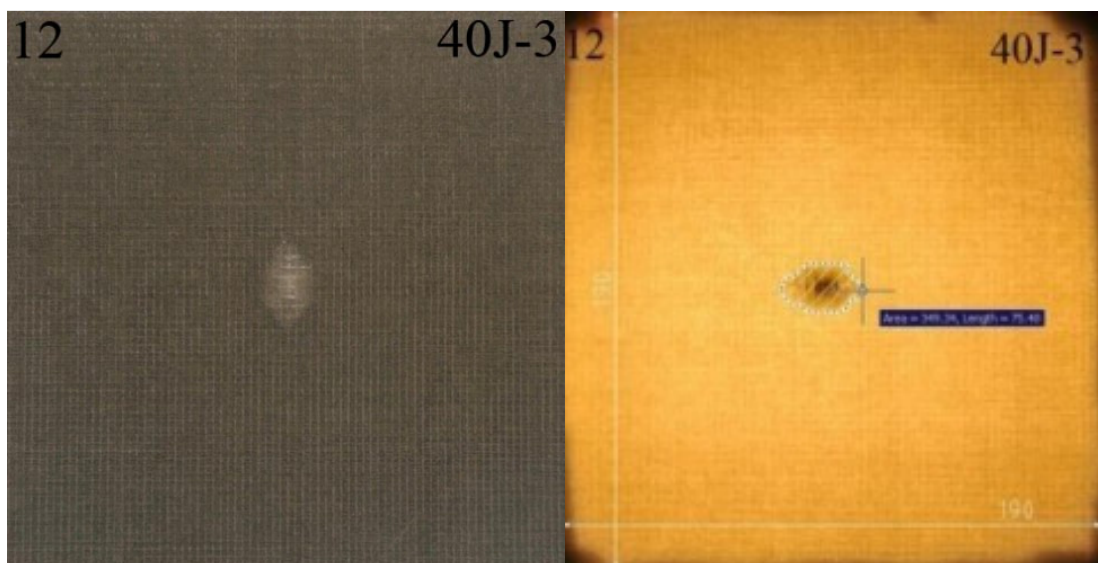
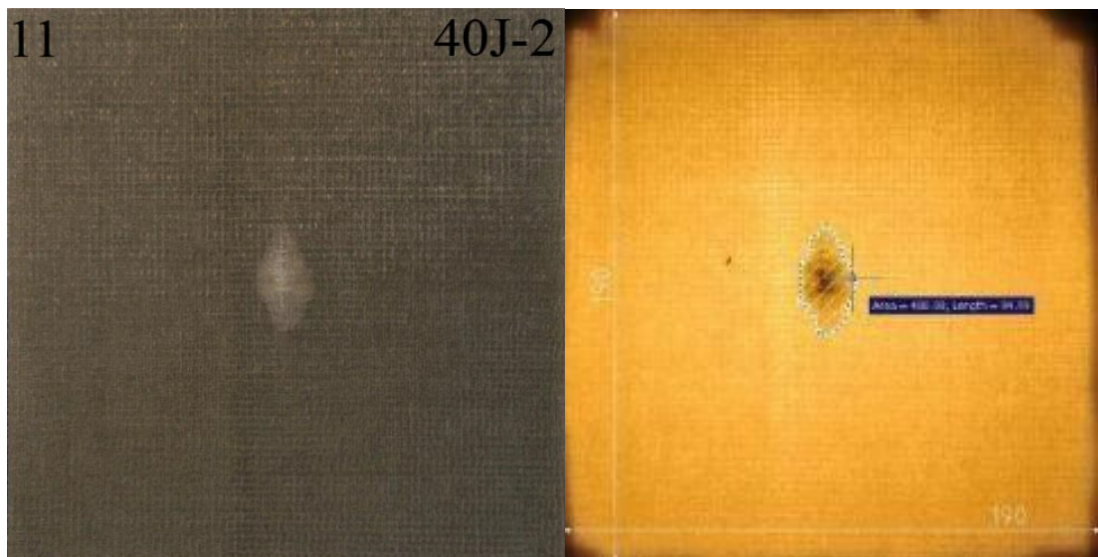
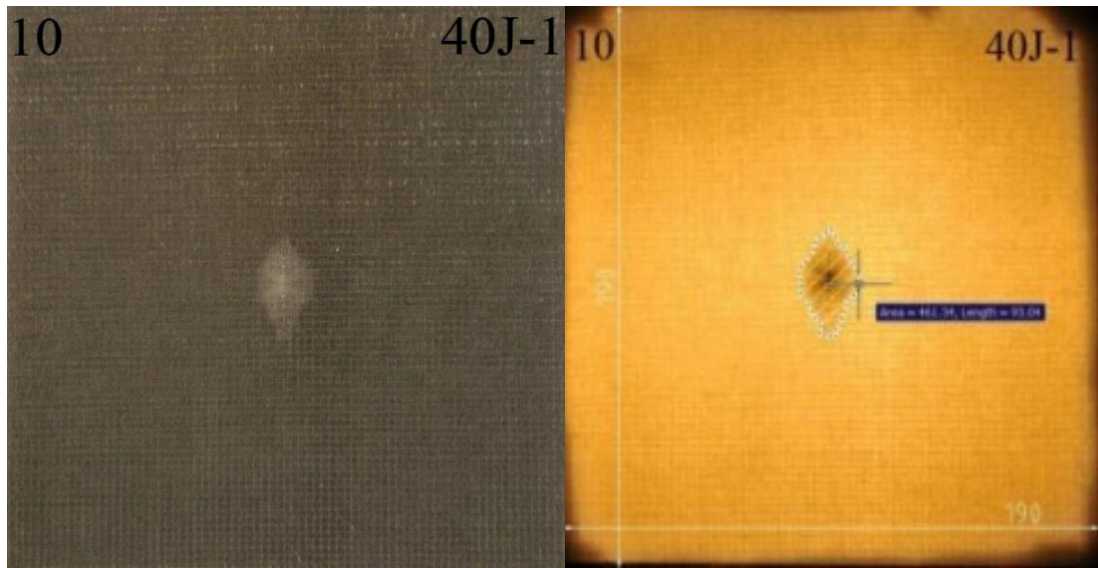
Figure 4.23 Damage area-Impact energy history of circle with 76 mm of diameter

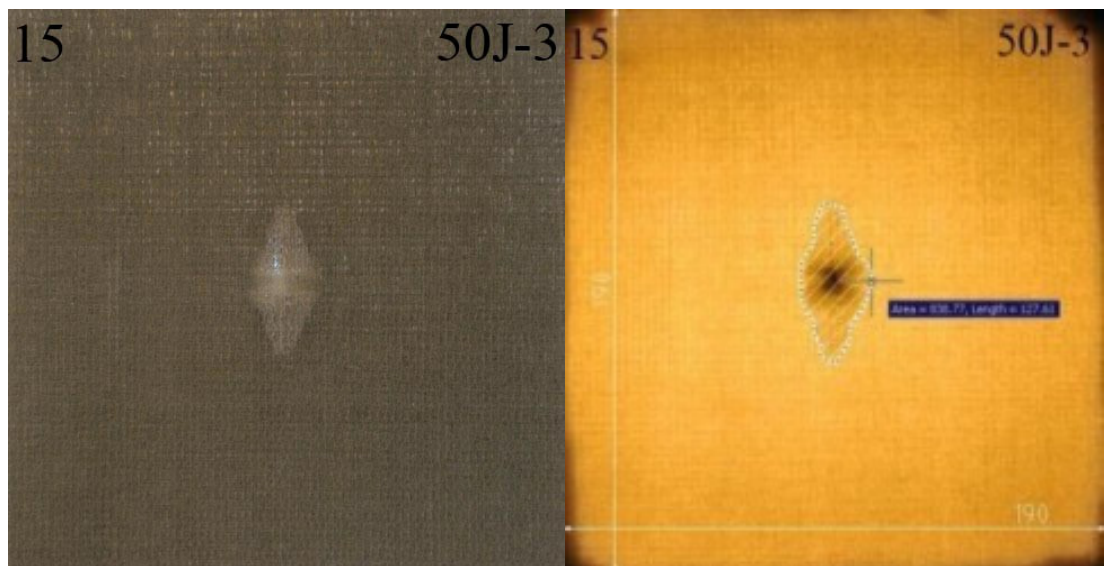
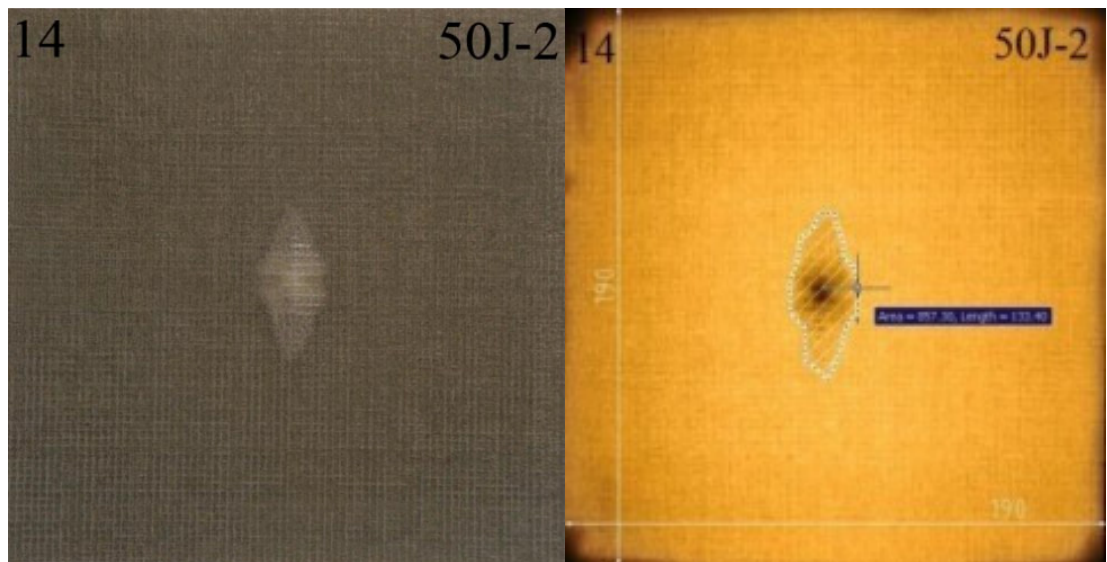
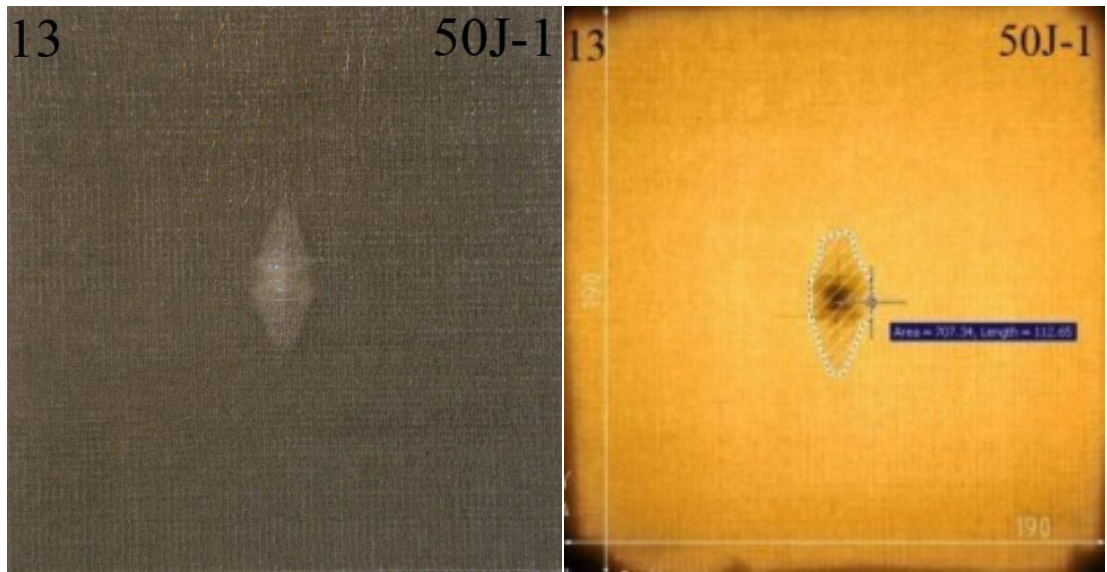
4.4.3 Square with 150 mm per Edge

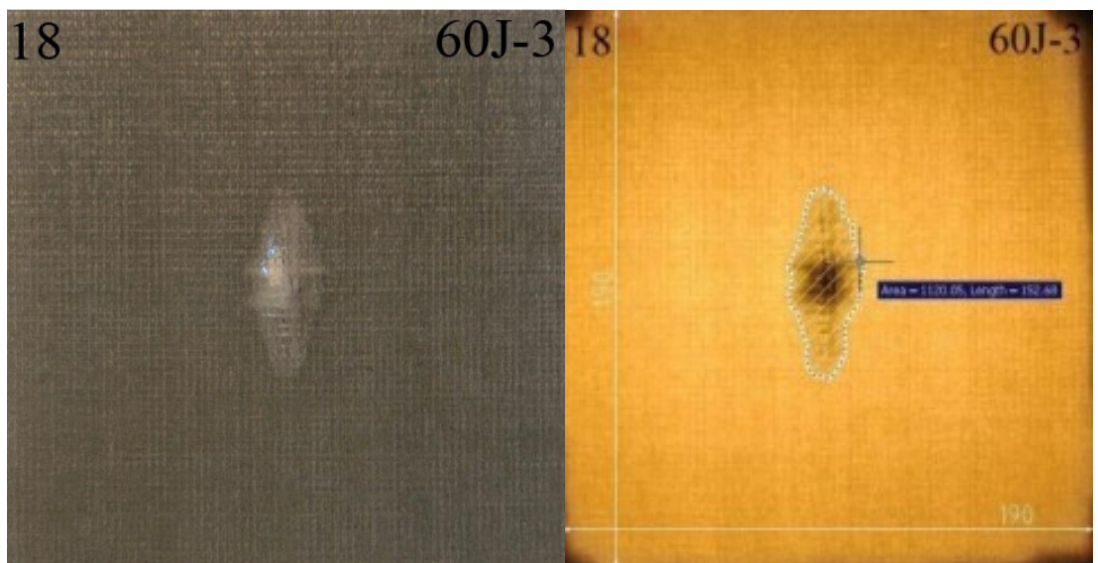
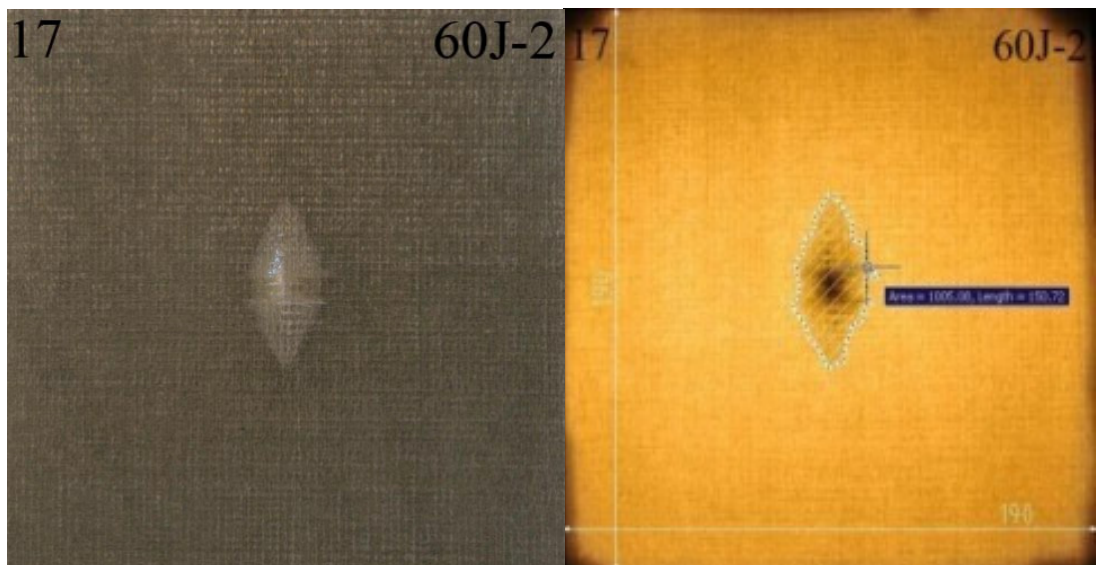
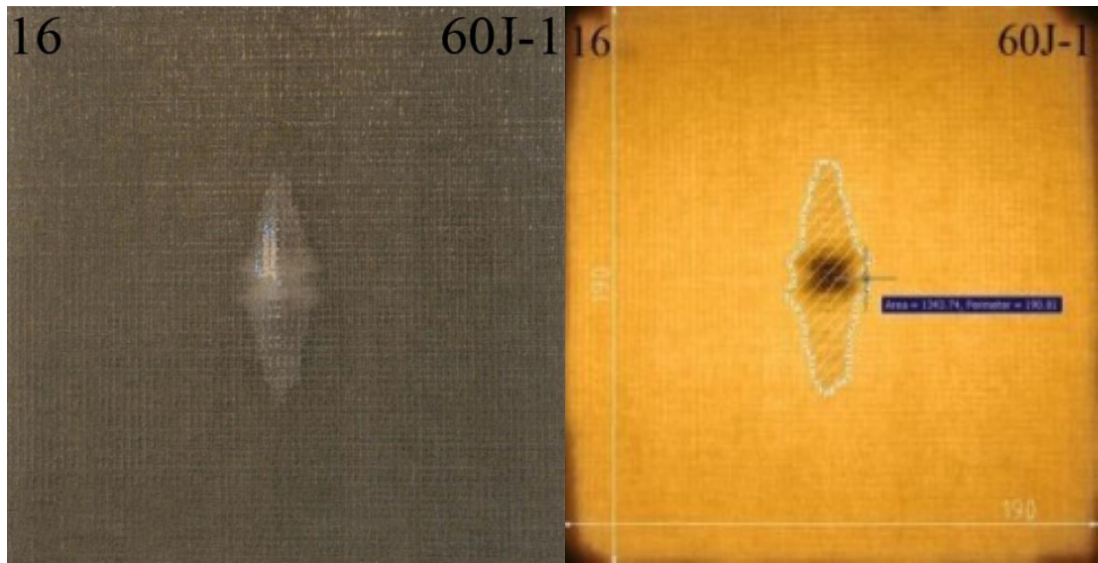


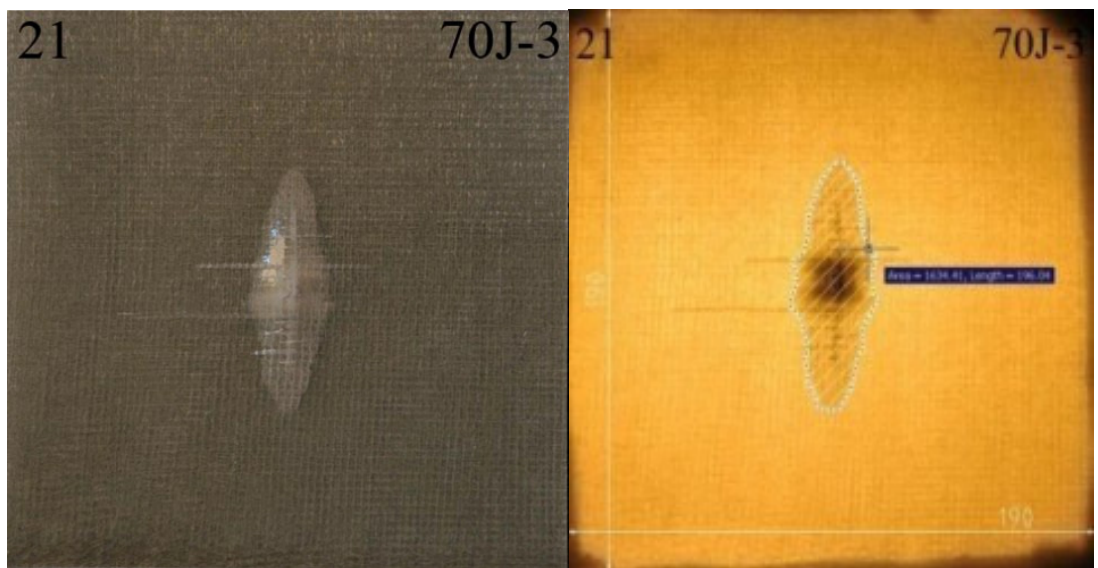


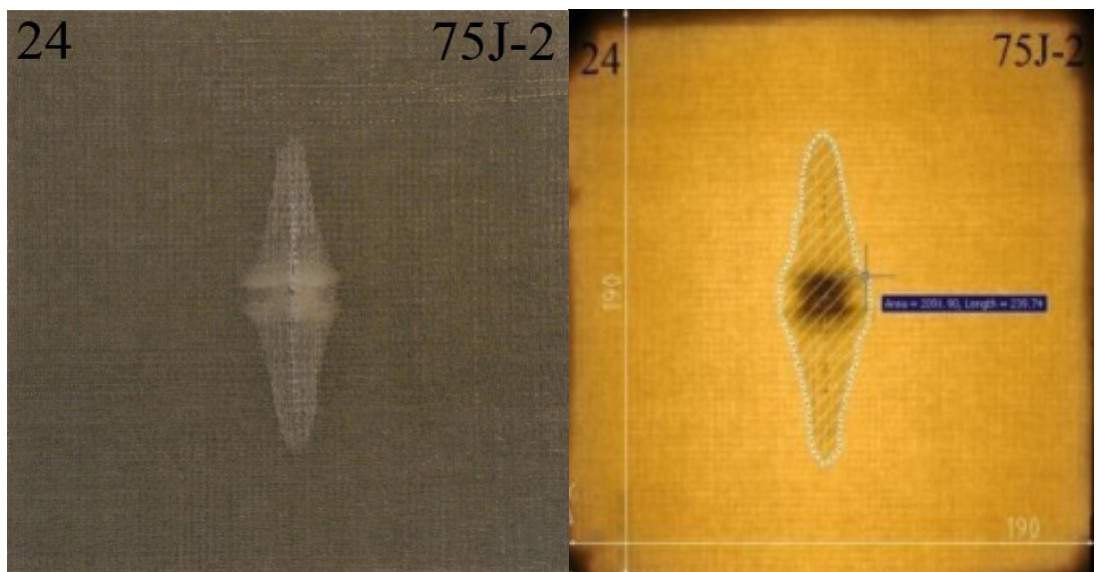
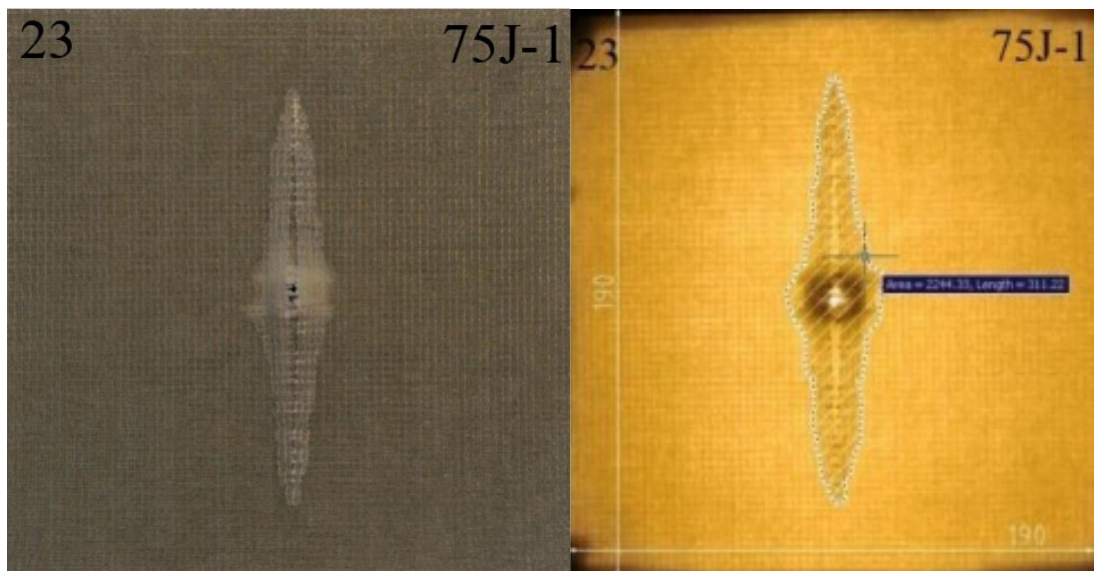
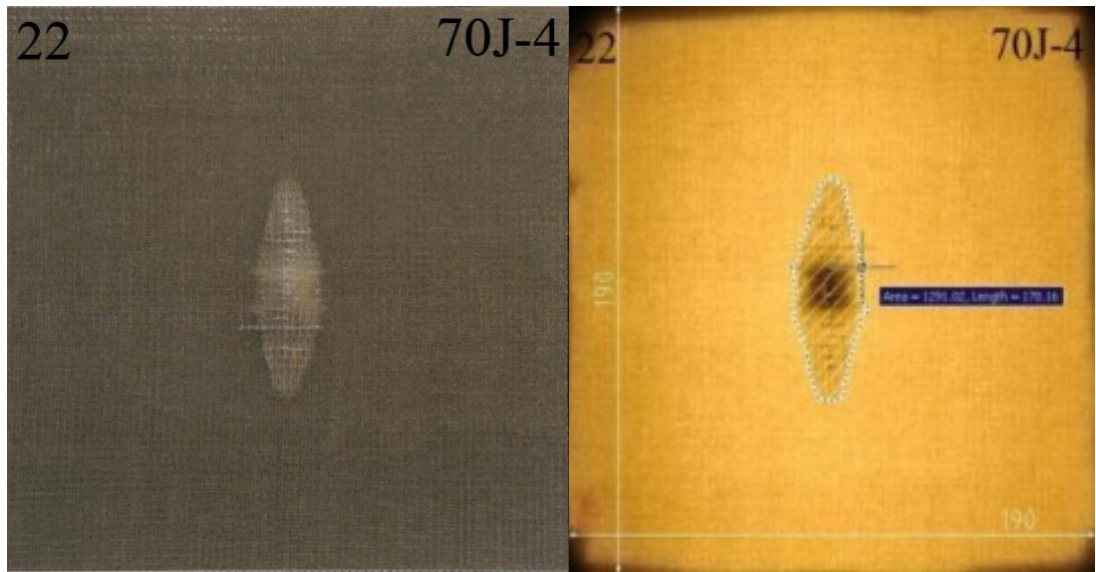


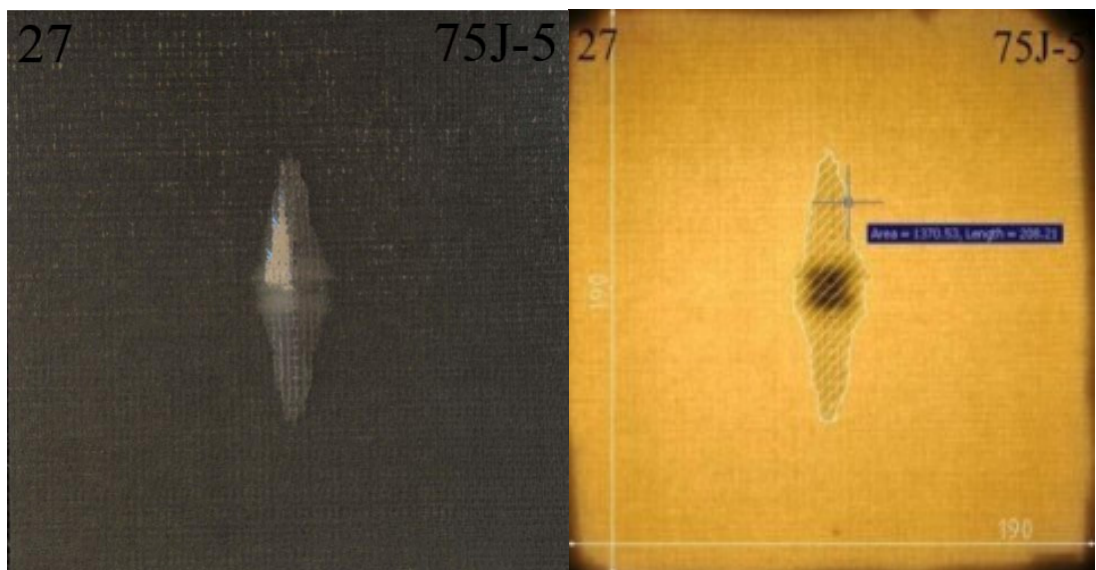
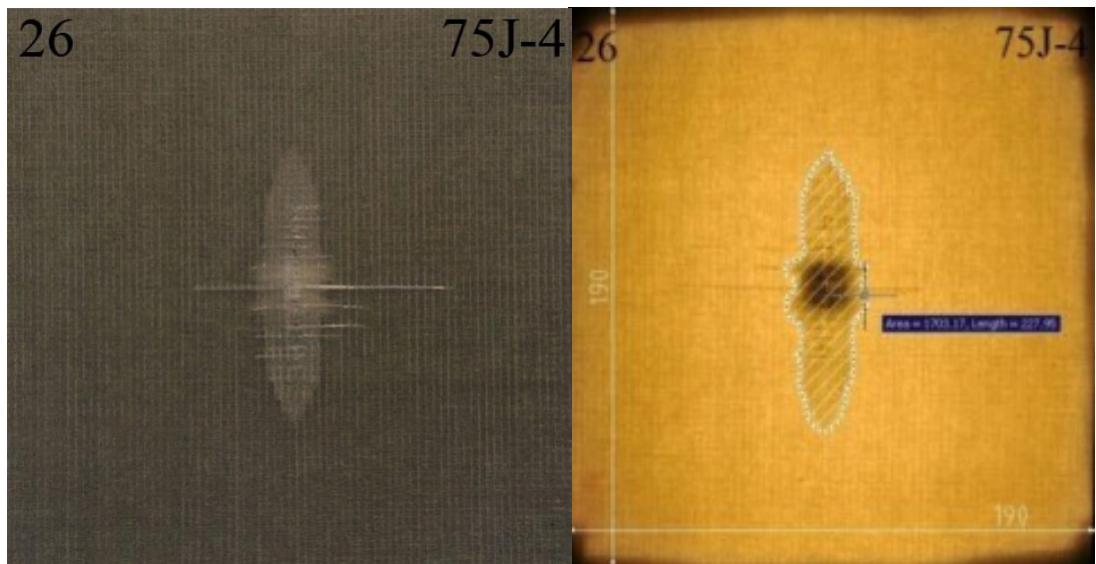
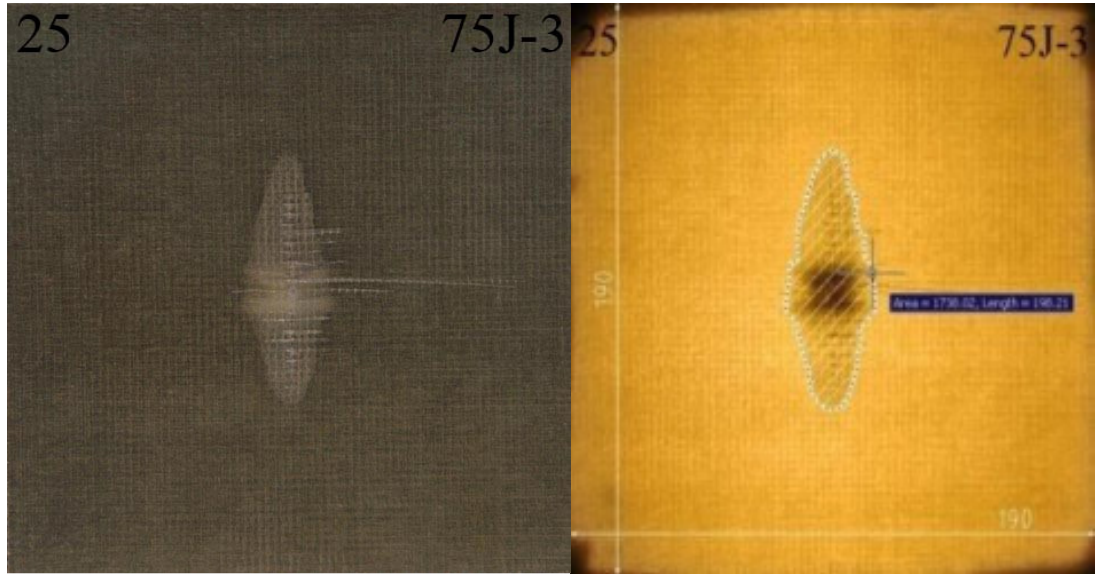


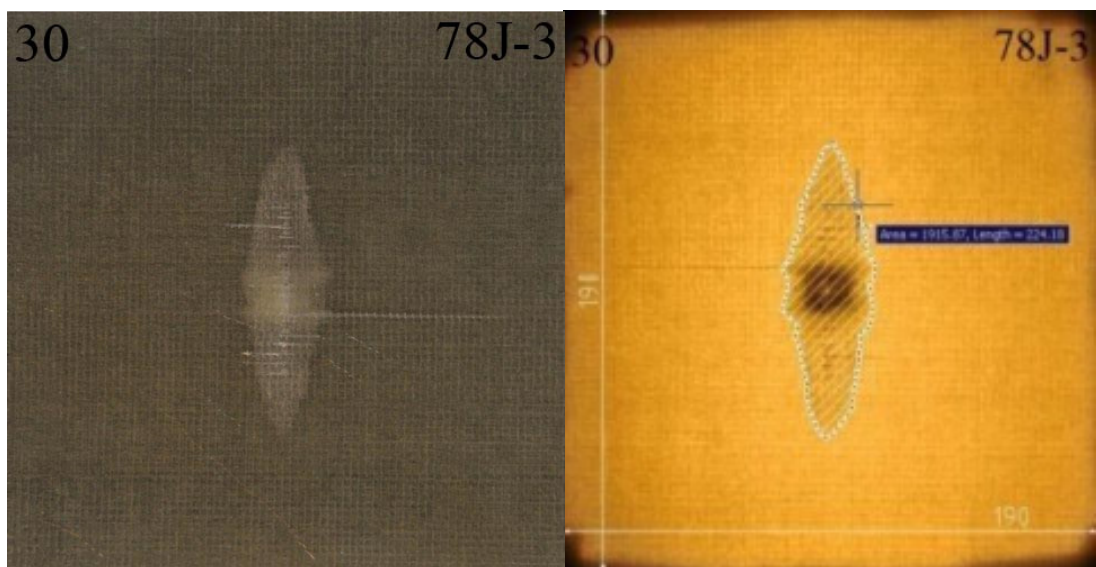
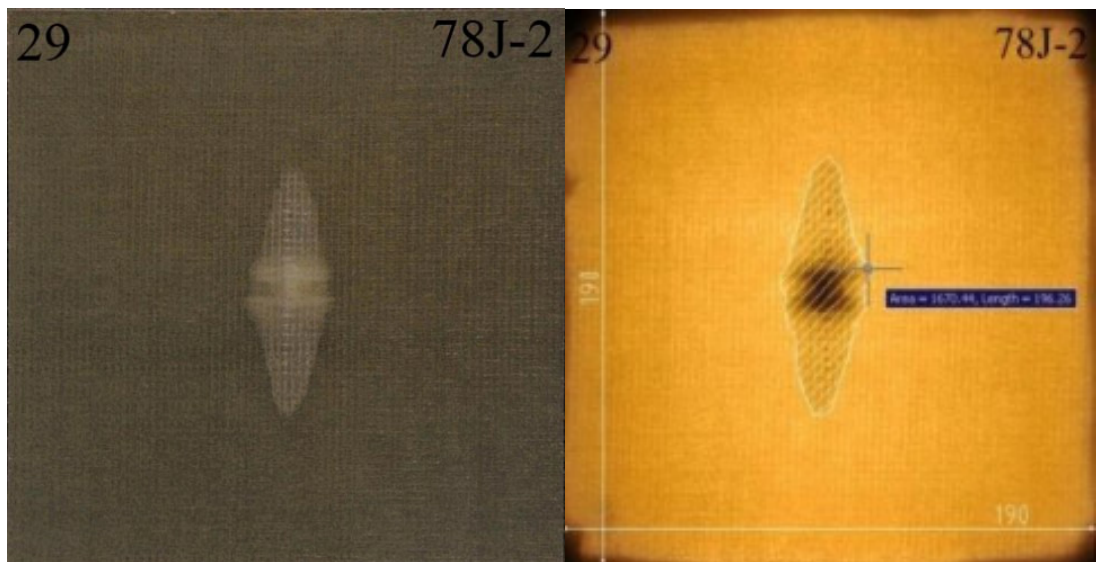
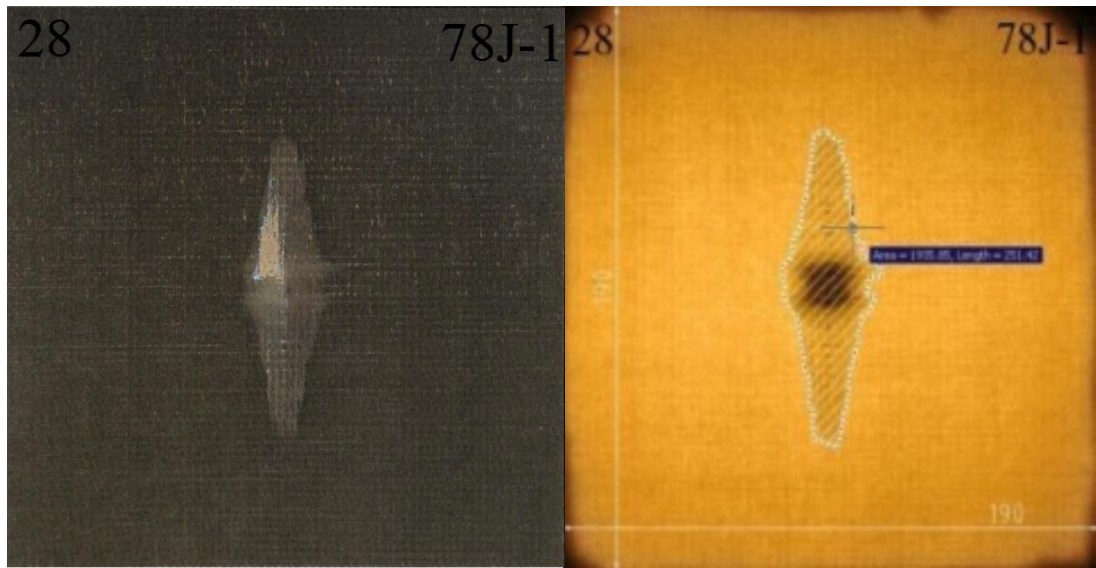


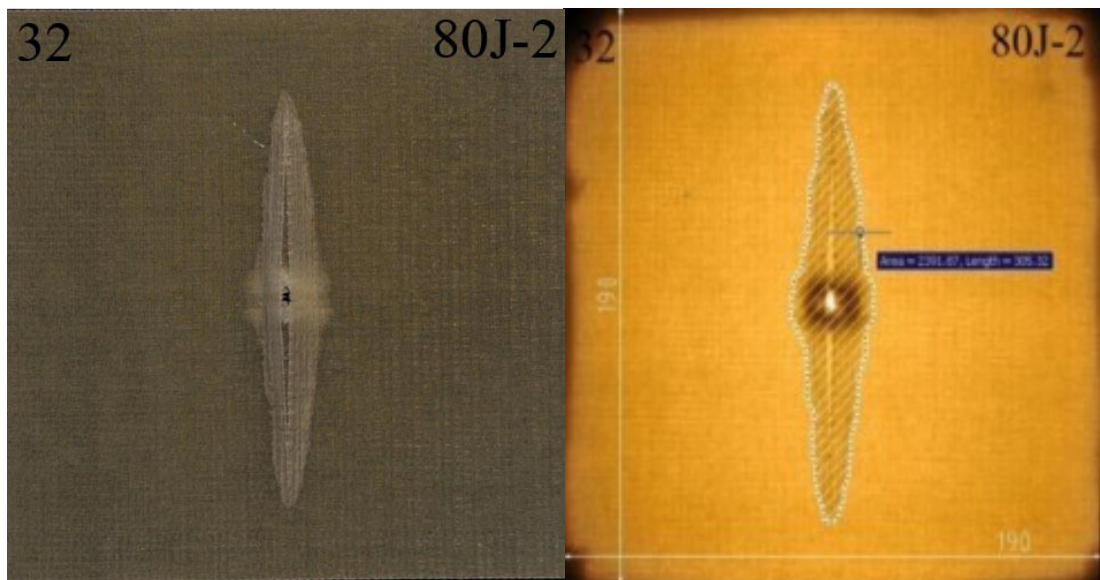
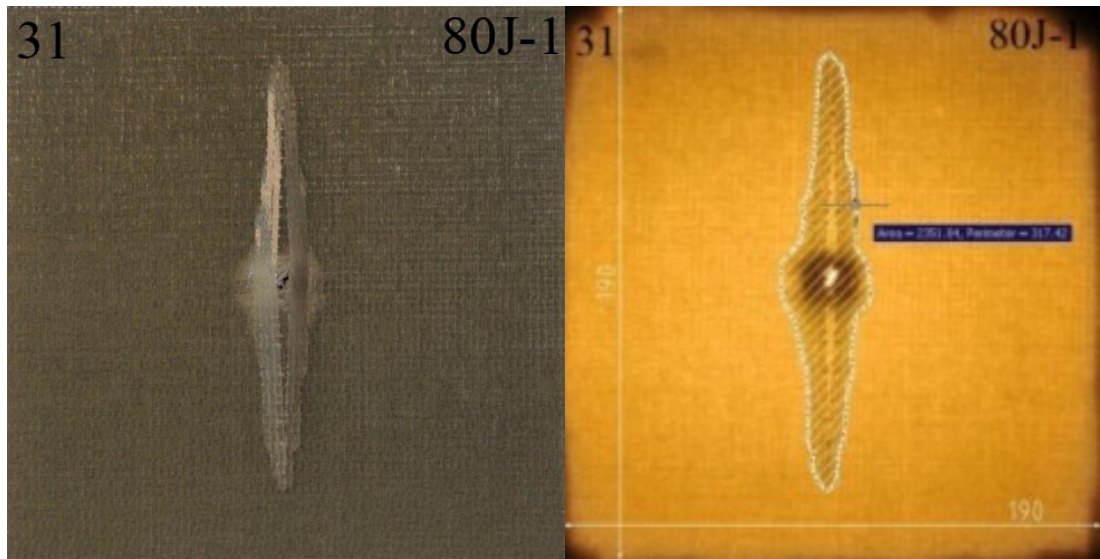


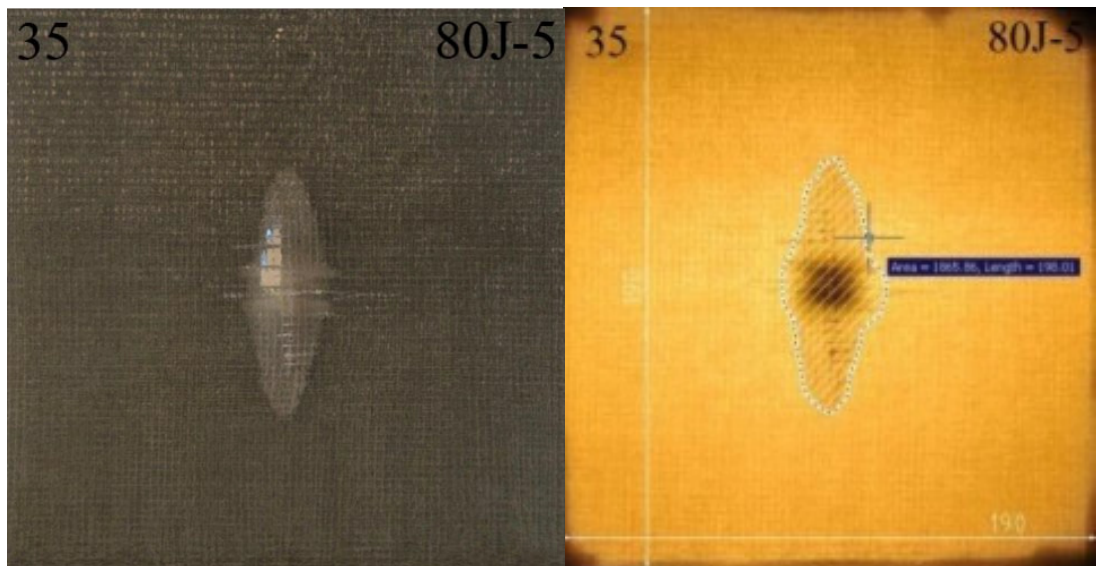
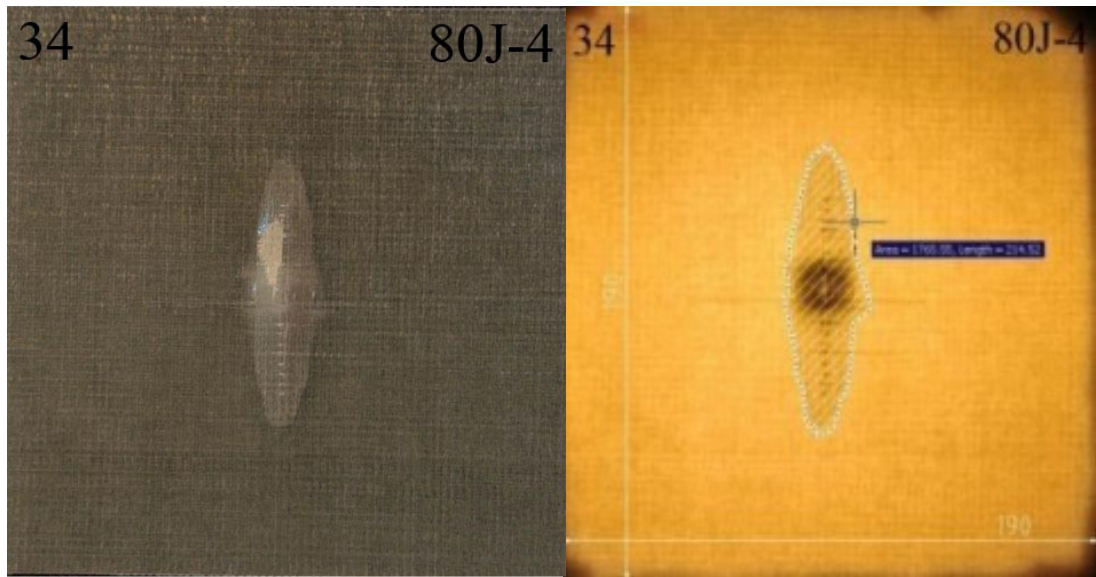


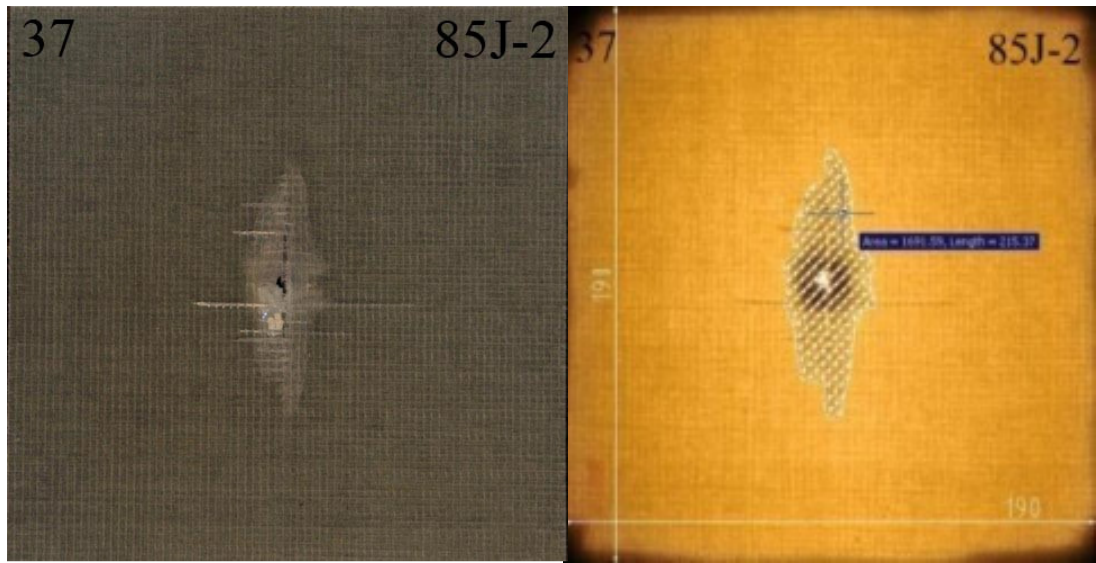


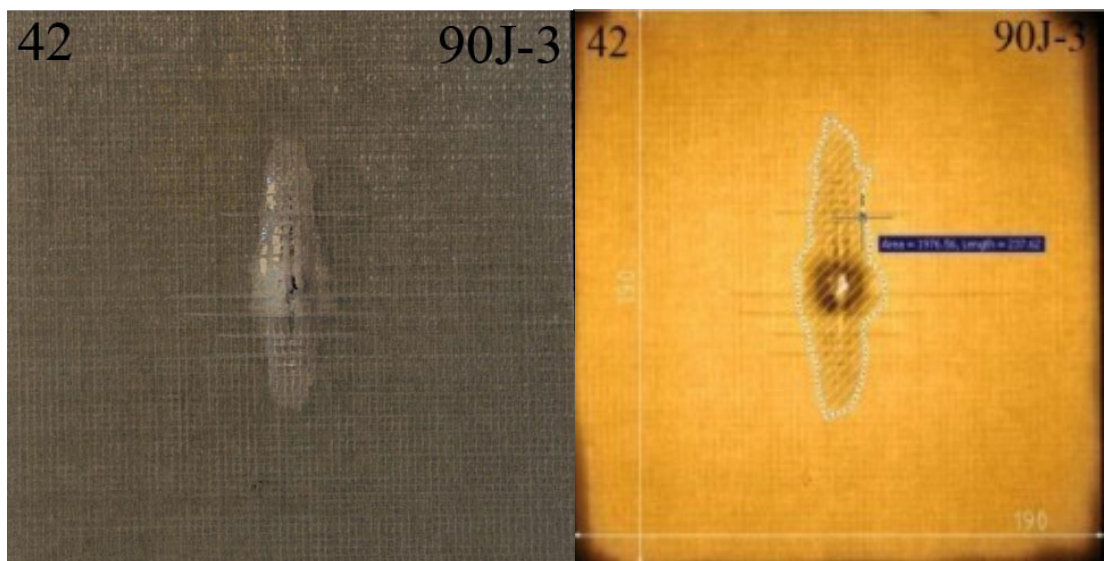
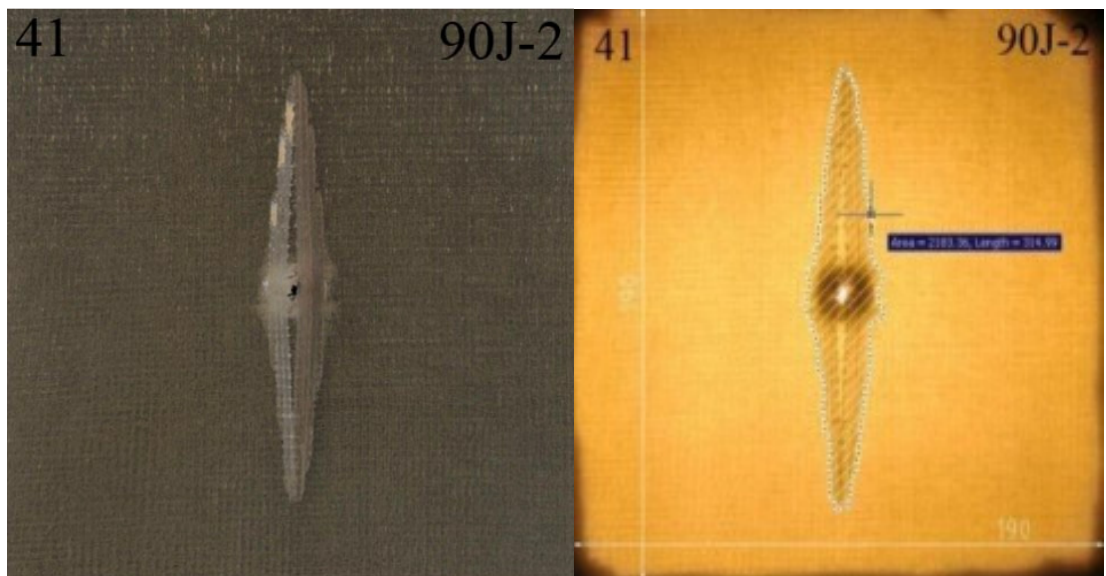
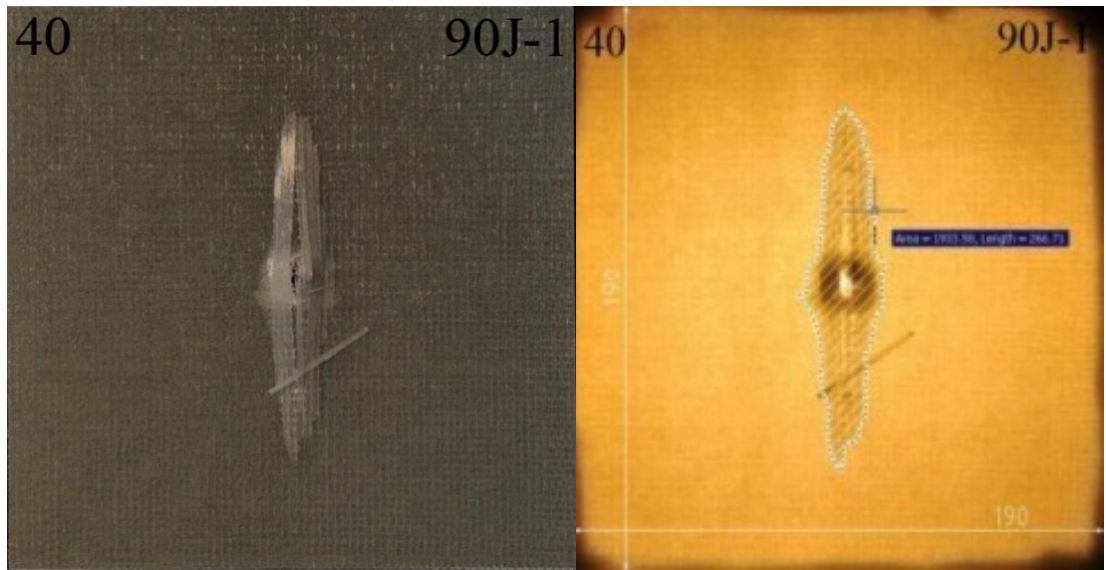


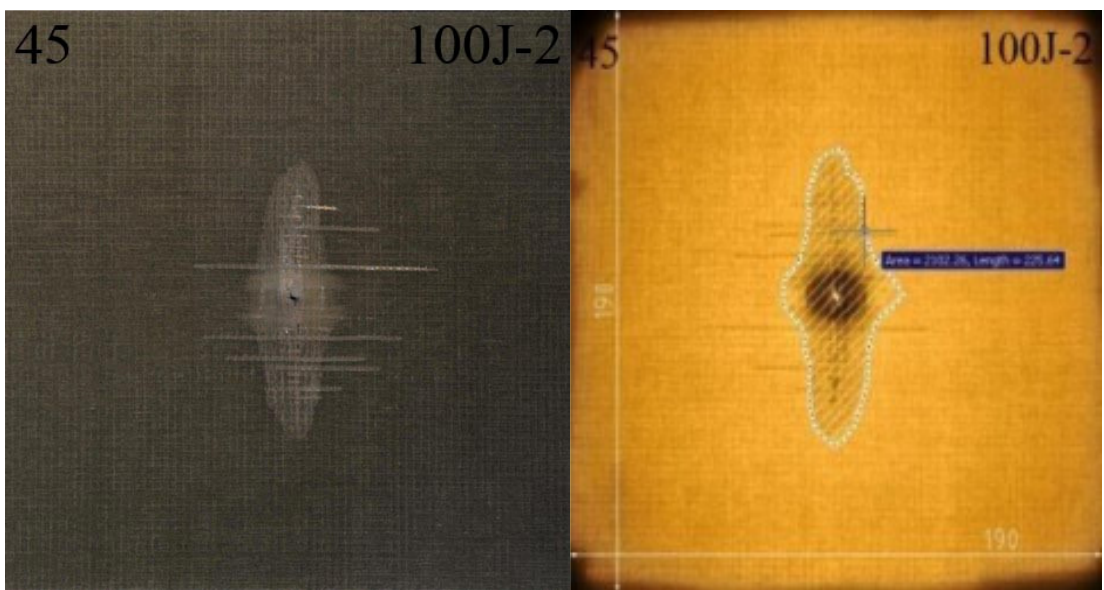
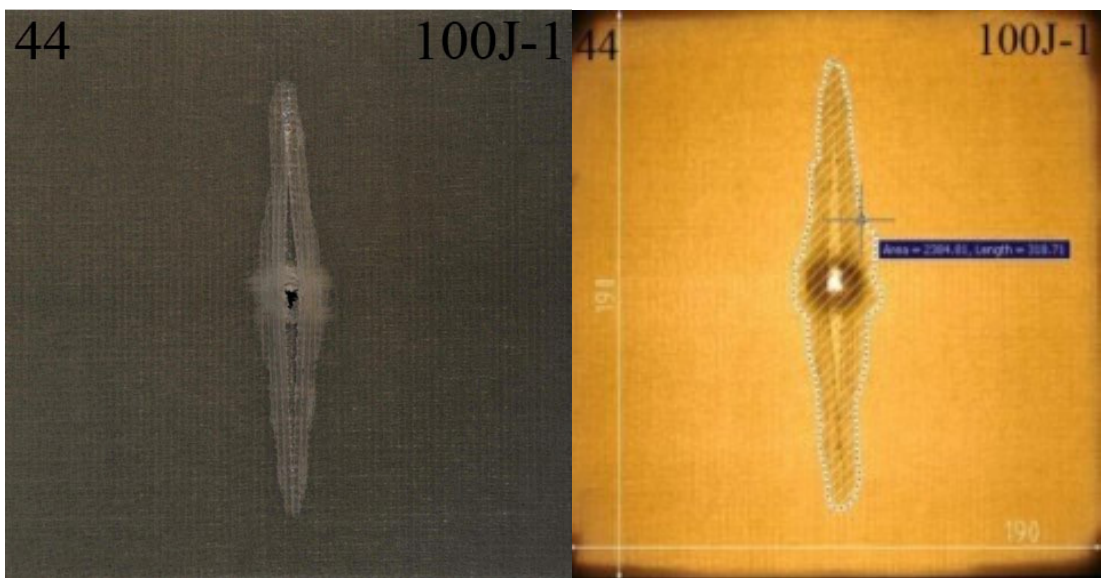
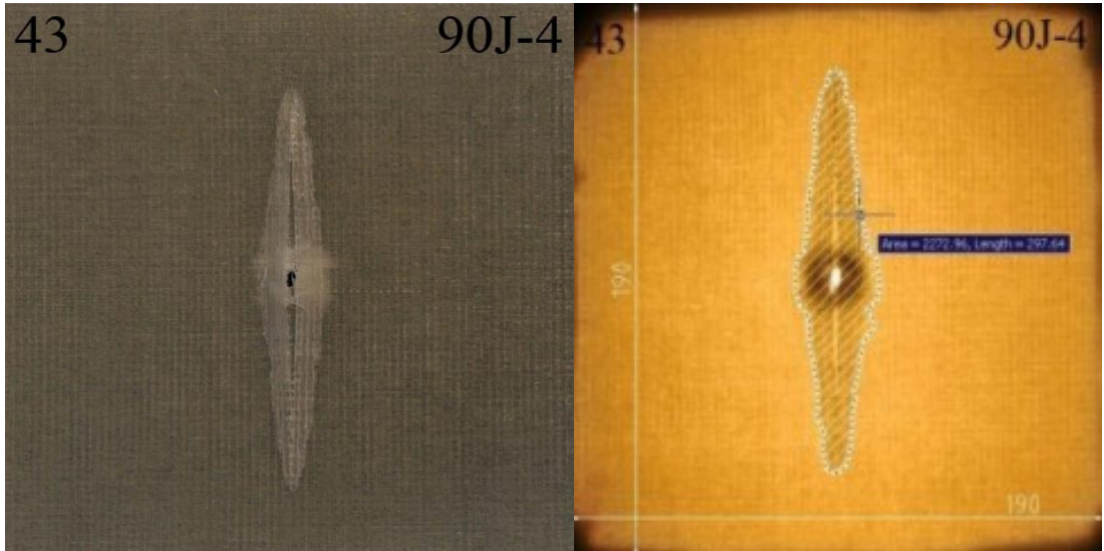












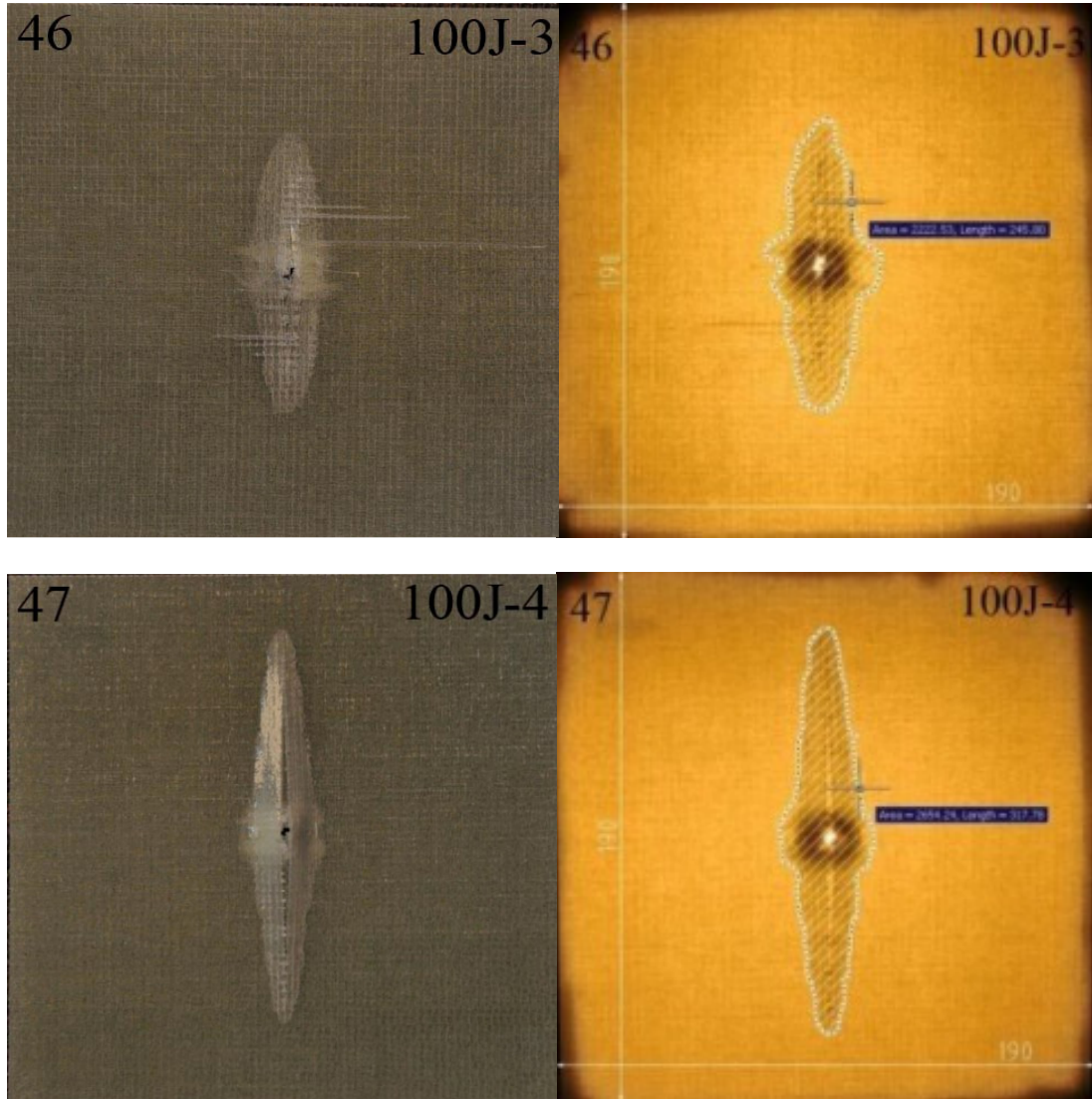


Figure 4.24 Photographs of the specimens (normal left, with a strong light behind right)

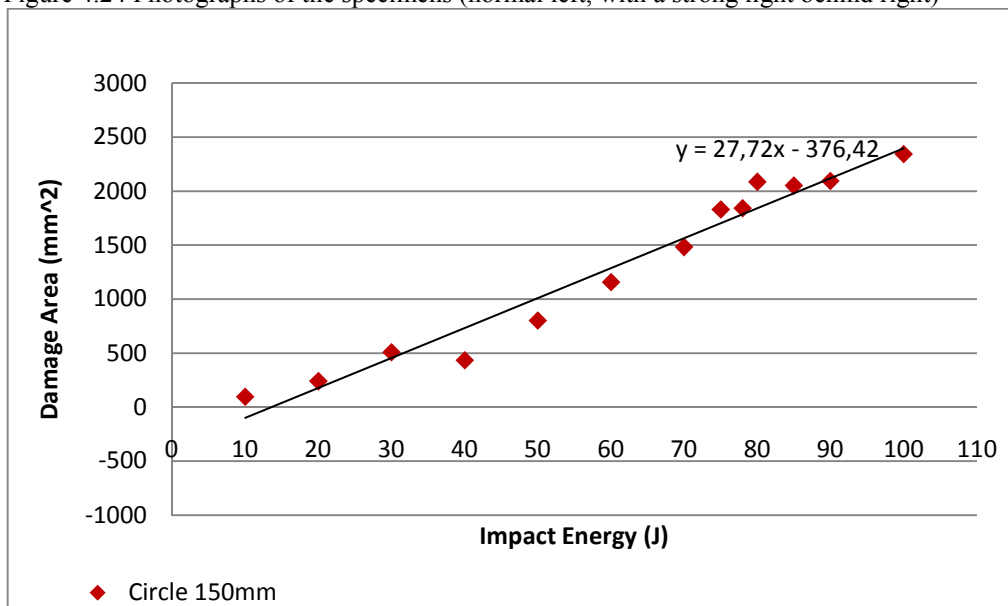


Figure 4.25 Damage area-Impact energy history of square with 150 mm per edge

4.5 Numerical Results

We have observed experimental results so far, both for comparing with experimental results and evaluating the delamination areas between interfaces by means of suitable stress analysis and damage criteria, we have also observed numerical results.

3D Impact is a FORTRAN based transient dynamic finite element analysis code which is used as a solver for our numerical analysis. We have used this code for determining the deflections of the composite plates, the contact force between impactor and the composite plates, and delamination shapes and areas between interfaces.

Specimen used for numerical analysis is modeled with three dimensional mesh. Four element layers are formed through the thickness as shown below and twelve element layers are formed for length and width. Thus, total numbers of elements are 576.

ELEMENT LAYER 1 :

PLY-ORIENTATION OF NO. 1 PLY = .00000E+00 DEGREES

PLY-ORIENTATION OF NO. 2 PLY = .00000E+00 DEGREES

PLY-ORIENTATION OF NO. 3 PLY = .90000E+02 DEGREES

PLY-ORIENTATION OF NO. 4 PLY = .90000E+02 DEGREES

ELEMENT LAYER 2 :

PLY-ORIENTATION OF NO. 1 PLY = .00000E+00 DEGREES

PLY-ORIENTATION OF NO. 2 PLY = .00000E+00 DEGREES

PLY-ORIENTATION OF NO. 3 PLY = .90000E+02 DEGREES

PLY-ORIENTATION OF NO. 4 PLY = .90000E+02 DEGREES

ELEMENT LAYER 3 :

PLY-ORIENTATION OF NO. 1 PLY = .90000E+02 DEGREES

PLY-ORIENTATION OF NO. 2 PLY = .90000E+02 DEGREES

PLY-ORIENTATION OF NO. 3 PLY = .00000E+00 DEGREES

PLY-ORIENTATION OF NO. 4 PLY = .00000E+00 DEGREES
 ELEMENT LAYER 4 :
 PLY-ORIENTATION OF NO. 1 PLY = .90000E+02 DEGREES
 PLY-ORIENTATION OF NO. 2 PLY = .90000E+02 DEGREES
 PLY-ORIENTATION OF NO. 3 PLY = .00000E+00 DEGREES
 PLY-ORIENTATION OF NO. 4 PLY = .00000E+00 DEGREES

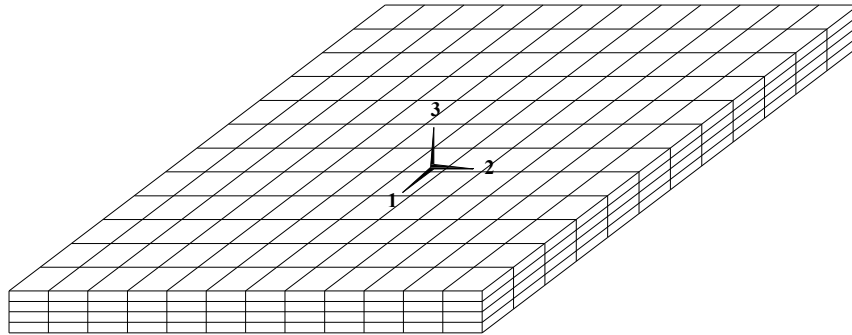
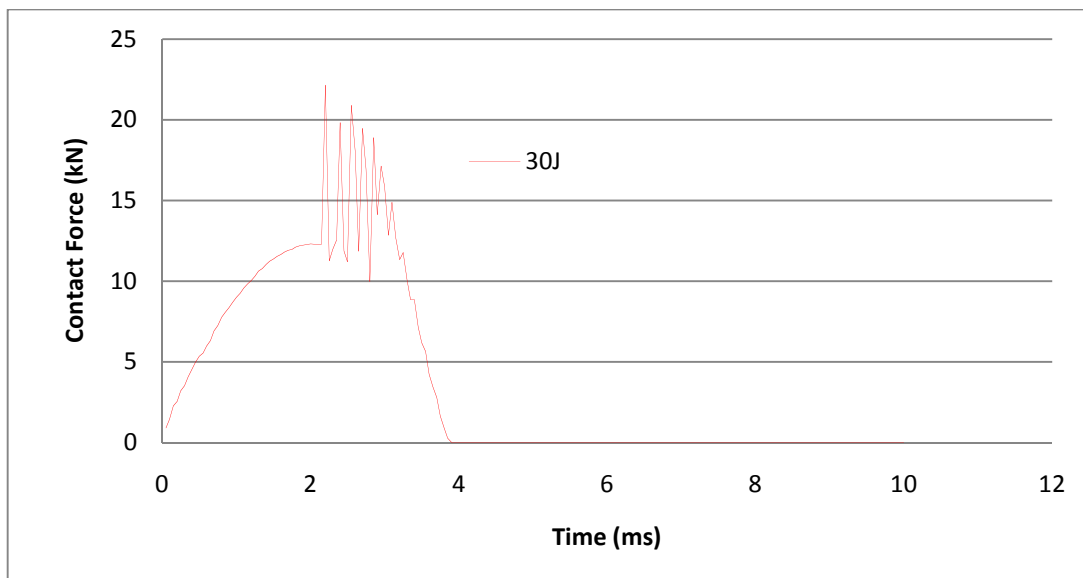
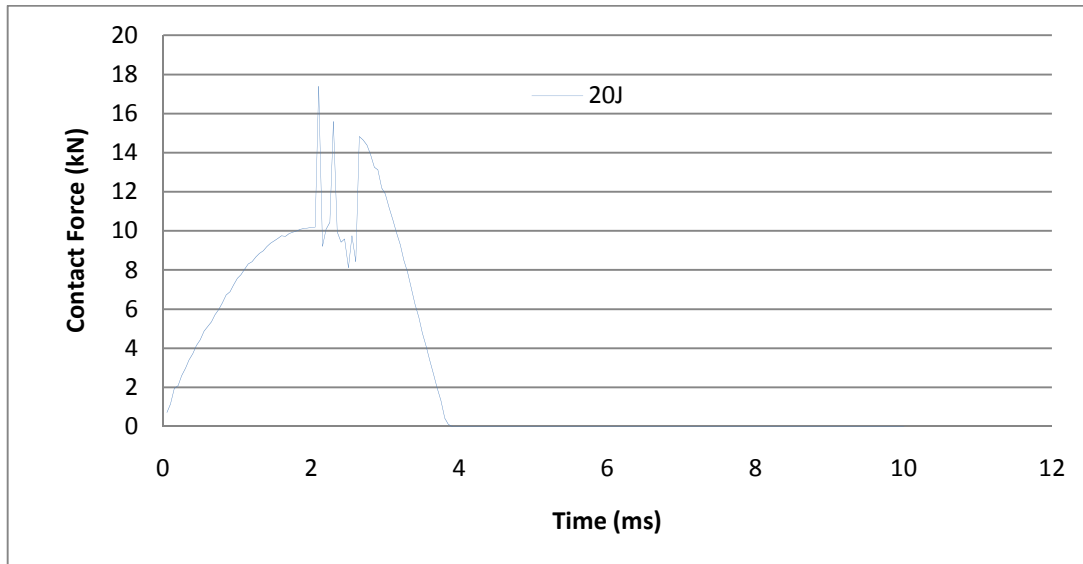
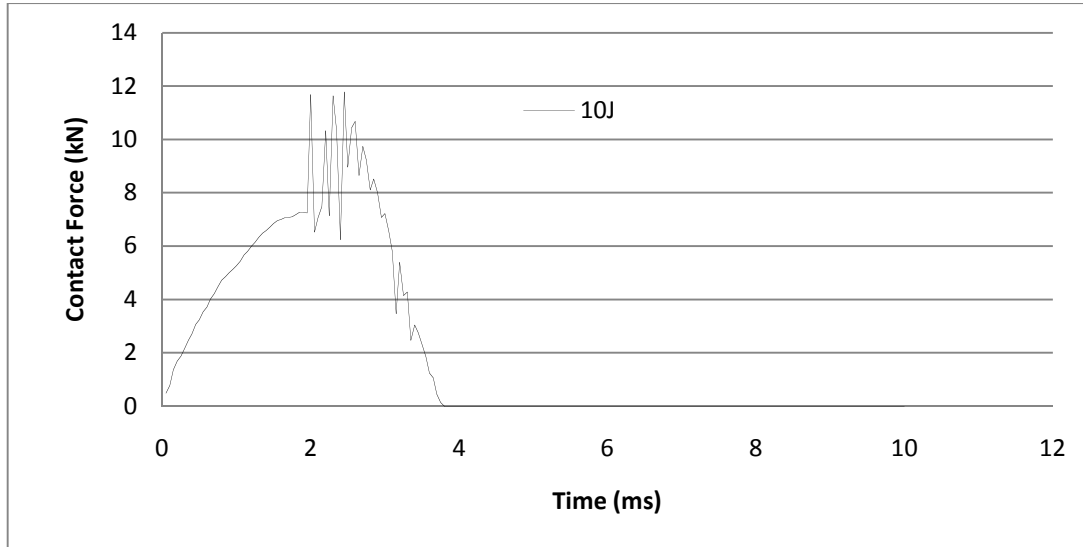


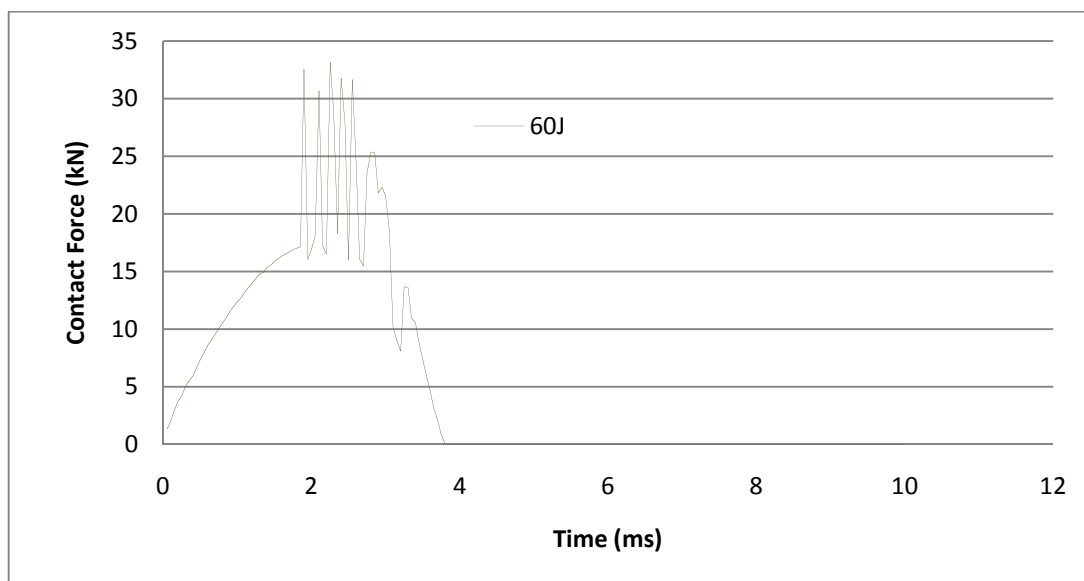
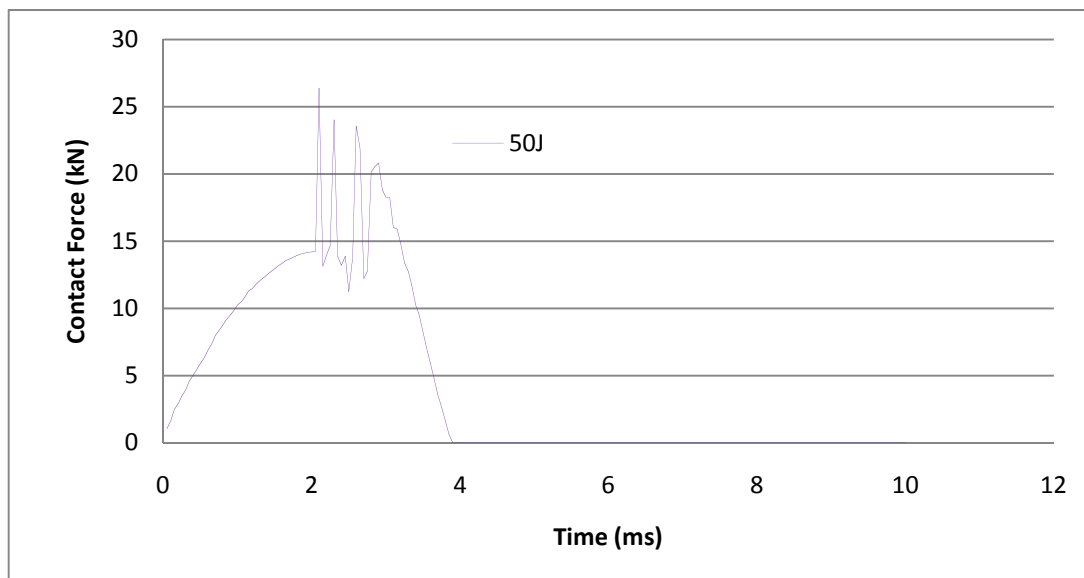
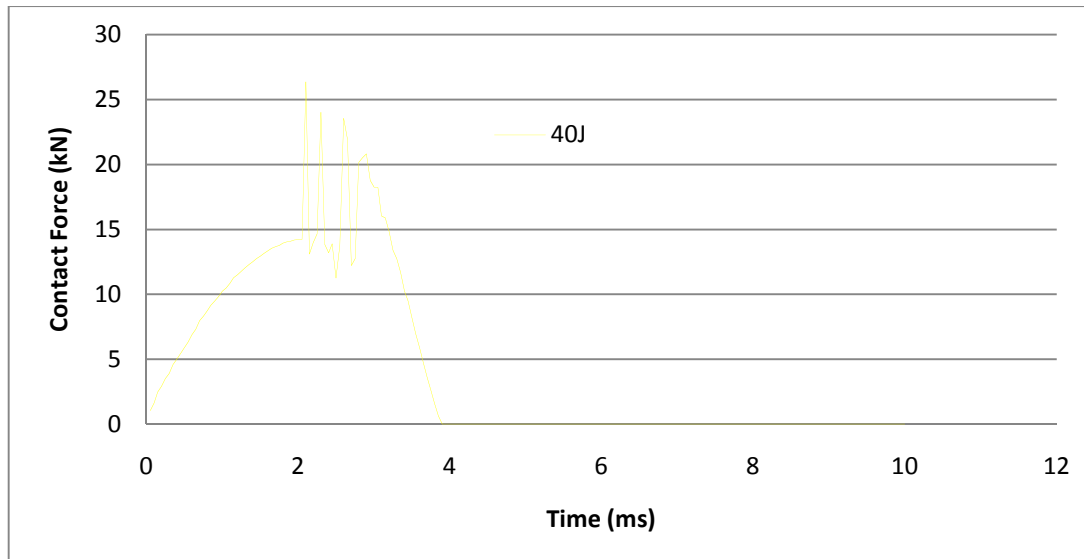
Figure 4.26 Finite element mesh of the simulated plate (Aktas,2007)

Four elements with specified ply orientations are formed and as a result we have the same orientation $[0/0/90/90/0/0/90/90]_s$ with the specimens we have used in experimental results.

First thing that we have made a comparison between experimental and numerical results was contact force – time graphs. We have observed contact force – time graphs for both square with 76 mm per edge and square with 150 mm per edge. (Circle with a diameter of 76 mm specimens are not observed because there was not so much difference between circle 76 mm and square 76 mm in experimental studies) These numerical analyses are completed up to penetration thresholds of the specimens, in other words only rebounding energies are applied to the specimens in numerical analyses because 3D Impact code does not include the fiber fracture criterion and that can cause us to have wrong results for higher energies.

Contact force – Time graphs for the square specimens with 76 mm per edge is given below. (10J, 20J, 30J, 40J, 50J, 60J)





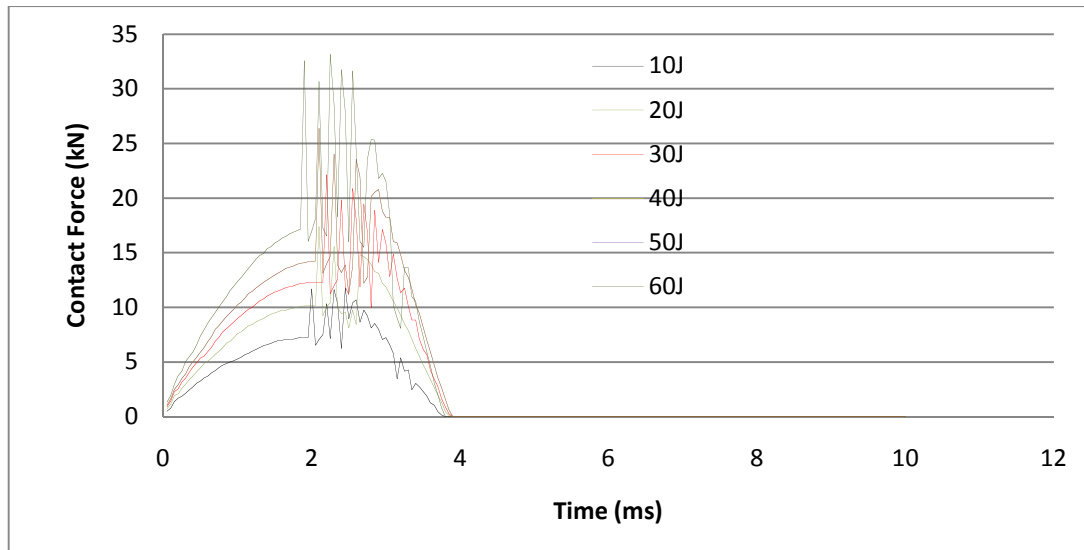
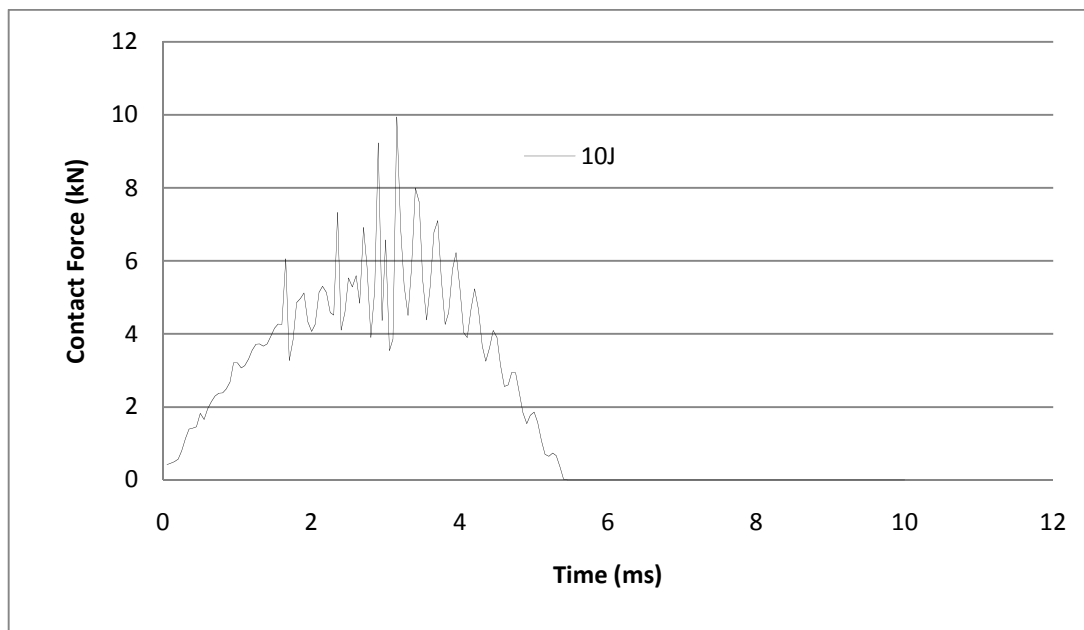
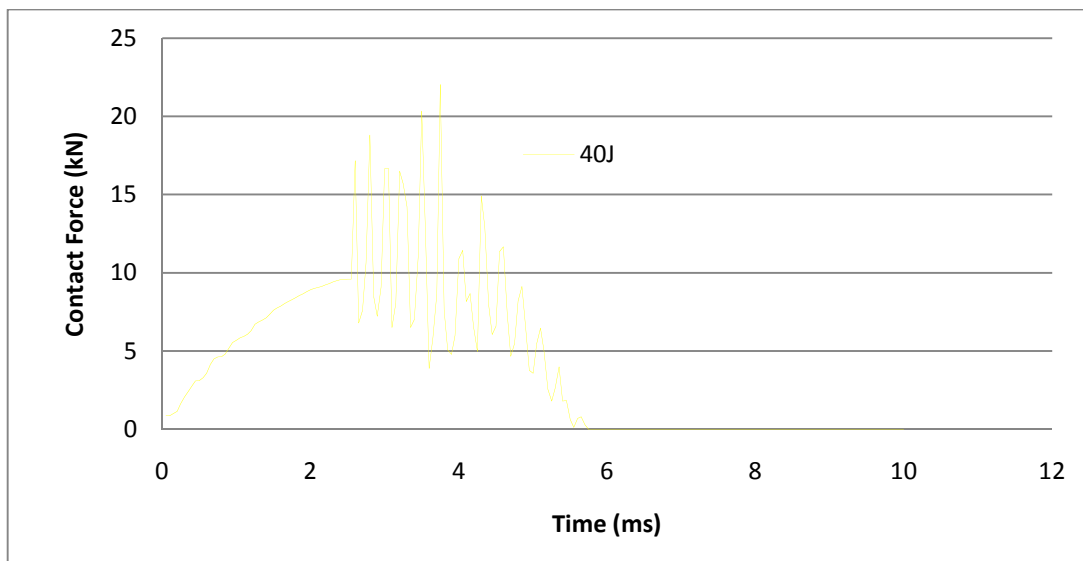
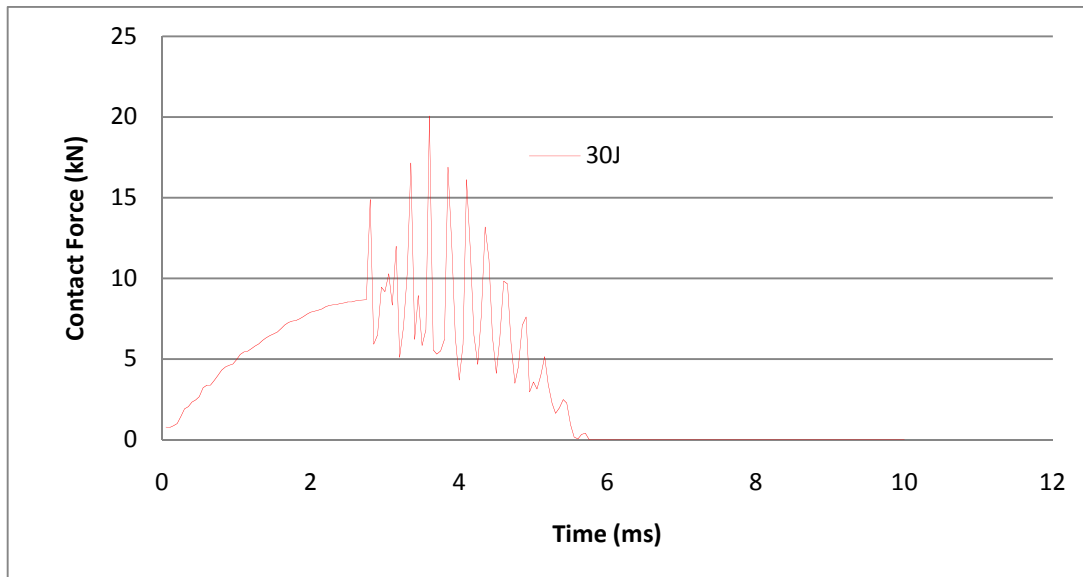
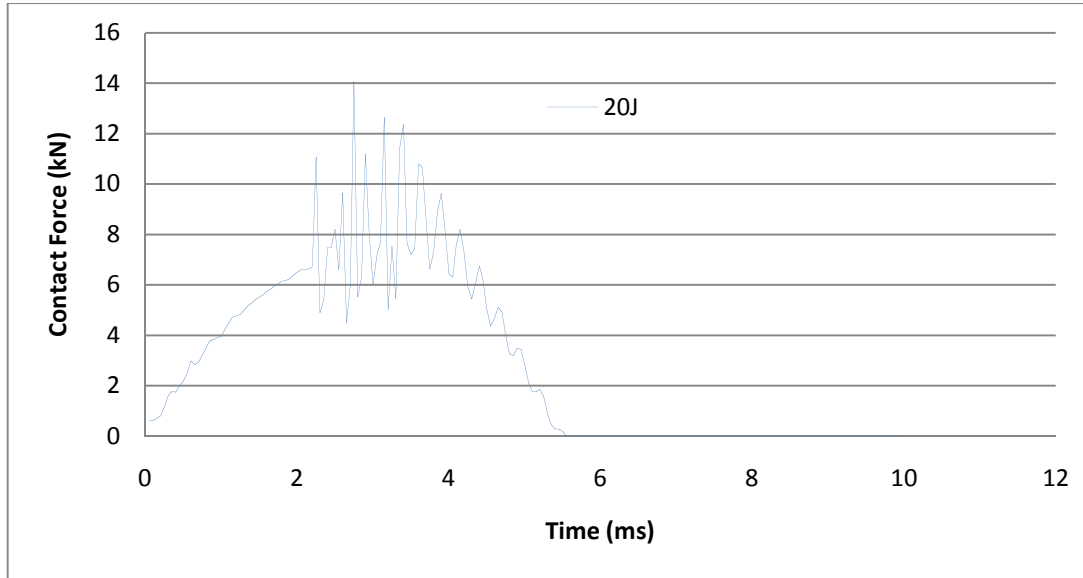


Figure 4.27 Numerical contact force-time diagrams, respectively for 10J, 20J, 30J, 40J, 50J, 60J and all together (square specimen with 76 mm per edge)

Contact force – Time graphs for the square specimens with 150 mm per edge is given below. (10J, 20J, 30J, 40J, 50J, 60J)





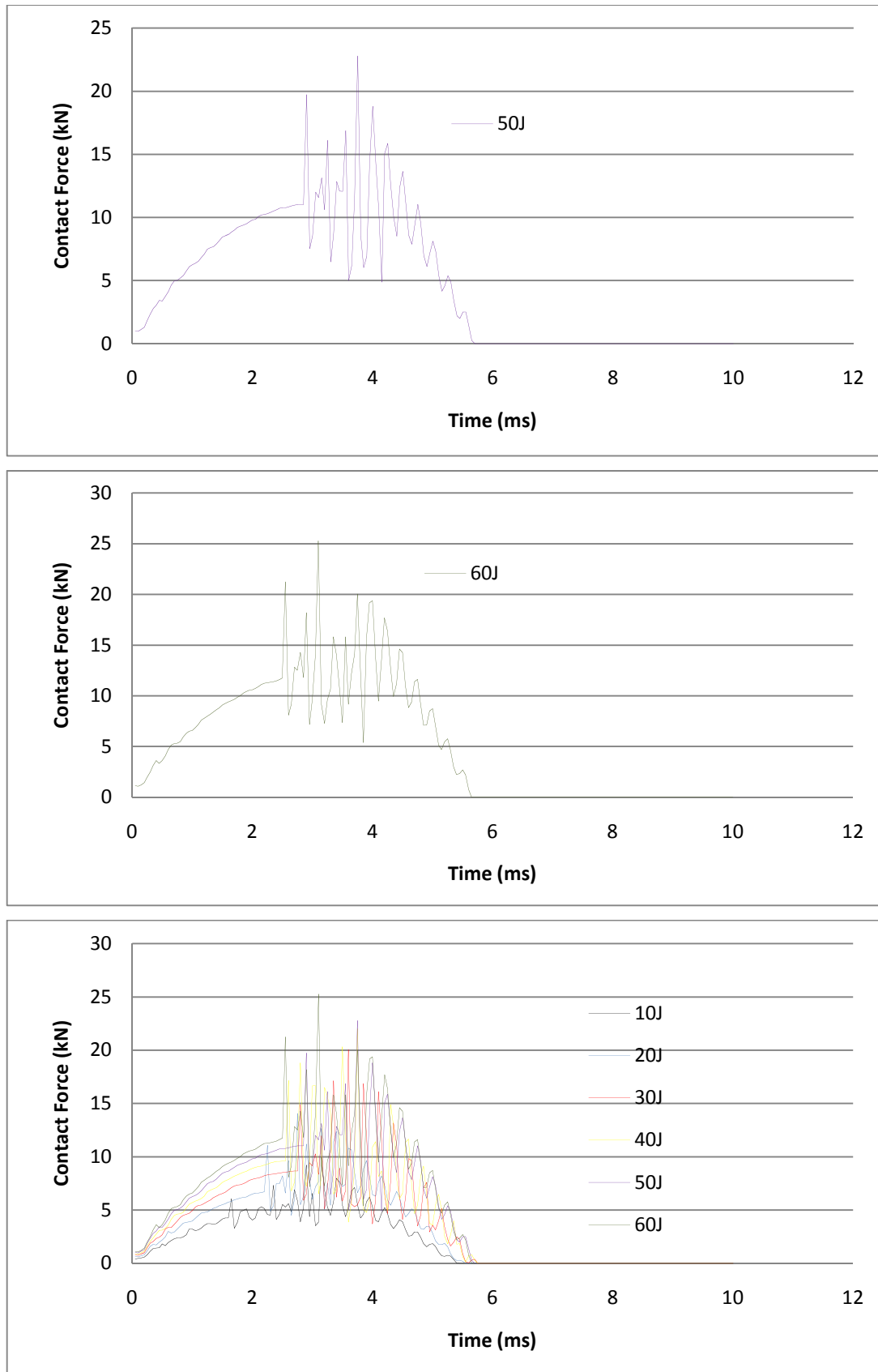


Figure 4.28 Numerical contact force-time diagrams, respectively for 10J, 20J, 30J, 40J, 50J, 60J and all together (square specimen with 150 mm per edge)

The last diagrams in Figure 4.27 and 4.28, it is clear that max. contact force increases by increasing impact energy. We have observed this before in experimental results. Another issue that we must see is, in square specimens with 150 mm per edge max. contact forces have lower values than the max. contact force in square specimens with 76 mm per edge, in same energy values. Energy level does not significantly affect on the contact time although it seems to increase by increasing impact energy.

In order to have better idea and to compare more circumstantial, we have given a random energy level diagram (40J) of both numerical and experimental tests at same time.

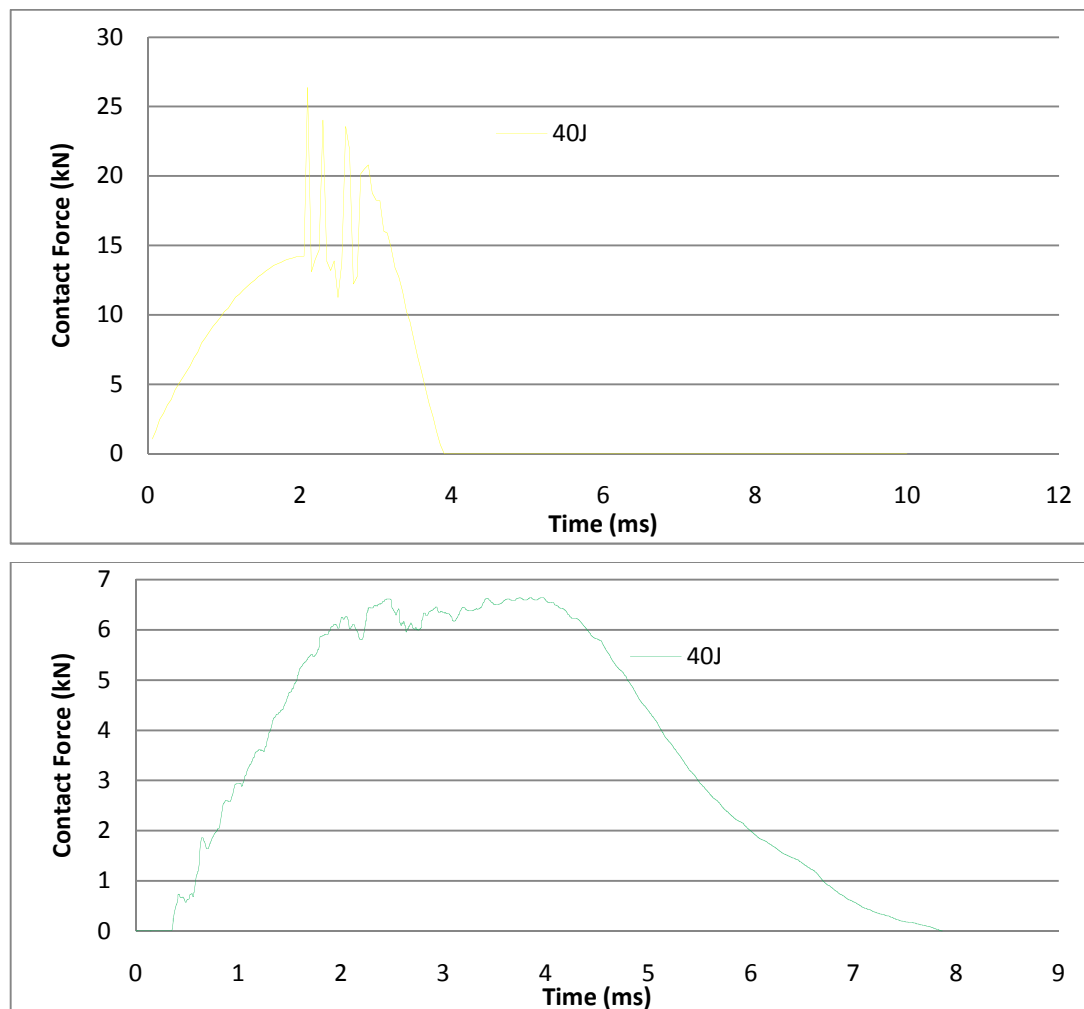


Figure 4.29 Comparison of contact force-time diagrams for the specimen with 76 mm per edge at 40J. (Numerical result, top-Experimental result, bottom.)

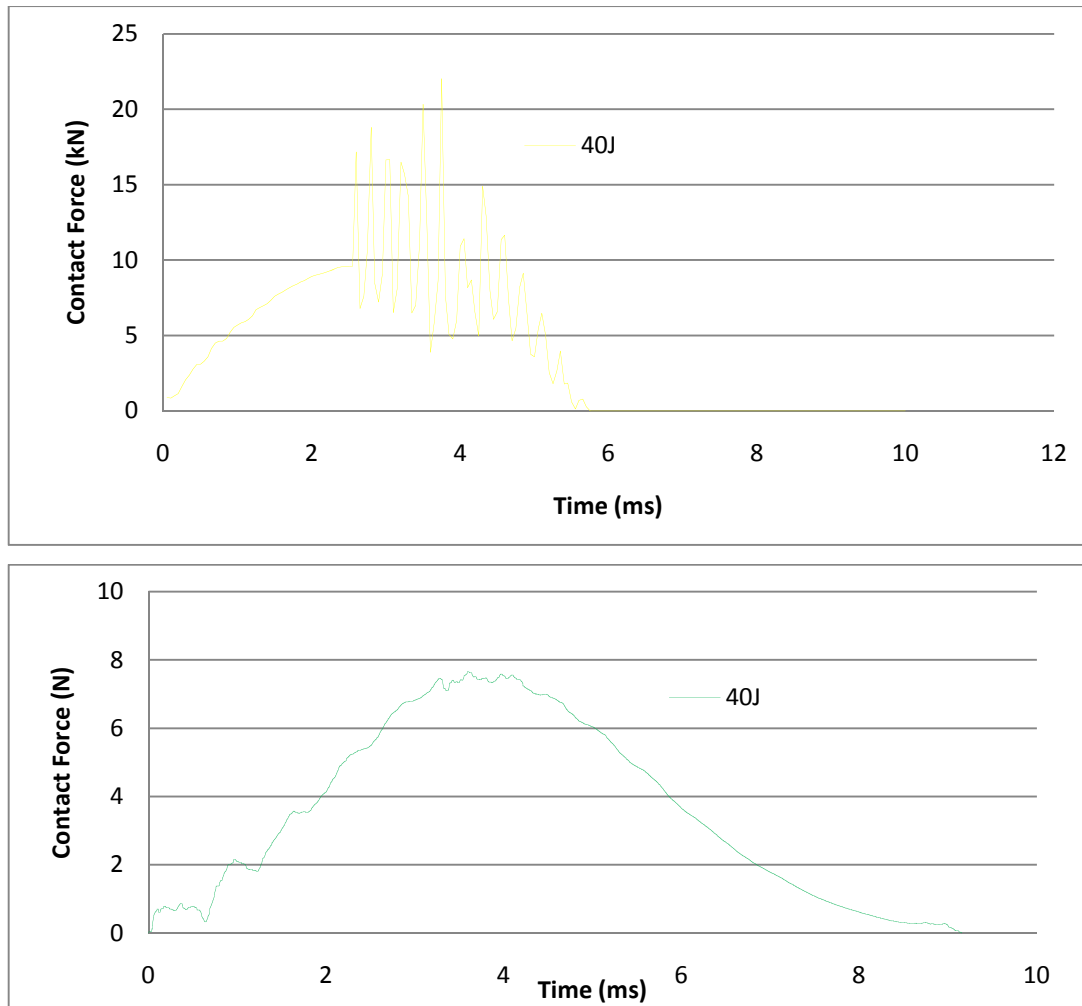


Figure 4.30 Comparison of contact force-time diagrams for the specimen with 150 mm per edge at 40J. (Numerical result, top-Experimental result, bottom.)

From Figures 4.29 and 4.30 it can be said that in numerical results, contact forces have higher values this is because of fiber fracture criterion. We can say that; the more specimens absorb energy, the more results differ from each other. Also it can be associated with rebounding rate of the specimen. Experimental results may get closer to numerical results if specimen's rebounding rate is high enough, that is why we are observing the specimens only at rebounding region.

Another important issue which must be highlighted during numerical tests is delamination areas between interfaces. This is one of the advantages that 3D impact provides us, delamination areas between interfaces can be seen below for square specimens with 76 mm per edge and 150 mm per edge for 10J energy level. Also

overall delamination areas can be ascertained by joining them together. Other energy levels except 10J are represented with the last interface because it is better to compare last interface delamination area with the back lighted photographs. In this thesis, the laminated composite is composed of eight layers so there are seven interfaces but there is no delamination occurred in the mid-plane interface due to the two same orientations adjacent plies.

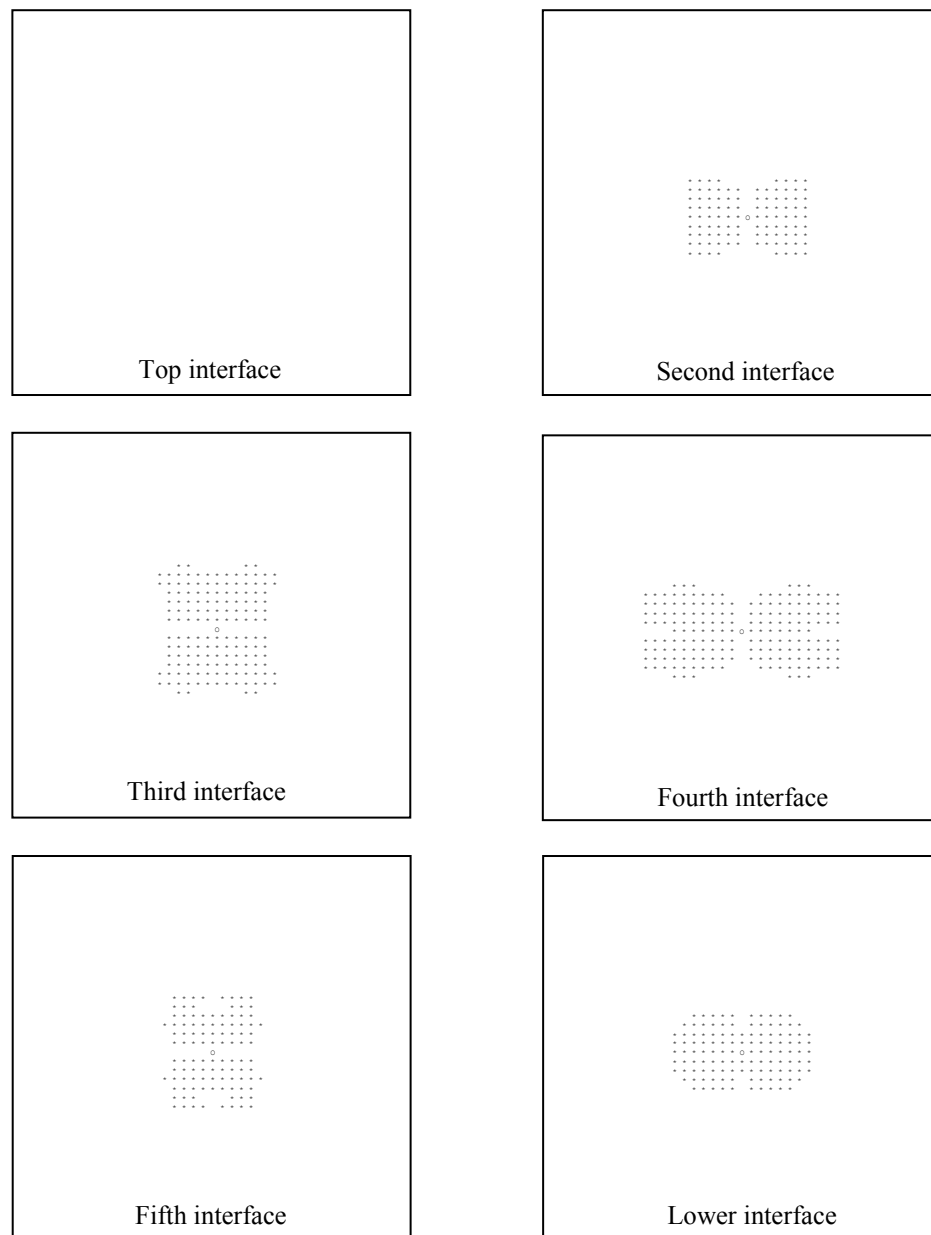


Figure 4.31 Delamination areas between interfaces of 76x76 mm square (10J)

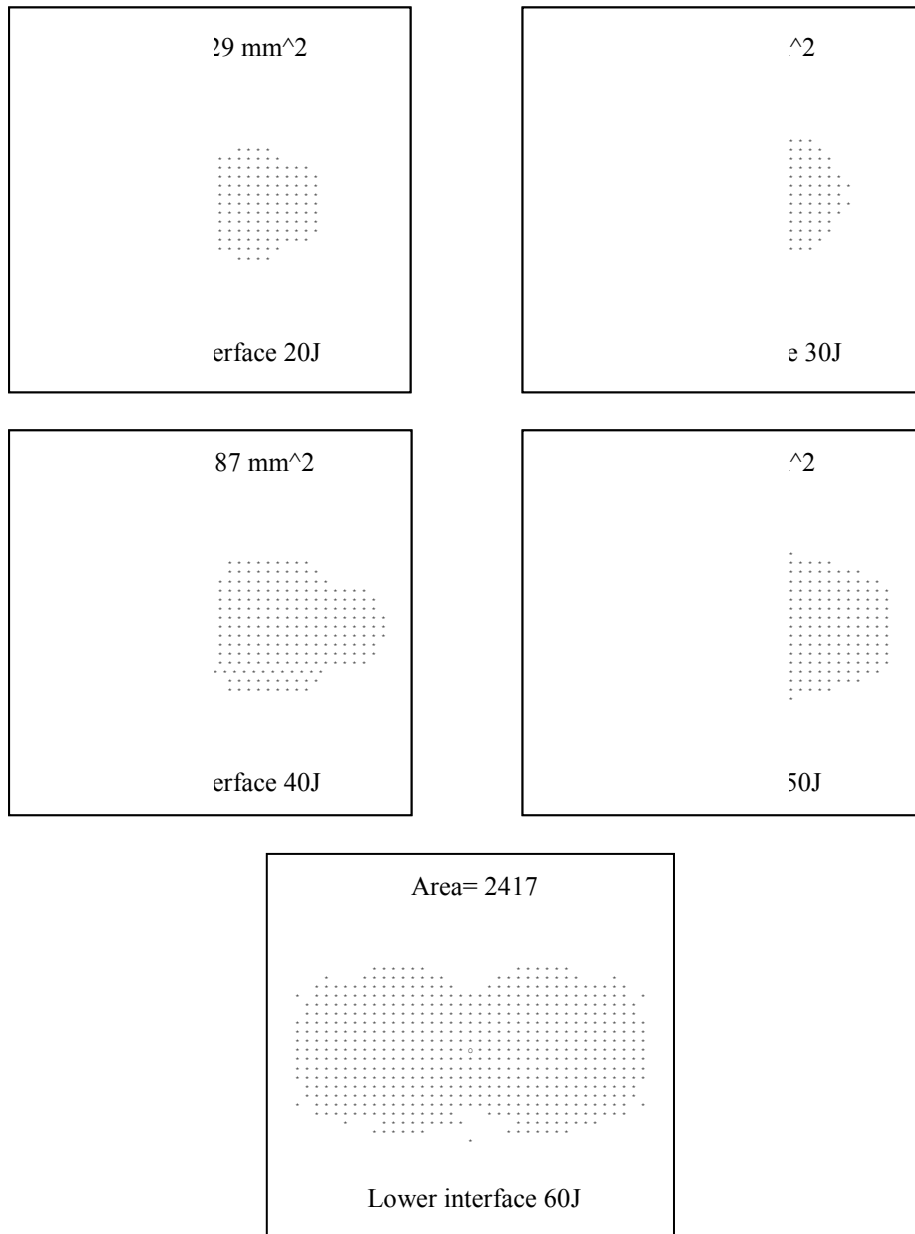


Figure 4.32 Delamination areas between last interfaces of respectively 20J, 30J, 40J, 50J, 60J energy levels (76x76 mm square)

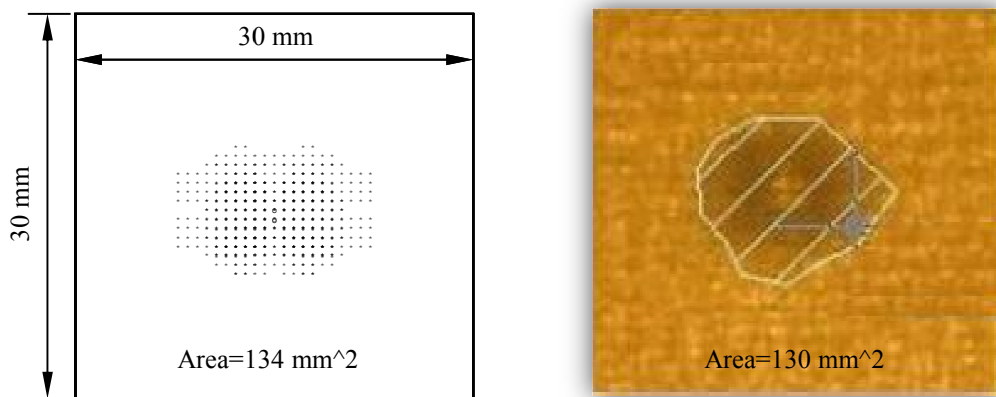


Figure 4.33 Overall delamination area for 10J energy level (76x76 square)



Figure 4.34 Delamination areas between interfaces of 150x150 mm square (10J)

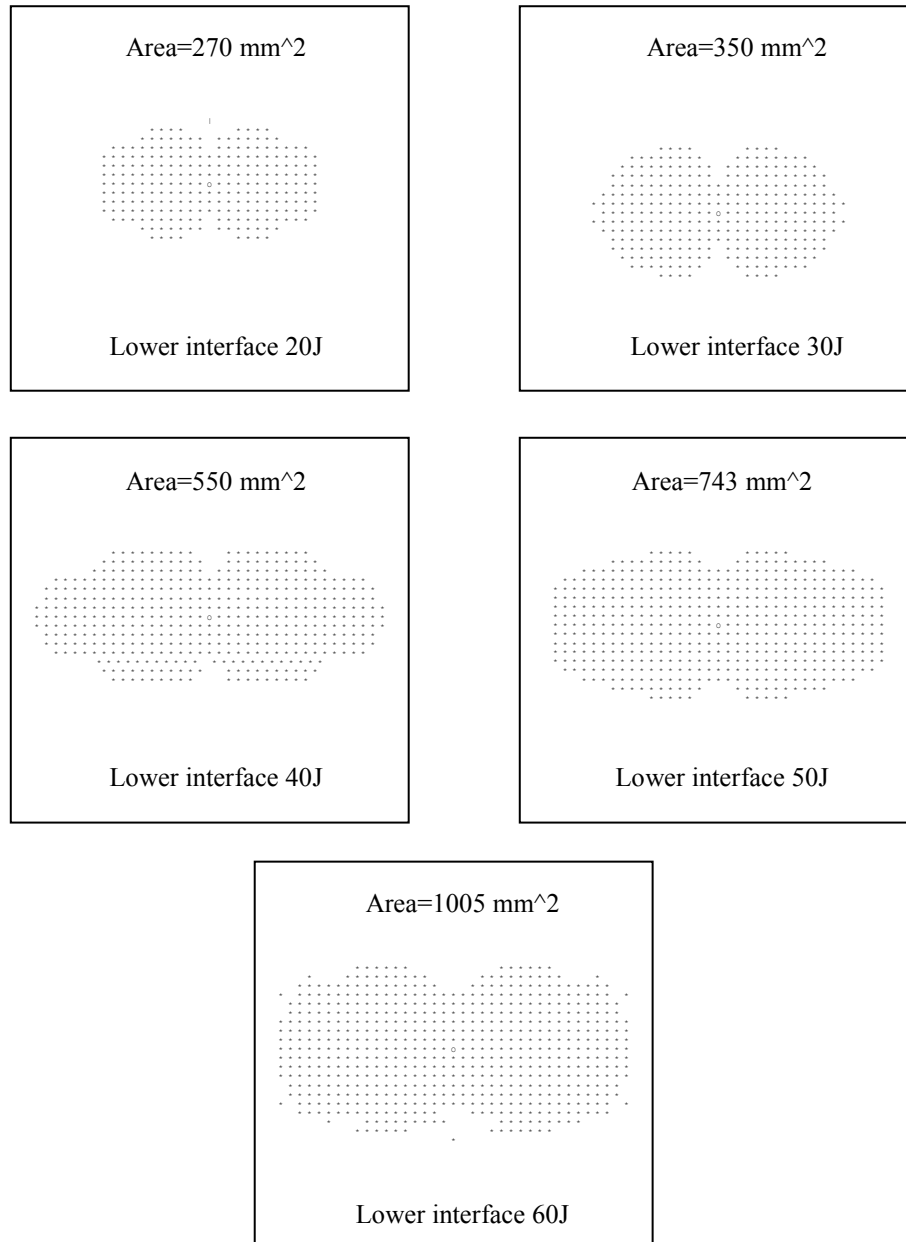


Figure 4.35 Delamination areas between last interfaces of respectively 20J, 30J, 40J, 50J, 60J energy levels (150x150 mm square)

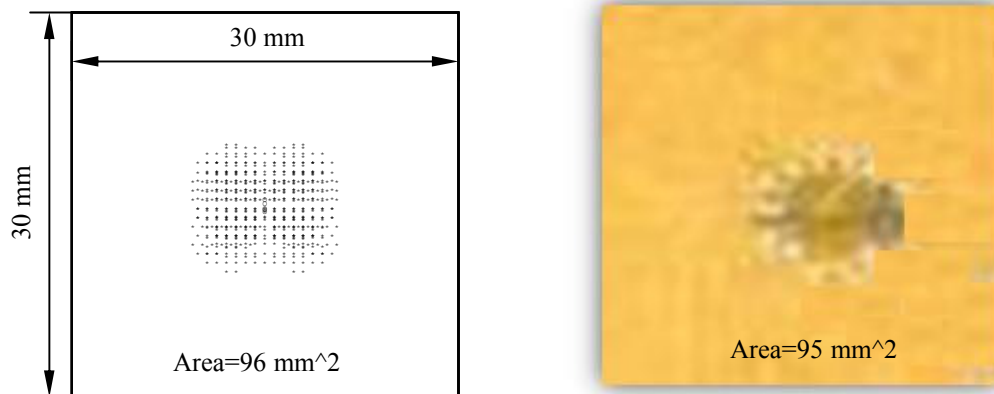


Figure 4.36 Overall delamination area for 10J energy level (150x150 square)

Numerical results regarding damage areas of the specimens were given, another issue is damage area - impact energy graphs for numerical results. Figure 4.37 and 4.38 shows comparison of numerical and experimental results regarding damage area – impact energy values.

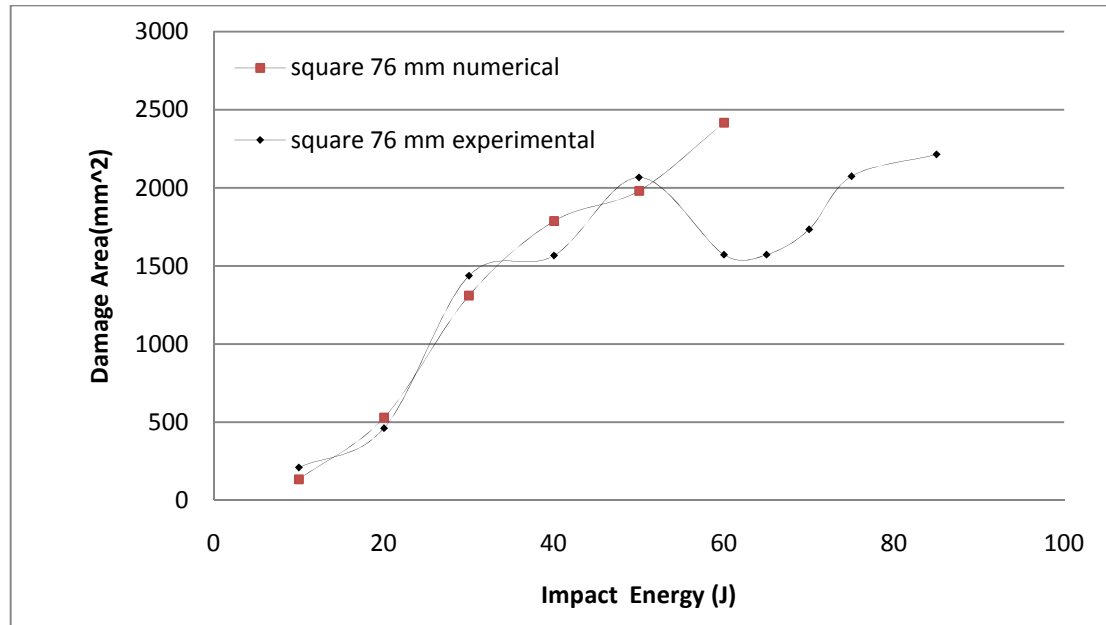


Figure 4.37 Comparison of damage area – impact energy graphs for numerical and experimental results (76x76 square)

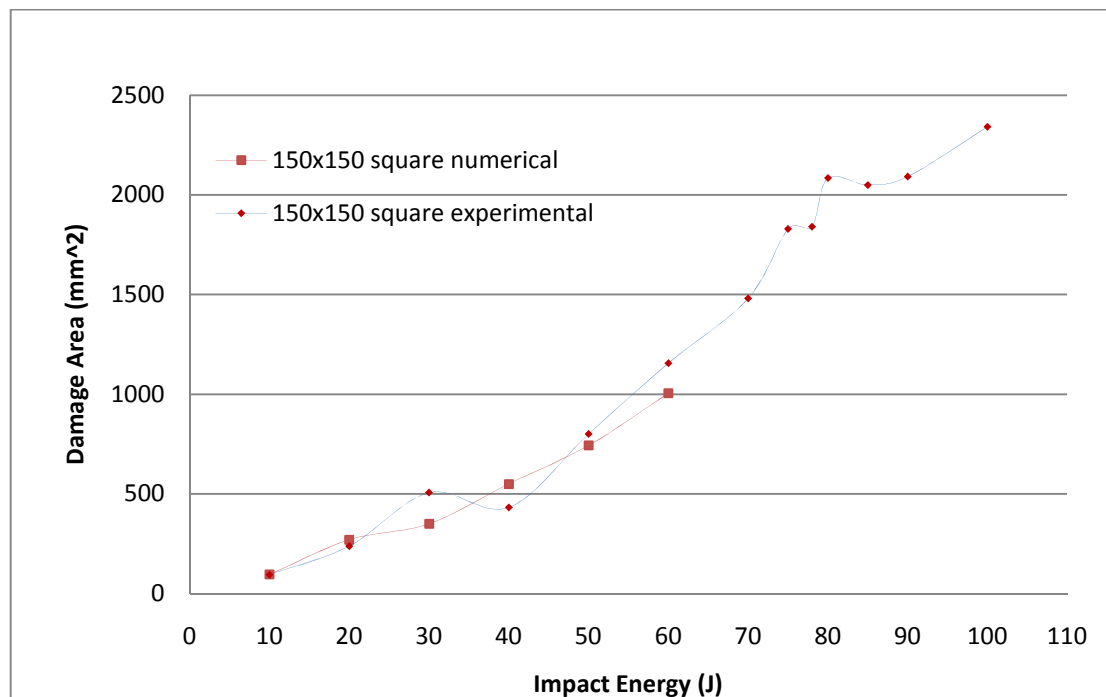


Figure 4.37 Comparison of damage area – impact energy graphs for numerical and experimental results (150x150 square)

CHAPTER SIX

CONCLUSIONS

In this study, the impact behavior of the glass/epoxy laminated composite plates at room temperature is observed by comparing numerical and experimental results. Energy and contact force histories of a 12.7 mm impactor striking to laminated composites with different dimensions were obtained. The whole energy profiles obtained from these tests are presented here. The energy profiles were used to characterize the impact perforation resistance of the composites. From the results obtained, the following conclusions can be drawn:

- Increasing the impact energy makes the contact force and the deflection increase.
- There existed an increase in absorbed energy as the impact energy increase but it is obtained that absorbed energy can decrease after perforation threshold point.
- Contact durations cannot be said as it is inversely proportional with impact energy although in many condition it decreases by increasing impact energy.
- The back face damage area of composites is obtained much bigger than the impacted face due to tensile crack by bending and delamination of back part of the plate.
- Damage areas for both impacted and back faces increase by increasing impact energy.
- For lower impact energies (less than 50 J), the main damage mode is detected as delamination and matrix cracks rather than fiber fracture. However, for the higher impact energies, splitting between fiber and matrix and fiber fractures are dominant damage modes around point of impact.
- In the lower interface, the delamination seems to have a larger area. It is because of bending and fiber fractures and is obtained from numerical results which are in good agreement with experimental results at this issue.
- Peak contact forces in numerical tests have bigger values when it is compared with experimental contact forces.

- Specimens with damage zones “circle with 76 mm of diameter” and “square with 76 mm per edge” have similar response to the impact.
- For all specimens, the absorbed energy curves are congruent till 30J.
- Square specimens with 150 mm per edge as an impact zone, differs from the other two specimens in higher impact energy levels. Having a larger area, it resists better to impact and need more energy for penetration, but it absorbs lesser energy than other specimens.
- Beginnings of material failures are abrupt, because there is no plastic deformation. Instead there is a region of fiber breakage and pullout ending with an abrupt break. The fiber breakage region is characterized by oscillations in loading curves of the diagrams so far.

REFERENCES

- Abrate, S. (1998). *Impact on composite structures* (1st ed.). Cambridge: Cambridge University Press.
- Aktaş, M. (2007). *Temperature effect on impact behavior of laminated composite plates*. Phd Thesis. Dokuz Eylül University.
- Aslan, Z. (2002). *Behavior of laminated composite structures subjected to low velocity impact*. Phd Thesis. Dokuz Eylül University.
- Aslan, Z., Karakuzu, R. & Okutan, B. (2003). The response of laminated composite plates under low-velocity impact loading. *Composites Science and Technology*, 59, 119–127.
- Belingardi, G., & Vadori, R. (2002). Low velocity impact tests of laminate glass-fiber-epoxy matrix composite material plates. *International Journal of Impact Engineering*, 27, 213–229.
- Breen, C., Guild, F., & Pavier, M. (2005). Impact of thick CFRP laminates: the effect of impact velocity. *Composites: Part A*, 36, 205–211.
- Caprino, G., Langella, A., & Lopresto, V. (2003). Indentation and penetration of carbon fibre reinforced plastic laminates.
- Carlsson, L. A., & Pipes, R. B. (1997). *Experimental Characterization of Advanced Composite Materials* (2nd ed.). USA: Technomic Publishing Company.
- Cesari, F., Re, V. D., Minak, G., & Zucchelli, A. (2007). Damage and residual strength of laminated carbon–epoxy composite circular plates loaded at the centre. *Journal of Composites: Part A*, 38, 1162–1170.
- Chakraborty, D., & Kumar, M. (2005). Response of laminated FRP composites under multiple impact loading. *Journal of Reinforced Plastics and Composites*, 24 (14), 1457–1477.

- Chang, L., Zhang, Z., & Breidt, C. (2004). Impact resistance of short fibre/particle reinforced epoxy. *Applied Composite Materials*.
- Choi, H. Y. (1990). *Damage in graphite/epoxy laminated composites due to low velocity impact*. PhD Thesis. Stanford University.
- Daniel, I. M., & Ishai, O. (1994). *Engineering Mechanics of Composite Materials* (1st ed.). New York: Oxford University Press.
- Finn, S. R. (1991). *Delamination in composite plates under transverse static or impact loads*. PhD Thesis, Stanford University.
- Floyd, A. M. (1994). *An engineering approach to the simulation of gross damage development in composite laminates*. PhD Thesis, The University of British Columbia.
- Groves, S. E. (1986). *A study of damage mechanics in continuous fiber composite laminates with matrix cracking and internal delaminations*. PhD Thesis, Texas A & M University.
- Guan, Z., & Yang, C. (2002). Low-velocity impact and damage process of composite laminates. *Journal of Composite Materials*, 36 (7), 851–871.
- Hull, D., & Clyne T. W. (1981). An introduction to composite materials. *Cambridge University Press*.
- Her, S. C., & Liang, Y. C. (2004). The finite element analysis of composite laminates and shell structures subjected to low velocity impact. *Composite Structures*, 66, 277–285.
- Herup, E. J. (1996). *Low-velocity impact on composite sandwich plates*. PhD Thesis, Air University.
- Hou, J. P., Petrinic, N., Ruiz, C., & Hallett, S. R. (2000). Prediction of impact damage in composite plates. *Composites Science and Technology*, 60, 273–281.

- Houde, M. (1990). *Impact force model for composite materials*. Msc Thesis, University of Toronto.
- Iannucci, L., & Ankersen, J. (2006). An energy based damage model for thin laminated composites. *Composites Science and Technology*, 66, 934–951.
- İçten, B. M. (2006). *Damage in laminated composite plates subjected to low-velocity impact*. PhD Thesis, Dokuz Eylül University.
- Jones, R. M. (1998). *Mechanics of Composite Materials* (2nd ed.). Tokyo: McGraw-Hill.
- Kumar, C. R., Radhakrishna, K., & Rao, R. M. V. G. K. (2005). Postcuring effects on impact behavior of glass/epoxy composite laminates. *Journal of Reinforced Plastics and Composites*, 24 (9), 949–960.
- Liu, D., Raju, B. B., & Dang, X. (1998). Size effects on impact response of Composite laminates. *International Journal of Impact Engineering*, 21 (10), 837–852.
- Matthews, F. L., Rawlings, R. D. (1994). *Composite materials: Engineering and science*. Woodhead Publishing Limited.
- Roy, T., & Chakraborty, D. (in press). Delamination in FRP laminates with holes under transverse impact. *Materials and Design*.
- Sankar, B. V., & Sun, C. T. (1985). Low-velocity impact response of laminated beams subjected to initial stresses. *AIAA Journal*.
- Zhang, Y., Zhu, P., & Lai, X. (2006). Finite element analysis of low-velocity impact damage in composite laminated plates. *Materials and Design*.
- Zhao, G. P., & Cho, C. D. (2007). Damage initiation and propagation in composite shells subjected to impact. *Composite Structures*, 78, 91–100.